Mathematical analysis of models for the transmission dynamics of mosquito borne diseases

by

Usman Ahmed Danbaba

Submitted in partial fulfilment of the requirements for the degree
Philosophiae Doctor

in the Faculty of Natural & Agricultural Sciences
University of Pretoria
Pretoria

August 2019

Declaration

I, Usman Ahmed Danbaba declare that the thesis, which I hereby submit for the degree Philosophiae Doctor at the University of Pretoria, is my own work and has not previously been submitted by me for a degree at this or any other tertiary institution.

Signature: 

Date: August 2019

Acknowledgement

I would like to start by expressing my sincere gratitude to my supervisor, Dr. S.M. Garba of the Department of Mathematics and Applied Mathematics, University of Pretoria. His expertise, encouragement, warm advices, and kind guidance can not be overemphasized. My appreciation also goes to the entire staff members, and postgraduate students of the Department of Mathematics and Applied Mathematics, University of Pretoria.

My study wouldn't have been possible without the financial support of the DST-NRF Centre of Excellence in Mathematical and Statistical Sciences (CoE-MaSS), and the University of Pretoria.

The support, encouragement and love from the entire members of my family have been the best, I wouldn't have been what I am without your trust, patience, motivations, and understanding. Finally, I wouldn't have been here without the encouragement and support of Dr. A. A. Yusuf and his family, thank you for everything, words can't express my appreciation. I love you all, and God bless.

Dedication

This work is dedicated to my lovely family for their unconditional love and support.

Title:	Mathematical analysis of models for the transmission dynamics of mosquito borne diseases
Name:	Usman Ahmed Danbaba
Supervisor:	Dr. S. M. Garba
Department:	Mathematics and Applied Mathematics
Degree:	Philosophiae Doctor

Summary

Mosquitoes are long-legged, two winged flies that are responsible for the transmission of many diseases such as Zika fever, malaria, yellow fever, chikungunya and dengue hemorrhagic fever. Mosquito borne diseases account for substantial amount of parasitic and infectious diseases, they have profound effects on economic growth of many developing countries. There have been continuous efforts to optimize and improve on existing mosquito control strategies, as well as to develop new tools aimed at reducing burden of mosquito borne diseases. Control strategies are either applied alone or in combination depending on available resources, education, health risk and burden of the disease.

The main aim of this thesis is to mathematically study three mosquito borne diseases in the presence of control, the diseases are Zika fever (this is because, in addition to the disease being transmitted vertically, it is the first mosquito borne disease known to be transmitted sexually), yellow fever (because despite having effective vaccine for the disease, it has continue to pose sporadic challenges in different regions of the world), and malaria (because it has the highest global burden among mosquito borne diseases despite continuous efforts to eradicate it).

Some major highlights of the thesis include: Roles of mosquito vertical transmission in the transmission dynamics of mosquito borne diseases, and effects of incorporating human-human transmission are evaluated. Assessment of impact of using different control measures both in human and mosquito populations, and effects of controlling population of adult male (non-disease transmitting) mosquitoes through sterilization are conducted. Implication of incorporating aquatic stage of mosquito development in models for the transmission of mosquito borne diseases, as well as effect of temperature variation in the transmission dynamics of malaria are also studied.

In Chapter 1, brief introduction to the epidemiology of mosquito borne diseases is presented. Basic results and definitions in mathematical epidemiology are also discussed. In addition, some important mathematical theories and definitions used in subsequent chapters are also presented. A Zika model that incorporates vectorial vertical transmission, human-human horizontal transmission, as well as human-mosquito and mosquito-human transmissions is studied in Chapter 2. Another Zika model is considered in Chapter 3, the model incorporated human-human transmission in the presence of mosquito sterilization. In Chapter 4, a yellow fever model with vaccination, use of bed nets and mosquito control at both aquatic and non-aquatic stages is constructed and analysed. Chapter 5 considered a temperature dependent malaria model in the presence of control. General conclusion is given in Chapter 6.

Contents

List of Figures

List of Tables

Table 1: List of Abbreviations

Abbreviation	**Meaning**
Zv	Zika virus
YF	Yellow fever
DFE	Disease free equilibrium
EE	Endemic equilibrium
LAS	Locally asymptotically stable
GAS	Globally asymptotically stable
BB	Backward bifurcation
ODE	Ordinary differential equations
MBD	Mosquito borne diseases
IMM	Integrated mosquito management
VBD	Vector borne diseases
PRCC	Partial rank correlation coefficient
ULV	Ultra low volume
EYE	Eliminating yellow fever epidemics
ULV	Ultra low volume
NIAID	National Institute of Allergy and Infectious Diseases

Chapter 1

General introduction

This thesis is aimed at mathematical study of three different mosquito borne diseases in the presence of control measures. In particular, mathematical models for the transmission dynamics of Zika virus, yellow fever and Malaria will be presented. Because the thesis is presented in the form of articles that are either published or submitted to be considered for publication, there are some overlaps of literature and theorems in some chapters. In this chapter, brief introduction to physiology of mosquitoes, mosquito borne diseases (MBD) and mosquito control are presented. In addition, basic mathematical and epidemiological concepts required for the understanding of subsequent chapters are also presented.

1.1 Mosquitoes

Mosquitoes are delicate, long-legged two winged flies (order Diptera, family Culicidae) that are easily recognized by their long proboscis and scaly wings and legs [70]. There are over three thousand five hundred species and subspecies of mosquitoes in the world [70, 92], the majority of mosquito species fall into three groups, commonly referred to as the anophelines, the culicines, and the aedines [92]. Mosquitoes are found everywhere in the world where standing water occurs, which is needed for the development of their aquatic (immature) stages that include eggs, larvae and pupae [92, 122]. Because of their ability to spread many deadly diseases, mosquitoes are considered as the most important group of arthropods of medical importance on the planet [92, 120].

1.2 Mosquito borne diseases

Mosquito borne diseases (MBD) are spread by blood-sucking female mosquitoes which require blood for the development of their eggs. Usually, warm-blooded animals are their common source of blood, but there are many mosquito species that feed on cold blooded animals such as snakes, turtles, toads, frogs and other insects. Some mosquito species are active at night or twilight while others are active during the daytime [70]. Mosquitoes use human blood almost exclusively to nurture their eggs [122]. The

most important mosquitoes have a marked tendency of feeding on humans and are exquisitely adapted to living around humans (domestic environments) [70, 92, 122]. Mosquitoes are responsible for the transmission of many important diseases, some of which include Zika virus, yellow fever, malaria, Chikungunya, West Nile virus, dengue haemorrhagic fever, and Japanese encephalitis [70, 95, 120]. MBD are responsible for 17% of the global burden of parasitic and infectious diseases. They result in avoidable ill-health and death, economic hardship for affected communities and are a serious impediment to economic development [95].

1.2.1 Mosquito control

Mosquito control simply refers to any or all methods (i.e., chemical, biological, environmental, and genetic) used in reducing mosquito longevity, density, and/or human-mosquito contact in an area [135]. A question of significant importance is whether it necessary to eradicate the messenger (mosquito) when it is really the message (pathogens and parasites) that is the enemy of public health [70]. On the other hand, mathematical control theory deals with basic principles underlying the analysis and design of control systems. To control an object means to influence its behavior so as to achieve a desired goal [130].

1.2.1.1 Genetic and larval control

Genetic control refers to controlling mosquitoes by releasing sterile males or genetically modified mosquitoes into an area [135]. On the other hand, larval control refers to the management of aquatic (immature) mosquito life stages using environmental management, larvicides, and biological control [135].

1.2.1.2 Adult mosquito management and personal protection

The management of adult mosquito population is aimed at reducing the population of biting mosquitoes. This involves the use of adulticides (usually spread from aircrafts and truck-mounted equipments), such as ultra-low volume application of malathionor chlorpyrifos or chlorpyrifos + permethrin, thermal fogging with malathion or chlorpyrifos or chlorpyrifos + permethrin as space treatment against adult mosquitoes at night or early morning when the air is calm, or applying insecticide residual spray as barrier treatments to tall grasses, weeds, shrubs, fences and other harborages surrounding parks, playgrounds and residences to help reduce adult mosquito populations [121].

Personal protection simply refers to mosquito control using methods like application of repellents, use of bed nets and protective clothing to reduce exposure to mosquito bite at an individual or community level [135].

1.2.1.3 Integrated mosquito management (IMM)

The integrated mosquito management scheme is a rational decision-making process to optimize the use of resources for mosquito control [145]. It considers available mosquito control techniques and integrate those appropriate measures that reduce mosquito populations while keeping pesticides and other interventions to justifiable

level. It is based on evidence and integrated management, promoting the use of a range of interventions, alone or in combination, selected on the basis of local knowledge about the mosquitoes and the disease [135, 145]. Integrated approaches can address several diseases at a time, this is because some mosquitoes can transmit multiple diseases and interventions are effective against different species [145].

1.2.2 Roles of mosquitoes in the ecosystem

Although mosquito borne diseases are deadly, there are however many positive impacts of mosquitoes to our ecosystem. Elimination of mosquitoes might make the biggest ecological difference in the Arctic tundra, where migratory birds depend on them [53]. The larvae of mosquitoes serve as food for fish and insect predators [70]. In fact, in the absence of their larvae, hundreds of species of fish would have to change their diet to survive [53]. Adult mosquitoes pollinate plants and are eaten by spiders, birds, bats, reptiles, and amphibians. The larvae of several genera use a modified breathing tube to pierce the stems and roots of aquatic plants to obtain oxygen, the botfly also depends on mosquitoes to carry its larvae to hosts [53, 70].

1.3 Mathematical Preliminaries

In this section, we briefly discuss some basic definitions and results in the study of dynamical systems that are relevant to this thesis and are not explicitly defined or stated in the subsequent chapters.

1.3.1 Introduction

Consider the system of ordinary differential equation (ODE) below,

$$\dot{x} = f(x,t) \quad x(0) = x_0, \tag{1.3.1}$$

where $f : U \times \mathbb{R}_+ \to \mathbb{R}^n$ with $x \in U \subset \mathbb{R}^n$, $t \in \mathbb{R}_+$, $n \in \mathbb{N}$ and U open in $\mathbb{R}^n$. The system (1.3.1) is autonomous if the function f is explicitly independent of time. Most of our study is restricted to the autonomous systems, hence for $x \in U \subset \mathbb{R}^n$,

$$\dot{x} = f(x), \quad x(0) = x_0. \tag{1.3.2}$$

Definition 1.3.1. By a solution of (1.3.2), we mean a continuously differentiable function $x : I(X) \to \mathbb{R}^n$ such that $x(t)$ satisfies (1.3.2), where $I(X)$ is an interval of $\mathbb{R}_+$ containing the origin [133].

Definition 1.3.2. System (1.3.2) defines a dynamical system in a subset E of $\mathbb{R}^n$ if for every $X \in E$, there exist a unique solution of (1.3.2) which is defined and remains in E for all $t \in \mathbb{R}_+$ [133].

Definition 1.3.3. Let U be an open subset of $\mathbb{R}^n$. A function $f : U \to \mathbb{R}^n$ is Lipschitz if for all $x, y \in U$, there is a K called Lipschitz constant such that

$$||f(x) - f(y)|| \leq K||x - y||.$$

Here $||.||$ stands for the Euclidean norm in $\mathbb{R}^n$. If f is Lipschitz on every bounded subset of $\mathbb{R}^n$, then f is said to be globally Lipschitz [97].

Theorem 1.3.1. Let $f : \mathbb{R}^n \to \mathbb{R}^n$ be globally Lipschitz on $\mathbb{R}^n$. Then there exist a unique solution $x(t)$ to (1.3.2) $\forall\ t \in \mathbb{R}_+$. Therefore the system defines a dynamical system in $\mathbb{R}^n$ [133].

Theorem 1.3.2. Let $C \subset U \subseteq \mathbb{R}^n \times \mathbb{R}_+$ be a compact set containing (x_0, t_0). The solution $x(t, t_0, x_0)$ can be uniquely extended forward in t up to the boundary of C [151].

Definition 1.3.4. An equilibrium (stationary) point of (1.3.2) is a point $\bar{x} \in \mathbb{R}^n$ such that $x_0 = \bar{x}$ and $f(\bar{x}) = 0$.

Clearly, the constant function $x(t) \equiv \bar{x}$ is a solution of (1.3.2) and by uniqueness of solutions, no other solution curve can pass through $\bar{x}$.

Theorem 1.3.3. Gronwall's Lemma Let $x(t)$ satisfy

$$\frac{dx}{dt} \leq px + q, \quad x(0) = x_0,$$

for p, q constants. Then for $t \geq 0$

$$x(t) \leq e^{pt}x_0 + \frac{q}{p}(e^{pt} - 1), \quad p \neq 0$$

and

$$x(t) \leq x_0 + qt, \quad p = 0 \quad [133].$$

1.3.2 Hartman-Grobman theorem

Let $\bar{x} \in \mathbb{R}^n$ be an equilibrium point of a dynamical system on E defined by (1.3.2). Then $\bar{x}$ is said to be:

1. stable if for any $\epsilon > 0$, there exist $\delta = \delta(\epsilon) > 0$ such that if $||\bar{x} - y(0)|| < \delta$, then, $||\bar{x} - y(t)|| < \epsilon$ for all $t \geq 0$,

2. locally attractive if $||\bar{x} - y(t)|| \to 0$ as $t \to \infty$ for all $||\bar{x} - y(0)||$ sufficiently small,

3. locally asymptotically stable if $\bar{x}$ is stable and locally attractive. For an asymptotically stable equilibrium point $\bar{x}$ of (1.3.2), the set of all initial data $x(0)$ such that
$$\lim_{t\to\infty} \Phi(t)x(0) = \bar{x}$$
is said to be the basin of attraction of $\bar{x}$,

4. globally attractive if (2) holds for any $x(0) \in E$, i.e. the basin of attraction of $\bar{x}$ is E,

5. globally asymptotically stable if (1) and (4) hold,

6. unstable if (1) fails

Definition 1.3.5. The Jacobian matrix of f at the equilibrium $\bar{x}$, denoted by $Df(\bar{x})$, is the matrix of partial derivatives of f evaluated at $\bar{x}$ [97].

One of the easiest ways of investigating the stability of an equilibrium point (if the derivatives do not vanish at the equilibrium) is by considering the linearized form of (1.3.2) given by

$$\dot{U} = JU \tag{1.3.3}$$

near $\bar{x}$, where $J = Df(\bar{x})$ is the Jacobian of the function f at $\bar{x}$. It is assumed that f is differentiable.

Definition 1.3.6. Let $\bar{x}$ be an equilibrium solution of (1.3.2), $\bar{x}$ is called a hyperbolic equilibrium point if none of the eigenvalues of $Df(\bar{x})$ have zero real part [151]. An equilibrium point that is not hyperbolic is called non hyperbolic.

Let X and Y be two topological spaces.

Definition 1.3.7. A function $f : X \to Y$ is a homeomorphism if it is continuous, bijective with a continuous inverse [97].

Definition 1.3.8. A function $h : X \to Y$ is a C^1 diffeomorphism if it is invertible and both h and it's inverse (h^{-1}) are C^1 maps [97].

Consider two functions $f : \mathbb{R}^n \to \mathbb{R}^n$ and $g : \mathbb{R}^m \to \mathbb{R}^m$.

Definition 1.3.9. f and g are said to be conjugate if there exist a homeomorphism $h : \mathbb{R}^n \to \mathbb{R}^m$ such that $g(h(x)) = h(f(x)), x \in \mathbb{R}^n$ [97].

Definition 1.3.10. A $C^r(r \geq 1)$ function $\Phi : U \times \mathbb{R}_+ \to \mathbb{R}^n$, $U \subset \mathbb{R}^n$ is called a flow for (1.3.2) if it satisfies the following properties

- $\Phi(x_0, 0) = x_0$
- $\Phi(x_0, s + t) = \Phi(\Phi(x_0, s), t)$

Definition 1.3.11. The set of all points in a flow $\Phi(t; x_o)$ for (1.3.2) is called the orbit or trajectory of $f(x)$ with initial condition x_0, we write the orbit $\Phi(x_0)$. When we consider $t \geq 0$, we say that, $\Phi(t; x_o)$ is a forward orbit or forward trajectory.

Proposition 1.3.4. If f and g are C^k conjugate, $k \geq 1$, and x_0 is a fixed point of f, then the eigenvalues of $Df(x_0)$ are equal to the eigenvalues of $Dg(h(x_0))$.

Theorem 1.3.5. (Hartman and Grobman) Assume that $f : \mathbb{R}^n \to \mathbb{R}^n$ is of class C^1 and consider a hyperbolic equilibrium point $\bar{x}$ of the dynamical system defined by (1.3.2). Then there exist $\delta > 0$, a neighborhood $\mathcal{N} \subset \mathbb{R}^n$ of the origin and a homeomorphism h defined from the ball $B = \{x \in R^n : ||x - \bar{x}|| < \delta\}$ onto $\mathcal{N}$ such that

$$u(t) = h(x(t)) \text{ solves (1.3.3) if and only if } x(t) \text{ solves (1.3.2).}$$

The direct application of the Hartman-Grobman theorem is that an orbit structure near a hyperbolic equilibrium solution is qualitatively the same as the orbit structure given by the associated linearized (around the equilibrium) dynamical system.

Theorem 1.3.6. Suppose all the eigenvalues of $Df(\bar{x})$ have negative real parts. The equilibrium solution $\bar{x}$ of the non linear vector field (1.3.2) is asymptotically stable [151].

1.3.3 Lyapunov functions

A function $V : \mathbb{R}^n \longrightarrow \mathbb{R}$ is said to be positive definite if,

- $V(x) > 0$, for all $x \neq 0$,
- $V(x) = 0$, if and only if $x = 0$,
- $V(x) \longrightarrow \infty$ as $x \longrightarrow \infty$.

The function V is locally positive definite if there exists $U \subset \mathbb{R}^n$ containing a fixed point $\bar{x}$ such that

- $V(\bar{x}) = 0$,
- $V(x) > 0$ for all $x \in U \backslash \{\bar{x}\}$.

Definition 1.3.12. Assume that (1.3.2) defines a dynamical system on an open subset $U \subset \mathbb{R}^n$ and $\bar{x}$ is an equilibrium point. A function $V \in C^1(U, \mathbb{R})$ is called a Lyapunov function of the system (1.3.2) for $\bar{x}$ on a neighborhood $B \subset U$ of $\bar{x}$ if

$$\dot{V}(x) := \lim_{h \to 0} \frac{V(x + hf(x)) - V(x)}{h} = \bigtriangledown V(x).f(x) \leq 0, \quad \forall x \in B, \tag{1.3.4}$$

where $\dot{V}(x)$ is the directional derivative of V in the direction of f. If in addition, $V(\bar{x}) = 0$ and $V(x) > 0$ $\forall x \in U \backslash \{\bar{x}\}$, then V is said to be a positive definite Lyapunov function at $\bar{x}$.

Theorem 1.3.7. Let V be a positive definite Lyapunov function of the dynamical system (1.3.2) on a neighborhood U of an equilibrium point $\bar{x}$. Then $\bar{x}$ is stable. If, in addition, $\dot{V}(x) < 0$ $\forall x \in U \backslash \{\bar{x}\}$, then $\bar{x}$ is asymptotically stable, and $\bar{x}$ is unstable if $\dot{V}(x) > 0$, $\forall x \in U \backslash \{\bar{x}\}$.

1.3.4 Limit sets and invariance principle

Epidemiology models generally deal with population dynamics, thus it is important to consider non-negative feasible regions where the property of non-negativity is preserved.

Definition 1.3.13. Let $x(t)$ be a solution of (1.3.2). A point p is said to be a positive limit of $x(t)$, if there exists a sequence $\{t_n\}$ with $t_n \longrightarrow \infty$ as $n \longrightarrow \infty$, such that $x(t_n) \longrightarrow p$ as $n \longrightarrow \infty$. The set of all positive limit points of $x(t)$ is called the positive limit set of $x(t)$.

Definition 1.3.14. Let ϕ be the flow of (1.3.1). A point $x_0 \in \mathbb{R}^n$ is called ω-limit point of $x \in \mathbb{R}^n$, denoted by $\omega(x)$, if there exists a sequence $\{t_n\}, t_n \longrightarrow \infty$ such that,

$$\phi(t_n, x) \longrightarrow x_0.$$

Similarly, a point $x_0 \in \mathbb{R}^n$ is called α-limit point of $x \in \mathbb{R}^n$, denoted by $\alpha(x)$, if there exists a sequence $\{t_n\}, t_n \longrightarrow -\infty$ such that,

$$\phi(t_n, x) \longrightarrow x_0.$$

The set of all ω-limit points of a flow is called the ω-limit set, while the set of all α-limit points of a flow is called the α-limit set [151].

Definition 1.3.15. A set M is said to be an invariant set with respect to the autonomous ODE given by (1.3.2) if,

$$x(0) \in M \Rightarrow x(t) \in M, \forall t \in \mathbb{R}.$$

That is, if any trajectory starts in M, it will stay in M for all time [131].

If we restrict $t \geq 0$ in the above definition, then M is said to be positively invariant set. In other words, any solution in a positively invariant set remains there for all positive time.

Theorem 1.3.8. (LaSalle's invariance principle)
Let $\bar{x}$ be an equilibrium point of (1.3.2) defined on $\Omega \subset \mathbb{R}^n$. Let V be a positive definite Lyapunov function for $\bar{x}$ on the set Ω. Furthermore let $\Omega_a = \{x \in \bar{\Omega} : \dot{V}(x) = 0\}$ and if

$$S = \{\text{the union of all trajectories that start and remain in } \Omega_a \text{ for all } t > 0\},$$

that is, S is the largest positively invariant subset of Ω_a such that $S \subset \Omega$, then $\bar{x}$ is globally asymptotically stable on Ω if and only if it is globally asymptotically stable on S [151].

1.4 Mathematical epidemiology

This section is aimed at discussing some of the basic principles and methods associated with modelling in epidemiology.

1.4.1 Incidence function

Let N be total human population in a community. Divide N into non-intersecting compartments of susceptible (S), infectious (I) and immune (R). Disease incidence is defined as the infection rate of susceptible individuals through their contact with infectious individuals [36, 139]. It is characterized by an incidence function (that describes the mixing pattern within a community), and infections are transmitted through contact.

The number of times an infectious individual comes into contact with other members per unit time is defined as the contact rate $C(N)$, let β_0 be a probability of infection by every contact, then $\beta_0 C(N)$ is called the effective contact rate, it shows the ability of an infected individual to infect others (depending on environment, toxicity of pathogen, etc.). Therefore, the mean adequate contact rate of an infective to susceptible individuals is $\beta_0 C(N)\frac{S(t)}{N(t)}$, which is called the infection rate. Furthermore, the total number of new infected individuals resulting per unit time at time t is $\beta_0 C(N)\frac{S(t)}{N(t)}I(t)$, which is called the incidence of a disease.

If $C(N) = kN$, the incidence is $\beta_0 kS(t)I(t) = \beta S(t)I(t)$ (where $\beta_0 k = \beta$ is the transmission coefficient) is called the bilinear incidence or simple mass-action incidence

[134]. When $C(N) = k$, the incidence becomes $\beta_0 k \frac{S(t)}{N(t)} I(t) = \beta \frac{s(t)}{N(t)} I(t)$ (where $\beta_0 k = \beta$), this type of incidence function is termed as the standard incidence [134].

For malaria (mosquito borne disease), Chitnis et.al proposed a function ($b = b(N_H, N_V)$) to model the total number of mosquito bites on humans as

$$b = b(N_H, N_V) = \frac{\sigma_V \sigma_H N_V N_H}{\sigma_V N_V + \sigma_H N_H} = \frac{\sigma_V \sigma_H}{\sigma_V \frac{N_V}{N_H} + \sigma_H} N_V,$$

where σ_V is the number of times one mosquito would want to bite humans per unit time if humans were freely available, σ_H is the maximum number of mosquito bites a human can have per unit time [27]. N_V and N_H are respectively total mosquito and human populations. They defined $b_H b_H(N_H, N_V) = \frac{b(N_H, N_V)}{N_H}$ as the number of bites per human per unit time, and $b_V = b_V(N_H, N_V) = \frac{b(N_H, N_V)}{N_V}$ as the number of bites per mosquito per unit time [27].

Other contact rates were also proposed, such as those with saturation as introduced by Dietz in 1982 [134] and Heesterbeek and Metz in 1993 [21], with contacts respectively given by

$$C(N) = \frac{\alpha N}{1 + \omega N}, \quad \text{and,} \quad C(N) = \frac{\alpha N}{1 + bN + \sqrt{1 + 2bN}}$$

satisfying

$$C(0) = 0, \quad C'(N) \geq 0, \quad \left(\frac{C(N)}{N}\right)' \leq 0 \quad \lim_{N \to \infty} C(N) = C_0 \quad [134].$$

Other incidences for special cases such as $\beta S^p I^q$, $\frac{\beta S^p I^q}{N}$ are also been used [134].

1.4.2 Basic reproduction number

One of the most important results in mathematical epidemiology is that, for epidemic models, there is difference in epidemic behavior when the average number of secondary infections caused by a single infectious individual in a wholly susceptible population, over the course of his/her infection, called the basic reproduction number (R_0), is less than one and when this quantity exceeds one [30, 59]. The famous threshold criterion states that: The disease can invade the population if $R_0 > 1$, whereas it cannot invade the population if $R_0 < 1$ [43, 139]. Mathematically, if $R_0 < 1$, the disease-free equilibrium is approached by solutions of the model describing the situation. If $R_0 > 1$, the disease-free equilibrium is unstable and solutions flow away from it, there is also an endemic equilibrium with a positive number of infective individuals, therefore, the disease remains in the population [30]. However, the situation may be more complicated with more than one stable equilibrium when the basic reproduction number is less than one.

1.4.2.1 Non-periodic reproduction number

The next generation method is used to establish the local asymptotic stability of the disease-free equilibrium (DFE). The method was first introduced by [43] and refined for epidemiological models by [139].

Consider a heterogeneous population whose individuals are distinguishable by their disease status and can be grouped into n homogeneous compartments. The idea is based on computing a matrix whose (i, j) element represents the number of secondary infections in compartment i caused by an individual in compartment j. We refer to disease compartment as the compartment where individuals are infected. We should note that, we will consider the disease compartment in a broader way compared to the clinical method, hence it includes stages of infections like exposed stage, in which infected individuals are not necessarily infectious.

Suppose there are n disease compartments and m non disease compartments, and let $x \in \mathbb{R}^n$ and $y \in \mathbb{R}^m$ be the sub populations in each of these compartments. Further, we denote by $\mathfrak{F}_i$ the rate at which secondary infections increase the i^{th} disease compartment and by $\mathcal{V}_i$, the rate at which disease progression, death and recovery decrease the i^{th} compartment. The compartmental model can then be written in the form

$$\begin{aligned} x_i^{'} &= \mathfrak{F}_i(x, y) - \mathcal{V}_i(x, y), \quad i = 1, 2, ...n, \\ y_j^{'} &= \mathrm{g}_j(x, y), \quad j = 1, 2, ..., m. \end{aligned} \tag{1.4.5}$$

Note that the decomposition of the dynamics into $\mathfrak{F}$ and $\mathcal{V}$ and the designation of compartments as infected or uninfected may not be unique; different decompositions correspond to different epidemiological interpretations of the model.

The derivation of the basic reproduction number is based on the linearization of the ODE model about a disease-free equilibrium. For an epidemic model with a line of equilibria, it is customary to use the equilibrium with all members of the population susceptible. We assume:

- $\mathfrak{F}_i(0, y) = 0$ and $\mathcal{V}_i(0, y) = 0$ for all $y = 0$ and $i = 1, ..., n$.
- The disease-free system $y^{'} = \mathrm{g}(0, y)$ has a unique equilibrium that is asymptotically stable, that is, all solutions with initial conditions of the form $(0, y)$ approach a point $(0, y_0)$ as $t \to \infty$. We refer to this point as the disease-free equilibrium.

The first assumption says that all new infections are secondary infections arising from infected hosts; there is no immigration of individuals into the disease compartments. It ensures that the disease-free set, which consists of all points of the form $(0, y)$, is invariant. That is, any solution with no infected individuals at some point in time will be free of infection for all time. The second assumption ensures that the disease-free equilibrium is also an equilibrium of the full system. The uniqueness of the disease-free equilibrium in the second assumption is required for models with demographics. Although it is not satisfied in epidemic models, the specification of a particular disease-free equilibrium with all members of the population susceptible is sufficient to validate the results.
Next, we assume:

- $\mathfrak{F}_i(x,y) \geq 0$ for all nonnegative x and y and $i = 1, ..., n$.
- $\mathcal{V}_i(x,y) \leq 0$ whenever $x_i = 0, i = 1, ..., n$.
- $\sum_{i=1}^{n} \mathcal{V}_i(x,y) \geq 0$ for all nonnegative x and y.

The reasons for these assumptions are that the function $\mathfrak{F}$ represents new infections and cannot be negative, each component $\mathcal{V}_i$ represents a net outflow from compartment i and must be negative (inflow only) whenever the compartment is empty, and the sum $\sum_{i=1}^{n} \mathcal{V}_i(x,y)$ represents the total outflow from all infected compartments. Terms in the model leading to increases in $\sum_{i=1}^{n} x_i$ are assumed to represent secondary infections and therefore belong to $\mathfrak{F}$.

Suppose that a single infected person is introduced into a population originally in the absence of disease. The initial ability of the disease to spread through the population is determined by an examination of the linearization of (1.4.5) about the disease-free equilibrium $(0, y_0)$. It is easy to see that the assumption $\mathfrak{F}_i(0,y) = 0, \mathcal{V}_i(0,y) = 0$ implies

$$\frac{\partial \mathfrak{F}_i}{\partial y_j}(0, y_0) = \frac{\partial \mathcal{V}_i}{\partial y_j}(0, y_0) = 0$$

for every pair (i,j). This implies that the linearized equations for the disease compartments x are decoupled from the remaining equations and can be written as

$$x^{'} = (F - V)x, \tag{1.4.6}$$

where F and V are the $n \times n$ matrices with entries

$$F = \frac{\partial \mathfrak{F}_i}{\partial x_j} \quad \text{and} \quad V = \frac{\partial \mathcal{V}_i}{\partial x_j}.$$

Because of the assumption that the disease-free system $y^{'} = \mathrm{g}(0,y)$ has a unique asymptotically stable equilibrium, the linear stability of the system (1.4.5) is completely determined by the linear stability of the matrix $(F - V)$ in (1.4.6).

The number of secondary infections produced by a single infected individual can be expressed as the product of the expected duration of the infectious period and the rate at which secondary infections occur [59].

Definition 1.4.1. The Matrix $K = FV^{-1}$ is referred to as the next generation matrix for the system (1.4.5) at the disease-free equilibrium [59].

The (i,j) entry of K is the expected number of secondary infections in compartment i produced by individuals initially in compartment j, assuming, of course, that the environment experienced by the individual remains homogeneous for the duration of its infection [59].

Lemma 1.4.1. The basic reproduction number $R_0 = \rho(FV^{-1}) = \max_{\lambda}\{|\lambda| : \lambda$ is an eigenvalue of $FV^{-1}\}$ and the disease-free equilibrium is asymptotically-stable if $R_0 < 1$ and unstable if $R_0 > 1$ [59].

Notice that Periodic reproduction number and Type reproduction number are discussed in subsequent chapters.

1.4.3 Backward Bifurcations

Bifurcation analysis is the mathematical study of changes in qualitative properties of solutions of a system of differential equations when changing its parameters. These changes in the dynamics of the system are called bifurcations. The parameter values where they occur are called bifurcation points. By analysing the existence of behavior of the model in such points, one can derive much about the systems properties.

It is well known in disease transmission modeling that a disease can be eradicated when the basic reproduction number $R_0 < 1$. However, when a backward bifurcation occurs, stable endemic equilibria may also exist for $R_0 < 1$, this means that, the condition that $R_0 < 1$ is only a necessity, but not sufficient to guarantee the elimination of the disease, indeed, the quantity R_0 must be reduced further to avoid endemic states and guarantee eradication. The scenario is qualitatively described as follows: in the neighborhood of 1, for $R_0 < 1$, a stable disease-free equilibrium coexists with stable endemic equilibrium. The endemic equilibrium disappears by saddle-node bifurcation when R_0 is decreased below a critical value $R_c < 1$ [24, 66].

Definition 1.4.2. A forward bifurcation occurs when R_0 crosses unity from below; a small positive asymptotically-stable equilibrium appears and the disease-free equilibrium losses its stability.

Definition 1.4.3. Backward bifurcation happens when R_0 is less than unity; a small positive unstable equilibrium appears while the disease-free equilibrium and a larger positive endemic equilibrium are locally-asymptotically stable [26].

Chapter 2

Zika virus with vertical transmission in mosquitoes and horizontal transmission in humans

General introduction

In this chapter, a Zika model that takes into account vertical transmission in mosquitoes, and human-human sexual transmission is constructed and rigorously analysed for its qualitative properties. The model also considers the conventional human-mosquito and mosquito-human Zika transmission.

Abstract

We construct and analyse a compartmental model for the transmission dynamics of Zika virus. In addition to horizontal transmissions (human-mosquito, mosquito-human and human-human), the model also incorporates vertical transmission of Zika virus in mosquito population, therefore, both aquatic and non-aquatic stages of mosquito development are considered. The aquatic stage is divided into infectious and non-infectious compartments, depending on whether oviposition is by infected mosquito (and the virus is vertically transmitted) or otherwise. The basic offspring number (N_0), basic reproduction number $(\mathcal{R}_0)$, and type reproduction number (T_I) of the model are computed. The relationship between type and basic reproduction numbers are established. Using the method based on center manifold theory, the model is shown to undergo backward bifurcation. Furthermore, condition under which the system does not undergo backward bifurcation at $\mathcal{R}_0 = 1$ is obtained. Global asymptotic stability of the disease free equilibrium (DFE) is presented under those conditions. Numerical simulations, local and global sensitivity analysis of the model parameters are also presented.

2.1 Introduction

Currently, emerging infectious diseases such as Zika virus (Zv) are of great socioeconomic importance, especially due to their numerous modes of transmissions. Zv is an arthropod-borne virus (arbovirus) that is related to West Nile virus, yellow fever, dengue and Japanese encephalitis, this is because their primary mode of transmission is through bites by Aedes mosquitoes (usually *Aedes aegypti* and *Aedes albopictus*). The clinical presentation of Zika infection is not specific (mild fever, rash, arthralgia, and conjunctivitis), it is also often confused with other diseases like dengue and Chikungunya [103, 105]. In addition to the conventional human-mosquito and mosquito-human modes of transmissions of the disease, human vertical transmission of Zv is linked to incidences of microcephaly and Guillain-Barr syndrome [98, 125]. Direct (human-human) transmissions (due to sexual contacts) have also been reported [58, 60, 104]. Furthermore, vertical transmission within Aedes aegypti and Aedes albopictus have also been observed, and it may even play significant role in the spread and maintenance of the disease [31, 54, 88, 90, 137]. Cases of vertical transmissions in other mosquito borne flavivirus such as yellow fever, Chikungunya and dengue, which could even be the probable mechanism for the persistence of arboviruses during periods that are unfavorable for horizontal transmission have been reported [68, 75, 87].

Gao et al [61] constructed a deterministic model for the transmission dynamics of Zika without demographic factors, but took into account sexual transmission of the disease. Brauer et al [22] considered another model with direct (sexual) transmission and computed the basic reproduction number. Agusto et al [4] analysed gender structured compartmental model with further subdivisions (compartments) based on disease status, and also considered sexual transmission. Agusto et al [5] presented another Zika model with vertical transmission in humans. Maxian et al [96] developed a model that evaluated the relative contribution of sexual transmission route to the overall epidemic. Imran et al [74] also considered vertical transmission in both human and mosquito populations with constant recruitment. Although vertical transmission in humans is attributed to microcephaly and Guillain-Barr syndrome, it is ignored in this study, and this is due to the fact that symptomatic children usually receive adequate treatment and hence, their transmission is assumed to be negligible.

Adams and Boots [2] constructed a dengue model with vertical transmission in the mosquito population. Both the aquatic and non-aquatic stages were considered in their model which assumes a constant oviposition, where fraction of the eggs become infected. We extend the formulation of [2] to capture vertical transmission at the point of oviposition (transovarial transmission), by considering oviposition that is proportional to the population of reproductive mosquitoes (infected and non-infected), where fraction of the eggs laid by infected mosquitoes are transmitted vertically.

The work is organized as follows; Introduction to Zika virus and review of related literature is presented in Section 2.1. The compartmental model for the transmission dynamics of Zika is constructed and rigorously analysed for its dynamical features in Section 2.2. Numerical and sensitivity analysis is presented in Section 2.3.

2.2 Model formulation

The designed model assumes a homogeneous mixing of the human and mosquito populations, so that each mosquito bite has equal chance of transmitting (acquiring) the disease to (from) susceptible (infectious) human. The model divides the total human population at a time t into non-intersecting compartments according to their disease status as susceptible (S_H), infectious (I_H), and recovered (R_H) humans. Notice that, recovery here refers to the case where the virus is cleared from the blood stream, but it may still be present in the sperm cells and saliva, and hence the probability of sexual (vaginal or oral) transmission [58, 60, 104], so that the total human population at time t is given by,

$$N_H(t) = S_H(t) + I_H(t) + R_H(t).$$

The mosquito population is split according to their developmental stages, that is aquatic (which includes egg, larvae and pupae) and the non-aquatic (adult) stages. The aquatic (A) mosquito population is further sub-divided into infected (A_I) and non-infected (A_N) mosquitoes, so that the total mosquito population in the aquatic stage is given by

$$A(t) = A_N(t) + A_I(t)$$

Similarly, the total adult mosquito population (N_V) is sub-divided into susceptible (S_V) and infected (I_V), so that the total mosquito population at the non-aquatic stage is given by

$$N_V(t) = S_V(t) + I_V(t).$$

The susceptible human population is generated via recruitment of humans (by birth or immigration) into the population (at a rate b_H). This population is decreased following infection, which could be acquired via sexual contact with infectious humans at a rate

$$\lambda_{HH} = \frac{\beta_{HH}\left(I_H + \eta_H R_H\right)}{N_H} \tag{2.2.1}$$

or from infectious mosquitoes at a rate

$$\lambda_{MH} = \frac{\beta_{VH} I_V}{N_V} \tag{2.2.2}$$

where $\beta_{HH} = \rho_{HH} b_{HH}$ is an effective contact rate between infectious and susceptible humans, ρ_{HH} is a probability of sexual transmission from infectious to susceptible humans and b_{HH} is a sexual contact rate between infectious and susceptible humans, η_H is a reduction parameter in the transmissibility of recovered humans when compared with infectious humans, similarly, $\beta_{VH} = \rho_{VH} b_{VH}$ is an effective contact rate between infectious mosquitoes and susceptible humans, ρ_{VH} is a probability of transmission from infectious mosquitoes to susceptible humans and b_{VH} is a biting rate of infectious mosquitoes. Therefore, the force of infection in human population (which is the sum of (2.2.1) and (2.2.2)) is given by

$$\lambda_H = \frac{\beta_{HH}\left(I_H + \eta_H R_H\right)}{N_H} + \frac{\beta_{VH} I_V}{N_V} \tag{2.2.3}$$

Individuals in each human compartment reduce due to natural death (at a rate μ_H). So that the rate of change of susceptible human population is given by

$$\frac{dS_H}{dt} = b_H - \lambda_H S_H - \mu_H S_H.$$

The population of infected humans (I_H) increases through the infection of susceptible humans (at the rate λ_H). This population is decreased by recovery (at a rate γ_H) and due to Zika infection (at a rate δ_H). This gives

$$\frac{dI_H}{dt} = \lambda_H S_H - (\delta_H + \gamma_H + \mu_H) I_H.$$

The population of recovered humans is generated by recovery of infected individuals (at the rate γ_H) and reduces due to natural death. So that

$$\frac{dR_H}{dt} = \gamma_H I_H - \mu_H R_H.$$

The population of non-infected aquatic mosquitoes (A_N) is generated through oviposition by susceptible (S_V) or infectious (I_V) mosquitoes at rates ϕ_V and $\eta_V \phi_V$ respectively (where η_V is the proportion of non-infected eggs). Oviposition rate per susceptible and infectious female mosquitoes is assumed to be proportional to their density, since breeding site can only support limited number of aquatic mosquitoes, we assume a maximum aquatic mosquito effect with a carrying capacity $\mathcal{K}$, similar formulation was considered by [45, 46]. This population is decreased by maturation (at a rate b_V) and natural death (at a rate μ_A). Similar to [46, 61, 140], it is assumed that $\mathcal{K} \propto N_H$, which implies $\mathcal{K} = mN_H$. Therefore

$$\frac{dA_N}{dt} = \phi_V \Big(1 - \frac{A_N + A_I}{\mathcal{K}}\Big) \big[S_V + \eta_V I_V\big] - b_V A_N - \mu_A A_N$$

The population of infected aquatic mosquitoes (A_I) is generated by oviposition of infected eggs laid by infectious mosquitoes (through vertical transmission at a rate $1 - \eta_V$). Similarly, maximum aquatic mosquito effect is considered. This population is reduced by maturation (at the rate b_V) and natural death (at the rate μ_A). This gives

$$\frac{dA_I}{dt} = \phi \Big(1 - \frac{A_N + A_I}{\mathcal{K}}\Big) [1 - \eta_V] I_V - b_V A_I - \mu_A A_I.$$

The population of susceptible adult mosquitoes (S_V) is generated by maturation of non-infected aquatic mosquitoes (at the rate b_V) and decrease by infection at a rate

$$\lambda_{HM} = \frac{\beta_{HV} I_H}{N_H} \tag{2.2.4}$$

where $\beta_{HV} = \rho_{HV} b_{HV}$ is an effective contact rate between infectious humans and susceptible mosquitoes, ρ_{HV} is a probability of transmission from infectious humans to susceptible mosquitoes and b_{HV} is a biting rate of susceptible mosquitoes and due

to natural death (at a rate μ_V). So that

$$\frac{dS_V}{dt} = b_V A_N - \lambda_{HM} S_V - \mu_V S_V.$$

Finally, the population of infectious adult mosquitoes (I_V) is generated by maturation of infected aquatic mosquitoes (at the rate b_V), by infection of susceptible mosquitoes at the rate λ_{HM} and decrease due to natural death (at the rate μ_V). So that

$$\frac{dI_V}{dt} = \lambda_{HM} S_V + b_V A_I - \mu_V I_V.$$

2.2.1 Incidence function

The most commonly used forms of disease transmissions is either the density-dependent (mass action) or the frequency-dependent (standard incidence). Although there is no rule of choice, standard incidence has thrive in modelling vector and sexually transmitted diseases [79]. Thus, the choice of the transmission functions given by (2.2.3) and (2.2.4). Furthermore, it is a known fact that, for the total number of bites to be conserved, the total number of mosquitoes bites must be equal to the total number of bites received by humans [19, 22, 62, 108]. Thus,

$$\beta_{VH}(N_H, N_V) N_H = \beta_{HV} N_V,$$

therefore

$$N_V = \frac{\beta_{VH}(N_H, N_V)}{\beta_{HV}} N_H, \tag{2.2.5}$$

Substituting (2.2.5) into (2.2.2) we have

$$\lambda_H = \lambda_{MH} + \lambda_{HH} = \frac{\beta_{HV} I_V + \beta_{HH}\Big(I_H + \eta_H R_H\Big)}{N_H}. \tag{2.2.6}$$

2.2.2 Model equations

The above formulation gives the model for the transmission dynamics of Zika virus with human-human transmission and vertical transmission in mosquito population, which

is represented by the following system of equations

$$\begin{aligned}
\frac{dS_H}{dt} &= b_H - \lambda_H \frac{S_H}{N_H} - \mu_H S_H,\\
\frac{dI_H}{dt} &= \lambda_H \frac{S_H}{N_H} - \delta_H I_H - \gamma_H I_H - \mu_H I_H,\\
\frac{dR_H}{dt} &= \gamma_H I_H - \mu_H R_H,\\
\frac{dA_N}{dt} &= \phi_V \Big(1 - \frac{A_N + A_I}{\mathcal{K}}\Big)\big[S_V + \eta_V I_V\big] - b_V A_N - \mu_A A_N,\\
\frac{dA_I}{dt} &= \phi_V \Big(1 - \frac{A_N + A_I}{\mathcal{K}}\Big)[1 - \eta_V] I_V - b_V A_I - \mu_A A_I,\\
\frac{dS_V}{dt} &= b_V A_N - \beta_{HV} \frac{I_H}{N_H} S_V - \mu_V S_V,\\
\frac{dI_V}{dt} &= \beta_{HV} \frac{I_H}{N_H} S_V + b_V A_I - \mu_V I_V.
\end{aligned} \tag{2.2.7}$$

With the assumption that all the model parameters are positive and initial conditions are non-negative. In addition, since $A_N + A_I = A$ we have

$$\frac{dA}{dt} = \phi_V \Big(1 - \frac{A}{\mathcal{K}}\Big)[S_V + I_V] - b_V A - \mu_A A. \tag{2.2.8}$$

Lemma 2.2.1. The following biologically feasible region

$$\begin{aligned}
\Omega = \Bigg\{ & S_H, I_H, R_H, A_N, A_I, S_V, I_V \in \mathbb{R}^7_+ : S_H + I_H + R_H \le \frac{b_H}{\mu_H},\\
& A_N + A_I \le \mathcal{K}, \quad S_V + I_V \le \frac{\mathcal{K} b_V}{\mu_V} \Bigg\}
\end{aligned} \tag{2.2.9}$$

is positively-invariant with respect to the model (2.2.7).

Proof. Since the system (2.2.7) is C^1 in $\mathbb{R}^7_+$, local existence and uniqueness of solution obviously follow. Observe from (2.2.8) that $A_N + A_I \le \mathcal{K}$. Also, let $N_V = S_V + I_V$, then by Gronwall's lemma we have

$$\begin{aligned}
& N_H(t) \le N_H(0) e^{-\mu_H t} + \frac{b_H}{\mu_H}\Big(1 - e^{-\mu_H t}\Big)\\
& \text{and}\\
& N_V(t) \le N_V(0) e^{-\mu_V t} + \frac{\mathcal{K} b_H}{\mu_V}\Big(1 - e^{-\mu_V t}\Big),
\end{aligned} \tag{2.2.10}$$

which are bounded and hence solution exists for all $t \ge 0$. In addition, $N_H(t) \le \frac{b_H}{\mu_H}$ if $N_H(0) \le \frac{b_H}{\mu_H}$, and $N_V(t) \le \frac{\mathcal{K} b_V}{\mu_V}$ if $N_V(0) \le \frac{\mathcal{K} b_V}{\mu_V}$. Consequently, solution of the

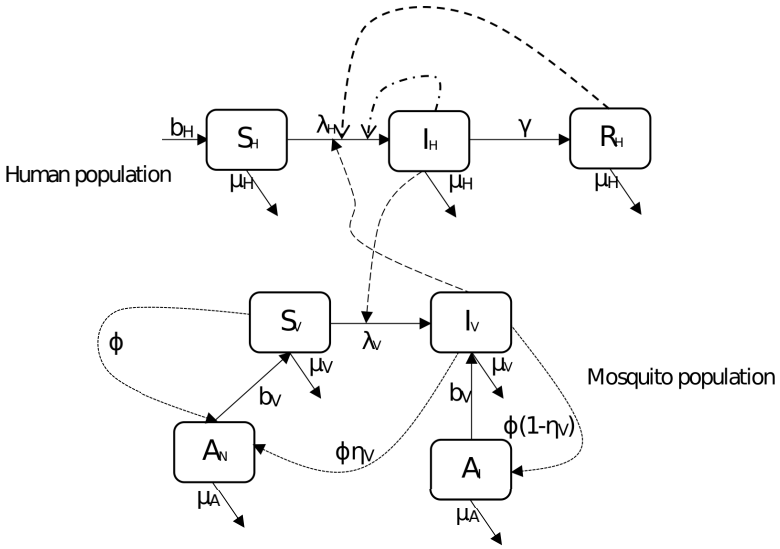

Figure 2.1: Model diagram showing the interaction between mosquitoes and humans.

model with initial condition in Ω remains in Ω for all $t \geq 0$. □

2.2.3 Analysis of mosquito only population

In this section, we analyse the model (2.2.7) in the absence of humans. Consider the mosquito component of the model (2.2.7) given by

$$\begin{aligned} \frac{dA_N}{dt} &= \phi_V\Big(1 - \frac{A_N}{\mathcal{K}}\Big)S_V - b_V A_N - \mu_A A_N, \\ \frac{dS_V}{dt} &= b_V A_N - \mu_V S_V. \end{aligned} \tag{2.2.11}$$

In the absence of interaction with humans, the average number of offspring produced by a single female mosquito through out her entire lifespan, in the presence of abundant resources, space and absence of disease is given by

$$N_0 = \frac{\phi_V b_V}{(b_V + \mu_A)\mu_V}. \tag{2.2.12}$$

It is interpreted as follows. The probability that an aquatic mosquito mature to be an adult female mosquito is $\frac{b_V}{b_V+\mu_A}$, where $\frac{1}{b_V+\mu_A}$ is the average time spent at aquatic stage, and b_V is the rate at which aquatic mosquitoes mature to become female mosquitoes. The life expectancy of adult female mosquito is $\frac{1}{\mu_V}$, while ϕ_V is their oviposition rate, thus the average number of eggs laid by a female mosquito is $\frac{\phi_V}{\mu_V}$. Therefore (2.2.12) is the average number of offspring produced by a susceptible mosquito in her entire life (basic offspring number).

The mosquito component of the model given by (2.2.11) has an extinction disease

Table 2.1: Description of variables and parameters used for the model given by (2.2.7).

Variable	**Interpretation**
S_H	Population of susceptible humans
I_H	Population of infectious humans
R_H	Population of recovered humans
N_H	Total population of humans
A_N	Population of non-infected aquatic mosquitoes
A_I	Population of infected aquatic mosquitoes
S_V	Population of susceptible mosquitoes
I_V	Population of infectious mosquitoes
A	Total population of aquatic mosquitoes
N_V	Total population of adult female mosquitoes

Parameter	**Interpretation**
ϕ_V	Oviposition rate of mosquitoes
γ_H	Recovery rate for humans
b_H	Recruitment rate of humans
b_V	Maturation rate of mosquitoes
μ_H	Natural death rate of humans
μ_V	Natural death rate of adult mosquitoes
μ_A	Natural death rate of aquatic mosquitoes
η_V	Rate (proportion) of non-vertical transmission
$\mathcal{K}$	Mosquito carrying capacity
m	Ratio of mosquitoes to humans (number of mosquitoes per human)
η_H	Modification parameter for the transmission by recovered humans
δ_H	Disease induced death rate of humans
b_{VH}	Biting rate of infected mosquitoes
b_{HV}	Biting rate of susceptible mosquitoes
ρ_{VH}	Probability of transmission from infectious mosquito to humans
ρ_{HV}	Probability of transmission from infectious humans to mosquito
b_{HH}	Sexual contact rate between infectious and susceptible humans
ρ_{HH}	Probability of sexual transmission from infectious to susceptible humans
β_{VH}	Transmissions rate from infectious mosquitoes to susceptible humans
β_{HV}	Transmissions rate from infectious humans to susceptible mosquitoes
β_{HH}	Transmissions rate from sexually infectious humans to susceptible humans

free equilibrium $\mathcal{E}_0$, and non-extinction disease free equilibrium $\mathcal{E}_1$ given by

$$\mathcal{E}_0 = \Big(A_N^*, A_I^*, S_V^*, I_V^*\Big) = \Big(0, 0, 0, 0\Big), \tag{2.2.13}$$

and

$$\mathcal{E}_1 = \Big(A_N^*, A_I^*, S_V^*, I_V^*\Big) = \Big(\mathcal{K}[1 - \frac{1}{N_0}], 0, \frac{b_V \mathcal{K}}{\mu_V}[1 - \frac{1}{N_0}], 0\Big). \tag{2.2.14}$$

To establish the stability of $\mathcal{E}_0$ and $\mathcal{E}_1$, we use the following Theorem.

Consider an autonomous dynamical system given by $\dot{x} = f(x)$, where $D \subseteq \mathbb{R}_+^n$ and $f : D \longrightarrow \mathbb{R}_+^n$ is continuous. Then

Theorem 2.2.2. [8] Let $a, b \in D$ be such that $a < b$, $[a, b] \subseteq D$ and $f(b) \leq 0 \leq f(a)$. Then the system defines a (positive) dynamical system on $[a, b]$. Moreover, if $[a, b]$ contains a unique equilibrium q, then q is globally asymptotically stable on $[a, b]$.

Rewriting (2.2.11) in the form $\dot{x} = f(x)$, where $f : D \longrightarrow \mathbb{R}_+^2$ and $D \subseteq \mathbb{R}_+^2$. Then we have the following result

Theorem 2.2.3. The extinction equilibrium $\mathcal{E}_0$ is globally asymptotically stable (GAS) when $N_0 \leq 1$ and unstable otherwise. The equilibrium $\mathcal{E}_1$ exists and LAS when $N_0 > 1$.

Proof. Consider $[a, b] = [0, b] \subseteq \mathbb{R}_+^2$, where $b = (p, \frac{(b_V + \mu_A)p}{\phi_V})$ and $p > 0$. It is easy to see that $f(0) = 0$, and

$$f(b) = \begin{pmatrix} -\big[b_V + \mu_A\big]\frac{p^2}{\mathcal{K}} \\ \\ b_V p[1 - \frac{1}{N_0}] \end{pmatrix} \text{ therefore } f(b) < 0 \text{ provided } N_0 \leq 1. \tag{2.2.15}$$

Thus, $f(b) \leq 0 \leq f(0)$ provided $N_0 \leq 1$. By Theorem (2.2.2), the system given by (2.2.11) defines a positive dynamical system on $[0, b]$ and $\mathcal{E}_0$ is GAS on $[0, b]$. Moreover, since p is arbitrary, b can be extended to be bigger than any $x \in \mathbb{R}_+^2$. Hence the result holds on $\mathbb{R}_+^2$. The second part of the proof follows by linearization. □

The epidemiological implication of Theorem (2.2.3) is that, if the basic offspring number can be brought to a value below unity, mosquito population would go to extinction and horizontal transmission between humans and mosquitoes can be avoided.

2.2.4 Mosquito extinction DFE

Let $\mathcal{E}_2$ be the DFE of (2.2.7) when the basic offspring number of the mosquito population (N_0) is less than or equal to one, that is

$$\mathcal{E}_2 = \Big(S_H^*, E_H^*, I_H^*, R_H^*, A_N^*, A_I^*, S_V^*, E_V^*, I_V^*\Big) = \Big(\frac{b_H}{\mu_H}, 0, 0, 0, 0, 0, 0, 0\Big). \tag{2.2.16}$$

Local stability of $\mathcal{E}_2$ can be established using the next generation method [139]. We employ the approach described by [22, 44, 139] to compute the next generation matrix (K).

The matrix F for the new infection terms and V for the transmission terms are given, respectively by,

$$F = \begin{pmatrix} \beta_{HH} & \beta_{HH}\eta_H & 0 & \beta_{HV} \\ 0 & 0 & 0 & 0 \\ 0 & 0 & 0 & \frac{\phi_V(1-\eta_V)}{N_0} \\ 0 & 0 & 0 & 0 \end{pmatrix}, \qquad V = \begin{pmatrix} K_1 & 0 & 0 & 0 \\ -\gamma_H & \mu_H & 0 & 0 \\ 0 & 0 & K_2 & 0 \\ 0 & 0 & -b_V & \mu_V \end{pmatrix}, \tag{2.2.17}$$

where $K_1 = \gamma_H + \mu_H + \delta_H$, $K_2 = \mu_A + b_V$. The next generation matrix with large domain (K_L) is

$$K_L = FV^{-1} = \begin{pmatrix} \beta_{HH} & \beta_{HH}\eta_H & 0 & \beta_{HV} \\ 0 & 0 & 0 & 0 \\ 0 & 0 & 0 & \frac{\phi_V(1-\eta_V)}{N_0} \\ 0 & 0 & 0 & 0 \end{pmatrix} \times \begin{pmatrix} \frac{1}{K_1} & 0 & 0 & 0 \\ \frac{\gamma_H}{K_1\mu_H} & \frac{1}{\mu_H} & 0 & 0 \\ 0 & 0 & \frac{1}{K_2} & 0 \\ 0 & 0 & \frac{b_V}{K_2\mu_V} & \frac{1}{\mu_V} \end{pmatrix}$$

$$= \begin{pmatrix} \frac{\beta_{HH}(\mu_H+\eta_H\gamma_H)}{K_1\mu_H} & \frac{\beta_{HH}\eta_H}{\mu_H} & \frac{\beta_{HV}b_V}{K_2\mu_V} & \frac{\beta_{HV}}{\mu_V} \\ 0 & 0 & 0 & 0 \\ 0 & 0 & \frac{\phi_V(1-\eta_V)b_V}{N_0K_2\mu_V} & \frac{\phi_V(1-\eta_V)}{N_0\mu_V} \\ 0 & 0 & 0 & 0 \end{pmatrix}. \tag{2.2.18}$$

Thus, using the approach of [44] with an auxiliary matrix E, the NGM (K) is

$$K = E^T K_L E = E^T F V^{-1} E = \begin{pmatrix} \frac{\beta_{HH}(\mu_H+\eta_H\gamma_H)}{K_1\mu_H} & \frac{\beta_{HV}b_V}{K_2\mu_V} \\ 0 & \frac{\phi_V(1-\eta_V)b_V}{N_0K_2\mu_V} \end{pmatrix}, \quad \text{where } E = \begin{pmatrix} 1 & 0 \\ 0 & 0 \\ 0 & 1 \\ 0 & 0 \end{pmatrix}, \tag{2.2.19}$$

Therefore the mosquito extinction basic reproduction number denoted by $\mathcal{R}_1$ is given by

$$\mathcal{R}_1 = \max\left\{\mathcal{R}_{HH}, \mathcal{R}_{VV}\right\}$$

where $\mathcal{R}_{HH} = \frac{\beta_{HH}(\mu_H+\eta_H\gamma_H)}{K_1\mu_H}$ and $\mathcal{R}_{VV} = \frac{\phi_V(1-\eta_V)b_V}{N_0K_2\mu_V} = 1 - \eta_V$. The NGM with large domain, (K_L), is always the matrix with highest dimension, therefore the NGM (K) eliminates irrelevant information and has detailed biological meaning (which we employed in the interpretation of $\mathcal{R}_0$ that comes later) [44].

Theorem 2.2.4. If $N_0 \leq 1$. The mosquito extinction disease free equilibrium $\mathcal{E}_2$ is globally asymptotically stable when the basic reproduction number $\mathcal{R}_1 \leq 1$ and unstable otherwise.

Proof. By Theorem (2.2.3), the extinction equilibrium of the mosquito component of (2.2.7) $(I_V = 0)$ is GAS when $N_0 \leq 1$, thus the model reduces to an SIR model with

infection by both I and R compartments. The function

$$V = \mathcal{R}_1 I_H + \mathcal{R}_1 \frac{\beta_{HH}\eta_H}{\mu_H} R_H, \tag{2.2.20}$$

is a suitable Lyapunov function where,

$$\begin{aligned}
\dot{V} &= \mathcal{R}_1\Big(\beta_{HH}\frac{I_H}{N_H}S_H + \beta_{HH}\eta_H\frac{R_H}{N_H}S_H - K_1 I_H\Big) + \mathcal{R}_1\frac{\beta_{HH}\eta_H}{\mu_H}\Big(\gamma_H I_H - \mu_H R_H\Big),\\
&= \mathcal{R}_1 I_H\Big(\beta_{HH}\frac{S_H}{N_H} + \beta_{HH}\frac{\eta_H\gamma_H}{\mu_H} - K_1\Big) + \mathcal{R}_1 R_H\Big(\beta_{HH}\eta_H\frac{S_H}{N_H} - \beta_{HH}\frac{\eta_H}{\mu_H}\mu_H\Big),\\
&\leq \mathcal{R}_1 K_1 I_H\Big(\beta_{HH}\frac{[\mu_H + \eta_H\gamma_H]}{K_1\mu_H} - 1\Big) + \mathcal{R}_1\beta_{HH}R_H\Big(\eta_H - \eta_H\Big) \text{ since } \frac{S_H}{N_H} \leq 1,\\
&= \mathcal{R}_1 K_1 I_H\Big(\mathcal{R}_1 - 1\Big).
\end{aligned} \tag{2.2.21}$$

Thus, $\dot{V} \leq 0$ if $\mathcal{R}_1 \leq 1$ with $\dot{V} = 0$ if and only if $I_H = R_H = 0$. Furthermore, the largest compact invariant set in $\{(S_H, I_H, R_H, A_N, A_I, S_V, I_V) \in \Omega : \dot{V} = 0\}$ is the set $\mathcal{E}_2$. Using LaSalle's invariance principle, every solution with initial conditions in Ω converge to the DFE $(\mathcal{E}_2)$ provided that $N_0 \leq 1$ and $\mathcal{R}_1 \leq 1$. □

It is worth mentioning that, this situation is biologically less plausible due to the absence of mosquitoes in the population. We now consider the case when $N_0 > 1$.

2.2.5 Mosquito persistent DFE

Let $\mathcal{E}_3$ be the DFE of (2.2.7) when the basic offspring number of the mosquito population is greater than one $(N_0 > 1)$, then

$$\mathcal{E}_3 = \Big(S_H^*, I_H^*, R_H^*, A_N^*, A_I^*, S_V^*, I_V^*\Big) = \Big(\frac{b_H}{\mu_H}, 0, 0, \mathcal{K}[1 - \frac{1}{N_0}], 0, \frac{b_V}{\mu_V}\mathcal{K}[1 - \frac{1}{N_0}], 0\Big) \tag{2.2.22}$$

Using similar approach to that of Section 2.4.4, the next generation matrix K is given by

$$K = \begin{pmatrix} \frac{\beta_{HH}(\mu_H + \eta_H\gamma_H)S_H^*}{N_H^* K_1 \mu_H} & \frac{\beta_{HV}S_H^*}{N_H^*\mu_V} \\ \frac{\beta_{HV}S_V^*}{N_H^* K_1} & \frac{\phi_V(1-\eta_V)b_V}{N_0 K_2 \mu_V} \end{pmatrix} = \begin{pmatrix} \mathcal{R}_{HH} & \mathcal{R}_{VH} \\ \mathcal{R}_{HV} & \mathcal{R}_{VV} \end{pmatrix}. \tag{2.2.23}$$

Thus, the basic reproduction number (which is the spectral radius of K) is given by

$$\mathcal{R}_0 = \frac{1}{2}\left(\mathcal{R}_{VV} + \mathcal{R}_{HH} + \sqrt{\Big(\mathcal{R}_{HH} - \mathcal{R}_{VV}\Big)^2 + 4\mathcal{R}_{HV}\mathcal{R}_{VH}}\right), \tag{2.2.24}$$

where $\mathcal{R}_{HV} = \frac{\beta_{HV}S_V^*}{N_H^* K_1}$ and $\mathcal{R}_{VH} = \frac{\beta_{HV}S_H^*}{N_H^*\mu_V}$, with $\mathcal{R}_{HH}$ and $\mathcal{R}_{VV}$ as presented in Section 2.4.4.

Lemma 2.2.5. The disease free equilibrium $\mathcal{E}_3$ of the model represented by (2.2.7) is locally asymptotically stable if $\mathcal{R}_0 < 1$, and unstable if $\mathcal{R}_0 > 1$ [139].

The threshold quantity $\mathcal{R}_0$ is the basic reproduction number. It is the average number of secondary cases generated by a single infectious individual that is introduced into a completely susceptible population throughout its period of infectivity. It is interpreted as follows. A sexually infectious (infected or recovered) human can transmit the disease sexually to a susceptible human. The number of new human-human sexual infection generated by an infected human (I_H) (near DFE) is the product of its infection rate ($\frac{\beta_{HH}}{N_H^*}$) and the average time spent in the infected class ($\frac{1}{K_1}$). In a similar way, the number of new sexual transmissions by a recovered human (near DFE) is the product of its infection rate ($\frac{\beta_{HH}\eta_H}{N_H^*}$), the average lifespan of a recovered human ($\frac{1}{\mu_H}$) and the probability that an individual survives compartment I_H and moves to R_H compartment ($\frac{\gamma_H}{K_1}$). So that the average human to human infection (noting that $S_H^* = N_H^*$) is given by

$$\mathcal{R}_{HH} = \frac{\beta_{HH}}{N_H^* K_1} S_H^* + \frac{\beta_{HH}\eta_H\gamma_H}{N_H^* K_1 \mu_H} S_H^* = \frac{\beta_{HH}(\mu_H + \eta_H\gamma_H)}{K_1\mu_H}. \tag{2.2.25}$$

Susceptible humans acquire infection from infected mosquitoes following effective contact capable of disease transmission. The number of human infections generated by an infected mosquito (near DFE) is given by the product of its rate of infection ($\frac{\beta_{HV}}{N_H^*}$) and the average duration in infected class ($\frac{1}{\mu_V}$). Thus, (noting that $S_H^* = N_H^*$)

$$\mathcal{R}_{HV} = \frac{\beta_{HV}}{N_H^*\mu_V} S_H^* = \frac{\beta_{HV}}{\mu_V}. \tag{2.2.26}$$

Similarly, susceptible mosquitoes acquire infection following effective contact with an infected human (I_H). The number of infections in the class S_V generated by one infected human (near the DFE) is the product of the infection rate of infected humans ($\frac{\beta_{HV}}{N_H^*}$) and the average time spent in the infected class ($\frac{1}{K_1}$). Therefore

$$\mathcal{R}_{VH} = \frac{\beta_{HV}}{N_H^* K_1} S_V^* \tag{2.2.27}$$

Unlike transstadial transmission which may occur at a different stage, transovarial transmission is direct, hence, the number of vectorial vertical transmissions is the percentage of infection passed by an infected mosquito per oviposition ($\mathcal{R}_{VV} = 1 - \eta_V$). The basic reproduction number is therefore given by (2.2.24).

For a homogeneous population, the basic reproduction number defines the threshold for control or elimination of a disease. This is not always the case for a heterogeneous population. In fact $\mathcal{R}_0$ could be of less importance when effort is to be targeted at a particular host, or if the cycle of infection includes other types such as vectors [123]. Therefore it is imperative to compute another threshold quantity named the type reproduction number.

2.2.6 Type reproduction number

The type-reproduction number T is a threshold quantity that correctly determines the critical control effort for a heterogeneous population [72]. A method to estimate the required effort(s) needed to control an infectious disease by targeting a specific

sub-population of hosts, considering the fact that infection will pass through other sub-populations before causing secondary infections is described by [72, 123]. Let K be the next generation matrix with large domain and the host types 1, 2 and 3 denote the populations of I_H, A_I and I_V. The type i reproduction number is given by

$$T_I = e^T K(I-(I-P)K)^{-1}e, \tag{2.2.28}$$

where I is an identity matrix, P is a projection matrix and e is a unit vector with all elements equal to zero except the ith. Let

$$K = \begin{pmatrix} K_{11} & K_{12} & K_{13} & K_{14} \\ 0 & 0 & 0 & 0 \\ 0 & 0 & K_{33} & K_{34} \\ K_{41} & 0 & 0 & 0 \end{pmatrix},$$

where,

$$K_{11} = \frac{\beta_{HH}(\mu_H+\eta_H\gamma_H)}{K_1\mu_H}, \quad K_{12} = \frac{\beta_{HH}\eta_H}{\mu_H}, \quad K_{13} = \frac{\beta_{HV}b_V}{K_2\mu_V},$$
$$K_{14} = \frac{\beta_{HV}}{\mu_V}, \quad K_{33} = \frac{\phi_V(1-\eta_V)b_V}{N_0K_2\mu_V}, \quad K_{34} = \frac{\phi_V(1-\eta_V)}{N_0\mu_V}, \quad K_{41} = \frac{\beta_{HV}S_V^*}{N_H^*K_1},$$

so that from (2.2.28) the type-reproduction number for infectious human is given by

$$T_1 = K_{11} + \frac{K_{13}K_{34}K_{41}}{1-K_{33}} + K_{41}K_{14} = \mathcal{R}_{HH} + \frac{\mathcal{R}_{HV}\mathcal{R}_{VH}}{1-\mathcal{R}_{VV}}. \tag{2.2.29}$$

This is the expected number of cases in humans caused by one infected human in a completely susceptible population, the infection might be directly or through chains of infections passing through individuals of other types, it singles out the required control effort when targeting the human population [72]. If $\mathcal{R}_0 > 1$, after some simplifications it can be shown that

$$\mathcal{R}_{HV}\mathcal{R}_{VH} > \big(1-\mathcal{R}_{VV}\big)\big(1-\mathcal{R}_{HH}\big) = \eta_V\big(1-\mathcal{R}_{HH}\big). \tag{2.2.30}$$

On the other hand $R_0 < 1$ implies

$$\mathcal{R}_{HV}\mathcal{R}_{VH} < \big(1-\mathcal{R}_{VV}\big)\big(1-\mathcal{R}_{HH}\big) = \eta_V\big(1-\mathcal{R}_{HH}\big). \tag{2.2.31}$$

Now $T_1 < 1$ if

$$\mathcal{R}_{HH} + \frac{\mathcal{R}_{HV}\mathcal{R}_{VH}}{1-\mathcal{R}_{VV}} < 1 \implies \mathcal{R}_{HV}\mathcal{R}_{VH} < \big(1-\mathcal{R}_{VV}\big)\big(1-\mathcal{R}_{HH}\big).$$

Thus, $T_1 < 1 \iff \mathcal{R}_0 < 1$. Similarly, the type-reproduction number for infected aquatic mosquito A_I is given by

$$T_2 = \frac{K_{11}+K_{14}K_{41}}{1+K_{14}K_{41}-K_{11}} = \frac{\mathcal{R}_{HH}+\mathcal{R}_{HV}\mathcal{R}_{VH}}{1+\mathcal{R}_{HV}\mathcal{R}_{VH}-\mathcal{R}_{HH}}. \tag{2.2.32}$$

It is the expected number of cases within aquatic mosquitoes generated by one infected aquatic mosquito in a completely susceptible population of mosquitoes. Observe that infection does not occur directly at this stage, it has to pass through chains of infections between mosquitoes and humans. It is straightforward to see that $T_2 < 1 \Longrightarrow \mathcal{R}_{HH} < \frac{1}{2}$.

The expected number of cases by one infected mosquito in a population of completely susceptible mosquitoes denoted by T_3 is given by

$$T_3 = \frac{K_{11}}{1 - K_{11}} = \frac{\mathcal{R}_{HH}}{1 - \mathcal{R}_{HH}}. \tag{2.2.33}$$

Likewise for infection to occur at this stage, it has to pass through chains of infections between humans to mosquitoes. Also $T_3 < 1 \Longrightarrow \mathcal{R}_{HH} < \frac{1}{2}$. Notice that the next generation matrix here cannot be used to compute the type reproduction number of recovered humans, this is because no new infection occurs by R_H population.

2.2.7 Endemic equilibrium (EE) and backward bifurcation (BB)

In this section we compute the endemic equilibrium of the model (2.2.7), and analyse the direction of bifurcation at $\mathcal{R}_0 = 1$.

2.2.7.1 Endemic equilibrium

Though the endemic equilibrium of the system given by (2.2.7) is not straight forward, by letting $A_I + A_N = A$ with the fact that $A \leq \mathcal{K}$, it can be shown that the model has a unique EE provided $N_0 > 1$ given by

$$\begin{aligned}
S_H^{**} &= \frac{b_H}{\lambda_H^{**} + \mu_H}, \quad I_H^{**} = \frac{\lambda_H^{**} b_H}{K_1\Big(\lambda_H^{**} + \mu_H\Big)}, \quad R_H^{**} = \frac{\lambda_H^{**} b_H \gamma_H}{K_1\Big(\lambda_H^{**} + \mu_H\Big)\mu_H}, \\
A^{**} &= \frac{\mathcal{K} K_2 \mu_V \Big(N_0 - 1\Big)}{b_V}, \quad A_N^{**} = \frac{\phi_V\Big(1 - \frac{A^{**}}{\mathcal{K}}\Big)\big[S_V^{**} + \eta_V I_V^{**}\big]}{K_2}, \\
A_I^{**} &= \frac{\phi_V\Big(1 - \frac{A^{**}}{\mathcal{K}}\Big)[1 - \eta_V] I_V^{**}}{K_2}, \quad S_V^{**} = \frac{b_V \phi_V\Big(1 - \frac{A^{**}}{\mathcal{K}}\Big)\big[S_V^{**} + \eta_V I_V^{**}\big]}{\Big(\lambda_V^{**} + \mu_V\Big)K_2}, \\
I_V^{**} &= \frac{\lambda_V^{**} K_2 b_V A^{**} + b_V \mu_V \phi_V\Big(1 - \frac{A^{**}}{\mathcal{K}}\Big)[1 - \eta_V] I_V^{**}}{\Big(\lambda_V^{**} + \mu_V\Big)K_2 \mu_V},
\end{aligned} \tag{2.2.34}$$

where

$$\lambda_H^{**} = \frac{\beta_{HV} I_V^{**} + \beta_{HH} I_H^{**} + \beta_{HH}\eta_H R_H^{**}}{N_H^{**}},$$

and

$$\lambda_V^{**} = \beta_{HV}\frac{I_H^{**}}{N_H^{**}}, \quad N_H^{**} = S_H^{**} + I_H^{**} + R_H^{**}.$$

Some previous studies on vector borne disease models that undergo backward bifurcation (a phenomenon where stable DFE coexists with a stable EE when $\mathcal{R}_0 < 1$) include [18], [24], [27], [35] and [62].

2.2.7.2 Backward bifurcation (BB)

Here, we apply the method described by [26, 139], which is based on center manifold theory to prove the existence of backward bifurcation or otherwise at $\mathcal{R}_0 = 1$ for the model (2.2.7). Let,

$$\big(S_H, I_H, R_H, A_N, A_I, S_V, I_V\big) = \big(x_1, x_2, x_3, x_4, x_5, x_6, x_7\big),$$

so that the total human population, and total mosquito population at aquatic and non-aquatic stages are respectively given by

$$N_H = x_1 + x_2 + x_3, \quad A = x_4 + x_5, \quad \text{and} \quad N_V = x_6 + x_7.$$

The transformed model (2.2.7) is represented by

$$\begin{aligned}
\frac{dx_1}{dt} &= b_H - \Big(\frac{\beta_{HV}x_7 + \beta_{HH}x_2 + \beta_{HH}\eta_H x_3}{x_1 + x_2 + x_3}\Big)x_1 - \mu_H x_1,\\
\frac{dx_2}{dt} &= \Big(\frac{\beta_{HV}x_7 + \beta_{HH}x_2 + \beta_{HH}\eta_H x_3}{x_1 + x_2 + x_3}\Big)x_1 - \delta_H x_2 - \gamma_H x_2 - \mu_H x_2,\\
\frac{dx_3}{dt} &= \gamma_H x_2 - \mu_H x_3,\\
\frac{dx_4}{dt} &= \phi_V\Big(1 - \frac{x_4 + x_5}{\mathcal{K}}\Big)\big[x_6 + \eta_V x_7\big] - b_V x_4 - \mu_A x_4,\\
\frac{dx_5}{dt} &= \phi_V\Big(1 - \frac{x_4 + x_5}{\mathcal{K}}\Big)[1 - \eta_V]x_7 - b_V x_5 - \mu_A x_5,\\
\frac{dx_6}{dt} &= b_V x_4 - \frac{\beta_{HV}x_2}{x_1 + x_2 + x_3}x_6 - \mu_V x_6,\\
\frac{dx_7}{dt} &= \frac{\beta_{HV}x_2}{x_1 + x_2 + x_3}x_6 + b_V x_5 - \mu_V x_7.
\end{aligned} \tag{2.2.35}$$

The associated forces of infection are given by

$$\lambda_H = \frac{\beta_{HV}x_7 + \beta_{HH}x_2 + \beta_{HH}\eta_H x_3}{x_1 + x_2 + x_3}x_1, \quad \lambda_V = \frac{\beta_{HV}x_2}{x_1 + x_2 + x_3}x_6.$$

Let $\mathcal{R}_0 = 1$, so that $\mathcal{R}_{HV}\mathcal{R}_{VH} = (1-\mathcal{R}_{VV})(1-\mathcal{R}_{HH})$. Suppose $\beta_{HV} = \beta^*_{HV}$ is chosen to be the bifurcation parameter. The Jacobian matrix (J^*) at the DFE with $\beta_{HV} = \beta^*_{HV}$ is given by

$$J^* = \begin{pmatrix} -\mu_H & -\beta_{HH} & -\beta_{HH}\eta_H & 0 & 0 & 0 & -\beta^*_{HV} \\ 0 & \beta_{HH} - K_1 & \beta_{HH}\eta_H & 0 & 0 & 0 & \beta^*_{HV} \\ 0 & \gamma_H & -\mu_H & 0 & 0 & 0 & 0 \\ 0 & 0 & 0 & -\frac{\phi_V b_V}{\mu_V} & -K_2(N_0-1) & \frac{K_2\mu_V}{b_V} & \frac{K_2\mu_V\eta_V}{b_V} \\ 0 & 0 & 0 & 0 & -K_2 & 0 & \frac{K_2\mu_V(1-\eta_V)}{b_V} \\ 0 & -\frac{\beta^*_{HV}S^*_V}{S^*_H} & 0 & b_V & 0 & -\mu_V & 0 \\ 0 & \frac{\beta^*_{HV}S^*_V}{S^*_H} & 0 & 0 & b_V & 0 & -\mu_V \end{pmatrix}.$$

The Jacobian has left (v_I) and right (w_I) eigenvectors associated with the zero eigenvalue respectively given by

$$\begin{aligned} &v_1 = 0, \quad v_2 = \frac{1}{S^*_H K_2\mu_V^2\eta_V^2\Big(\beta_{HH}\gamma_H\eta_H + \mu_H^2\Big) + S^*_V\beta^2_{HV}\mu_H^2\Big([1-\eta_V] + K_2\eta_V\Big)}, \\ &v_3 = \frac{\beta_{HH}\eta_H}{\mu_H}v_2 \quad v_4 = 0, \quad v_5 = \frac{\beta_{HV}b_V}{K_2\mu_V\eta_V}v_2, \quad v_6 = 0, \quad v_7 = \frac{\beta_{HV}}{\mu_V\eta_V}v_2, \end{aligned} \tag{2.2.36}$$

and

$$\begin{aligned} &w_1 = -\frac{K_1}{\mu_H}\Big(\mathcal{R}_{HH} + \mathcal{R}_{HV}\mathcal{R}_{VH}\frac{1}{\eta_V}\Big)w_2 \quad w_2 = S^*_H K_2\mu_H^2\mu_V^2\eta_V^2, \\ &w_3 = \frac{\gamma_H}{\mu_H}w_2, \quad w_4 = -\frac{\beta_{HV}S^*_V(1-\eta_V)}{S^*_H b_V\eta_V}w_2, \\ &w_5 = \frac{\beta_{HV}S^*_V(1-\eta_V)}{S^*_H b_V\eta_V}w_2, \quad w_6 = -\frac{\beta_{HV}S^*_V}{S^*_H\mu_V\eta_V}w_2, \quad w_7 = \frac{\beta_{HV}S^*_V}{S^*_H\mu_V\eta_V}w_2. \end{aligned} \tag{2.2.37}$$

Using the afore listed vectors in (2.2.36) and (2.2.37) we have

$$\begin{aligned} \mathbf{a} = \sum_{k,i,j=1}^{n} V_k W_I W_j \frac{\partial^2 f_k}{\partial x_I \partial x_j}(0,0) = \frac{-2w_2^2 v_2}{N^*_H\mathcal{K}}\Bigg[&\frac{2\beta_{HH}S^*_H\mathcal{K}(\gamma_H\eta_H+\mu_H)(\gamma_H+\mu_H)}{\mu_H^2} + \\ &8\beta^2_{HV}\frac{S^*_V\mathcal{K}}{\mu_V\eta_V} + \frac{\beta^2_{HV}S^*_V\mathcal{K}(\gamma_H+\mu_H)}{\mu_V\mu_H\eta_V} + \beta_{HV}S^*_V\mathcal{K}\Big(\frac{4\mu_H+5\gamma_H}{\mu_H} - 3\frac{K_1}{\mu_H}\{\mathcal{R}_{HH} + \\ &\frac{\mathcal{R}_{HV}\mathcal{R}_{VH}}{(1-\mathcal{R}_{VV})}\}\Big)\Bigg] \end{aligned} \tag{2.2.38}$$

while,

$$\mathbf{b} = \sum_{k,i=1}^{n} v_k w_I \frac{\partial^2 f_k}{\partial x_I \partial \phi_V}(0,0) = \frac{S_V^* w_2 v_2}{S_H^*}\Big(\frac{\beta_{HV}}{\mu_V \eta_V} + 8\Big) > 0. \tag{2.2.39}$$

Since **b** is positive, it follows from Theorem 4.1 in [26] that the Zika model (2.2.7) will undergo backward bifurcation if the bifurcation coefficient **a** given by (2.2.38) is positive. □

The public health impact of BB phenomenon of model (2.2.7) is that the epidemiological requirement of having the threshold quantity ($\mathcal{R}_0$) to be less than unity is although necessarily, but no longer sufficient for effective control of the disease. Hence the cause of such phenomenon is now explored.

2.2.8 Non-existence of backward bifurcation

Observe that

$$\frac{4\mu_H + 5\gamma_H}{\mu_H} - 3\frac{K_1}{\mu_H}\Big[\mathcal{R}_{HH} + \mathcal{R}_{HV}\mathcal{R}_{VH}\Big] \leq \frac{5(\mu_H + \gamma_H)}{\mu_H} - 3\frac{K_1}{\mu_H}\Big[\mathcal{R}_{HH} + \mathcal{R}_{HV}\mathcal{R}_{VH}\Big]. \tag{2.2.40}$$

So that if $\delta_H = 0$ and K_1 reduces to $\gamma_H + \mu_H$, then we have

$$\begin{aligned}\mathbf{a} \leq & \frac{-2K_1 w_2^2 v_2}{N_H^* \mathcal{K}}\Bigg[\frac{2\beta_{HH} S_H^* \mathcal{K}(\gamma_H \eta_H + \mu_H)}{\mu_H^2} + \frac{8\beta_{HV}^2 S_V^* \mathcal{K}}{K_1 \mu_V \eta_V} + \frac{\beta_{HV}^2 S_V^* \mathcal{K}}{\mu_V \mu_H \eta_V} + \frac{3\beta_{HV} S_V^* \mathcal{K}}{\mu_H} \\ & \Big(\frac{5}{3} - \{\mathcal{R}_{HH} + \frac{\mathcal{R}_{HV}\mathcal{R}_{VH}}{(1 - \mathcal{R}_{VV})}\}\Big)\Bigg].\end{aligned} \tag{2.2.41}$$

Corollary 1. The Zika model (2.2.7) does not undergo backward bifurcation at $\mathcal{R}_0 = 1$ if $\delta_H = 0$.

The result of the Corollary is consistent with that obtained numerically by Chitnis et. al [27] in their Malaria model which does not incorporate aquatic stages.

2.2.9 Global stability of the DFE $(\mathcal{E}_3)$

The global asymptotic stability of the DFE $(\mathcal{E}_2)$ obtained when $N_0 \leq 1$ is proved by Theorem (2.2.4). We use the method described in [77] to find the threshold condition under which the DFE $(\mathcal{E}_3)$ will be GAS with respect to a positively invariant region Ω.

The system is rewritten in a pseudo-triangular form as follows. From (2.2.7) and the property of the DFE, it is easy to see that the first equation of the system can be

rewritten in the form

$$\begin{aligned}\frac{dS_H}{dt} &= b_H - \beta_{HV}\frac{I_V}{N_H}S_H - \beta_{HH}\frac{I_H}{N_H}S_H - \beta_{HH}\eta_H\frac{R_H}{N_H}S_H - \mu_H S_H,\\ &= b_H - \beta_{HV}\frac{I_V}{N_H}S_H - \beta_{HH}\frac{I_H}{N_H}S_H - \beta_{HH}\eta_H\frac{R_H}{N_H}S_H - \mu_H S_H - b_H + \mu_H S_H^*,\\ &= -\mu_H(S_H - S_H^*) - \beta_{HV}\frac{I_V}{N_H}S_H - \beta_{HH}\frac{I_H}{N_H}S_H - \beta_{HH}\eta_H\frac{R_H}{N_H}S_H.\end{aligned} \tag{2.2.42}$$

The equation of the aquatic mosquitoes can also be rewritten in the form

$$\begin{aligned}\frac{dA_N}{dt} &= \phi_V\Big(1-\frac{A}{\mathcal{K}}\Big)\big[S_V + \eta_V I_V\big] - K_2 A_N,\\ &= \phi_V\Big(1-\frac{A}{\mathcal{K}}\Big)\big[S_V + \eta_V I_V\big] - K_2 A_N - \phi_V\Big(1-\frac{A_N^*}{\mathcal{K}}\Big)S_V^* + K_2 A_N^* + \phi_V\frac{S_V}{\mathcal{K}}A_N^*\\ &- \phi_V\frac{S_V}{\mathcal{K}}A_N^*,\\ &= -(A_N - A_N^*)\Big(K_2 + \phi_V\frac{S_V}{\mathcal{K}}\Big) + \phi_V(S_V - S_V^*)\Big(1-\frac{A_N^*}{\mathcal{K}}\Big) + \phi_V\eta_V I_V\Big(1-\frac{A}{\mathcal{K}}\Big)\\ &- \phi_V\frac{S_V}{\mathcal{K}}A_I.\end{aligned} \tag{2.2.43}$$

Similarly,

$$\begin{aligned}\frac{dA_I}{dt} &= \phi_V\Big(1-\frac{[A_I + A_N]}{\mathcal{K}}\Big)(1-\eta_V)I_V - b_V A_I - \mu_A A_I,\\ &= \phi_V(1-\eta_V)I_V - \phi_V(1-\eta_V)I_V\frac{A_I}{\mathcal{K}} - \phi_V(1-\eta_V)I_V\frac{A_N}{\mathcal{K}} - K_2 A_I,\\ &= -A_I\Big(K_2 + \phi_V(1-\eta_V)\frac{I_V}{\mathcal{K}}\Big) + \phi_V(1-\eta_V)I_V\Big(1-\frac{A_N}{\mathcal{K}}\Big).\end{aligned} \tag{2.2.44}$$

Furthermore, the fourth equation of the system (2.2.7) is rewritten as

$$\begin{aligned}\frac{dS_V}{dt} &= b_V A_N - \beta_{HV}\frac{I_H}{N_H}S_V - \mu_V S_V,\\ &= b_V A_N - \beta_{HV}\frac{I_H}{N_H}S_V - \mu_V S_V - b_V A_N^* + \mu_V S_V^*,\\ &= -\mu_V(S_V - S_V^*) + b_V(A_N - A_N^*) - \beta_{HV}\frac{I_H}{N_H}S_V.\end{aligned} \tag{2.2.45}$$

From the above simplification the system given by (2.2.7) can therefore be re-written

in a pseudo-triangular form as

$$\begin{cases} \dot{\mathbf{x}_1} &= A_{11}(\mathbf{x})(\mathbf{x}_1 - \bar{\mathbf{x}_1}) + A_{12}(\mathbf{x})\mathbf{x}_2 \\ \\ \dot{\mathbf{x}_2} &= A_{22}(\mathbf{x})\mathbf{x}_2, \end{cases} \tag{2.2.46}$$

where $\mathbf{x}_1 = (S_H, A_N, S_V)^T$ represents the naive (uninfected) component of the model (2.2.7), $\mathbf{x}_2 = (I_H, R_H, A_I, I_V)^T$ represents the infectious part of (2.2.7), $\bar{\mathbf{x}_1} = (S_H^*, A_N^*, S_V^*)^T$ is the DFE and

$$A_{11}(\mathbf{x}) = \begin{pmatrix} -\mu_H & 0 & 0 \\ 0 & -\big(K_2 + \phi_V \frac{S_V}{\mathcal{K}}\big) & \phi_V\big(1 - \frac{A_N^*}{\mathcal{K}}\big) \\ 0 & b_V & -\mu_V \end{pmatrix},$$

$$A_{12}(\mathbf{x}) = \begin{pmatrix} -\beta_{HH}\frac{S_H}{N_H} & -\beta_{HH}\eta_H\frac{S_H}{N_H} & 0 & -\beta_{HV}\frac{S_H}{N_H} \\ 0 & 0 & -\phi_V\frac{S_V}{\mathcal{K}} & \phi_V\eta_V\big(1 - \frac{A}{\mathcal{K}}\big) \\ -\beta_{HV}\frac{S_V}{N_H} & 0 & 0 & 0 \end{pmatrix}, \tag{2.2.47}$$

$$A_{22}(\mathbf{x}) = \begin{pmatrix} -m_{11} & \beta_{HH}\eta_H\frac{S_H}{N_H} & 0 & \beta_{HV}\frac{S_H}{N_H} \\ \gamma_H & -\mu_H & 0 & 0 \\ 0 & 0 & -m_{33} & m_{34} \\ \beta_{HV}\frac{S_V}{N_H} & 0 & b_V & -\mu_V \end{pmatrix},$$

where $m_{11} = K_1 + \beta_{HH}\frac{S_H}{N_H}$, $m_{33} = K_2 + \phi_V(1-\eta_V)\frac{I_V}{\mathcal{K}}$ and $m_{34} = \phi_V(1-\eta_V)\big(1 - \frac{A_N^*}{\mathcal{K}}\big)$.

Theorem 2.2.6. Consider (2.2.7). Let $\Omega \subset \mathbb{R}_+^{n_1+n_2}$ be a positively-invariant set. If

1. The system (2.2.7) is defined on the positively invariant set $\Omega \subset \mathbb{R}_+^{n_1+n_2}$.
2. The sub-system $\dot{x} = A_{11}(x)(x_1 - \bar{x_1})$ is globally asymptotically stable at the equilibrium $\bar{x_1}$.
3. For any $x \in \Omega$, the matrix $A_{22}(x)$ is Metzler and irreducible.
4. There exists an upper bound matrix $\bar{A_{22}}$ for the set $\mathcal{M} = \{A_{22}(x)/x \in \Omega\}$, with the property that either $\bar{A_{22}} \notin \mathcal{M}$ or if $\bar{A_{22}} \in \mathcal{M}$(i.e., $\bar{A_{22}} = \max_\Omega \mathcal{M}$), then for $\bar{x} \in \Omega$ such that $\bar{A_{22}} = A_{22}(\bar{x})$, then $\bar{x} \in \mathbb{R}^7 \times \{0\}$ (the DFE sub-manifold contains the points where the maximum is attained).
5. The stability modulus of $\bar{A_{22}}$ satisfies $\alpha(\bar{A_{22}}) \leq 0$.

Then, the associated DFE is GAS in Ω [77].

A similar technique was also employed by [45, 46, 136] for other mosquito borne diseases. The set Ω defined by (2.2.9) was shown to be positively invariant with

respect to the system (2.2.7). At $\mathcal{E}_3$, $A^* = \mathcal{K}(\frac{N_0-1}{N_0})$, thus the eigenvalues of the associated $A_{11}(x)$ matrix given by (2.2.47) are

$$-\mu_H \text{ and } -\frac{1}{2}\Big(K_2+\mu_V+\frac{\phi_V S_V}{\mathcal{K}}\Big) \pm \frac{1}{2}\sqrt{\Big(K_2+\mu_V+\frac{\phi_V S_V}{\mathcal{K}}\Big)^2 - 4\frac{S_V}{\mathcal{K}}\phi_V\mu_V},$$

using the fact that $\Big(K_2+\mu_V+\frac{\phi_V S_V}{\mathcal{K}}\Big)^2 - 4\frac{S_V}{\mathcal{K}}\phi_V\mu_V = \Big(K_2+\mu_V-\frac{\phi_V S_V}{\mathcal{K}}\Big)^2 > 0$, and $\Big(K_2+\mu_V+\frac{\phi_V S_V}{\mathcal{K}}\Big)^2 - 4\frac{S_V}{\mathcal{K}}\phi_V\mu_V = \Big(K_2+\mu_V-\frac{\phi_V S_V}{\mathcal{K}}\Big)^2 < \Big(K_2+\mu_V+\frac{\phi_V S_V}{\mathcal{K}}\Big)^2$, the eigenvalues of the Metzler matrix $A_{11}(\mathbf{x})$ are all real and negative. Therefore the subsystem $\dot{\mathbf{x}_1} = A_{11}(\mathbf{x})(\mathbf{x}_1 - \bar{\mathbf{x}_1})$ is globally asymptotically stable.

Definition 2.2.1. A square matrix $\mathbf{A}$ is said to be reducible if it has the form

$$\mathbf{A} = \begin{pmatrix} \mathbf{A}_1 & \mathbf{A}_2 \\ 0 & \mathbf{A}_3 \end{pmatrix} \tag{2.2.48}$$

where $\mathbf{A}_1$ and $\mathbf{A}_3$ are square matrices of order at least 1 or if $\mathbf{A}$ can be transformed into the form (2.2.48) by simultaneous permutations of rows and columns [55]. It is irreducible otherwise. Alternatively, a square matrix is irreducible if and only if its associated digraph is strongly connected.

Lemma 2.2.7. Let $\mathcal{M}$ be a Metzler matrix which is block decomposed as follows

$$\mathcal{M} = \begin{pmatrix} \mathbb{A} & \mathbb{B} \\ \mathbb{C} & \mathbb{D} \end{pmatrix} \tag{2.2.49}$$

where $\mathbb{A}$ and $\mathbb{D}$ are square matrices. Then $\mathcal{M}$ is Metzler stable if and only if $\mathbb{A}$ and $\mathbb{D} - \mathbb{C}\mathbb{A}^{-1}\mathbb{B}$ are Metzler stable.

Observe that $\mathcal{R}_{HH} < 1$ implies $\beta_{HH} < K_1$. Let $M_H^* = \frac{b_H}{\delta_H+\mu_H}$, then $N_H \geq M_H^*$ and $S_H \leq N_H$, so that $\frac{1}{M_H^*} \geq \frac{1}{N_H}$ and $\frac{S_H}{N_H} \leq 1$ in Ω with equality at the DFE. Furthermore $A_N \leq \mathcal{K}$ and $S_V \leq S_V^* \frac{N_0}{N_0-1}$ in Ω. Thus, the matrix $A_{22}(\mathbf{x})$ is Metzler irreducible (see Figure 2.2), hence conditions 1-3 of Theorem (2.2.6) are satisfied. The following matrix $\bar{A_{22}}(\mathbf{x})$ given by

$$\bar{A_{22}}(\mathbf{x}) = \begin{pmatrix} -(K_1-\beta_{HH}) & \beta_{HH}\eta_H & 0 & \beta_{HV} \\ \gamma_H & -\mu_H & 0 & 0 \\ 0 & 0 & -K_2 & \phi_V(1-\eta_V)\frac{1}{N_0} \\ \frac{\beta_{HV}S_V^* N_0}{(N_0-1)M_H^*} & 0 & b_V & -\mu_V \end{pmatrix} \tag{2.2.50}$$

is Metzler and an upper bound of $A_{22}(\mathbf{x}) \in \Omega$ provided $\mathcal{R}_{HH} < 1$. Thus, condition 4

of Theorem (2.2.6) is satisfied. In the case of the matrix $\bar{A_{22}}$ we have

$$\mathbb{A} = \begin{pmatrix} -\left[K_1 - \beta_{HH}\right] & \beta_{HH}\eta_H \\ \gamma_H & -\mu_H \end{pmatrix}, \quad \mathbb{B} = \begin{pmatrix} 0 & \beta_{HV} \\ 0 & 0 \end{pmatrix},$$

$$\mathbb{C} = \begin{pmatrix} 0 & 0 \\ \frac{\beta_{HV} S_V^* N_0}{(N_0-1)M_H^*} & 0 \end{pmatrix}, \quad \mathbb{D} = \begin{pmatrix} -K_2 & \phi_V(1-\eta_V)\frac{1}{N_0} \\ b_V & -\mu_V \end{pmatrix}. \tag{2.2.51}$$

Under the condition that $\mathcal{R}_{HH} < 1$, it is easy to verify that $\mathbb{A}$ is Metzler stable. Also

$$\mathbb{D} - \mathbb{C}\mathbb{A}^{-1}\mathbb{B} = \begin{pmatrix} -K_2 & \phi_V(1-\eta_V)\frac{1}{N_0} \\ b_V & -\mu_V\left[1 - \frac{\beta_{HV}^2 S_V^* N_0}{K_1 M_H^* \mu_V (N_0-1)\left[1-\frac{\beta_{HH}(\gamma_H\eta_H+\mu_H)}{K_1\mu_V}\right]}\right] \end{pmatrix}. \tag{2.2.52}$$

Let $Z = \frac{N_H^* N_0}{M_H^*(N_0-1)}$. Then $\mathbb{D} - \mathbb{C}\mathbb{A}^{-1}\mathbb{B}$ is Metzler if

$$\frac{\beta_{HV}^2 S_V^* N_H^* N_0}{K_1 N_H^* M_H^* (N_0-1)\left[1-\mathcal{R}_{HH}\right]\mu_V} = \frac{\mathcal{R}_{HV}\mathcal{R}_{VH}}{(1-\mathcal{R}_{HH})} Z < 1. \tag{2.2.53}$$

and Metzler stable if

$$K_2\mu_V\left(1 - \frac{\mathcal{R}_{HV}\mathcal{R}_{VH}}{(1-\mathcal{R}_{HH})}Z - \mathcal{R}_{VV}\right) \geq 0 \implies \frac{\mathcal{R}_{HV}\mathcal{R}_{VH}}{(1-\mathcal{R}_{HH})}Z + \mathcal{R}_{VV} \leq 1. \tag{2.2.54}$$

Notice that for $N_0 > 1$, $Z = \frac{N_H^* N_0}{M_H^*(N_0-1)} > 1$, therefore, the two conditions given by (2.2.53) and (2.2.54) are equivalent to

$$\frac{\mathcal{R}_{HV}\mathcal{R}_{VH}}{(1-\mathcal{R}_{HH})(1-\mathcal{R}_{VV})} \leq \frac{1}{Z} = \frac{M_H^*(N_0-1)}{N_H^* N_0} < 1 \text{ and, } \frac{\mathcal{R}_{HV}\mathcal{R}_{VH}}{(1-\mathcal{R}_{HH})} < \frac{M_H^*(N_0-1)}{N_H^* N_0}.$$

Thus, the necessarily and sufficient conditions for the GAS of $\mathcal{E}_3$ with respect to Ω is that $\mathcal{R}_{HH} < 1$ and $\frac{\mathcal{R}_{HV}\mathcal{R}_{VH}}{(1-\mathcal{R}_{HH})}Z + \mathcal{R}_{VV} \leq 1$.

Theorem 2.2.8. The DFE ($\mathcal{E}_3$) of the model (2.2.7) with respect to Ω is GAS if the associated human-human reproduction number $\mathcal{R}_{HH} = \frac{\beta_{HH}(\mu_H+\gamma_H\eta_H)}{K_1\mu_H} < 1$, and $\frac{\mathcal{R}_{HV}\mathcal{R}_{VH}}{(1-\mathcal{R}_{HH})}Z + \mathcal{R}_{VV} \leq 1$.

Notice that $\frac{\mathcal{R}_{HV}\mathcal{R}_{VH}}{(1-\mathcal{R}_{HH})}Z + \mathcal{R}_{VV} \leq 1$ is equivalent to $\frac{\mathcal{R}_{HV}\mathcal{R}_{VH}}{(1-\mathcal{R}_{HH})(1-\mathcal{R}_{VV})} \leq \frac{M_H^*(N_0-1)}{N_H^* N_0}$, since $M_H^* \leq N_H^*$ and $N_0 - 1 < N_0$, then $\frac{\mathcal{R}_{HV}\mathcal{R}_{VH}}{(1-\mathcal{R}_{HH})}Z + \mathcal{R}_{VV} \leq 1$ suffices that $\mathcal{R}_0 \leq 1$.

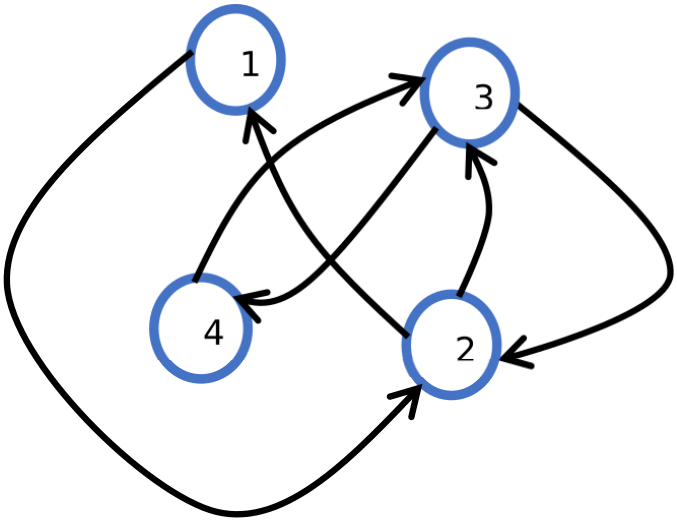

Figure 2.2: Strongly connected directed graph (di-graph) associated with the matrix $A_{22}(\mathbf{x})$. The square matrix $A_{22}(\mathbf{x})$ is thus irreducible (as the figure shows a strongly connected associated di-graph).

We next consider a special case for a positively invariant subset Ω^* of Ω given by

$$\Omega^* = \Big\{ S_H, I_H, R_H, A_N, A_I, S_V, I_V \in \mathbb{R}^7_+ : S_H + I_H + R_H \leq \frac{b_H}{\mu_H}, \quad A_N + A_I \leq \mathcal{K}, \\ S_V \leq S_V^* = \frac{\mathcal{K} b_V}{\mu_V}\big[1 - \frac{1}{N_0}\big], \quad \leq S_V + I_V \leq \frac{\mathcal{K} b_V}{\mu_V} \Big\}. \tag{2.2.55}$$

With respect to Ω^*, it can be shown that the condition for the global asymptotic stability of the DFE $\mathcal{E}_3$ is $\mathcal{R}_{HH} < 1$ and $\frac{\mathcal{R}_{HV}\mathcal{R}_{VH}}{(1-\mathcal{R}_{HH})(1-\mathcal{R}_{VV})} \leq \frac{M_H^*}{N_H^*}$.

If $\delta_H = 0$ ($M_H^* = N_H^*$), the condition reduces to $\frac{\mathcal{R}_{HV}\mathcal{R}_{VH}}{(1-\mathcal{R}_{HH})(1-\mathcal{R}_{VV})} \leq 1$. It should be observed that in Ω^*, $\bar{A}_{22} = A_{22}(\bar{x}_1, 0)$ provided $\delta_H = 0$. Therefore, in addition to $\mathcal{R}_{HH} < 1$, the condition for the GAS of $\mathcal{E}_3$ is $\frac{\mathcal{R}_{HV}\mathcal{R}_{VH}}{(1-\mathcal{R}_{HH})(1-\mathcal{R}_{VV})} \leq 1 \implies \mathcal{R}_0 \leq 1$.

Corollary 2. The DFE ($\mathcal{E}_3$) of the model (2.2.7) with respect to Ω^* is GAS if $\delta_H = 0$, the associated human-human reproduction number $\mathcal{R}_{HH} = \frac{\beta_{HH}(\mu_H + \gamma_H \eta_H)}{K_1 \mu_H} < 1$, and $\mathcal{R}_0 \leq 1$.

The proof can also be done using Corollary 4.4 of [77].

2.3 Numerical simulation and sensitivity analysis

Some numerical simulations, local and global sensitivity analysis of the basic reproduction number ($\mathcal{R}_0$) with respect to the model parameters are presented. Parameter

Table 2.2: Parameter values used in numerical simulations, with low baseline values that gives $R_0 = 0.1156 < 1$, while $R_0 = 2.9268 > 1$ for the high baseline

Parameter	Range	Low baseline	High baseline	References
γ_H	$0.07 - 0.33$ day^{-1}	0.14 day^{-1}	0.08 day^{-1}	[110]
m	$1 - 10$	2	5	[61, 140]
η_H	$0 - 1$ day^{-1}	0.04 day^{-1}	0.08 day^{-1}	assumed
η_V	$0 - 1$ day^{-1}	0.95 day^{-1}	0.90 day^{-1}	[2, 31]
δ_H	0.001 day^{-1}	0.001 day^{-1}	0.001 day^{-1}	[33, 62]
ϕ_V	$1 - 14$ day^{-1}	4 day^{-1}	6 day^{-1}	[45, 46]
b_H	$10 - 10^3$ day^{-1}	30 day^{-1}	10 day^{-1}	[19, 62]
b_V	$0.05 - 0.5$ day^{-1}	0.05 day^{-1}	0.1 day^{-1}	[46, 140]
$\frac{1}{\mu_A}$	$3 - 4$ days	3 days	4 days	[45, 46]
$\frac{1}{\mu_V}$	$4 - 35$ days	7 days	20 days	[7, 61]
$\frac{1}{\mu_H}$	$50 - 70$ years	65 years	50 years	[45, 46]
b_{VH}	$0.3 - 1$ day^{-1}	0.3 day^{-1}	0.5 day^{-1}	[96, 7]
b_{HV}	$0.3 - 1$ day^{-1}	0.414 day^{-1}	0.823 day^{-1}	[96, 7]
ρ_{VH}	$0.1 - 0.75$ day^{-1}	0.25 day^{-1}	0.55 day^{-1}	[7, 61]
ρ_{HV}	$0.5 - 1$ day^{-1}	0.35 day^{-1}	0.45 day^{-1}	[7, 61]
b_{HH}	$0 - 0.20$ day^{-1}	0.02 day^{-1}	0.02 day^{-1}	[96]
ρ_{HH}	$0 - 1$ day^{-1}	0.01 day^{-1}	0.01 day^{-1}	[61, 96]
β_{HH}	$0 - 0.2$ day^{-1}	0.0002 day^{-1}	0.0002 day^{-1}	[61, 96]
β_{HV}	$0.15 - 1$ day^{-1}	0.145 day^{-1}	0.37 day^{-1}	[61, 96]

ranges and values in Table 2.2 for high ($\mathcal{R}_0 > 1$) and low ($\mathcal{R}_0 < 1$) transmission regions are used.

2.3.1 Numerical simulations

From the parameter values in Table 2.2, low transmission baseline has $\mathcal{R}_0 = 0.1156 < 1$ and $N_0 = 3.65$. On the other hand, for high transmission baseline we obtained $\mathcal{R}_0 = 2.9268 > 1$ while $N_0 = 34.29$. Some numerical simulations for the Zika model (2.2.7) are performed for the two baseline parameter values. Figure 2.3 and Figure 2.4 depict the simulation of the Zika model showing infected humans (I_H) approaching the endemic equilibrium when $\mathcal{R}_0 > 1$, and approaching the DFE when $\mathcal{R}_0 < 1$ respectively. Figure 2.5 shows cumulative new cases in humans with different values of η_V, such that as η_V approaches 0 and $1-\eta_V$ approaches 1, that is proportion vertical transmission increases, the cumulative number of new human Zika cases increases.

2.3.2 Sensitivity analysis of $\mathcal{R}_0$

For a function depending on some parameters, the relative change in the function due to change in parameters can be measured using elasticity index. For a parameter α and a function $\mathcal{R}_0$, the elasticity index is given by

$$\Upsilon_{\alpha}^{\mathcal{R}_0} = \frac{\partial \mathcal{R}_0}{\partial \alpha} \times \frac{\alpha}{\mathcal{R}_0}. \tag{2.3.56}$$

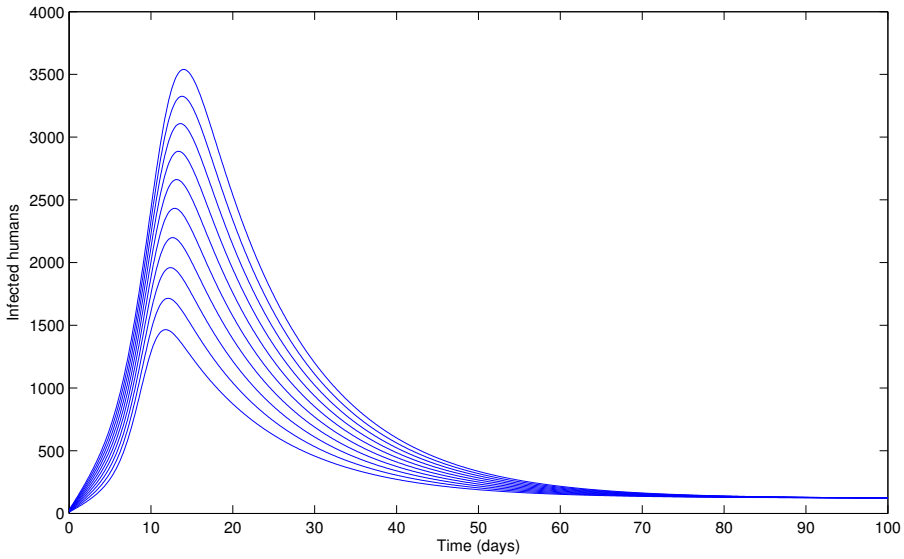

Figure 2.3: Simulation of the model (2.2.7) with infected humans converging to the EE when $\mathcal{R}_0 = 2.9268 > 1$ and different initial conditions.

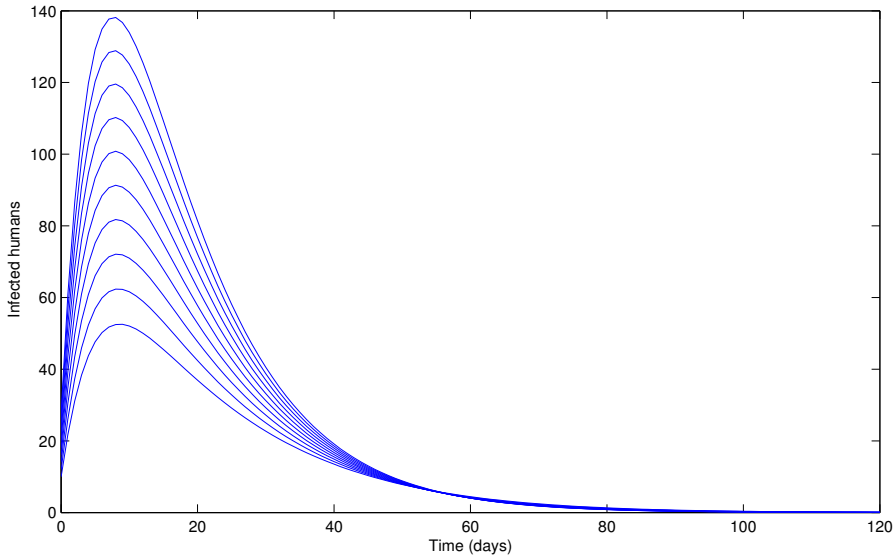

Figure 2.4: Simulation of the model (2.2.7) showing infected humans with different initial conditions converging to the DFE when $\mathcal{R}_0 = 0.1156 < 1$.

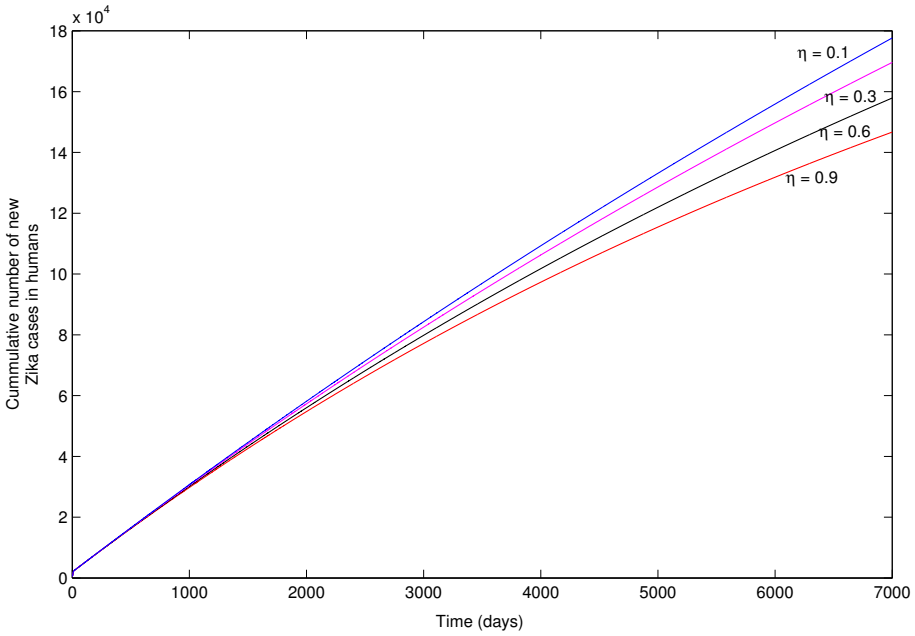

Figure 2.5: Simulation of the model (2.2.7) showing the cumulative number of new Zika cases in humans with different values of η_V and $R_0 = 2.0510 > 1$.

Because an explicit formula for the basic reproduction number is obtained, the above formula (2.3.56) can be used to analyse the sensitivity of $\mathcal{R}_0$ with respect to the model parameters. Using parameter values in Table 2.2 for both low and high transmission regions, the sensitivity index is given in Table 2.3 according to their degree of correlation with $\mathcal{R}_0$. For comparison, line plot for the sensitivity index of $\mathcal{R}_0$ for both low and high regions are give in Figure 2.6.

Although the same set of parameters are positively and negatively correlated with $\mathcal{R}_0$ for both low and high transmission regions, there are wide margins for some parameters as the value of $\mathcal{R}_0$ increases, in particular the parameter $v = 1-\eta_V$. Because of the observed variations for the sensitivity of $\mathcal{R}_0$ as parameter values change, there is therefore the need for more reliable sensitivity analysis which follows.

2.3.3 Global sensitivity analysis

Local sensitivity analysis is best suited when input parameters are known with little uncertainty. However, due to the uncertain nature of biological parameters, it is essential to perform global sensitivity analysis of the Zika model (2.2.7). Global sensitivity analysis allows other parameters to vary as the effect of a certain parameter is estimated. Using parameter ranges in Table 2.2, the partial rank correlation coefficient (PRCC) of the model parameters were computed and presented in Figure 2.7 with the output as the basic reproduction number. For instance, the proportion of vertical transmission $v = 1 - \eta_V$ is the most positively correlated to $\mathcal{R}_0$ while μ_V is the most negatively correlated.

Table 2.3: Local sensitivity index of $\mathcal{R}_0$ to the parameters of the Zika model (2.2.7) evaluated at the baseline parameter values ($\mathcal{R}_0 = 0.1156$ in column 2 and $\mathcal{R}_0 = 2.9268$ in column 4) given in Table 2.2. Parameters are arranged from the most to the least sensitive. Where $v = 1 - \eta_V$.

Parameter	**Sensitivity ($\mathcal{R}_0$)**	**Parameter**	**Sensitivity ($\mathcal{R}_0$)**
v	$+0.74352$	β_{HV}	$+0.91592$
β_{HV}	$+0.23176$	b_V	$+0.46779$
b_V	$+0.15384$	$\mathcal{K}$	$+0.45796$
$\mathcal{K}$	$+0.11588$	μ_H	$+0.40756$
μ_H	$+0.09284$	β_{HH}	$+0.05049$
ϕ_V	$+0.04366$	η_H	$+0.05006$
β_{HH}	$+0.02472$	v	$+0.03359$
η_H	$+0.02300$	ϕ_V	$+0.01376$
δ_H	-0.00100	δ_H	-0.00627
μ_A	-0.03796	μ_A	-0.00983
b_H	-0.11588	γ_H	-0.45177
γ_H	-0.11657	b_H	-0.45796
μ_V	-0.27542	μ_V	-0.92968

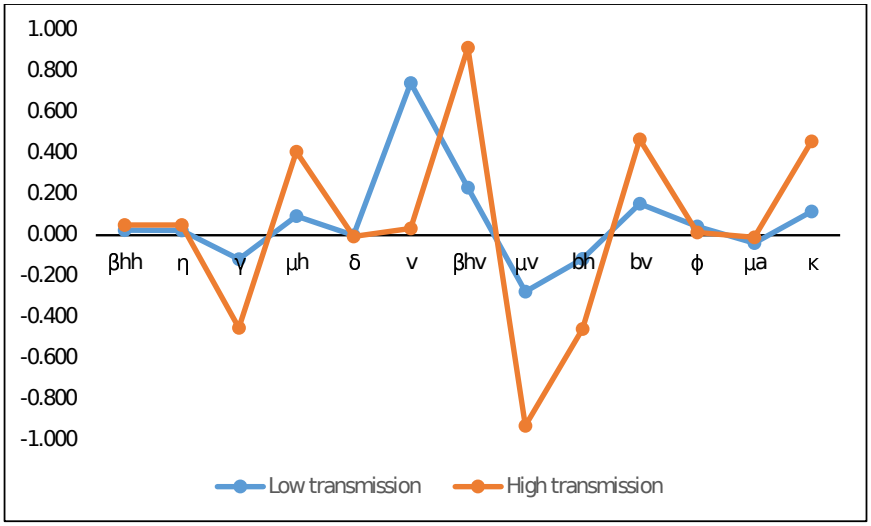

Figure 2.6: Line plot for the comparison of the local sensitivity index of $\mathcal{R}_0$ to the model parameters with low transmission having $\mathcal{R}_0 < 1$, and high transmission for $\mathcal{R}_0 > 1$. Where $v = 1 - \eta_V$.

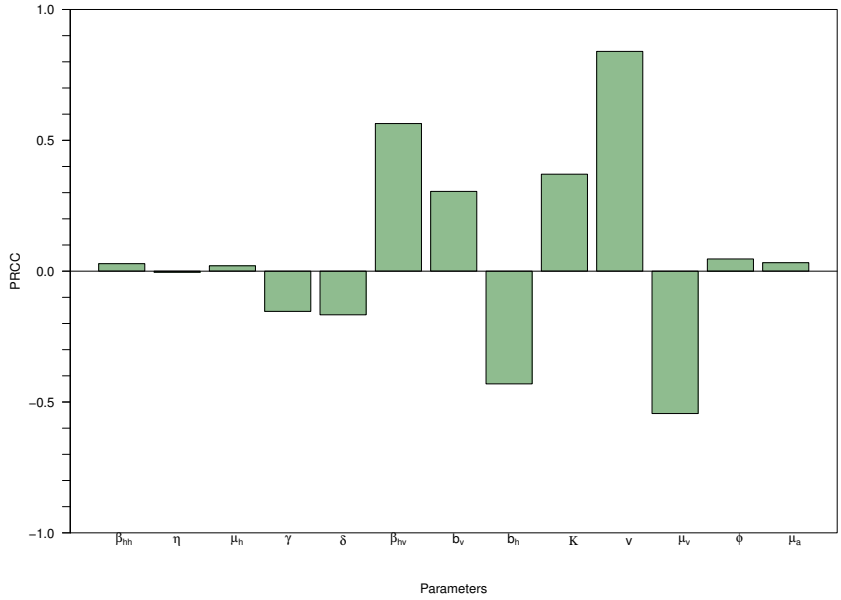

Figure 2.7: PRCC plot of the model parameters using $\mathcal{R}_0$ as the output function. Ranges of parameter values are as presented in Table 2.2.

Conclusion

Zika model that incorporates both vectorial vertical and sexual transmission of Zika virus is constructed and analysed. Some of the key findings include.

- The population of mosquito has a threshold parameter (basic offspring number N_0) which controls the extinction or existence of the mosquito population, such that if it is less than or equal to one, the mosquito population dies out and persist otherwise.
- In the case when $N_0 \leq 1$, the disease can be controlled if the associated reproduction number for human-human transmission is less than or equal to unity.
- The model undergo backward bifurcation (at $\mathcal{R}_0 = 1$) when the basic offspring number is greater than one. The cause of the bifurcation is disease induced death rate in humans.
- Relationships between the type reproduction numbers and the basic reproduction number are computed, with infected human type reproduction number (T_1) most closely related to $\mathcal{R}_0$.
- The condition for the global stability of disease free equilibrium $\mathcal{E}_3$ is $R_{HH} < 1$ and $\frac{\mathcal{R}_{HV}\mathcal{R}_{VH}N_0N_H^*}{M_H^*(N_0-1)(1-\mathcal{R}_{HH})} + \mathcal{R}_{VV} \leq 1$.
- Numerical simulation shows that increase in the proportion of vertical transmission in mosquitoes increase the cumulative number of Zika cases in humans.

- The most positively correlated parameter to the basic reproduction number is the proportion of vertical transmission in mosquito population $(1 - \eta_V = v)$.

Chapter 3

Mathematical modelling of Zika virus with mosquito sterilization

This work has appeared in

Danbaba UA, Garba SM. Modeling the transmission dynamics of Zika with sterile insect technique. *Math Meth Appl Sci*. 2018;1-26. https://doi.org/10.1002/mma.5336.

General introduction

In this chapter, we study a model for the transmission dynamics of Zika with mosquito sterilization. The model considers the interaction of humans and mosquitoes (where both aquatic and non-aquatic stages are considered) in a population.

Abstract

A deterministic model for the transmission dynamics of Zika is designed and rigorously analysed. A model consisting of mutually exclusive compartments representing the human and mosquito dynamics takes into account both direct (human-human) and indirect modes of transmissions. The basic offspring number of the mosquito population is computed and condition for existence and stability of equilibria is investigated. Using the centre manifold theory, the model (with and without direct transmission) is shown to exhibit the phenomenon of backward bifurcation (where a locally asymptotically stable disease free equilibrium coexists with a locally asymptotically stable endemic equilibrium) whenever the associated reproduction number is less than unity. The study shows that the models with and without direct transmission exhibit the same qualitative dynamics with respect to the local stability of their associated disease-free equilibrium and backward bifurcation phenomenon. The main cause of the backward bifurcation is identified as Zika induced mortality in humans. Sensitivity (local and global) analysis of the model parameters are conducted to identify crucial parameters that influence the dynamics of the disease. Analysis of the model shows that an increase in the mating rate with sterile mosquito decreases the mosquito population.

Numerical simulations, using parameter values relevant to the transmission dynamics of Zika are carried out to support some of the main theoretical findings.

3.1 Introduction

Zika is a mosquito borne disease caused by Zika virus (Zv) of genus Flavivirus. The virus was first identified in Uganda in 1947, through a monitoring network of sylvatic yellow fever in rhesus monkeys. Five years later, human infection was identified in Uganda and Tanzania. Since then, Zika outbreaks have been recorded in Africa, Americas, Asia and the Pacific [149]. The disease is primarily transmitted by a bite of an infected mosquito, mainly Aedes aegypti (a mosquito species that transmits yellow fever, dengue, Chikungunya, West Nile virus, and Japanese encephalitis viruses) [71, 149]. The virus is also transmitted through sexual contact between humans [58, 60, 42, 149], blood transfusion and parental transmission [149]. Recently, incidences of congenital neurological disorder (microcephaly) and auto-immune (Guillain-Barr syndrome) complications have been attributed to growing number of Zika incidences especially in the Americas [98, 149].

Unfortunately there is no specific treatment for Zika infection available. Fluid replacement therapy is used for individuals with symptoms such as fever, rash or arthralgia [149]. Although there is no effective vaccine for Zika at the moment, a number of candidate vaccines are undergoing various phases of clinical trials. One of the recent is the experimental vaccine known as rZIKV/D4Δ30-713 developed by scientist at the National Institute of Allergy and Infectious Diseases (NIAID), which is being evaluated in a phase 1 clinical trial (initiated in August 2018) [156]. It is acknowledged that mosquito control is one of the most important tools in the control and/or prevention of mosquito borne diseases (such as dengue and Zika). One of the most promising methods to control Zika is the Sterile Insect Technology (SIT), which is non-polluting method of insect control that relies on the release of sterile male mosquitoes. Mating of released sterile males with wild female mosquitoes leads to non-hatching of eggs and this results in the decline of the wild mosquitoes population [8, 47, 80, 112].

Since the introduction of SIT, numerous mathematical models have been developed and used to quantify the impact of SIT on the transmission dynamics of vector borne diseases (VBDs). These models fall into two main categories, namely, the deterministic or process-based models (which represent the dynamics of the disease using differential equations) some of which include [8, 12, 47, 51, 52] (and some of the references therein), and the statistical models (mainly stochastic processes which are typically based on the use of time-series data to describe the correlation, or relationship, between VBDs and the vector population). In this study, we extend the model designed in [8] by incorporating additional compartments for infectious mosquitoes (sterilized and non-sterilized) and human population. This allows us to assess the potential impact of sterilization on both mosquito and disease control. Furthermore, the model assumes that disease transmission between humans is possible, the recent findings which confirm the Zika transmission via sexual contact between humans include [58, 60, 96, 42, 149]. The purpose of incorporating sexual transmission is to investigate the potential

impact of combined direct (human-to-human) and indirect (human-vector-human) Zika transmission.

The work is organized as follows. A Zika model, which incorporates the dynamics of mosquitoes (sterilized and non-sterilized) and humans is formulated and analysed in Section 3.2. Mosquito-only model is analysed in Section 3.3. Analysis of the model in the absence of direct (human-to-human) transmission is presented in Section 3.4. The model with direct transmission is analysed in Section 3.5. Sensitivity analysis is performed in Section 3.6, while numerical simulation is reported in Sections 3.7.

3.2 Model formulation

The model assumes a homogeneous mixing of human and vector (mosquito) populations, so that each mosquito bite has equal chance of transmitting the virus to a susceptible human (or acquiring infection from infectious human) in the population. The total human population at time t, denoted by $N_H(t)$ is split into mutually exclusive compartments of susceptible $(S_H(t))$, infected $(I_H(t))$ and recovered $(R_H(t))$, so that

$$N_H(t) = S_H(t) + I_H(t) + R_H(t).$$

Similarly, the total mosquito population is split into aquatic (immature) and non-aquatic (adult) stages. For mathematical tractability, the aquatic stages (eggs, larvae and pupae) are lumped into one compartment denoted by $A(t)$. The adult mosquito population (non-aquatic stage) at time t is sub-divided into seven mutually exclusive compartments consisting of non-fertilized adult female mosquitoes $(Y(t))$, fertilized non-sterile susceptible females $(F_N(t))$, fertilized sterile susceptible females (those that could lay eggs but do not hatch due to mating with sterile male mosquitoes) $(F_S(t))$, fertilized non-sterile infected females $(F_{NI}(t))$, fertilized sterile infected females $(F_{SI}(t))$, sterile $(M_S(t))$ and non-sterile $(M_N(t))$ male mosquitoes. Sterile male mosquitoes are injected into the population at a constant rate. Thus, the total mosquito population at time t is given by

$$N_V(t) = Y(t) + F_N(t) + F_S(t) + F_{NI}(t) + F_{SI}(t) + M_N(t) + M_S(t).$$

It is assumed that humans can acquire infection following effective contact with infectious mosquitoes in the F_{NI} or F_{SI} classes at a rate λ_{H1} given by

$$\lambda_{H1} = \beta_{VH}\frac{(F_{NI} + \eta_1 F_{SI})}{N_V}, \tag{3.2.1}$$

where $\beta_{VH} = \rho_{VH}\xi_1$ is the effective contact rate between infectious mosquitoes and susceptible humans, it is defined as the product of the transmission probability from an infectious mosquito to susceptible human (ρ_{VH}) and the biting rate of infectious mosquitoes (ξ_1). The modification parameter $0 < \eta_1 < 1$ accounts for the assumed reduction in transmissibility of mosquitoes in F_{SI} class in comparison to those in F_{NI} class. Furthermore, it is assumed that humans can acquire Zika infection from infectious humans (in I_H or R_H class) via sexual contact at a rate λ_{H2} (this is in line with some recent clinical studies which suggest that, high viral load was found in

the semen and saliva of recovered patients weeks after recovery, hence, there is high chance of direct vaginal or oral sex transmission by recovered humans [48, 58, 60, 42, 149, 156]). It is worth mentioning that Zika is the first Flavivirus known to be transmitted sexually by infectious humans [60]. Thus,

$$\lambda_{H2} = \beta_{HH}\frac{(I_H + \eta_2 R_H)}{N_H},$$

where $\beta_{HH} = \rho_{HH}\xi_2$ is the effective contact rate between infectious and susceptible humans, which is the product of the transmission probability from infectious humans to susceptible humans (ρ_{HH}) and contact rate (usually sexual) between infectious and susceptible humans (ξ_2). The modification parameter $0 < \eta_2 < 1$ accounts for the assumed reduction in transmissibility of recovered humans (including fraction of recovered females) in comparison to infectious humans, so that the force of infection of humans is given by

$$\lambda_H = \lambda_{H1} + \lambda_{H2} = \beta_{VH}\frac{(F_{NI} + \eta_1 F_{SI})}{N_V} + \beta_{HH}\frac{(I_H + \eta_2 R_H)}{N_H}. \tag{3.2.2}$$

Similarly, a susceptible mosquito can acquire Zika infection from an infectious human at a rate λ_V (the force of infection of mosquitoes), given by

$$\lambda_V = \beta_{HV}\frac{I_H}{N_H},$$

where $\beta_{HV} = \rho_{HV}\xi_3$ is the effective contact rate between infectious humans and susceptible mosquitoes; it is defined as the product of the transmission probability from an infectious human to a susceptible mosquito (ρ_{HV}) and the biting rate of susceptible mosquitoes (ξ_3).

3.2.1 Incidence functions

In this section, the functional form of the incidence functions for the transmission dynamics of Zika will be derived. Using the well known fact that for mosquito borne diseases, the total number of bites made by mosquitoes must be equal to the total number of bites received by humans (see [19, 22, 34, 62, 108] for detailed justification), for the number of bites to be conserved, the following equation must hold

$$\beta_{VH}(N_H, N_V)N_H = \beta_{HV}N_V,$$

hence

$$N_V = \frac{\beta_{VH}(N_H, N_V)}{\beta_{HV}}N_H. \tag{3.2.3}$$

Substituting (3.2.3) in (3.2.1) gives

$$\lambda_{H1} = \frac{\beta_{HV}}{N_H}(F_{NI} + \eta_1 F_{SI}),$$

so that

$$\lambda_H = \lambda_{H1} + \lambda_{H2} = \frac{\beta_{HV}(F_{NI} + \eta_1 F_{SI}) + \beta_{HH}(I_H + \eta_2 R_H)}{N_H}. \tag{3.2.4}$$

3.2.2 Dynamics of human population

The population of susceptible humans is generated by birth or immigration at a constant rate b_H. This population is decreased by acquiring infection after receiving adequate amount of bites capable of disease transmission from an infectious mosquito (at the rate λ_{H1}) or via sexual transmission by an infectious human (at the rate λ_{H2}) and by natural death at a rate μ_H. This gives

$$\frac{dS_H}{dt} = b_H - \lambda_H S_H - \mu_H S_H.$$

The population of infectious humans is generated by infection of susceptible humans at the rate λ_H, and decreases due to recovery (at a rate γ_H), natural death (at the rate μ_H) and disease induced death (at a rate δ_H), so that

$$\frac{dI_H}{dt} = \lambda_H S_H - \delta_H I_H - \gamma_H I_H - \mu_H I_H.$$

The population of recovered humans is generated by the recovery of infectious individuals (at the rate γ_H) and reduces due to natural death (at the rate μ_H). Thus,

$$\frac{dR_H}{dt} = \gamma_H I_H - \mu_H R_H.$$

3.2.3 Dynamics of mosquito population

The population of mosquitoes in the aquatic stage (eggs, larvae and pupae) is increased through oviposition by reproductive mosquitoes at a rate ϕ_V. This population decreases due to natural death at a rate μ_V (note that apart from sterile male mosquitoes, it is assumed that natural death occurs in all other mosquito compartments at the same rate μ_V), by density dependent death at a rate μ, maturate and move out of aquatic stage at a rate b_V. Thus,

$$\frac{dA}{dt} = \phi_V F_{NI} + \phi_V F_N - \mu A^2 - \mu_V A - b_V A.$$

The population of non-sterile male mosquitoes evolves directly from the aquatic stage at a rate $(1-r)b_V$, and decreases due to natural death. Thus,

$$\frac{dM_N}{dt} = (1-r)b_V A - \mu_V M_N.$$

Sterile male mosquitoes (M_S) are released into the population at a rate $\omega(t)$ at time t. However, due to some environmental and geographical factors that may affect the mixing of sterile and wild mosquitoes, such as location of mosquito breeding site, it

is convenient to assume that, only a fraction p of the released mosquitoes will join the wild mosquito population. It is further believed that the sterile mosquitoes are in several ways the same as wild mosquitoes. In particular, they are able to mate with wild female mosquitoes. However, there are some differences, which include a change in mating competitiveness due to irradiation and population distributions (which depend on the released formula that could depends on the breeding site and feeding ground). The differences in mating competitiveness can be captured by a modification parameter g which represents the mean mating competitiveness of the sterile male mosquitoes [8, 34, 73], so that, if the number of wild mosquitoes equivalent of sterile mosquitoes is given by M_S, then the actual number of released sterile male mosquitoes is $\frac{1}{pg}M_S$. Therefore, the population of sterile male mosquitoes increases at a rate $pg\omega(t)$ at time t (see for instance [8]). This population decreases due to natural death at a rate μ_S (it also depends on the procedure), so that

$$\frac{dM_S}{dt} = pg\omega - \mu_S M_S.$$

It is assumed that mating of female mosquitoes with sterile male mosquitoes results to non-hatching of their eggs (that is, they lay infertile eggs). Thus, under the previously stated assumptions and adjustments to M_S, it is convenient to assume that the mosquitoes in the M_S and M_N classes have equal chances of mating. Thus, a female mosquito has probability $\frac{M_S}{M_S+M_N}$ of mating with sterile male mosquito and probability $\frac{M_N}{M_S+M_N}$ of mating with non-sterile male mosquito. Adult female mosquitoes evolve from the aquatic stage at a rate $rb_V A$, they mate with non-sterile male mosquito and progress to F_N compartment at a rate $\frac{\alpha M_N}{M_S+M_N}$, or with a sterile male mosquito and move to F_S compartment at a rate $\frac{\alpha M_S}{M_S+M_N}$ (where α is total mating rate). Note that the total mating rate $\frac{M_S}{M_S+M_N} + \frac{\alpha M_N}{M_S+M_N} = \alpha$ remain the same. Thus, we have

$$\frac{dY}{dt} = rb_V A - \frac{\alpha M_S}{M_N+M_S}Y - \frac{\alpha M_N}{M_N+M_S}Y - \mu_V Y.$$

The population of mosquitoes in the F_N class is generated from compartment Y through mating of female mosquitoes with a non-sterile male mosquitoes (M_N). In order to nourish their eggs before oviposition, they need blood, and hence they will probably bite an infectious human and move to the F_{NI} compartment at the rate λ_V. This population is reduced due to natural death, so that

$$\frac{dF_N}{dt} = \frac{\alpha M_N}{M_N+M_S}Y - \lambda_V F_N - \mu_V F_N.$$

Similarly, the population of mosquitoes in the F_S class is generated through mating of adult female mosquitoes with sterile male mosquitoes. This population is decreased by infections following contact with infectious humans and progress to the F_{SI} compartment at a rate λ_V. This gives

$$\frac{dF_S}{dt} = \frac{\alpha M_S}{M_N+M_S}Y - \lambda_V F_S - \mu_V F_S.$$

The population of mosquitoes in the F_{NI} class is generated by the infection of mosquitoes in F_N class, and are decreased by natural death. Hence,

$$\frac{dF_{NI}}{dt} = \lambda_V F_N - \mu_V F_{NI}.$$

Finally, the population of mosquitoes in the F_{SI} class is generated from F_S after biting an infectious human. Thus,

$$\frac{dF_{SI}}{dt} = \lambda_V F_S - \mu_V F_{SI}.$$

3.2.4 Model equations

Since there are only two mating possibilities, either with sterilized or non-sterilized male mosquitoes, we let $\frac{M_S}{M_N+M_S} = \theta$, so that $\frac{M_N}{M_N+M_S} = 1-\theta$. Thus, the Zika transmission model is given by the following system of non-linear differential equations (a flow diagram of the model is given in Figure 3.1 and the associated variables and parameters are described in Table 3.1)

$$\text{Humans} \begin{cases} \frac{dS_H}{dt} = b_H - \lambda_H S_H - \mu_H S_H, \\ \frac{dI_H}{dt} = \lambda_H S_H - \delta_H I_H - \gamma_H I_H - \mu_H I_H, \\ \frac{dR_H}{dt} = \gamma_H I_H - \mu_H R_H, \end{cases}$$

$$\text{Mosquitoes} \begin{cases} \frac{dA}{dt} = \phi_V F_{NI} + \phi_V F_N - \mu A^2 - \mu_V A - b_V A, \\ \frac{dY}{dt} = r b_V A - \alpha Y - \mu_V Y, \\ \frac{dF_N}{dt} = \alpha(1-\theta)Y - \lambda_V F_N - \mu_V F_N, \\ \frac{dF_S}{dt} = \alpha\theta Y - \lambda_V F_S - \mu_V F_S, \\ \frac{dF_{NI}}{dt} = \lambda_V F_N - \mu_V F_{NI}, \\ \frac{dF_{SI}}{dt} = \lambda_V F_S - \mu_V F_{SI}, \\ \frac{dM_N}{dt} = (1-r) b_V A - \mu_V M_N, \\ \frac{dM_S}{dt} = pg\omega(t) - \mu_V M_S. \end{cases} \tag{3.2.5}$$

Notice that, the last equation of (3.2.5) is controlled externally and it is independent of the other compartments. Therefore, given $\omega(t)$ continuous, as a linear equation it has the solution

$$M_S(t) = e^{-\mu_S t}\Big(M_S(0) + \int_0^t e^{\mu_S j} pg\omega(j)dj\Big). \tag{3.2.6}$$

It is worth mentioning that model (3.2.5) was also considered in a conference proceed-

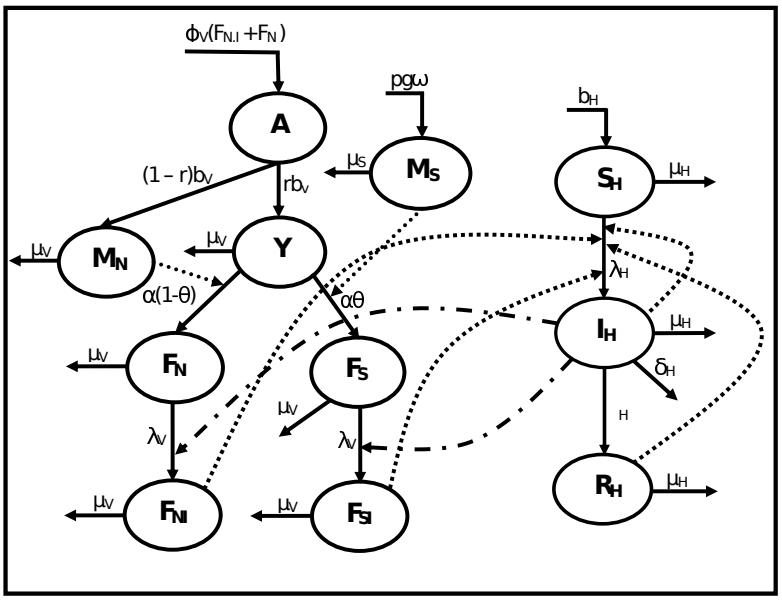

Figure 3.1: *Schematic diagram of the model* (3.2.5).

ing (reference [34] by the same authors). The focus and approach of the two studies are however different. This study gives a thorough rigorous theoretical and constructive analysis of the model, such as the global stability and backward bifurcation property, global sensitivity analysis, we also consider the model with and without human-human Zika transmission. The Zika model (3.2.5), to the author's knowledge is the first to incorporate sterile insect technique with both direct and indirect transmission modes. The model extends some Zika transmissions models and sterile insect technique (SIT) models in the literature, such as those in [4, 8, 12, 22, 47, 51, 52, 61, 74], by for instance:

- Incorporating mosquito sterilization in the model for the transmission of Zika, which is not considered in [4, 22, 61, 74].
- Incorporating the aquatic and non-aquatic stages of mosquitoes which allows us to evaluate the effects of the mosquito reproduction and sterilization on disease transmission, which is not considered in [8, 12, 22, 51, 52, 61].
- Allowing for the transmissions of Zika by both infectious and recovered humans, whereas only transmission by infectious human is assumed in [22, 61].

- Considering sub compartments of fertilized mosquitoes, that to our knowledge is not considered in the literature.

To understand the impact of controlling mosquito population, it is imperative to consider the mosquito-only population in the presence of sterilization. Thus, the following section.

3.3 Theoretical analysis of the mosquito-only model

Here, we carry out analysis of mosquito population in the absence of interaction with infectious humans, by considering the compartment for the non infectious mosquito population only, given by

$$\begin{aligned}
\frac{dA}{dt} &= \phi_V F_N - \mu A^2 - \mu_V A - b_V A,\\
\frac{dY}{dt} &= r b_V A - \alpha Y - \mu_V Y,\\
\frac{dF_N}{dt} &= \alpha(1-\theta)Y - \mu_V F_N,\\
\frac{dF_S}{dt} &= \alpha\theta Y - \mu_V F_S,\\
\frac{dM_N}{dt} &= (1-r)b_V A - \mu_V M_N.
\end{aligned} \tag{3.3.7}$$

3.3.1 Basic offspring number of the mosquito population

The basic offspring number of the mosquito population is given by

$$N_0 = \frac{\phi_V r b_V \alpha(1-\theta)}{(b_V+\mu_V)(\alpha+\mu_V)\mu_V}. \tag{3.3.8}$$

It can be interpreted as follows. A successful oviposition occurs after a female mosquito mates with a non-sterile (wild) male mosquito, which fertilizes and lays eggs. The average duration spent in aquatic stage by mosquito is $\frac{1}{b_V+\mu_V}$ (where b_V is the rate at which mosquitoes transform from aquatic to non-aquatic stage). Let r be the fraction of aquatic mosquitoes that become females, the probability that an egg survives the aquatic stage and becomes an adult female mosquito is

$$\frac{r b_V}{b_V+\mu_V}. \tag{3.3.9}$$

Similarly, $\frac{1}{(\alpha+\mu_V)}$ is the average duration spent by a female mosquito in Y compartment. The rate at which a mosquito in compartment Y move to compartment F_N (through mating with male mosquitoes in M_N compartment) is $\alpha(1-\theta)$. Thus, the probability

Table 3.1: Description of variables and parameters for the model (3.2.5).

Variable	**Interpretation**
S_H	Population of susceptible humans
I_H	Population of infected humans
R_H	Population of recovered humans
A	Population of aquatic mosquitoes
M_S	Population of sterile male mosquitoes
M_N	Population of non-sterile male mosquitoes
M	Total male mosquito population
Y	Population of non-fertilized female mosquitoes
F_S	Population of fertilized sterile susceptible female mosquitoes
F_N	Population of fertilized non-sterile susceptible female mosquitoes
F_{SI}	Population of fertilized sterile infected female mosquitoes
F_{NI}	Population of fertilized non-sterile infected female mosquitoes
Parameter	**Interpretation**
b_H	Recruitment rate of humans
γ_H	Recovery rate of humans
μ_H	Natural death rate of humans
δ_H	Disease induced death rate of humans
α	Mating rate of mosquitoes
b_V	Maturation rate of mosquitoes
ϕ_V	Oviposition rate of fertilized female mosquitoes
θ	Mating probability of a sterilized male mosquito
μ_V	Natural death rate of non-sterilized mosquitoes
μ_S	Natural death rate of sterilized male mosquitoes
μ	Density dependent death rate of aquatic mosquitoes
r	Proportion of matured mosquitoes that are female
η_1	Modification parameter for reduced infectiousness of sterilized mosquitoes in comparison to non-sterilized mosquitoes
η_2	Modification parameter for reduction in infectiousness of recovered humans in comparison to infected humans
ρ_{HH}	Transmission probability from infectious to susceptible humans
ρ_{VH}	Transmission probability from infectious mosquitoes to susceptible humans
ρ_{HV}	Transmission probability from infectious humans to susceptible mosquitoes
β_{HH}	Rate of infection from infectious to susceptible humans
β_{VH}	Rate of infection from infectious mosquitoes to susceptible humans
β_{HV}	Rate of infection from infectious humans to susceptible mosquitoes

that a female mosquito successfully moves from class Y to class F_N is given by

$$\frac{\alpha(1-\theta)}{(\alpha+\mu_V)}. \tag{3.3.10}$$

Furthermore, let the average lifespan of a mosquito in F_N class be $\frac{1}{\mu_V}$, and ϕ_V be its oviposition rate, then the average number of eggs deposited by each mosquito in F_N compartment during its lifetime is given by

$$\frac{\phi_V}{\mu_V}. \tag{3.3.11}$$

The product of the quantities in equations (3.3.9), (3.3.10) and (3.3.11) gives the number of offspring produced by a single female mosquito that mates with a non-sterile male mosquito in its entire lifespan.
Thus, If $N_0 > 1$, then the mosquito population persist, otherwise, if $N_0 \leq 1$ then, the mosquito population goes to extinction and the indirect (human-mosquito-human) transmission can be eliminated.

3.3.2 Existence and stability of equilibria in mosquito population

Setting the right hand side of the equations of system (3.3.7) to zero gives the following equilibria

$$\mathcal{E}_0 = (A^*, Y^*, F_N^*, F_S^*, M_N^*) = \left(A^*, \frac{rb_V A^*}{K_3}, \frac{(1-\theta)\alpha r b_V A^*}{K_3\mu_V}, \frac{\theta\alpha r b_V A^*}{K_3\mu_V}\frac{(1-r)b_V A^*}{K_3\mu_V}\right) \tag{3.3.12}$$

where

$$K_1 = \delta_H + \gamma_H + \mu_H, \quad K_2 = b_V + \mu_V, \text{ and } K_3 = \alpha + \mu_V,$$

and A^* satisfies

$$(A^*)^2 + \frac{K_2}{\mu}\Big[1 - \frac{\phi_V r b_V \alpha(1-\theta)}{K_2 K_3 \mu_V}\Big]A^* = 0,$$

or equivalently

$$A^*\left[A^* + \frac{K_2}{\mu}(1-N_0)\right] = 0. \tag{3.3.13}$$

The roots of A^* are controlled by the magnitude of N_0.
If $N_0 \leq 1$, then, the only biologically meaningful root of equation (3.3.13) is $A^* = 0$, which corresponds to the trivial (or mosquito extinction) equilibrium, $\mathcal{E}_1$, given by

$$\mathcal{E}_1 = (A^*, Y^*, F_N^*, F_S^*, M_N^*) = (0, 0, 0, 0, 0). \tag{3.3.14}$$

It is worth mentioning that the equilibrium, $\mathcal{E}_1$, is biologically less attractive due to the absence of mosquitoes in the population. However if $N_0 > 1$, then, the system

(3.3.7), has a non-zero positive equilibrium, $\mathcal{E}_2$, given by

$$\mathcal{E}_2 = (A^*, Y^*, F_N^*, F_S^*, M_N^*) = \left(A^*, \frac{b_V r A^*}{K_3}, \frac{b_V r\alpha(1-\theta)A^*}{K_3\mu_V}, \frac{b_V\theta\alpha r A^*}{K_3\mu_V}, \frac{b_V(1-r)A^*}{K_3\mu_V}\right) \tag{3.3.15}$$

where $A^* = \frac{K_2}{\mu}(N_0 - 1) > 0$.

Theorem 3.3.1. For the mosquito-only model (3.3.7), the extinction equilibrium, $\mathcal{E}_1$, is globally asymptotically stable (GAS) if $N_0 \leq 1$ and unstable otherwise. In addition, the positive equilibrium, $\mathcal{E}_2$, is locally asymptotically stable if $N_0 > 1$.

Proof. We shall give the proof of the first part of Theorem (GAS of $\mathcal{E}_1$) using similar approach to that in [8]. In particular Theorem 6 of [8], reproduced below for convenience will be used.
Consider $\dot{x} = f(x)$, where $D \subseteq \mathbb{R}^n$ and $f : D \longrightarrow \mathbb{R}^n$ is continuous. Then we have the following result

Theorem 3.3.2. [8] Let $a, b \in D$ be such that $a < b$, $[a, b] \subseteq D$ and $f(b) \leq 0 \leq f(a)$. Then $\dot{x} = f(x)$ defines a (positive) dynamical system on $[a, b]$. Moreover, if $[a, b]$ contains a unique equilibrium q then q is globally asymptotically stable on $[a, b]$.

To apply Theorem (3.3.2) to system (3.3.7), let $p \in \mathbb{R}_+ > \frac{3(\mu_V+b_V)}{\mu}$ and A_p be chosen so large such that

$$\begin{aligned}
A_p &\geq p,\\
F_{N_p} &= \frac{\mu_V + b_V + \mu A_p}{2\phi_V} A_p \geq p,\\
Y_p &= \frac{\mu_V F_{N_p}}{2\alpha(1-\theta)} = \frac{\mu_V(\mu_V + b_V + \mu A_p)}{4\phi_V\alpha(1-\theta)} A_p \geq p,\\
F_{S_p} &= \frac{\theta F_{N_p}}{(1-\theta)} = \frac{\theta(\mu_V + b_V + \mu A_p)}{2\phi_V(1-\theta)} A_p \geq p,\\
M_p &= \frac{2b_v(1-r)A_p}{\mu_V} \geq p.
\end{aligned} \tag{3.3.16}$$

Further, let $b_p = (A_p, Y_p, F_{N_p}, F_{S_p}, M_p)^T$, and consider the interval $[0, b_p] \in \mathbb{R}^5_+$. Then

$$f(b_p) = \begin{pmatrix} -\frac{(\mu_V+b_V+\mu A_p)}{2} A_p \\ r b_V A_p\left(1 - \frac{\mu_V+b_V+\mu A_p}{4N_0(\mu_V+b_V)}\right) \\ -\mu_V F_p \\ -\frac{\mu_V\phi_V F_{N_p}}{2(1-\theta)} \\ -(1-r)b_v A_p \end{pmatrix} \leq \begin{pmatrix} -\frac{(\mu_V+b_V+\mu A_p)}{2} A_p \\ r b_V A_p\left(1 - \frac{1}{N_0}\right) \\ -\mu_V F_p \\ -\frac{\mu_V\phi_V F_{N_p}}{2(1-\theta)} \\ -(1-r)b_v A_p \end{pmatrix} < 0, \text{ provided } N_0 \leq 1.$$

Therefore in the interval $[a, b] = [0, b_p] \in \mathbb{R}^5_+$, the condition $f(b) \leq 0 \leq f(a) = f(b_p) \leq 0 \leq f(0)$ is satisfied. However since p is arbitrary, then b_p can be selected

larger than any $x \in \mathbb{R}^5_+$. Thus the system defines a positive dynamical system on $\mathbb{R}^5_+$. Moreover if $N_0 \leq 1$, $\mathcal{E}_1$ is unique in $[0, b_p]$ and thus, $\mathcal{E}_1$ is globally asymptotically stable.
For local stability of the non-zero equilibrium $\mathcal{E}_2$, we use the property of eigenvalues of the Jacobian matrix J_1 below.

$$J_1 = \begin{pmatrix} -P_1 & 0 & \phi_V & 0 & 0 \\ rb_V & -K_3 & 0 & 0 & 0 \\ 0 & P_2 & -\mu_V & 0 & 0 \\ 0 & \theta\alpha & 0 & -\mu_V & 0 \\ (1-r)b_V & 0 & 0 & 0 & -\mu_V \end{pmatrix},$$

where $P_1 = 2\mu A^* + \mu_V + b_V = 2K_2(N_0 - 1) + \mu_V + b_V$, and $P_2 = (1-\theta)\alpha$. Notice that the system given by (3.3.7) is cooperative on $\mathbb{R}^5_+$, that is, growth in any compartment has positive effect on the growth of other compartments. Equivalently, a system is cooperative if the non-diagonal elements of its Jacobian matrix are non-negative.
Clearly, $-\mu_V$ is an eigenvalue of J_1. The remaining eigenvalues satisfy

$$\lambda^3 + \lambda^2(P_1 + K_3 + \mu_V) + \lambda(K_3\mu_V + P_1K_3 + P_1\mu_V) + P_1K_3\mu_V\Big(1 - \frac{b_V\phi_V\alpha r(1-\theta)}{K_3\mu_V(K_2 + 2\mu A^*)}\Big) = 0 \tag{3.3.17}$$

Applying Routh-Hurwitz criterion and Lienard-Chipart test [81], the roots of a polynomial of degree three are negative if and only if $a_i > 0$ with $i = 0, 1, 2, 3$ and $a_1a_2 - a_3 > 0$.
Its clear from (3.3.17) that a_0, a_1 and a_2 are positive, while the sign of $a_3 = P_1K_3\mu_V\big(1 - \frac{N_0}{2N_0-1}\big)$ depends on N_0. Also,

$$a_1a_2 - a_3 = (K_3 + P_1 + \mu_V)(K_3\mu_V + P_1K_3 + P_1\mu_V) + P_2b_V\phi_V r - P_1K_3\mu_V > 0.$$

If $N_0 > 1$, then $a_3 > 0$. On the other hand $1 - \frac{N_0}{2N_0-1} < 0$ if and only if $N_0 < 1$, hence, $\mathcal{E}_2$ is locally asymptotically stable. □

The epidemiological implication of Theorem 3.3.1 is that the model (3.3.7) does not undergo backward bifurcation when $N_0 \leq 1$ (since $\mathcal{E}_1$ is GAS when $N_0 \leq 1$). Thus bringing the value of N_0 to below unity is a sufficient condition for the control of a mosquito population, which could be achieved by increasing the mating rate of sterile mosquitoes (θ).
The full model is now analysed for its dynamical features, by first of all considering the model in the absence of direct (human-human) transmission.

3.4 Analysis of the model (in the absence of direct transmission)

Here, we analyse the model (3.2.5) in the absence of human-human transmission (obtained by setting $\beta_{HH} = 0$), so that, the forces of infections are now given by

$$\lambda_H = \frac{\beta_{HV}(F_{NI} + \eta_1 F_{SI})}{N_H} \text{ and } , \ \lambda_V = \beta_{HV}\frac{I_H}{N_H}. \tag{3.4.18}$$

3.4.1 Disease-free equilibrium (DFE)

The model (3.2.5) with (3.4.18) has the following disease-free equilibrium

$$\begin{aligned}\mathcal{E}_3 = \Big(S_H^*, I_H^*, R_H^*, A^*, Y^*, F_N^*, F_S^*, F_{NI}^*, F_{SI}^*, M_N^*\Big) = \Big(\frac{b_H}{\mu_H}, 0, 0, \frac{K_2}{\mu}[N_0 - 1],\\ \frac{b_V K_2 r[N_0-1]}{K_3\mu}, \frac{b_V K_2\alpha r(1-\theta)[N_0-1]}{K_3\mu_V\mu}, \frac{b_V K_2\theta\alpha r[N_0-1]}{K_3\mu_V\mu}, 0, 0,\\ \frac{b_V K_2(1-r)[N_0-1]}{K_3\mu_V\mu}\Big).\end{aligned} \tag{3.4.19}$$

Notice that:
If $N_0 \leq 1$, then, the only DFE of the model (3.2.5) is the trivial equilibrium (corresponding to human population free of mosquitoes), $\mathcal{E}_{31}$, given by

$$\mathcal{E}_{31} = (S_H^*, I_H^*, R_H^*, A^*, Y^*, F_N^*, F_S^*, F_{NI}^*, F_{SI}^*, M_N^*) = \left(\frac{b_H}{\mu_H}, 0, 0, 0, 0, 0, 0, 0, 0, 0\right). \tag{3.4.20}$$

This coincides with the mosquito extinction equilibrium, $\mathcal{E}_1$, which is shown to be GAS in Theorem 3.3.1.
If $N_0 > 1$, then, the system (3.2.5), has a non-zero positive disease-free equilibrium, $\mathcal{E}_{32}$ (which corresponds to human population in the presence of mosquitoes), given by

$$\begin{aligned}\mathcal{E}_{32} = \Big(S_H^*, I_H^*, R_H^*, A^*, Y^*, F_N^*, F_S^*, F_{NI}^*, F_{SI}^*, M_N^*\Big) = \Big(\frac{b_H}{\mu_H}, 0, 0, \frac{K_2}{\mu}[N_0 - 1],\\ \frac{b_V K_2 r[N_0-1]}{K_3\mu}, \frac{b_V K_2\alpha r(1-\theta)[N_0-1]}{K_3\mu_V\mu}, \frac{b_V K_2\theta\alpha r[N_0-1]}{K_3\mu_V\mu}, 0, 0,\\ \frac{b_V K_2(1-r)[N_0-1]}{K_3\mu_V\mu}\Big).\end{aligned} \tag{3.4.21}$$

As stated in Section 3.2, the equilibrium $\mathcal{E}_{31}$ is less attractive. Thus, the stability of $\mathcal{E}_{32}$ is now explored.

3.4.1.1 Local stability of the DFE ($\mathcal{E}_{32}$)

The local stability of the DFE, $\mathcal{E}_{32}$ (for the case when $N_0 > 1$) can be established using the next generation operator method on the system given by model (3.2.5). The matrices F (for the new infection terms) and V (of the transition terms) are respectively, given by

$$F = \begin{pmatrix} 0 & 0 & \beta_{HV} & \eta_1\beta_{HV} \\ 0 & 0 & 0 & 0 \\ \beta_{HV}\frac{F_N^*}{N_H^*} & 0 & 0 & 0 \\ \beta_{HV}\frac{F_S^*}{N_H^*} & 0 & 0 & 0 \end{pmatrix}, \quad V = \begin{pmatrix} K_1 & 0 & 0 & 0 \\ -\gamma_H & \mu_H & 0 & 0 \\ 0 & 0 & \mu_V & 0 \\ 0 & 0 & 0 & \mu_V \end{pmatrix}.$$

Following [139], the basic reproduction number of the Zika model (3.2.5) about $\mathcal{E}_{32}$, with the forces of infection given by (3.4.18) (and $N_0 > 1$) is

$$\mathcal{R}_1 = \rho(FV^{-1}) = \sqrt{\frac{\beta_{HV}^2 b_V \alpha r K_2 (N_0 - 1)\left[\theta\eta_1 + (1-\theta)\right]}{N_H^* K_1 K_3 \mu_V^2 \mu}}. \tag{3.4.22}$$

Lemma 3.4.1. The DFE $(\mathcal{E}_{32})$, of the model (3.2.5) with (3.4.18) (and $N_0 > 1$) is locally-asymptotically stable (LAS) if $\mathcal{R}_1 < 1$, and unstable if $\mathcal{R}_1 > 1$ [139].

The epidemiological implication of Lemma 2 is that, there will not be a disease outbreak for a small influx of infectious mosquitoes in the community if $\mathcal{R}_1 < 1$, and therefore the disease eventually dies out.

3.4.2 Interpretation of $\mathcal{R}_1$

In the absence of direct transmission (when $\beta_{HH} = 0$), the threshold quantity $(\mathcal{R}_1)$ is defined as the expected number of secondary cases generated by an infected case introduced into a completely susceptible population. It can be interpreted as follows. Susceptible humans can acquire infection following effective contact with infectious mosquitoes (in F_{NI} or F_{SI} classes). The number of human infections generated by mosquitoes in the F_{NI} class (near the DFE) is given by the product of the infection rate of infectious mosquitoes in the F_{NI} class ($\frac{\beta_{HV}}{N_H^*} = \frac{\beta_{HV}\mu_H}{b_H}$), the average duration in the F_{NI} class ($\frac{1}{\mu_V}$), and the probability that a female mosquito survives the fertilized non-sterilized class (F_N), and move to the F_{NI} compartment ($\frac{\alpha(1-\theta)}{\mu_V}$). This gives (noting that $S_H^* = \frac{b_H}{\mu_H}$)

$$\frac{\beta_{HV}\mu_H\alpha(1-\theta)}{b_H\mu_V^2}S_H^* = \frac{\beta_{HV}\alpha(1-\theta)}{\mu_V^2}. \tag{3.4.23}$$

Similarly, the number of human infections generated by infectious mosquitoes in the F_{SI} class (near the DFE) is given by the product of the infection rate of mosquitoes in the F_{SI} class ($\frac{\beta_{HV}\eta_1}{N_H^*} = \frac{\beta_{HV}\eta_1\mu_H}{b_H}$), the average duration in the F_{SI} class ($\frac{1}{\mu_V}$), and the probability that a female mosquito survives the fertilized and sterilized class (F_S)

and move to F_{SI} compartment ($\frac{\alpha\theta}{\mu_V}$), so that

$$\frac{\beta_{HV}\mu_H\alpha\theta\eta_1}{b_H\mu_V^2}S_H^* = \frac{\beta_{HV}\alpha\theta\eta_1}{\mu_V^2}. \tag{3.4.24}$$

Therefore, the sum of (3.4.23) and (3.4.24) gives the average number of new human infections generated by infectious mosquito (sterilized or non-sterilized). This gives

$$\mathcal{R}_{VH} = \frac{\beta_{HV}\alpha(1-\theta)}{\mu_V^2} + \frac{\beta_{HV}\alpha\theta\eta_1}{\mu_V^2} = \frac{\beta_{HV}\alpha\big[\theta\eta_1 + (1-\theta)\big]}{\mu_V^2}. \tag{3.4.25}$$

The number of mosquitoes infection generated by infectious human (near the DFE), is given by the product of infection rate of infectious humans ($\frac{\beta_{HV}}{N_H^*} = \frac{\beta_{HV}\mu_H}{b_H}$), and the average duration of humans in the infectious class $\frac{1}{K_1}$, so that (with $Y^* = \frac{A^* b_V r}{K_3}$)

$$\mathcal{R}_{HV} = \frac{\beta_{HV}}{N_H^* K_1}Y^* = \frac{\beta_{HV} b_V \mu_H r}{K_1 K_3 b_H}A^*. \tag{3.4.26}$$

The geometric mean of (3.4.25) and (3.4.26) gives the associated reproduction number (noting that $A^* = \frac{K_2(N_0-1)}{\mu} > 0$)

$$\mathcal{R}_1 = \sqrt{\frac{\beta_{HV}^2 b_V \mu_H \alpha r K_2 (N_0-1)\big[\theta\eta_1 + (1-\theta)\big]}{b_H K_1 K_3 \mu_V^2 \mu}} = \sqrt{\mathcal{R}_{HV}\mathcal{R}_{VH}},$$

where the quantities $\mathcal{R}_{HV}$ and $\mathcal{R}_{VH}$ are the reproduction thresholds associated with Zika transmission from human to mosquitoes and from mosquito to humans, respectively.

3.4.3 Endemic equilibrium and backward bifurcation

Let,

$$\mathcal{E}_4 = \big(S_H^{**}, I_H^{**}, R_H^{**}, A^{**}, Y^{**}, F_N^{**}, F_S^{**}, F_{NI}^{**}, F_{SI}^{**}, M_N^{**}\big) \tag{3.4.27}$$

represents an arbitrary positive endemic equilibrium point of the model (3.2.5) in the absence of human-human transmission. Furthermore, let

$$\lambda_H^{**} = \frac{\beta_{HV}F_{NI}^{**} + \beta_{HV}\eta_1 F_{SI}^{**}}{S_H^{**} + I_H^{**} + R_H^{**}}, \quad \lambda_V^{**} = \beta_{HV}\frac{I_H^{**}}{S_H^{**} + I_H^{**} + R_H^{**}}. \tag{3.4.28}$$

be the associated forces of infections at steady-state. Solving the equations of model (3.2.5) at steady state gives

$$
\begin{aligned}
&S_H^{**} = \frac{b_H}{\lambda_H^{**}+\mu_H}, \quad I_H^{**} = \frac{\lambda_H^{**} b_H}{K_1(\lambda_H^{**}+\mu_H)}, \quad R_H^{**} = \frac{\lambda_H^{**} b_H \gamma_H}{K_1\mu_H(\lambda_H^{**}+\mu_H)},\\
&A^{**} = \frac{K_2}{\mu}\big(N_0-1\big), \quad Y^{**} = \frac{rb_V K_2}{K_3\mu}\big(N_0-1\big), \quad F_N^{**} = \frac{b_V r\alpha(1-\theta)K_2}{K_3\mu(\lambda_V^{**}+\mu_V)}\big(N_0-1\big),\\
&F_S^{**} = \frac{b_V r\alpha\theta K_2}{K_3\mu(\lambda_V^{**}+\mu_V)}\big(N_0-1\big), \quad F_{NI}^{**} = \frac{b_V\lambda_V r\alpha(1-\theta)K_2}{K_3\mu_V\mu(\lambda_V^{**}+\mu_V)}\big(N_0-1\big),\\
&F_{SI}^{**} = \frac{b_V\lambda_V r\alpha\theta K_2}{K_3\mu_V\mu(\lambda_V^{**}+\mu_V)}\big(N_0-1\big), \quad M_N^{**} = \frac{(1-r)b_V K_2}{\mu_V\mu}\big(N_0-1\big).
\end{aligned}
\tag{3.4.29}
$$

Since the endemic equilibrium is dependent on λ_V^{**} and λ_H^{**}, it is imperative to find the possible roots of λ_H^{**}, which can be used to evaluate λ_V^{**}. This can be achieved by substituting $S_H^{**}, I_H^{**}, R_H^{**}, F_{NI}^{**}$ and F_{SI}^{**} from (**??**) in (3.4.28). After some algebraic simplification, it can be shown that, λ_H^{**} satisfies

$$
a_0(\lambda_H^{**})^5 + a_1(\lambda_H^{**})^4 + a_2(\lambda_H^{**})^3 + a_3(\lambda_H^{**})^2 + a_4\lambda_H^{**} = 0, \tag{3.4.30}
$$

where

$$
\begin{aligned}
a_0 =&\beta_{HV}b_H^2\mu_H^2K_1(\mu_H+\gamma_H) + b_H^2K_1\mu_H\mu_V(\mu_H+\gamma_H)^2,\\
a_1 =&2\beta_{HV}b_H^2\mu_H^3K_1(\mu_H+\gamma_H) + \beta_{HV}b_H^2\mu_H^3K_1^2 +\\
&2b_H^2K_1^2\mu_H^2\mu_V(\mu_H+\gamma_H) + 2b_H^2\mu_H^2K_1\mu_V(\mu_H+\gamma_H)^2 - \mathcal{R}_1^2K_1^3b_H^2\mu_H^2\mu_V,\\
a_2 =&2\beta_{HV}b_H^2K_1^2\mu_H^4 + \beta_{HV}b_H^2\mu_H^4K_1(\mu_H+\gamma_H) + 4b_H^2K_1^2\mu_H^3\mu_V\\
&(\mu_H+\gamma_H) + b_H^2K_1^3\mu_H^3\mu_V + b_H^2\mu_H^3K_1\mu_V(\mu_H+\gamma_H)^2 - 3\mathcal{R}_1^2K_1^3b_H^2\mu_H^3\mu_V,\\
a_3 =&2K_1^3\mu_H^4b_H^2\mu_V + K_1^2b_H^2\mu_H^5\beta_{HV} + 2K_1^2b_H^2\mu_H^4\mu_V(\mu_H+\gamma_H) - 3\mathcal{R}_1^2K_1^3b_H^2\mu_H^4\mu_V,\\
a_4 =&b_H^2K_1^3\mu_H^5\mu_V(1-\mathcal{R}_1^2).
\end{aligned}
\tag{3.4.31}
$$

Clearly, $\lambda_H^{**} = 0$ is a root of (3.4.30), which corresponds to the DFE. Notice from (3.4.31) that $a_0 > 0$ and $a_4 > 0$ $(a_4 < 0)$ whenever $\mathcal{R}_1 < 1$ $(\mathcal{R}_1 > 1)$. Further, the signs of the remaining coefficients (a_1, a_2 and a_3) depend on the magnitude of the associated parameters, different possibilities can be obtained by permuting their signs as presented in Table 3.2.

Theorem 3.4.2. The model (3.2.5) in the absence of human-human transmission has
i) Unique endemic equilibrium if $\mathcal{R}_1 > 1$ as in Cases 2, 4, 8 and 10 in Table 3.2.
ii) Two or more endemic equilibrium if $\mathcal{R}_1 < 1$ as in Cases 3, 5, 7, 9, 11, 13, and 15 in Table 3.2.
iii) No endemic equilibrium if $\mathcal{R}_1 < 1$, as in Case 1 in Table 3.2.

Theorem 3.4.2 (Case (ii)) indicates the possibility of backward bifurcation (where the locally-asymptotically stable DFE co-exists with a locally-asymptotically stable endemic

equilibrium when $\mathcal{R}_1 < 1$) in the model (3.2.5) (see, for instance, [62, 63, 64]). Furthermore, this is investigated using the center manifold theory below. We claim the following result.

Theorem 3.4.3. The Zika model (3.2.5) in the absence of direct transmission undergoes backward bifurcation at $\mathcal{R}_1 = 1$, whenever the bifurcation coefficient denoted by $\tilde{a}$ given by (3.4.34) in Appendix B is positive.

Proof. To prove the existence of backward bifurcation for the model given by (3.2.5), a method, which is based on the Centre Manifold Theory [26, 139], is used. The following change of variables are made on the model given by (3.2.5). Let,

$$\big(S_H, I_H, R_H, A, Y, F_N, F_S, F_{NI}, F_{SI}, M_N\big) = \big(x_1, x_2, x_3, x_4, x_5, x_6, x_7, x_8, x_9, x_{10}\big),$$

and hence, the total human and mosquito populations are:

$$N_H = x_1 + x_2 + x_3 \quad \text{and} \quad N_V = x_4 + x_5 + x_6 + x_7 + x_8 + x_9 + x_{10}.$$

Using vector notation, we have,

$$X = \big(x_1, x_2, x_3, x_4, x_5, x_6, x_7, x_8, x_9, x_{10}\big)^T,$$

and,

$$\frac{dX}{dt} = \big(f_1, f_2, f_3, f_4, f_5, f_6, f_7, f_8, f_9, f_{10}\big),^T$$

and therefore the transformed model (3.2.5) is represented by

$$\begin{aligned}
\frac{dx_1}{dt} &= f_1 = b_H - \Big(\frac{\beta_{HV}x_8 + \beta_{HV}\eta_1 x_9 + \beta_{HH}x_2 + \beta_{HH}\eta_2 x_3}{x_1+x_2+x_3}\Big)x_1 - \mu_H x_1,\\
\frac{dx_2}{dt} &= f_2 = \Big(\frac{\beta_{HV}x_8 + \beta_{HV}\eta_1 x_9 + \beta_{HH}x_2 + \beta_{HH}\eta_2 x_3}{x_1+x_2+x_3}\Big)x_1 - x_2K_1,\\
\frac{dx_3}{dt} &= f_3 = \gamma_H x_2 - \mu_H x_3,\\
\frac{dx_4}{dt} &= f_4 = \phi_V x_6 + \phi_V x_8 - \mu x_4^2 - K_2 x_4,\\
\frac{dx_5}{dt} &= f_5 = rb_V x_4 - K_3 x_5,\\
\frac{dx_6}{dt} &= f_6 = \alpha(1-\theta)x_5 - \frac{\beta_{HV}x_2x_6}{x_1+x_2+x_3} - \mu_V x_6,\\
\frac{dx_7}{dt} &= f_7 = \alpha\theta x_5 - \frac{\beta_{HV}x_2x_7}{x_1+x_2+x_3} - \mu_V x_7,\\
\frac{dx_8}{dt} &= f_8 = \frac{\beta_{HV}x_2x_6}{x_1+x_2+x_3} - \mu_V x_8,\\
\frac{dx_9}{dt} &= f_9 = \frac{\beta_{HV}x_2x_7}{x_1+x_2+x_3} - \mu_V x_9,\\
\frac{dx_{10}}{dt} &= f_{10} = (1-r)b_V x_4 - \mu_V x_{10},
\end{aligned} \tag{3.4.32}$$

so that the forces of infection are given by

$$\lambda_H = \frac{\beta_{HV}x_8 + \beta_{HV}\eta_1 x_9}{x_1+x_2+x_3}x_1, \quad \lambda_V = \frac{\beta_{HV}x_2}{x_1+x_2+x_3}.$$

Let β^*_{HV} be chosen as a bifurcation parameter obtained by solving for $\beta_{HV} = \beta^*_{HV}$, when $\mathcal{R}_0 = 1$, given by

$$\beta^*_{HV} = \sqrt{\frac{K_1 N^*_H}{F^*_N + \eta_1 F^*_S}}. \tag{3.4.33}$$

The Jacobian of the system (3.4.32), evaluated at the DFE, $\mathcal{E}_{32}$, is given by

$$J^* = \begin{pmatrix} -\mu_H & 0 & 0 & 0 & 0 & 0 & 0 & -\beta^*_{HV} & -\beta^*_{HV}\eta_1 & 0 \\ 0 & -K_1 & 0 & 0 & 0 & 0 & 0 & \beta^*_{HV} & \beta^*_{HV}\eta_1 & 0 \\ 0 & \gamma_H & -\mu_H & 0 & 0 & 0 & 0 & 0 & 0 & 0 \\ 0 & 0 & 0 & j_1 & 0 & \phi_V & 0 & \phi_V & 0 & 0 \\ 0 & 0 & 0 & rb_V & -K_3 & 0 & 0 & 0 & 0 & 0 \\ 0 & -\frac{\beta_{HV}F^*_N}{N^*_H} & 0 & 0 & j_3 & -\mu_V & 0 & 0 & 0 & 0 \\ 0 & -\frac{\beta_{HV}F^*_S}{N^*_H} & 0 & 0 & \alpha\theta & 0 & -\mu_V & 0 & 0 & 0 \\ 0 & \frac{\beta_{HV}F^*_N}{N^*_H} & 0 & 0 & 0 & 0 & 0 & -\mu_V & 0 & 0 \\ 0 & \frac{\beta_{HV}F^*_S}{N^*_H} & 0 & 0 & 0 & 0 & 0 & 0 & -\mu_V & 0 \\ 0 & 0 & 0 & j_2 & 0 & 0 & 0 & 0 & 0 & -\mu_V \end{pmatrix},$$

where $j_1 = -2\mu A^* - K_1$, $j_2 = (1-r)b_V$, $j_3 = \alpha(1-\theta)$. The Jacobian (J^*) of the linearised system has a simple zero eigenvalue (with all other eigenvalues having negative real part). Thus, the centre manifold theory can be used to analyse the dynamics of the system (3.4.32) around $\beta_{HV} = \beta^*_{HV}$.

For the case were equation (3.4.33) holds, the matrix J^* has left eigenvectors associated with zero eigenvalue given by $\mathbf{v} = [v_1, v_2, v_3, v_4, v_5, v_6, v_7, v_8, v_9, v_{10}]^T$

$$v_1 = 0, \quad v_2 = \frac{1}{\mu_H^2 N^*_H \mu_V^2 + \beta^2_{HV}\mu^2_H\left(F^*_N + \eta_1 F^*_S\right)}, \quad v_3 = 0, \quad v_4 = 0,$$

$$v_5 = 0, \quad v_6 = 0, \quad v_7 = 0, \quad v_8 = \frac{\beta_{HV}v_2}{\mu_V}, \quad v_9 = \frac{\beta_{HV}\eta_1 v_2}{\mu_V}, \quad v_{10} = 0,$$

and the right eigenvector (of the zero eigenvalue) denoted by $\mathbf{w} = [w_1, w_2, w_3, w_4, w_5, w_6, w_7, w_8, w_9, w_{10}]^T$ has elements given by:

$$w_1 = -\frac{K_1 w_2}{\mu_H} R_{HV} R_{VH} \quad w_2 = N^*_H \mu^2_H \mu^2_V, \quad w_3 = \frac{\gamma_H w_2}{\mu_H}, \quad w_4 = 0, \quad w_5 = 0,$$

$$w_6 = -\frac{\beta_{HV}F^*_N w_2}{N^*_H \mu_V}, \quad w_7 = -\frac{\beta_{HV}F^*_S w_2}{N^*_H \mu_V}, \quad w_8 = \frac{\beta_{HV}F^*_N w_2}{N^*_H \mu_V}, \quad w_9 = \frac{\beta_{HV}F^*_S w_2}{N^*_H \mu_V},$$

$$w_{10} = 0.$$

It can be shown, by computing the non-zero partial derivatives of the right-hand functions, that the associated backward bifurcation coefficients, $\tilde{a}$ and $\tilde{b}$, are respectively, given by (see Theorem 4.1 in [26])

$$\tilde{\mathbf{a}} = \sum_{k,i,j=1}^{n} v_k w_i w_j \frac{\partial^2 f_k}{\partial x_i \partial x_j}(0,0) = \frac{-2K_1 w_2^2 v_2}{N^*_H}\left[\mathcal{R}_{HV}\mathcal{R}_{VH}\left(\frac{2\left(\gamma_H + \mu_H\right)}{\mu_H} + \frac{\beta_{HV}}{\mu_V}\right) - \frac{K_1 \mathcal{R}^2_{HV}\mathcal{R}^2_{VH}}{\mu_H}\right] \tag{3.4.34}$$

Table 3.2: Number of possible roots for (3.4.30) for $\mathcal{R}_1 < 1$ and $\mathcal{R}_1 > 1$.

Case	a_0	a_1	a_2	a_3	a_4	Value of $\mathcal{R}_1$	Sign change	Real roots
1	+	+	+	+	+	$\mathcal{R}_1 < 1$	0	0
2	+	+	+	+	-	$\mathcal{R}_1 > 1$	1	1
3	+	+	+	-	+	$\mathcal{R}_1 < 1$	2	0, 2
4	+	+	+	-	-	$\mathcal{R}_1 > 1$	1	1
5	+	+	-	+	+	$\mathcal{R}_1 < 1$	2	0, 2
6	+	+	-	+	-	$\mathcal{R}_1 > 1$	3	1, 3
7	+	+	-	-	+	$\mathcal{R}_1 < 1$	2	0, 2
8	+	+	-	-	-	$\mathcal{R}_1 > 1$	1	1
9	+	-	-	-	+	$\mathcal{R}_1 < 1$	2	0, 2
10	+	-	-	-	-	$\mathcal{R}_1 > 1$	1	1
11	+	-	+	-	+	$\mathcal{R}_1 < 1$	4	0, 2, 4
12	+	-	+	-	-	$\mathcal{R}_1 > 1$	3	1, 3
13	+	-	+	+	+	$\mathcal{R}_1 < 1$	2	0, 2
14	+	-	+	+	-	$\mathcal{R}_1 > 1$	3	1, 3
15	+	-	-	+	+	$\mathcal{R}_1 < 1$	2	0, 2
16	+	-	-	+	-	$\mathcal{R}_1 > 1$	3	1, 3

and

$$\tilde{\mathbf{b}} = \sum_{k,i=1}^{n} v_k w_i \frac{\partial^2 f_k}{\partial x_i \partial \phi_V}(0,0) = \frac{\beta_{HV} v_2 w_2 K_2 b_V (N_0 - 1) r \alpha \Big([1-\theta] + \eta_1 \theta \Big)}{N_H^* K_3 \mu_V^2 \mu} > 0 \tag{3.4.35}$$

Since the bifurcation coefficient, b is positive, it follows from Theorem 4.1 in [26] that the Zika model (or its transform equivalent (3.4.31)) will undergo backward bifurcation if the bifurcation coefficient, $\tilde{a}$, given by (3.4.34), is positive. □

The public health implication of backward bifurcation phenomenon of the model (3.2.5) is that the classical epidemiological requirement of having the reproduction number ($\mathcal{R}_1$) to be less than unity, while necessary is no longer sufficient for the effective control of the disease. In other words, the backward bifurcation property of the model (3.2.5) makes effective Zika control difficult. Further, as a consequence, it is instructive to try to determine the cause of the backward bifurcation phenomenon in the model (3.2.5). This is explored below.

3.4.4 Non-existence of Backward bifurcation

Consider the model (3.2.5) with Zika induced death assumed to be negligible (obtained by setting $\delta_H = 0$) so that, K_1 reduces to $\mu_H + \gamma_H$, thus we have the coefficients in

(3.4.31) reduces to

$$\begin{aligned} a_0 =&\beta_{HV} b_H^2 \mu_H^2 K_1^2 + b_H^2 K_1^3 \mu_H \mu_V, \\ a_1 =&3\beta_{HV} b_H^2 \mu_H^3 K_1^2 + K_1^3 b_H^2 \mu_H^2 \mu_V (4 - \mathcal{R}_1^2), \\ a_2 =&3\beta_{HV} b_H^2 K_1^2 \mu_H^4 + 3K_1^3 b_H^2 \mu_H^3 \mu_V (2 - \mathcal{R}_1^2) \\ a_3 =&\beta_{HV} K_1^2 b_H^2 \mu_H^5 + K_1^3 b_H^2 \mu_H^4 \mu_V (4 - 3\mathcal{R}_1^2), \quad a_4 = b_H^2 K_1^3 \mu_H^5 \mu_V (1 - \mathcal{R}_1^2). \end{aligned} \tag{3.4.36}$$

Clearly $a_0 > 0$, the sign of a_1, a_2, a_3, and a_4 depend on the magnitude of R_1. Noticed that, if $R_1 \leq 1$, there is no sign change, hence, by Routh-Hurwitz criterion, there is no endemic equilibrium whenever $R_1 \leq 1$.

Lemma 3.4.4. The Zika model in the absence of direct transmission given by (3.2.5), with $\delta_H = 0$ has no endemic equilibrium whenever $R_1 \leq 1$.

The epidemiological implication of Lemma 3.4.4 is that the Zika model without direct transmission given by (3.2.5), with $\delta_H = 0$ does not undergo backward bifurcation (since the occurrence of backward bifurcation requires the existence of at least two equilibria when $\mathcal{R}_1 < 1$).

Furthermore, it is worth noticing that, substituting $\delta_H = 0$ in the expression for the bifurcation coefficient $\tilde{\mathbf{a}}$, given by equation (3.4.34) in Appendix B reduces $\tilde{\mathbf{a}}$ reduces to

$$\tilde{\mathbf{a}} = \frac{-2w_2^2 v_2}{N_H^*} \Big[\frac{\mathcal{R}_{HV}\mathcal{R}_{VH}K_1^2}{\mu_H} \big(2 - \mathcal{R}_{HV}\mathcal{R}_{VH}\big) + \frac{\mathcal{R}_{HV}\mathcal{R}_{VH}K_1\beta_{HV}}{\mu_V} \Big] < 0, \tag{3.4.37}$$

provided $\mathcal{R}_1 \leq 1$. Thus, it follows from Theorem 4.1 of [26] that, the model (3.2.5) does not undergoes backward bifurcation if the disease induced death rate is negligible. This result is similar to that obtained numerically by Chitnis et al [27] in their malaria model.

The Zika model with both direct (human-human) and indirect (human-mosquito-human) transmission is now analysed for its dynamical features. The aim is to find out if incorporating direct transmission will change the dynamics of the disease.

3.5 Analysis of the model with direct transmission

In this section, we consider the full Zika model in the presence of human-human transmission (i.e with the forces of infection given by (3.2.1) and (3.2.4)).

3.5.1 Disease-free equilibrium

The model (3.2.5) (with direct transmission) has two disease-free equilibria given by:

$$\mathcal{E}_5 = \big(S_H^*, I_H^*, R_H^*, A^*, Y^*, F_N^*, F_S^*, F_{NI}^*, F_{SI}^*, M_N^*\big) = \left(\frac{b_H}{\mu_H}, 0, 0, 0, 0, 0, 0, 0, 0, 0\right), \tag{3.5.38}$$

which occurs when $N_0 \leq 1$. And

$$\mathcal{E}_6 = \Big(S_H^*, I_H^*, R_H^*, A^*, Y^*, F_N^*, F_S^*, F_{NI}^*, F_{SI}^*, M_N^*\Big) = \Big(\frac{b_H}{\mu_H}, 0, 0, \frac{K_2}{\mu}(N_0 - 1), \frac{rb_V K_2(N_0-1)}{K_3\mu}, \frac{(1-\theta)\alpha r b_V K_2(N_0-1)}{K_3\mu_V\mu}, \frac{\theta\alpha r b_V K_2(N_0-1)}{K_3\mu_V\mu}, 0, 0, \frac{(1-r)b_V K_2(N_0-1)}{K_3\mu_V\mu}\Big), \tag{3.5.39}$$

which is obtained when $N_0 > 1$.

3.5.2 Local stability of $\mathcal{E}_6$

The local stability of the DFE, $\mathcal{E}_6$, is established using the next generation method on model (3.2.5). The F and V matrices about $\mathcal{E}_5$ are respectively given by

$$F = \begin{pmatrix} \beta_{HH} & \eta_2\beta_{HH} & \beta_{HV} & \eta_1\beta_{HV} \\ 0 & 0 & 0 & 0 \\ \beta_{HV}\frac{F_N^*}{N_H^*} & 0 & 0 & 0 \\ \beta_{HV}\frac{F_S^*}{N_H^*} & 0 & 0 & 0 \end{pmatrix}, \quad V = \begin{pmatrix} K_1 & 0 & 0 & 0 \\ -\gamma_H & \mu_H & 0 & 0 \\ 0 & 0 & \mu_V & 0 \\ 0 & 0 & 0 & \mu_V \end{pmatrix}.$$

Following [139], the associated reproduction number of the system model (3.2.5) (with $N_0 > 1$) denoted by $\mathcal{R}_0$ is given by

$$\begin{aligned} \mathcal{R}_0 &= \frac{\beta_{HH}\big(\eta_2\gamma_H + \mu_H\big)}{2K_1\mu_H} + \\ &\sqrt{\Big[\frac{\beta_{HH}\big(\eta_2\gamma_H + \mu_H\big)}{2K_1\mu_H}\Big]^2 + \frac{\beta_{HV}^2 b_V r\alpha\mu_H K_2(N_0-1)\big[\theta\eta_1 + (1-\theta)\big]}{K_1K_3b_H\mu_V^2\mu}}. \\ &= \frac{1}{2}\left(\mathcal{R}_{HH} + \sqrt{\mathcal{R}_{HH}^2 + 4\mathcal{R}_{VH}\mathcal{R}_{HV}}\right). \end{aligned}$$

where, $\mathcal{R}_{HH}$ is the threshold quantity associated with the direct (human-to-human) transmissions.

Lemma 3.5.1. The disease-free equilibrium $(\mathcal{E}_6)$, of model (3.2.5) with (3.2.1), (3.2.4) and $N_0 > 1$ is locally asymptotically stable if $\mathcal{R}_0 < 1$, and unstable if $\mathcal{R}_0 > 1$ [139].

The threshold quantity $\mathcal{R}_{HH}$ can be interpreted as follows. The number of new human-human infections (via sexual transmission), generated by an infectious human (I_H) (near the DFE) is given by the product of the infection rate of infectious human $(\frac{\beta_{HH}S_H^*}{N_H^*})$, and the average duration in the infectious class $(\frac{1}{K_1})$, this gives

$$\frac{\beta_{HH}}{K_1}. \tag{3.5.40}$$

Similarly, the number of new human infections generated by humans in the R_H class (near the DFE), is given by the product of the infection rate of infectious human ($\frac{\beta_{HH}\eta_2 S_H^*}{N_H^*}$), the probability that human survives the infectious class I_H and move to recovered class ($\frac{\gamma_H}{K_1}$), and the average duration in the recovered class ($\frac{1}{\mu_H}$), this gives

$$\frac{\beta_{HH}\eta_2\gamma_H}{K_1\mu_H}. \tag{3.5.41}$$

Hence, the sum of (3.5.40) and (3.5.41) gives the threshold quantity associated with the human-human Zika transmissions

$$\mathcal{R}_{HH} = \frac{\beta_{HH}}{K_1} + \frac{\beta_{HH}\eta_2\gamma_H}{K_1\mu_H} = \frac{\beta_{HH}\big(\mu_H + \eta_2\gamma_H\big)}{K_1\mu_H}. \tag{3.5.42}$$

Notice that in the absence of direct Zika transmission, $\mathcal{R}_0 = \mathcal{R}_1$. This result is consistent with those obtained in Brauer et al [19] and Chitnis et al [29] for epidemic model of vector borne diseases with both direct and indirect transmissions.

3.5.3 Endemic equilibrium and backward bifurcation

Let

$$\mathcal{E}_7 = \big(S_H^{***}, I_H^{***}, R_H^{***}, A^{***}, Y^{***}, F_N^{***}, F_S^{***}, F_{NI}^{***}, F_{SI}^{***}, M_N^{***}\big), \tag{3.5.43}$$

represents an arbitrary positive endemic equilibrium point (EE) of the model (3.2.5). Furthermore, let

$$\lambda_H^{***} = \frac{\beta_{HV}(F_{NI}^{***} + \eta_1 F_{SI}^{***}) + \beta_{HH}(I_H^{***} + \eta_2 R_H^{***})}{S_H^{***} + I_H^{***} + R_H^{***}}, \quad \lambda_V^{***} = \beta_{HV}\frac{I_H^{***}}{S_H^{***} + I_H^{***} + R_H^{***}}$$

be the associated forces of infections at the steady-state. Solving equations of model (3.2.5) at the steady-state (with $N_0 > 1$) gives

$$\begin{aligned}
&S_H^{***} = \frac{b_H}{\lambda_H^{***} + \mu_H}, \quad I_H^{***} = \frac{\lambda_H^{***} b_H}{K_1(\lambda_H^{***} + \mu_H)}, \quad R_H^{***} = \frac{\lambda_H^{***} b_H \gamma_H}{K_1\mu_H(\lambda_H^{***} + \mu_H)},\\
&A^{***} = \frac{K_2}{\mu}\big(N_0 - 1\big), \quad Y^{***} = \frac{r b_V K_2}{K_3\mu}\big(N_0 - 1\big), \quad F_N^{***} = \frac{b_V r\alpha(1-\theta)K_2}{K_3\mu(\lambda_V^{***} + \mu_V)}\big(N_0 - 1\big),\\
&F_S^{***} = \frac{b_V r\alpha\theta K_2}{K_3\mu(\lambda_V^{***} + \mu_V)}\big(N_0 - 1\big), \quad F_{NI}^{***} = \frac{b_V\lambda_V^{***} r\alpha(1-\theta)K_2}{K_3\mu_V\mu(\lambda_V^{***} + \mu_V)}\big(N_0 - 1\big)\\
&F_{SI}^{***} = \frac{b_V\lambda_V^{***} r\alpha\theta K_2}{K_3\mu_V\mu(\lambda_V^{***} + \mu_V)}\big(N_0 - 1\big), \quad M_N^{***} = \frac{(1-r)b_V K_2}{\mu_V\mu}\big(N_0 - 1\big).
\end{aligned} \tag{3.5.44}$$

we claim the following result.

Theorem 3.5.2. The Zika model (3.2.5) with direct transmission undergoes backward bifurcation at $\mathcal{R}_0 = 1$, whenever the bifurcation coefficient denoted by $\tilde{\mathbf{a}}_2$ given by equation (3.5.45) is positive.

Proof. Using similar approach as in the proof of Theorem 3.4.3. It can be shown that the associated bifurcation coefficient $\tilde{\mathbf{a}}$, is now given by

$$\tilde{\mathbf{a}}_2 = \sum_{k,i,j=1}^{n} v_k w_i w_j \frac{\partial^2 f_k}{\partial x_i \partial x_j}(0,0) = \frac{-2K_1 w_2^2 v_2}{N_H^*}\Big[\frac{\mathcal{R}_{HH}\big(\gamma_H+\mu_H\big)}{\mu_H}+$$
$$\frac{2\mathcal{R}_{HV}\mathcal{R}_{VH}\big(\gamma_H+\mu_H\big)}{\mu_H}+\frac{\mathcal{R}_{HV}\mathcal{R}_{VH}\beta_{HV}}{\mu_V}-K_1\Big(\frac{\mathcal{R}_{HH}\mathcal{R}_{VH}\mathcal{R}_{HV}}{\mu_H}+\frac{\mathcal{R}_{HV}^2\mathcal{R}_{VH}^2}{\mu_H}\Big)\Big] \tag{3.5.45}$$

and

$$\tilde{\mathbf{b}}_2 = \sum_{k,i=1}^{n} v_k w_i \frac{\partial^2 f_k}{\partial x_i \partial \phi_V}(0,0) = \frac{2\beta_{HV} v_2 w_2 K_2 b_V (N_0-1) r\alpha\Big([1-\theta]+\eta_1\theta\Big)}{N_H^* K_3 \mu_V^3 \mu} > 0. \tag{3.5.46}$$

□

Notice that if $\delta_H = 0$, then K_1 reduces to $\gamma_H + \mu_H$ and $\tilde{\mathbf{a}}_2$ reduces to

$$\tilde{\mathbf{a}}_2 = \frac{-2w_2^2 v_2}{N_H^*}\Big[\frac{\mathcal{R}_{HH}K_1^2}{\mu_H}\big(1-\mathcal{R}_{HV}\mathcal{R}_{VH}\big)+\frac{\mathcal{R}_{HV}\mathcal{R}_{VH}K_1^2}{\mu_H}\big(2-\mathcal{R}_{HV}\mathcal{R}_{VH}\big)+$$
$$\frac{\mathcal{R}_{HV}\mathcal{R}_{VH}K_1\beta_{HV}}{\mu_V}\Big] < 0, \tag{3.5.47}$$

provided $\mathcal{R}_0 \leq 1$.

Lemma 3.5.3. The Zika model (3.2.5) does not undergoes backward bifurcation at $\mathcal{R}_0 = 1$ if $\delta_H = 0$.

Thus, as in Section 4, this result completely rules out the existence of backward bifurcation when $\delta_H = 0$.

3.6 Sensitivity analysis

Sensitivity analysis is a tool used in studying the variation of an output of a model due to change in the input parameters. We perform both local sensitivity analysis (where all other parameters are held at a certain baseline) for the basic reproduction number $(\mathcal{R}_0)$, and global sensitivity analysis, where a multidimensional parameter space is studied globally [91].

3.6.1 Local sensitivity analysis of $\mathcal{R}_0$ with respect to model parameters

The basic reproduction number $(\mathcal{R}_0)$ is used to measure the potential impact of a disease. Using elasticity index, we perform local sensitivity analysis of the parameters of $\mathcal{R}_0$. The method is used to measure the percentage change of a parameter say α,

Table 3.3: Two sets of parameter values used in numerical simulations, with low baseline values that gives $\mathcal{R}_0 = 0.2461 < 1$, while $\mathcal{R}_0 = 4.3250 > 1$ for the high baseline values

Parameters	Range (day^{-1})	Low baseline	High baseline	References
r	$(0,1)$	0.5	0.5	[47, 51]
δ_H	0.001	0.001	0.001	[33, 62]
θ	$(0,1)$	0.2	0.4	assumed
α	$(0,1)$	0.7	0.7	[47]
μ	0.00001	0.00001	0.00001	[8]
ϕ_V	$100-200$	100	120	[32]
b_H	30	30	30	[19]
b_V	$0.05-0.1$	0.05	0.08	[45, 46, 47]
η_1	$(0,1)$	0.5	0.5	assumed
η_2	$(0,1)$	0.04	0.2	assumed
γ_H	$0.059-0.167$	0.14	0.08	[110]
ξ_1	$0.3-1$	0.3	0.5	[61, 96, 93]
ξ_2	$0.01-0.20$	0.001	0.01	[96]
ξ_3	$0.3-1$	0.3	0.5	[96, 93]
μ_V	$0.029-0.25$	0.25	0.09	[61, 93]
μ_H	0.00004	0.00004	0.00004	[45, 46, 47]
ρ_{HH}	$0-1$	0.02	0.04	[61, 96]
ρ_{VH}	$0.1-0.75$	0.2	0.7	[61, 93]
ρ_{HV}	$0.3-0.75$	0.3	0.5	[61, 93]

with respect to a percentage change of a quantity say $R(\alpha)$. The normalized sensitivity index (elasticity indices) of $R(\alpha)$ with respect to α is [28],

$$\Upsilon_{\alpha}^{R} = \frac{\partial R}{\partial \alpha} \times \frac{\alpha}{R}.$$

Using the parameter values in Table 3.3, we give the sensitivity index of the parameters for low and high baseline values in Table 3.4. For both low and high transmission regions, $\mathcal{R}_0$ is most negatively correlated to μ_V, where $\Upsilon_{\mu_V}^{\mathcal{R}_0} = -0.71355$ in low region and $\Upsilon_{\mu_V}^{\mathcal{R}_0} = -0.66732$ in high region, both are followed by b_H and μ (note that $\Upsilon_{b_H}^{\mathcal{R}_0} = \Upsilon_{\mu}^{\mathcal{R}_0}$). Similarly, $\mathcal{R}_0$ is most positively correlated to r then b_V and β_{HH} in both regions. Given that

$$\mathcal{R}_0 = \frac{\mathcal{R}_{HH}}{2} + \sqrt{\left(\frac{\mathcal{R}_{HH}}{2}\right)^2 + \mathcal{R}_{HV}\mathcal{R}_{VH}} \tag{3.6.48}$$

where $\mathcal{R}_{HH}$, $\mathcal{R}_{VH}$ and $\mathcal{R}_{HV}$ are as defined in (3.5.42), (3.4.25) and (3.4.26) respectively. The computation of sensitivity index is presented as follows:

$$\Upsilon^{\mathcal{R}_0}_{\beta_{HH}} = \frac{\mathcal{R}_{HH}}{2\mathcal{R}_0}\Big(1+\frac{\mathcal{R}_{HH}}{2\sqrt{(\frac{\mathcal{R}_{HH}}{2})^2+\mathcal{R}_{HV}\mathcal{R}_{VH}}}\Big),$$

$$\Upsilon^{\mathcal{R}_0}_{\phi_V} = \frac{\mathcal{R}_{HV}\mathcal{R}_{VH}N_0}{2\mathcal{R}_0(N_0-1)\sqrt{(\frac{\mathcal{R}_{HH}}{2})^2+\mathcal{R}_{HV}\mathcal{R}_{VH}}},$$

$$\Upsilon^{\mathcal{R}_0}_{\alpha} = \frac{\mathcal{R}_{HV}\mathcal{R}_{VH}N_0(K_3-1)^2}{2\mathcal{R}_0K_3^2\alpha(N_0-1)\sqrt{(\frac{\mathcal{R}_{HH}}{2})^2+\mathcal{R}_{HV}\mathcal{R}_{VH}}},$$

$$\Upsilon^{\mathcal{R}_0}_{\eta_2} = \frac{\beta_{HH}\eta_2\gamma_H}{2\mathcal{R}_0K_1\mu_H}\Big(1+\frac{\mathcal{R}_{HH}}{2\sqrt{(\frac{\mathcal{R}_{HH}}{2})^2+\mathcal{R}_{HV}\mathcal{R}_{VH}}}\Big),$$

$$\Upsilon^{\mathcal{R}_0}_{\eta_1} = \frac{\mathcal{R}_{HV}\mathcal{R}_{VH}\theta\eta_1}{2\mathcal{R}_0\Big[\theta\eta_1+(1-\theta)\Big]\sqrt{(\frac{\mathcal{R}_{HH}}{2})^2+\mathcal{R}_{HV}\mathcal{R}_{VH}}},$$

$$\Upsilon^{\mathcal{R}_0}_{\mu_V} = -\frac{\mathcal{R}_{HV}\mathcal{R}_{VH}\mu_V\Big[K_3+K_2(N_0-1)\Big]}{2K_2K_3\mathcal{R}_0(N_0-1)\sqrt{(\frac{\mathcal{R}_{HH}}{2})^2+\mathcal{R}_{HV}\mathcal{R}_{VH}}},$$

$$\Upsilon^{\mathcal{R}_0}_{b_V} = \frac{\mathcal{R}_{HV}\mathcal{R}_{VH}}{2K_2(N_0-1)\mathcal{R}_0\sqrt{(\frac{\mathcal{R}_{HH}}{2})^2+\mathcal{R}_{HV}\mathcal{R}_{VH}}}\big(2N_0K_2-2b_V-\mu_V\big),$$

$$\Upsilon^{\mathcal{R}_0}_{\beta_{HV}} = \frac{\mathcal{R}_{HV}\mathcal{R}_{VH}}{\mathcal{R}_0\sqrt{(\frac{\mathcal{R}_{HH}}{2})^2+\mathcal{R}_{HV}\mathcal{R}_{VH}}}, \quad \Upsilon^{\mathcal{R}_0}_{b_H} = -\frac{\mathcal{R}_{HV}\mathcal{R}_{VH}}{2\mathcal{R}_0\sqrt{(\frac{\mathcal{R}_{HH}}{2})^2+\mathcal{R}_{HV}\mathcal{R}_{VH}}},$$

$$\Upsilon^{\mathcal{R}_0}_{r} = \frac{\mathcal{R}_{HV}\mathcal{R}_{VH}(2N_0-1)}{2\mathcal{R}_0(N_0-1)\sqrt{(\frac{\mathcal{R}_{HH}}{2})^2+\mathcal{R}_{HV}\mathcal{R}_{VH}}}, \quad \Upsilon^{\mathcal{R}_0}_{\mu} = -\frac{\mathcal{R}_{HV}\mathcal{R}_{VH}}{2\mathcal{R}_0\sqrt{(\frac{\mathcal{R}_{HH}}{2})^2+\mathcal{R}_{HV}\mathcal{R}_{VH}}},$$

$$\Upsilon^{\mathcal{R}_0}_{\mu_H} = \frac{\beta_{HH}}{2K_1\mathcal{R}_0} - \frac{\mathcal{R}_{HH}(K_1+\mu_H)}{2K_1\mathcal{R}_0} - \frac{(\mathcal{R}_{HH}\mu_H+\mathcal{R}_{HH}K_1-\beta_{HH})}{4\mathcal{R}_0K_1\sqrt{(\frac{\mathcal{R}_{HH}}{2})^2+\mathcal{R}_{HV}\mathcal{R}_{VH}}} -$$
$$\frac{\mathcal{R}_{HV}\mathcal{R}_{VH}(K_1-\mu_H)}{2\mathcal{R}_0K_1^2\sqrt{(\frac{\mathcal{R}_{HH}}{2})^2+\mathcal{R}_{HV}\mathcal{R}_{VH}}},$$

$$\Upsilon^{\mathcal{R}_0}_{\gamma_H} = \frac{\beta_{HH}\eta_2\gamma_H}{2\mathcal{R}_0K_1\mu_H}\Big(1+\frac{1}{2\sqrt{(\frac{\mathcal{R}_{HH}}{2})^2+\mathcal{R}_{HV}\mathcal{R}_{VH}}}\Big) - \frac{\Big(\mathcal{R}_{HH}+2\mathcal{R}_{HV}\mathcal{R}_{VH}\Big)}{4K_1\sqrt{(\frac{\mathcal{R}_{HH}}{2})^2+\mathcal{R}_{HV}\mathcal{R}_{VH}}}$$
$$-\frac{\mathcal{R}_{HH}\gamma_H}{2\mathcal{R}_0K_1},$$

$$\Upsilon^{\mathcal{R}_0}_{\theta} = \frac{\mathcal{R}_{HV}\mathcal{R}_{VH}\theta\eta_1}{2\mathcal{R}_0[\theta\eta_1+(1-\theta)]\sqrt{(\frac{\mathcal{R}_{HH}}{2})^2+\mathcal{R}_{HV}\mathcal{R}_{VH}}} - \frac{\mathcal{R}_{HV}\mathcal{R}_{VH}}{\sqrt{(\frac{\mathcal{R}_{HH}}{2})^2+\mathcal{R}_{HV}\mathcal{R}_{VH}}},$$
$$\frac{N_0\theta}{2\mathcal{R}_0(N_0-1)(1-\theta)},$$

$$\Upsilon_{\delta_H}^{\mathcal{R}_0} = -\frac{\mathcal{R}_{HH}\delta_H}{2\mathcal{R}_0 K_1}\Big(1+\frac{\mathcal{R}_{HH}}{2\sqrt{(\frac{\mathcal{R}_{HH}}{2})^2+\mathcal{R}_{HV}\mathcal{R}_{VH}}}\Big) - \frac{\mathcal{R}_{HV}\mathcal{R}_{VH}\delta_H}{2\mathcal{R}_0 K_1\sqrt{(\frac{\mathcal{R}_{HH}}{2})^2+\mathcal{R}_{HV}\mathcal{R}_{VH}}}.$$

Table 3.4: Sensitivity index of $\mathcal{R}_0$ with respect to parameters of the model (3.2.5) for $\mathcal{R}_0 = 0.2461 < 1$ and $\mathcal{R}_0 = 4.3250 > 1$ using the values of Table 3.3

Parameter	Low baseline	Sensitivity index	High baseline	Sensitivity index
r	0.5	+0.40271	0.5	+0.41333
δ_H	0.001	−0.00344	0.001	−0.00662
θ	0.2	−0.07344	0.4	−0.18978
γ_H	0.14	−0.19457	0.08	−0.19978
α	0.7	+0.10598	0.7	+0.04709
μ	0.00001	−0.19610	0.00001	−0.20585
ϕ_V	100	+0.20661	120	+0.20749
η_1	0.5	+0.02179	0.5	+0.05146
η_2	0.04	+0.28729	0.2	+0.32992
μ_V	0.2	−0.71355	0.09	−0.66732
μ_H	0.00004	−0.09133	0.00004	−0.12435
b_H	30	−0.19610	30	−0.20585
b_V	0.05	+0.40096	0.08	+0.41274
β_{HV}	0.09	+0.39219	0.25	+0.41169
β_{HH}	0.0001	+0.28934	0.0004	+0.33075

3.6.2 Global sensitivity analysis

Unlike local sensitivity analysis, global sensitivity analysis allows other parameters to vary as the effect of a certain parameter is estimated. Using ranges and baseline values in Table 3.3 (high baseline), the partial rank correlation coefficient (PRCC) of the model parameters were computed and presented in Figure 3.2. Total infectious humans $(I_H + R_H)$ is taken as the output function. Other parameters considered are defined as $k_2 = b_V + \mu_V$ and $k_3 = \alpha + \mu_V$. Also $k_4 = \alpha\theta$ and $k_8 = \alpha(1-\theta)$ are the rates of fertilization of F_N and F_S compartments respectively, $k_5 = (1-r)b_v$ and $k_9 = rb_V$ are respectively the rates of maturation to M_N and Y compartments. Input parameters were sampled using Latin Hypercube Sampling (LHS) method (a statistical method for generating a sample of plausible collections of parameter values from a multidimensional distribution), and a total of 1000 simulations were ran. The value of the PRCC in Figure 3.2 gives the correlation between the parameters and the chosen output $(I_H + R_H)$. The parameters with large PRCC values are considered to be the most important (in determining the value/size of the chosen response function). The figures shows that the total infectious humans is most positively correlated to b_H and negatively correlated with ϕ_V, γ_H and k_5 thus they can be targeted in reducing

the number of infectious humans.

The Scatter plots of the most sensitive parameters (that is b_H, ϕ_V, γ_H and k_5) are presented in Figure 3.3. The vertical axis represent the residual of the linear regression between the rank transformed values of the parameters b_H, ϕ_V, γ_H and k_5 and the transformed values of other parameters. The ordinate gives the residual of the linear regression between the rank-transformed values of the output function $(I_H + R_H)$ and the transformed values of all other parameters.
The value of the PRCC of the threshold parameters $\mathcal{R}_1$ and $\mathcal{R}_0$ are given in Figures 3.4 and 3.5, respectively. In either case, μ_V is the most negatively correlated parameter to the threshold quantities, followed by θ, μ and b_H. Thus, this sensitivity study shows the significance of θ in controlling both $\mathcal{R}_1$ and $\mathcal{R}_0$.

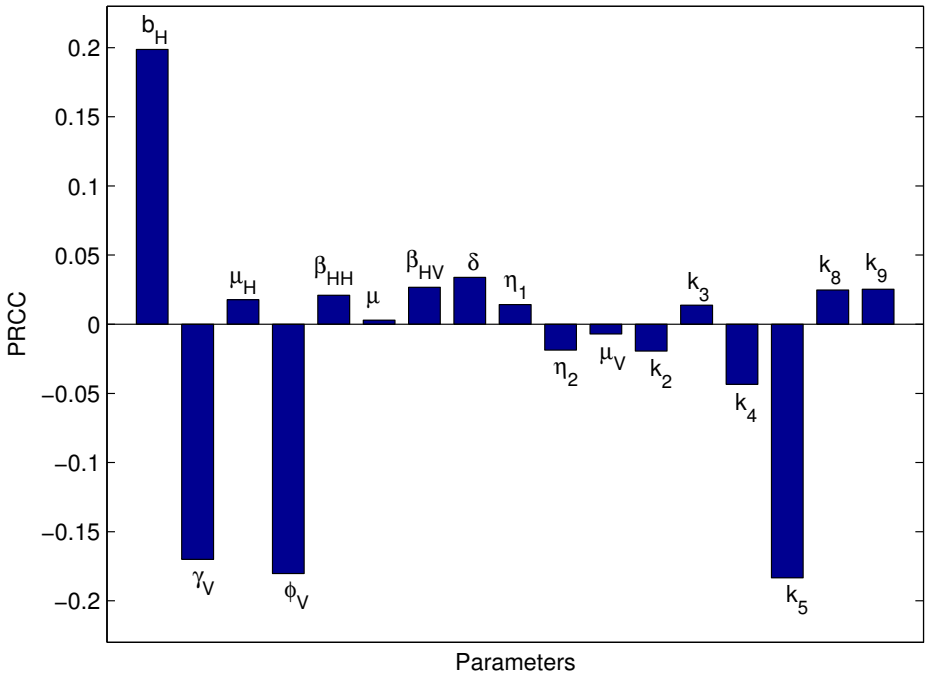

Figure 3.2: PRCC plots of the various parameters of the model (3.2.5), using total infectious humans $(I_H + R_H)$ as the output function.

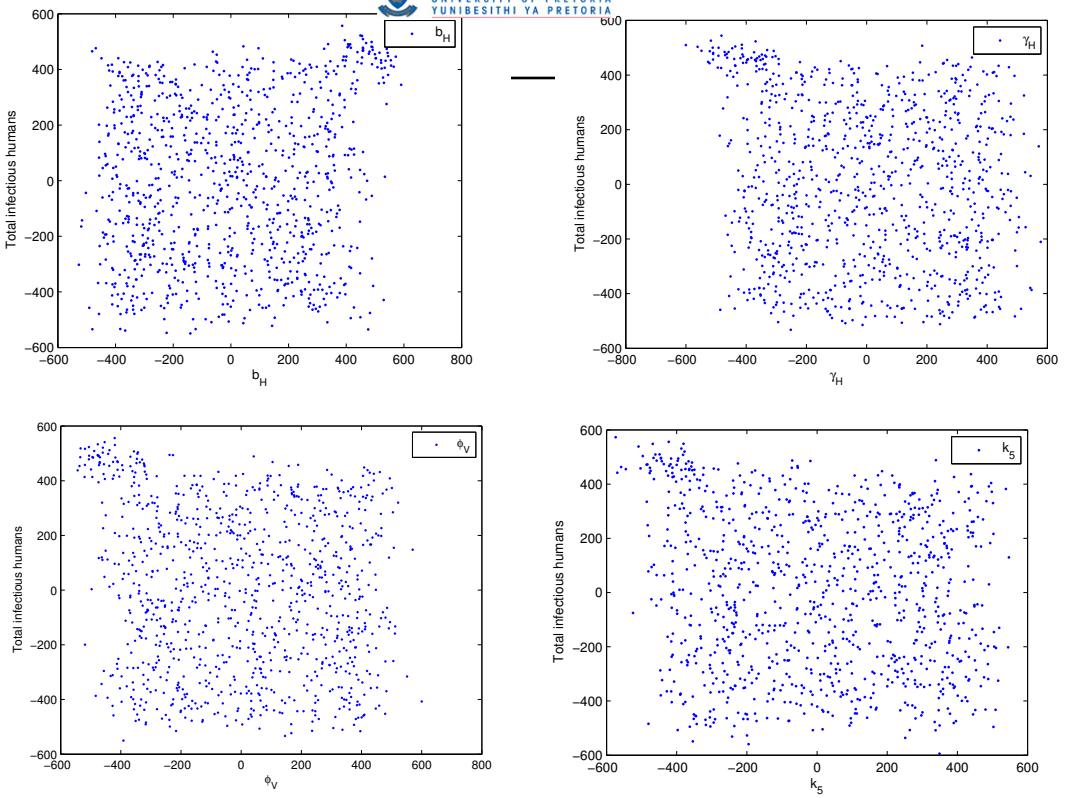

Figure 3.3: Scatter plots of the most sensitive parameters b_H, γ_H, ϕ_V and k_5.

3.7 Numerical simulations

In this section, the Zika model (3.2.5) is simulated using parameter values in Table 3.3, this is aimed at illustrating some of the established analytical results in the previous sections. Two different set of parameter values are used, the low baseline values give $R_0 = 0.2461 < 1$, while the high baseline values give $\mathcal{R}_0 = 4.3250 > 1$. Different simulations were obtained using both low and high baseline parameter values for comparison purposes. Initial conditions used through out our simulations are $S_H(0) = 600$, $I_H(0) = 20$, $R_H(0) = 0$, $A(0) = 2400$, $Y(0) = 500$, $F_N(0) = 300$, $F_S(0) = 100$, $F_{NI}(0) = 100$, $F_{SI}(0) = 50$, and $M_N(0) = 150$.

Figure 3.6 and Figure 3.7 depict population of infected humans with different initial conditions. Figure 3.6 shows the convergence of solution profile to the disease-free equilibrium when $\mathcal{R}_0 = 0.2461 < 1$ and Figure 3.7 shows the convergence of solutions to a non zero equilibrium (endemic equilibrium) when $\mathcal{R}_0 = 4.3250 > 1$. The solution profile of the model (3.2.5) showing cumulative number of new Zika cases in humans, with different values of θ (the probability of a female mosquito mating with a sterile male mosquito) is illustrated in Figure 3.8. The figure shows how increase in the value of θ can drastically reduce the cumulative new human cases. As such, introduction and successful mating of female mosquitoes with sterile male mosquitoes is negatively correlated to new human cases. In Figure 3.9, the effect of θ on the population of reproductive mosquitoes is shown, as the value of θ increases, total reproductive mosquitoes is reduced. Figure 3.10 and Figure 3.11 give a comparison between solution profile of the model showing total number of adult mosquitoes with varying values of ϕ_V and θ respectively, both have positive effect in reducing the size of adult mosquito population, although θ can be controlled (through increase in the release of sterile male mosquitoes at the right location), ϕ_V is not easily controlled.

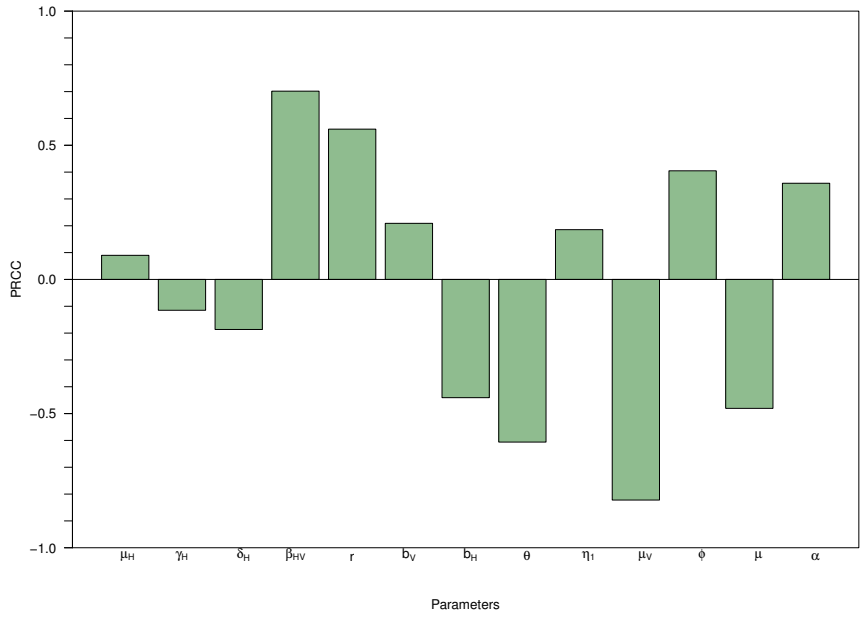

Figure 3.4: PRCC plots of the various parameters of the Zika model (3.2.5), using $\mathcal{R}_1$ as the output function. Parameter ranges used are in Table 3.3.

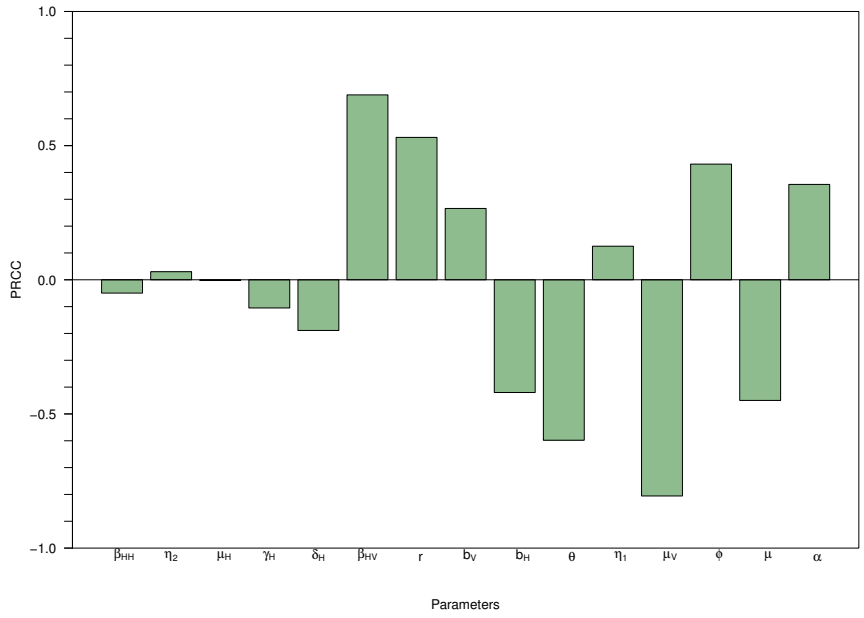

Figure 3.5: PRCC plots of the various parameters of the Zika model (3.2.5), using $\mathcal{R}_0$ as the output function. Parameter ranges used are in Table 3.3.

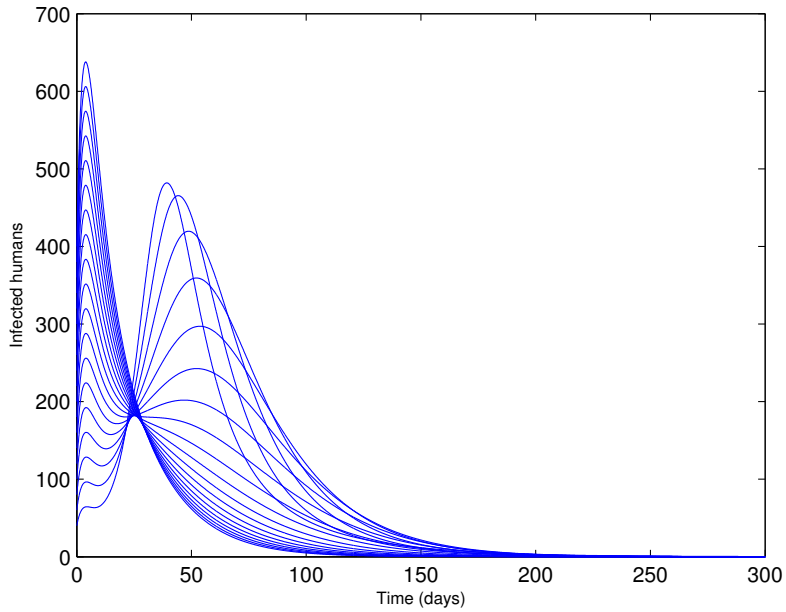

Figure 3.6: Simulation of the model (3.2.5) showing solution profile of infected humans. Parameter values used are as given in Table 3.3, with different initial conditions so that $\mathcal{R}_0 = 0.2461 < 1$.

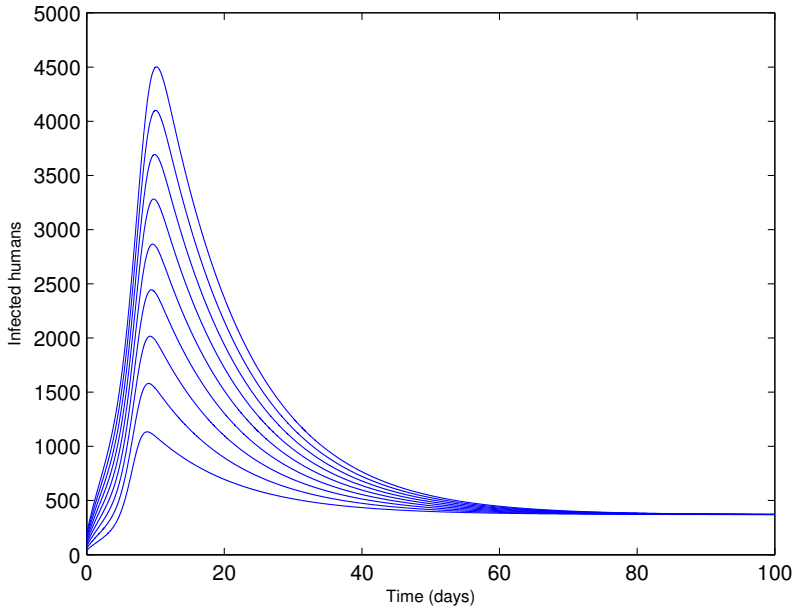

Figure 3.7: Simulation of the model (3.2.5) showing solution profile of infected humans. Parameter values used are as given in Table 3.3, with different initial conditions so that $\mathcal{R}_0 = 4.3250 > 1$.

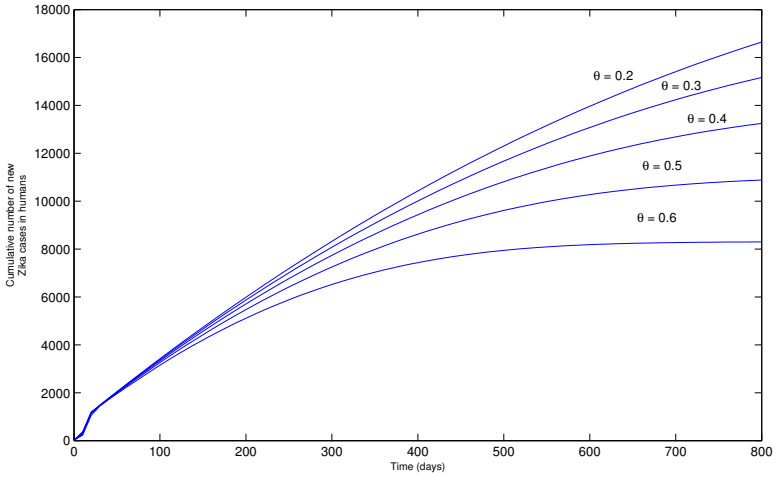

Figure 3.8: Simulation of the model (3.2.5) showing the cumulative number of new cases in human population. Parameter values used are as given in Table 3.3, with various values of θ (chances of mating with sterilized male mosquitoes).

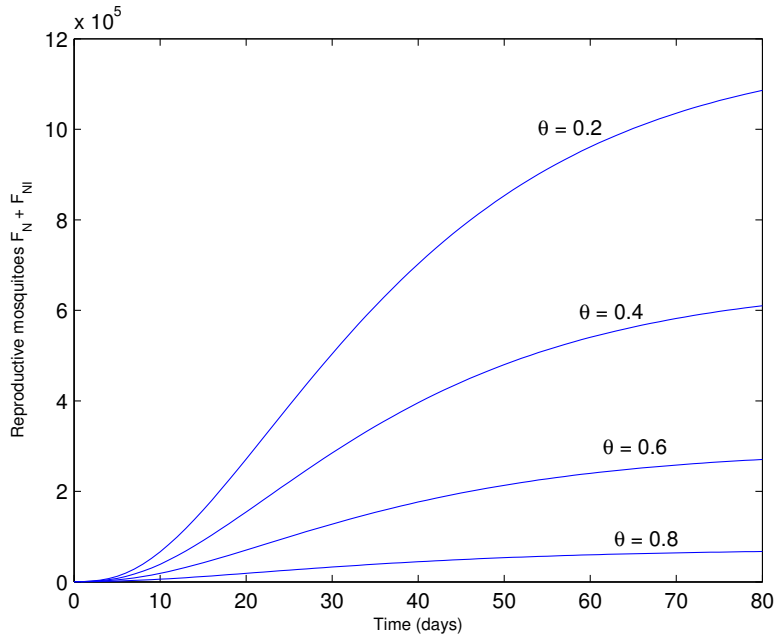

Figure 3.9: Simulation of the model (3.2.5) showing solution profile of reproductive mosquitoes. Parameter values used are as given in Table 3.3, with $\theta = 0.2$, $\theta = 0.4$, $\theta = 0.6$ and $\theta = 0.8$.

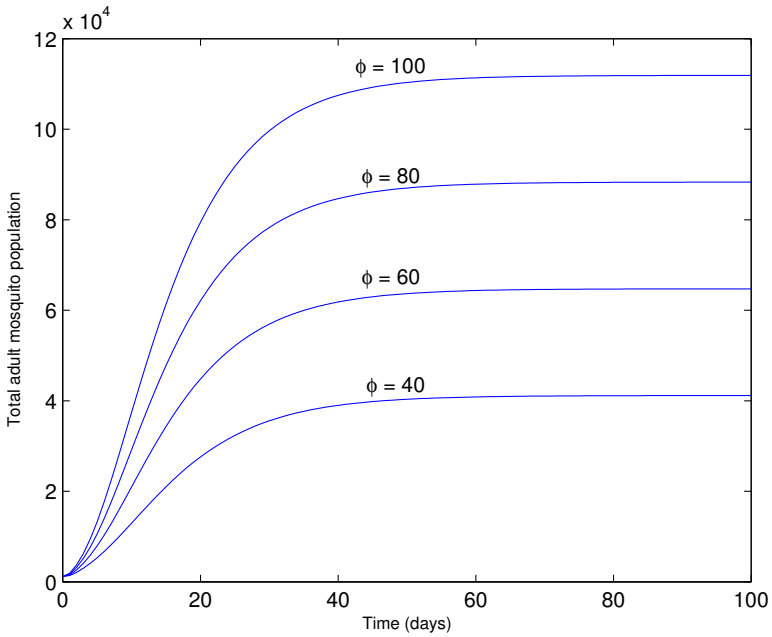

Figure 3.10: Simulation of the model (3.2.5) showing the total number of adult mosquitoes. Parameter values used are as given in Table 3.3, with $\phi_V = 100$, $\phi_V = 80$, $\phi_V = 60$ and $\phi_V = 40$ which respectively give $N_0 = 19.6491$, $N_0 = 15.7193$, $N_0 = 11.7895$ and $N_0 = 7.8596$.

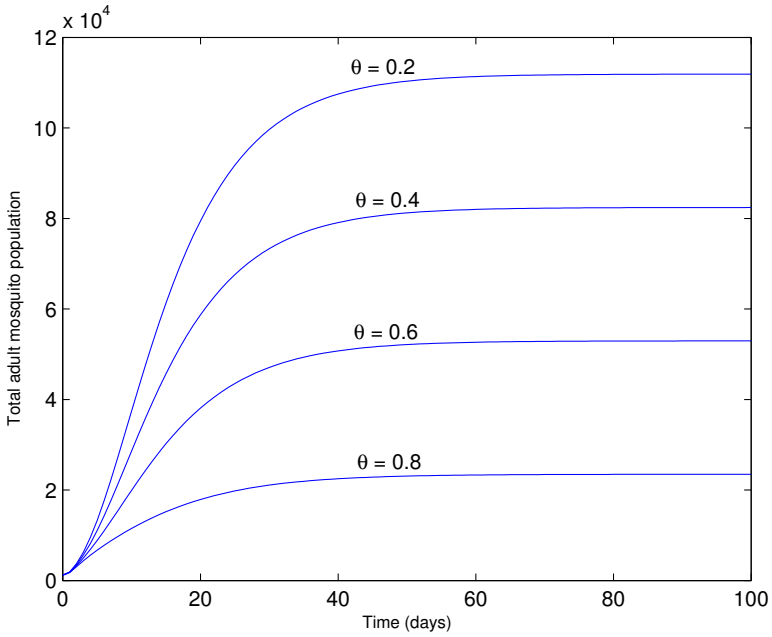

Figure 3.11: Simulation of the model (3.2.5) showing the number of reproductive mosquitoes. Parameter values used are as given in Table 3.3, with $\theta = 0.2$, $\theta = 0.4$, $\theta = 0.6$ and $\theta = 0.8$ which respectively give $N_0 = 19.6491$, $N_0 = 14.7368$, $N_0 = 9.8246$ and $N_0 = 4.9123$.

Conclusion

In this study, we design a new deterministic model for the transmission dynamics of Zika in a population consisting of humans and mosquitoes. The model which adopts a standard incidence formulation incorporates the aquatic stage of mosquito development and mosquito sterilization. Some of the key findings of the study are as follows.

1. The mosquito extinction equilibrium, $\mathcal{E}_0$, is shown to be globally-asymptotically stable when the associated threshold quantity (N_0) called the basic offspring number is less than unity.

2. An increase in the mating rate of sterilized mosquitoes, could be sufficient to bring the value of N_0 to value less than unity, there by decreases the mosquito population.

3. The model (with $N_0 > 1$) in the absence of direct transmission undergoes backward bifurcation, where the stable DFE co-exist with a stable endemic equilibrium when the associated reproduction number is less than unity. This study identifies a sufficient condition for the emergence of backward bifurcation in the model, namely disease induced death in humans ($\delta_H = 0$).

4. Similarly, the model with direct transmission also undergoes backward bifurcation at $\mathcal{R}_0 = 1$. The backward bifurcation property can be removed when the Zika-induced mortality in humans is negligible ($\delta_H = 0$). Thus, the major parameter responsible for backward bifurcation in both models (with and without direct transmission) is the disease-induced mortality in humans. This result is similarly shown by Garba et al [62] for dengue model and numerically for a Malaria model by Chitnis et al [27].

5. The DFE of both models (with and without direct transmissions) in the presence of mosquito population (when $N_0 > 1$) are shown to be locally-asymptotically stable when the associated reproduction numbers are less than unity.

6. The two models exhibit the same qualitative dynamics with respect to the local stability of the associated disease-free equilibrium and backward bifurcation phenomenon.

7. Using elasticity index (local sensitivity analysis), it is shown that, the most effective parameter for the control of the basic reproduction number in both areas of high and low transmission is mosquito death rate.

Chapter 4

Stability analysis and optimal control for yellow fever virus

General introduction

A yellow fever model with vertical transmission in mosquito population, mosquito control, vaccination and use of treated bed nets is constructed and rigorously analysed for its qualitative properties. Optimal control and sensitivity analysis are also presented. This Chapter is under review [37].

Abstract

In this work, a deterministic model for the transmission dynamics of yellow fever virus in a human-mosquito setting in the presence of control is constructed and rigorously analyzed. In addition to horizontal transmissions, vertical transmission of yellow fever within mosquito population is also considered. The model is analysed for its qualitative properties, where the mosquito-only component is shown to have a globally asymptotically stable equilibrium, whenever the basic offspring number (N_0) of the mosquito population is less than or equal to unity. The vaccinated and type reproduction numbers of the autonomous model are computed. Also, condition for global asymptotic stability of the disease free equilibrium of the autonomous form of the model when $N_0 > 1$ is computed. Optimal control theory is applied to the non-autonomous version of the model and optimal controls are characterized. Numerical simulations to assess the effect of fractional vaccine dosing on the vaccinated reproduction number, global sensitivity analysis (where vaccinated reproduction number is most sensitive to the rate of vertical transmission of mosquitoes), and simulations for the optimal control model are also presented.

4.1 Introduction

Yellow fever (YF) is an acute viral haemorrhagic fever that is transmitted by mosquitoes of the Aedes and Haemogogus species. It is endemic in Africa, Central and South

America, where approximately one billion people in fourty seven countries are at risk. Symptoms of the disease include fever, headache, jaundice, muscle pain, nausea, vomiting and fatigue [13, 129, 147, 144]. In broad terms, YF can either be jungle or urban. Jungle YF occurs in tropical rain-forest and it is usually transmitted to humans by incidence, in Africa, it is transmitted by Aedes africanus while in South America by Haemagogus species [15, 147, 144]. Urban YF is transmitted by Aedes aegypti, it is characterized by rapid amplification, capacity for international spread and devastating effect on public health, economic, social and political life [144]. The agent of YF (yellow fever virus) is an arthropod-borne viruses (arboviruses), a group of viruses that are transmitted among vertebrate hosts by arthropod vectors and must replicate in both vertebrate and vector to perpetuate transmission [13, 15]. The host vertebrates in the case of YF are primates where as the host arthropods are normally mosquitoes. Once a mosquito is infected, it lives with the disease for the rest of its life and hence they can be considered as the reservoir for the virus, on the other hand, monkeys have brief viremias and can be considered to be amplifying hosts [15].

Unfortunately, the threats posed by YF have largely been forgotten, just a bit more than a century ago, it was a source of terror, decimating populations of cities, destroying economies and driving political choices. Extensive, repeated epidemics in North American and European port cities during the 18th and 19th centuries spread panic, shutting down affected cities and killing hundreds of thousands of people [144]. Despite the availability of very effective YF vaccine, the disease has however continuously persist in Africa and South America, often with high mortality rate [13]. For instance, the world health organization reported that between 1st of July 2017 and 28th of February 2018, there were 723 confirmed human cases of YF that were reported in Brazil, with at least 237 deaths [148]. In general terms, fourty seven countries are either YF endemic or have some regions that are YF endemic, thirty four of those countries are in Africa with thirteen in South and Central America. A modelling study based on African data sources estimated that, the burden of YF during 2013 was between 84,000 to 170,000 severe cases, and 29,000 to 60,000 deaths [144].

Vertical transmission of YF virus occurs when orally infected female mosquitoes pass the virus to their progeny (transovarial transmission) [41]. First evidence of vertical transmission of YF virus was reported as far back as 1997 [57]. Apart from experimental proof for the vertical transmission of YF, entomological surveys also provided more evidence of vertical transmission of YF virus by mosquitoes. The virus was isolated from wild males and recently emerged adults from larvae collected in the field [41]. In fact, during dry seasons (when mosquito breeding is not favourable), YF virus survival can be attributed to vertical transmission from infected female mosquitoes to their eggs, at which point the viral particles are stable for long periods and can be reactivated when the progeny emerges under better conditions [15, 132]. Thus, vertical transmission is incorporated in this study.

YF has attracted less modeling attention when compared with other mosquito borne diseases such as malaria, dengue, West Nile and Zika virus. To study population dynamics of YF mosquitoes (Aedes aegypti), Dye [49] proposed an appropriate continuous time model that described a field population of adult Aedes aegypti mosquito. Recently, Martorano et al constructed and analysed a compartmental model for the transmission of YF with vaccination [94], although vertical transmission is not

accounted for in their model, both aquatic and non-aquatic stages of mosquito development were considered. An urban YF epidemic model was also formulated and used to study the 2016 YF outbreak in Luanda, Angola by Zhao et al [157]. The complex vector-host dynamics of the system was explored by taking into account mosquito abundance, vaccination and asymptomatic infections in the human population, their model successfully fits the time series of weekly reported YF cases and deaths during the epidemic in Angola [157]. Monica et al [101] looked at a YF model in a human-vector-primate setting with vaccination in human population. To estimate the incubation periods of YF virus in both human and mosquito populations, four statistical models of incubation periods were fitted with historical data in [76]. In this work, we extend the model in [94] by incorporating vertical transmission in mosquito population, in addition to vaccination, the proposed model also incorporates the use of treated bed nets, larvicides and adulticides in mosquito control.

The work is organized as follows: Introduction to YF, short review of relevant literature, brief introduction to vaccination, vector control, treatment and eliminating YF strategy are discussed in Section 4.1. An autonomous deterministic model for the transmission dynamics of YF is constructed and its basic properties are presented in Section 4.2. Threshold quantities and stability analysis of equilibria are also explored. In addition, condition for the global asymptotic stability of the disease free equilibrium (DFE) is presented in Section 4.2. Optimal control analysis for the non-autonomous form of the model is discussed in Section 4.3. Sensitivity analysis and numerical simulations are presented in Section 4.4.

4.1.1 Vaccination

After the isolation of YF in 1927, there were unsuccessful efforts to produce inactivated vaccines in the early 20th century, thus, subsequent developments focused on live virus products and yield the production of a safe, effective vaccine against YF called the 17D strain, it was originally developed by Theiler and Smith in 1936 by attenuating the wild-type Asibi strain in mouse and chick tissue [13, 99]. YF vaccines are manufactured by inoculation of 17D virus seed into chicken embryos and harvesting the infected embryos under standards developed by World Health Organization (WHO) [99]. One dose of the effective, affordable and safe YF vaccine can provides lifelong immunity [144].

4.1.2 Treatment

There is no specific treatment for YF infection, but care to specifically treat cases of dehydration, liver failure, fever and kidney failure is often administered to improve outcomes. Thus, early detection and good supportive treatment in hospitals improve possibility of survival. In the case of bacterial infections, it can also be treated with antibiotics [147].

4.1.3 Vector control

Mosquito control is an important (perhaps the most important) component of preventing and controlling transmission of vector borne diseases. It requires knowledge of both mosquito biology and local conditions to be used in choosing the best interventions (habitat modification, water management, sanitation or pesticides) on a site-specific basis [126]. Only the use of pesticides is considered in this work, it can be achieved either by the use of adulticides (agents to clear adult mosquitoes) or larvicides (agents aimed at eliminating potential mosquito breeding sites) [126, 147]. Adulticides are most often applied as a very fine ultra low-volume (ULV) droplet spray from a truck or aircraft, it is usually organophosphate insecticides and/or synthetic pyrethroids and their combinations [121, 126]. Some larvicide agents are specific to mosquitoes and when used according to directions will have relatively little impact on the environment and human health. They can prevent the emergence of adult mosquitoes for up to 1 month, which decreases labour costs [126].

4.1.4 Eliminating Yellow Fever Epidemics (EYE) Strategy

The most powerful known tool to prevent YF infection is vaccination. One vaccine dose can provide life-long immunity at an affordable rate of 1 US dollar. Angola was in 2016 hit by an unprecedented outbreak of urban YF which spread to beyond its boarders and generated local transmissions. The epidemic created an urgent need for more than 28 million doses of YF vaccines, the demand exhausted the existing global vaccine supply. It also diverted health authorities from tackling other important public health issues, which impacted on health care delivery in general [144, 147].

In order to ensure adequate supply of vaccine especially in high risk regions, the Eliminate Yellow Fever Epidemics (EYE) strategy, steered by World Health Organization, UNICEF and Gavi, the Vaccine Alliance was inaugurated. The vision of EYE is to have a world without YF epidemics. Its mission is to coordinate international action and help countries at risk of the disease to prevent outbreaks and prepare the inevitable cases, to minimize suffering, damage and spread through early and reliable detection as well as a rapid and appropriate response. The initiative has three strategic objectives: they include protecting at-risk populations, preventing international spread, and containing outbreaks rapidly [144].

4.2 Yellow fever model

Following compartmental modeling approach, total human population at time t, denoted by $N_H(t)$ is divided into five mutually exclusive compartments of susceptible ($S_H(t)$), vaccinated ($V_H(t)$), exposed ($E_H(t)$), infected ($I_H(t)$) and recovered ($R_H(t)$) humans, so that

$$N_H(t) = S_H(t) + V_H(t) + E_H(t) + I_H(t) + R_H(t).$$

Susceptible human population is generated at a constant rate b_H, fraction of which are vaccinated at a rate c_V which wanes at a rate ω_H, because the vaccination is

not perfect, vaccinated individuals get infection at a reduced rate (which depends on vaccine efficacy) in comparison to susceptible humans. After infection, individuals move to exposed class before the disease progresses, when they move to infected class at a rate γ_H, infected humans recover and move to recovered class at a rate τ_H, humans die naturally at a rate μ_H and due to disease in the infected compartments at a rate δ_H.

Mosquito population is split into aquatic (immature) and non-aquatic (mature) stages, this is aimed at incorporating vertical transmission and to allow for assessing the impact of controlling mosquitoes using larvicides (to eliminate potential breeding sites). For mathematical tractability, different development stages of the aquatic mosquito population (eggs, larvae and pupae) are lumped into a single compartment denoted by A. Aquatic mosquitoes are further divided into infectious (A_I) and non-infectious (A_N) mosquitoes, thus, the total mosquitoes population at the aquatic stage at time t, is given by

$$A(t) = A_I(t) + A_N(t).$$

Aquatic mosquitoes mature to adulthood at a rate b_V, die naturally at a rate μ_A and due to the use of larvicides at a rate $c_L = r_L e_L$ (where r_L is the rate of applying larvicides and e_L is the efficacy of larvicides). The total mosquito population at non-aquatic stage (adult) at time t, denoted by $N_V(t)$, is sub-divided into susceptible ($S_V(t)$) and infectious ($I_V(t)$) mosquitoes, so that

$$N_V(t) = S_V(t) + I_V(t).$$

Matured susceptible mosquitoes get infection and move to infectious class, they die naturally at a rate μ_V and due to the use of adulticides at a rate $c_A = r_A e_A$ (where r_A is the rate of applying adulticides and e_A is the efficacy of adulticides). Once a mosquito is infected, it remains with the infection. Only female matured mosquitoes are considered (since male mosquitoes are not infectious).

In addition to the use of vaccination, larvicides and adulticides for the control of mosquitoes, prevention effort by reducing mosquito-human contact through the use of treated bed-net is also incorporated.

4.2.1 Incidence function

The frequency-dependent (standard) incidence function is the most widely used form of incidence in vector borne disease models. Infection from mosquitoes to humans occur after an infectious mosquito bites a susceptible human at a rate b_{VH}, let ρ_{VH} be a transmission probability from an infectious mosquito to susceptible human, then the infection rate of humans is $\beta_{VH} = \rho_{VH} b_{VH}$. Therefore the force of infection in humans is given by

$$\lambda_H = \rho_{VH} b_{VH} \frac{I_V}{N_V} = \beta_{VH} \frac{I_V}{N_V}. \tag{4.2.1}$$

Similarly, let $\beta_{HV} = \rho_{HV} b_{HV}$ be the rate at which susceptible mosquitoes acquire infection from infectious human, where ρ_{HV} is the probability of transmission from an infectious human to a susceptible mosquito and b_{HV} is the biting rate of a susceptible mosquito. Then the force of infection in mosquito population (due to horizontal

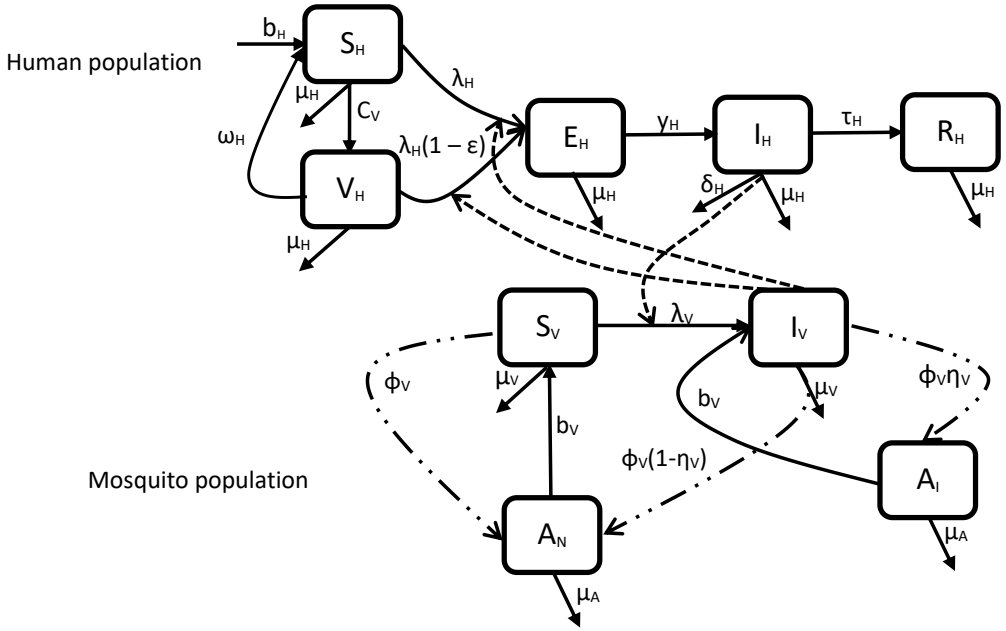

Figure 4.1: *Schematic diagram of the model* (4.2.5).

transmission) is given by

$$\lambda_V = \rho_{HV} b_{HV} \frac{I_H}{N_H} = \beta_{HV} \frac{I_H}{N_H}. \tag{4.2.2}$$

Since mosquitoes bite both susceptible and infected humans, for the total number of bites to be conserved, it is assumed that the total number of bites by the mosquitoes must be equal to the total number of bites received by humans (and this depends on the total sizes of the populations of humans and mosquitoes), see [19, 22, 34, 35, 62, 64, 108]. Thus

$$\beta_{VH}(N_H, N_V) N_H = \beta_{HV} N_V, \text{ so that, } N_V = \frac{\beta_{VH}(N_H, N_V)}{\beta_{HV}} N_H, \tag{4.2.3}$$

Substituting equation (4.2.3) into equation (4.2.1), we have

$$\lambda_H = \beta_{HV} \frac{I_V}{N_H}. \tag{4.2.4}$$

4.2.2 Model equations

Let $c_B = r_B e_B$ be a rate of reducing mosquito-human contact through the use of bed nets, where r_B is the rate of using treated bed-nets and e_B is the efficacy of bed nets. The time independent YF transmission model with vertical transmission,

vaccination, mosquito-human prevention and mosquito control is represented by the following system of equations;

$$\text{Humans}\begin{cases}\dfrac{dS_H}{dt} = b_H + \omega_H V_H - c_V S_H - \beta_{HV}(1-c_B)\dfrac{I_V}{N_H}S_H - \mu_H S_H,\\ \dfrac{dV_H}{dt} = c_V S_H - \beta_{HV}(1-c_B)(1-\epsilon)\dfrac{I_V}{N_H}V_H - \omega_H V_H - \mu_H V_H,\\ \dfrac{dE_H}{dt} = \beta_{HV}(1-c_B)\dfrac{I_V}{N_H}\Big[S_H + (1-\epsilon)V_H\Big] - \gamma_H E_H - \mu_H E_H,\\ \dfrac{dI_H}{dt} = \gamma_H E_H - \delta_H I_H - \tau_H I_H - \mu_H I_H,\\ \dfrac{dR_H}{dt} = \tau_H I_H - \mu_H R_H,\end{cases} \tag{4.2.5}$$

$$\text{Mosquitoes}\begin{cases}\dfrac{dA_N}{dt} = \phi_V\Big(1-\dfrac{A}{\mathcal{K}}\Big)\Big[S_V + (1-\eta_V)I_V\Big] - b_V A_N - \mu_A A_N - c_L A_N,\\ \dfrac{dA_I}{dt} = \phi_V\eta_V\Big(1-\dfrac{A}{\mathcal{K}}\Big)I_V - b_V A_I - \mu_A A_I - c_L A_I,\\ \dfrac{dS_V}{dt} = b_V A_N - \beta_{HV}(1-c_B)\dfrac{I_H}{N_H}S_V - \mu_V S_V - c_A S_V,\\ \dfrac{dI_V}{dt} = \beta_{HV}(1-c_B)\dfrac{I_H}{N_H}S_V + b_V A_I - \mu_V I_V - c_A I_V.\end{cases}$$

It is assumed that, all the model parameters are positive and initial conditions are non-negative. In addition, let $A_N + A_I = A$ so that

$$\frac{dA}{dt} = \phi_V\Big(1-\frac{A}{\mathcal{K}}\Big)[S_V + I_V] - b_V A - \mu_A A - c_L A, \tag{4.2.6}$$

which is the standard formulation for aquatic mosquitoes where breeding sites are limited by number of aquatic mosquitoes they can support, see [45, 46].

Lemma 4.2.1. The following biologically feasible region of the model (4.2.5)

$$\Omega = \Bigg\{S_H, V_H, E_H, I_H, R_H, A_N, A_I, S_V, I_V \in \mathbb{R}^9_+ : S_H + V_H + E_H + I_H + R_H \le \frac{b_H}{\mu_H}, \quad A_N + A_I \le \mathcal{K}, \quad S_V + I_V \le \frac{\mathcal{K} b_V}{\mu_V + c_A}\Bigg\} \tag{4.2.7}$$

is positively-invariant and attracting.

Proof. It is easy to see that solution to the system (4.2.5) exists locally and it is unique ((4.2.5) is C^1 in $\mathbb{R}^{10}_+$). Observe from (4.2.6) that $A_N + A_I \le \mathcal{K}$. Also by

Gronwall's lemma we have

$$\begin{aligned} N_H(t) &\leq N_H(0)e^{-\mu_H t} + \frac{b_H}{\mu_H}\Big(1 - e^{-\mu_H t}\Big), \\ N_V(t) &\leq N_V(0)e^{-(\mu_V + c_A)t} + \frac{\mathcal{K}b_H}{\mu_V + c_A}\Big(1 - e^{-(\mu_V + c_A)t}\Big), \end{aligned} \tag{4.2.8}$$

which are bounded and hence solution exists for all $t \geq 0$. In addition, $N_H(t) \leq \frac{b_H}{\mu_H}$ if $N_H(0) \leq \frac{b_H}{\mu_H}$, and $N_V(t) \leq \frac{\mathcal{K}b_V}{\mu_V + c_A}$ if $N_V(0) \leq \frac{\mathcal{K}b_V}{\mu_V + c_A}$. Consequently, solution of the system (4.2.5) with initial condition in Ω remains in Ω for all $t > 0$ (the ω-limits set of the system are contained in Ω). □

Having obtained the positively-invariant and attracting domain for the system (4.2.5), it is sufficient to consider the asymptotic properties of the dynamics of the flow generated by the system.

4.2.3 Mosquito only equilibria

Consider the mosquito component of the model given by (4.2.5) in the absence of interaction with humans, by direct computation, we obtained a threshold termed as the basic offspring number (N_0) given by

$$N_0 = \frac{\phi_V b_V}{(b_V + \mu_A + c_L)(\mu_V + c_A)}. \tag{4.2.9}$$

It is defined as the average number of offspring produced by a female mosquito in her entire lifespan in the absence of interaction with humans. It can be interpreted as follows: The average time spent by a mosquito at the aquatic stage is $\frac{1}{b_V + \mu_A + c_L}$, while b_V is the rate at which aquatic mosquitoes mature to become female mosquitoes, thus, $\frac{b_V}{b_V + \mu_A + c_L}$ is the probability that an aquatic mosquito mature to be an adult female mosquito. The average life expectancy of an adult female mosquito is $\frac{1}{\mu_V + c_A}$, whereas ϕ_V is the oviposition rate of a female mosquito, therefore the total average number of eggs laid by a female mosquito is $\frac{\phi_V}{\mu_V + c_A}$. Consequently (4.2.9) is the basic offspring number of a mosquito. The mosquito component of (4.2.5) has an extinction disease free equilibrium $\mathcal{E}_0$ given by,

$$\mathcal{E}_0 = \Big(A_N^*, A_I^*, S_V^*, I_V^*\Big) = \Big(0, 0, 0, 0, 0\Big), \tag{4.2.10}$$

obtained when $N_0 \leq 1$ and non-extinction disease free equilibrium $\mathcal{E}_1$ that is obtained when $N_0 > 1$ given by

$$\mathcal{E}_1 = \Big(A_N^*, A_I^*, S_V^*, I_V^*\Big) = \Big(\mathcal{K}[1 - \frac{1}{N_0}], 0, \frac{b_V \mathcal{K}}{[\mu_V + c_A]}[1 - \frac{1}{N_0}], 0\Big). \tag{4.2.11}$$

Let $f : G \longrightarrow \mathbb{R}^4$ be continuous where $G \subseteq \mathbb{R}^n$. Consider a system given by $\dot{x} = f(x)$, then the following theorem follows.

Theorem 4.2.2. [8] Let $a, b \in G$ be such that $a < b$, $[a, b] \subseteq G$ and $f(b) \leq 0 \leq f(a)$.

Table 4.1: Description of the variables and parameters for the model (4.2.5).

Var	Interpretation
S_H	Susceptible humans
V_H	Vaccinated humans
E_H	Exposed humans
I_H	Infected humans
R_H	Recovered humans
A_N	Non-infected aquatic mosquitoes
A_I	Infected aquatic mosquitoes
S_V	Susceptible mosquitoes
I_V	Infected mosquitoes
N_H	Total human population
N_V	Total matured mosquitoes
N_M	Total mosquito population

Par	Interpretation	Range	Ref
c_V	Successful rate of vaccination	$0 - 0.043$/day	[94, 114, 129]
ϵ	Vaccine efficacy	$0.8 - 0.99$/dose	[67, 99, 114]
ω_H	Waning rate of vaccination	$(0, 1)$/dose	[94]
c_B	Rate of successful use of bed net	$0 - 0.95$	[20]
b_H	Recruitment rate of humans	$10 - 800$/day	[3, 19]
μ_H	Natural death rate of humans	3×10^{-5}-6×10^{-5}/day	[7, 62, 94]
γ_H	Progression rate of YF	$0.167 - 0.3$/day	[147, 76, 157]
δ_H	Disease induced death rate of humans	$0.0001 - 0.0004$/day	[34, 94]
τ_H	Recovery rate of humans	$0.25 - 0.33$/day	[94, 147, 157]
μ_A	Natural death rate of aquatic mosquito	$0.2 - 0.33$/day	[45, 46]
μ_V	Natural death rate of mosquitoes	$0.0287 - 0.25$/day	[7, 94, 157]
c_L	Mosquito death rate due to larvicides	$(0, 1)$/day	Assumed
c_A	Mosquito death rate due to adulticides	$(0, 1)$/day	[18, 20]
ϕ_V	Mosquito oviposition rate	$(1, 50)$/day	[8, 45, 46]
η_V	Vertical transmission rate	$(0, 1)$/oviposition	[41, 57]
b_V	Mosquito maturation rate	$0.05 - 0.1$/day	[8, 45, 46]
$\mathcal{K}$	Mosquito carrying capacity	$5 \times 10^1 - 9.8 \times 10^7$	[3, 94]
b_{HV}	Biting rate of mosquitoes	$0.3 - 1$/day	[7, 45, 157]
ρ_{HV}	Transmission probability from I_H to S_V	$0.5 - 1$/day	[7, 157]
ρ_{VH}	Transmission probability from I_V to S_H	$0.1 - 0.75$/day	[7, 45, 157]
β_{VH}	Infection rate of humans	$0.03 - 0.75$/day	[7, 157]
β_{HV}	Infection rate of mosquitoes	$0.15 - 1$/day	[7, 157]

Then $\dot{x} = f(x)$ defines a (positive) dynamical system on $[a, b]$. Moreover, if $[a, b]$ contains a unique equilibrium q then q is globally asymptotically stable on $[a, b]$.

Theorem 4.2.3. The extinction equilibrium $\mathcal{E}_0$ is globally asymptotically stable (GAS) when $N_0 \leq 1$ and unstable otherwise. The equilibrium $\mathcal{E}_1$ exists and it is locally asymptotically stable (LAS) when $N_0 > 1$.

Proof. By rewriting the mosquito component of (4.2.5) in the form of $\dot{x} = f(x)$ and considering the interval $[a, b] = [0, b] \in \mathbb{R}^2_+$, where $b = (q, \frac{(b_V+\mu_A+c_L)q}{\phi_V})$ with $q > 0$. Clearly $f(a) = f(0) = 0$ while

$$f(b) = \begin{pmatrix} -\frac{q^2}{\mathcal{K}}\left[b_V + \mu_A + c_L\right] \\ \\ b_V q[1 - \frac{1}{N_0}] \end{pmatrix} < 0 \text{ provided } N_0 \leq 1. \tag{4.2.12}$$

Therefore $f(b) \leq 0 \leq f(0)$ provided $N_0 \leq 1$, thus by Theorem (4.2.2), the mosquito component of the system given by (4.2.5) defines a positive dynamical system on $[0, b]$, moreover, the equilibrium $(\mathcal{E}_0)$ is GAS on $[0, b]$. Because q is arbitrary, b can be chosen such that its bigger than any $x \in \mathbb{R}^2_+$. Hence the result holds on $\mathbb{R}^2_+$. The second part of the proof follows by linearization.

The epidemiological implication of Theorem (4.2.3) is that, if the basic offspring number can brought to below 1, mosquito population goes to extinction and horizontal transmission can be avoided.

4.2.4 Disease free equilibria

The disease free equilibrium of the model given by (4.2.5) depends on N_0. If $N_0 \leq 1$ a mosquito free DFE $\mathcal{E}_2$ is obtained, while a mosquito persistent equilibrium $\mathcal{E}_3$ is obtained when $N_0 > 1$. Thus

$$\mathcal{E}_2 = \Big(S_H^*, V_H^*, E_H^*, I_H^*, R_H^*, A_N^*, A_I^*, S_V^*, I_V^*\Big) = \Big(\frac{b_H(\omega_H + \mu_H)}{K_1\mu_H}, \frac{c_V b_H}{K_1\mu_H}, 0, 0, 0, 0, 0, 0, 0\Big), \tag{4.2.13}$$

while

$$\mathcal{E}_3 = \Big(S_H^*, V_H^*, E_H^*, I_H^*, R_H^*, A_N^*, A_I^*, S_V^*, I_V^*\Big) = \Big(\frac{b_H(\omega_H + \mu_H)}{K_1\mu_H}, \frac{c_V b_H}{K_1\mu_H}, 0, 0, \mathcal{K}\big[1 - \frac{1}{N_0}\big], 0, \frac{\mathcal{K}b_V}{K_5}\big[1 - \frac{1}{N_0}\big], 0, 0\Big), \tag{4.2.14}$$

where $K_1 = c_V + \omega_H + \mu_H$, $K_2 = \gamma_H + \mu_H$, $K_3 = \delta_H + \tau_H + \mu_H$, $K_4 = b_V + \mu_A + c_L$ and $K_5 = \mu_V + c_A$.

Following [139], the linear stability of the disease free equilibria can be established using the next generation operator method on the model (4.2.5).

4.2.4.1 Stability of $\mathcal{E}_2$

For $\mathcal{E}_2$, the matrix of new infection terms and that of transition terms are respectively given by

$$F = \begin{pmatrix} 0 & 0 & 0 & 0 & \frac{\beta_{HV}(1-c_B)\left[S_H^*+V_H^*(1-\epsilon)\right]}{N_H^*} \\ 0 & 0 & 0 & 0 & 0 \\ 0 & 0 & 0 & 0 & \frac{\phi_V \eta_V}{N_0} \\ 0 & \frac{\beta_{HV}(1-c_B)S_V^*}{N_H^*} & 0 & 0 & 0 \end{pmatrix}, \tag{4.2.15}$$

$$V = \begin{pmatrix} K_2 & 0 & 0 & 0 \\ -\gamma & K_3 & 0 & 0 \\ 0 & 0 & K_4 & 0 \\ 0 & 0 & -b_V & K_5 \end{pmatrix}.$$

The next generation matrix with large domain ($K_L = FV^{-1}$) is

$$K_L = \begin{pmatrix} 0 & 0 & \frac{\beta_{HV} b_V (1-c_B)\left[S_H^*+V_H^*(1-\epsilon)\right]}{N_H^* K_4 K_5} & \frac{\beta_{HV}(1-c_B)\left[S_H^*+V_H^*(1-\epsilon)\right]}{N_H^* K_5} \\ 0 & 0 & 0 & 0 \\ 0 & 0 & \frac{\phi_V b_V \eta_V}{N_0 K_4 K_5} & \frac{\phi_V \eta_V}{N_0 K_5} \\ 0 & 0 & 0 & 0 \end{pmatrix}, \tag{4.2.16}$$

Thus using the approach of [44] with an auxiliary matrix E, the NGM (K) is

$$K = E^T K_L E = E^T F V^{-1} E = \begin{pmatrix} 0 & \frac{\beta_{HV} b_V (1-c_B)\left[S_H^*+V_H^*(1-\epsilon)\right]}{N_H^* K_4 K_5} \\ 0 & \frac{\phi_V \eta_V b_V}{N_0 K_4 K_5} \end{pmatrix}, \tag{4.2.17}$$

where

$$E = \begin{pmatrix} 1 & 0 \\ 0 & 0 \\ 0 & 1 \\ 0 & 0 \end{pmatrix},$$

Therefore the mosquito extinction basic reproduction number is $R_{vv} = \frac{\phi_V \eta_V b_V}{N_0 K_4 K_5} = \eta_V$.

Lemma 4.2.4. The mosquito extinction DFE given by $\mathcal{E}_2$ is locally asymptotically stable if the vectorial vertical transmission reproduction number $R_{vv} = \eta_V \leq 1$ and unstable otherwise [139].

The mosquito extinction disease free equilibrium is of less interest (as it is highly unattainable), it can easily be shown to be globally asymptotically stable when $N_0 \leq 1$. Next we look at the DFE obtained in the presence of mosquitoes ($N_0 > 1$).

4.2.4.2 Stability of $\mathcal{E}_3$

For the case of $\mathcal{E}_3$ when $N_0 > 1$, applying similar method to that of section 2.4.1., the NGM with large domain K_L is given by

$$\begin{pmatrix} 0 & 0 & \frac{\beta_{HV} b_V (1-c_B)\left[S_H^* + V_H^*(1-\epsilon)\right]}{N_H^* K_4 K_5} & \frac{\beta_{HV}(1-c_B)\left[S_H^* + V_H^*(1-\epsilon)\right]}{N_H^* K_5} \\ 0 & 0 & 0 & 0 \\ 0 & 0 & \frac{\phi_V \eta_V b_V}{N_0 K_4 K_5} & \frac{\phi_V \eta_V}{N_0 K_5} \\ \frac{\beta_{HV} S_V^* (1-c_B)\gamma_H}{N_H^* K_2 K_3} & \frac{\beta_{HV} S_V^* (1-c_B)}{N_H^* K_3} & 0 & 0 \end{pmatrix}. \tag{4.2.18}$$

Thus using the approach of [44] with an auxiliary matrix E, the NGM (K) is

$$K = \begin{pmatrix} 0 & \frac{\beta_{HV} b_V (1-c_B)\left[S_H^* + V_H^*(1-\epsilon)\right]}{N_H^* K_4 K_5} & \frac{\beta_{HV}(1-c_B)\left[S_H^* + V_H^*(1-\epsilon)\right]}{N_H^* K_5} \\ 0 & \frac{\phi_V \eta_V b_V}{N_0 K_4 K_5} & \frac{\phi_V \eta_V}{N_0 K_5} \\ \frac{\beta_{HV} S_V^* (1-c_B)\gamma_H}{N_H^* K_2 K_3} & 0 & 0 \end{pmatrix}, \tag{4.2.19}$$

where

$$E = \begin{pmatrix} 1 & 0 & 0 \\ 0 & 0 & 0 \\ 0 & 1 & 0 \\ 0 & 0 & 1 \end{pmatrix}.$$

Thus, the vaccinated reproduction number is

$$R_{0v} = \frac{\eta_V}{2} + \sqrt{\left[\frac{\eta_V}{2}\right]^2 + \frac{\beta_{HV}^2 S_V^* (1-c_B)^2 \gamma_H}{N_H^* K_2 K_3 K_5}\left[1 - \frac{V_H^*}{N_H^*}\epsilon\right]} \tag{4.2.20}$$

The threshold quantity, R_{0v} is the average number of new secondary cases that one infection can produce in a totally naive population, where a fraction of the population is vaccinated.

4.2.4.3 Threshold analysis and vaccine impact

Here we analyse impact of a single dose and a fractional dosing of vaccine. Since not all vaccines have positive impact in a population, it is therefore instructive to first of all assess the impact of YF vaccine. In the absence of vaccination ($S_H^* = N_H^*$ when $V_H^* = 0$), the vaccinated reproduction reduces to

$$R_0 = R_{0v}\Big|_{V_H^*=0} = \frac{\eta_V}{2} + \sqrt{\left(\frac{\eta_V}{2}\right)^2 + \frac{\beta_{HV}^2 S_V^* (1-c_B)^2 \gamma_H}{N_H^* K_2 K_3 K_5}}. \tag{4.2.21}$$

Notice that $R_{0v} \leq R_0$ since $\frac{V_H^* \epsilon}{N_H^*} \geq 0$. Thus, vaccination of individuals will have positive impact in the community by reducing the value of the associated reproduction number R_0.

Furthermore, the impact of vaccination can be analysed qualitatively by differentiating R_{0v} with respect to the fraction of vaccinated individuals (V). It can be shown that

$$\frac{\partial R_{0v}}{\partial V} = \frac{-\beta_{HV}^2 S_V^*(1-c_B)^2\gamma_H\epsilon}{2K_2K_3K_5N_H^*\sqrt{\left[\frac{\eta_V}{2}\right]^2 + \frac{\beta_{HV}^2 S_V^*(1-c_B)^2\gamma_H}{(N_H^*)^2K_2K_3K_5}\left[S_H^* + V_H^*(1-\epsilon)\right]}} < 0. \quad (4.2.22)$$

Thus, R_{0v} is a decreasing function of V. Since the reproduction number measures disease burden, for whatever fraction of the population that is vaccinated with whatever level of efficacy, the vaccination will have a positive impact in disease control.

4.2.4.4 Standard dosing

Based on the available clinical data [144], the minimum standard dose administered should preferentially contain 3000 international units (IU)/dose, but no less than 1000 IU/dose. Let $V = \frac{V_H^*}{N_H^*}$ $(V \leq 1)$ be the fraction of the vaccinated individuals at the steady state when standard dose of YF vaccine is issued. Then solving for $R_{0v} = 1$ we obtained

$$V_c = \frac{1}{\epsilon}\Big[1 - \frac{\{1-\eta_V\}N_H^*K_2K_3K_5}{\beta_{HV}^2 S_V^*(1-c_B)^2\gamma_H}\Big]. \quad (4.2.23)$$

Thus, for the vaccination to be effective in bringing $R_{0v} < 1$, the fraction of vaccinated individuals (V_c) at steady state must be greater than the vaccinated threshold ratio $(V > V_c)$ defined in 4.2.23.

Notice that if $\eta_V = 1$, that is the case when all eggs laid by infected female mosquitoes are infected, then there is no amount of vaccination that will make $R_{0v} < 1$ (in this settings) since the critical vaccination rate reduces to $V_c = \frac{1}{\epsilon} > 1$.

Lemma 4.2.5. The DFE, $\mathcal{E}_3$, of the model (4.2.5) is locally-asymptotically stable if $\eta_V < 1$ and $V > V_c$. It is unstable otherwise.

The proof follows from Theorem 2 of [139] and the fact that $R_{0v} < 1$ if and only if $\eta_V < 1$ and $V > V_c$.

4.2.4.5 Fractional dosing

The best way to stretch vaccine supplies and protect as many people as possible to stop the spread of yellow fever in emergency situations is by using fractional dosing. Based on the available evidence, the Strategic Advisory Group of Experts (SAGE) on Immunization affirms that a fractional dose can be used as part of an exceptional response when there is a large outbreak and a shortage of vaccine [144, 147]. In the case of dose fractionation, a smaller amount of antigen would be used per dose in order to increase the number of persons who can be vaccinated with a given quantity of vaccine. Studies show that the yellow fever vaccine given as one fifth of the regular dose, still provides full immunity against the disease for at least 12 months and likely longer [144, 147]. This strategy was previously proposed to extend pre-pandemic influenza vaccine supplies [152]. Suppose each dose of vaccination is fractioned into m number of doses, so that the efficacy of the fractioned vaccine (e_{Vf}) becomes

$e_{Vf} = \frac{\epsilon}{m}$, then

$$V_{cf} = \frac{m}{\epsilon}\Big[1 - \frac{\{1-\eta_V\}N_H^* K_2 K_3 K_5}{\beta_{HV}^2 S_V^*(1-c_B)^2\gamma_H}\Big] = m \times V_c > V_c$$

and

$$e_{Vcf} = \frac{m}{V}\Big[1 - \frac{\{1-\eta_V\}N_H^* K_2 K_3 K_5}{\beta_{HV}^2 S_V^*(1-c_B)^2\gamma_H}\Big] = m \times e_{Vc} > e_{Vc}.$$

Figure 4.2 shows the simulation of the vaccinated reproduction number as a function of vaccine efficacy with single dose and fractionated 2-fold. Simulation of $R_{0V}(\epsilon)$ with fractioned 3-fold and 5-fold are depicted in Figure 4.3. Although when $\epsilon = 0$, all the simulations have the same value of $R_{0V} = R_0$ (about 1.143), the vaccinated reproduction number becomes less than unity when $\epsilon > 0.4$ (for a single dose), while for the case of 2-fold fractionated vaccine, ϵ needs to be about 0.7 for R_{0V} to be less than unity, while for 3-fold and 5-fold fractionated vaccine, a higher vaccine efficacy, ϵ is required to possibly bring R_{0V} to a value below unity. This result is consistent with those in [144],which stated that a fractional YF vaccination does not meet YF vaccination requirements under the International Health Regulations (IHR).

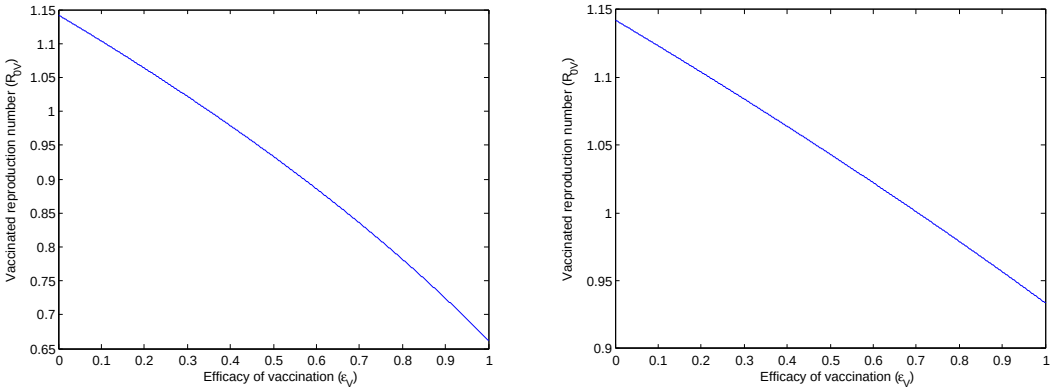

Figure 4.2: Vaccinated reproduction number (R_{0V}) as a function of efficacy of vaccination with standard dose and fractionated 2-fold vaccines.

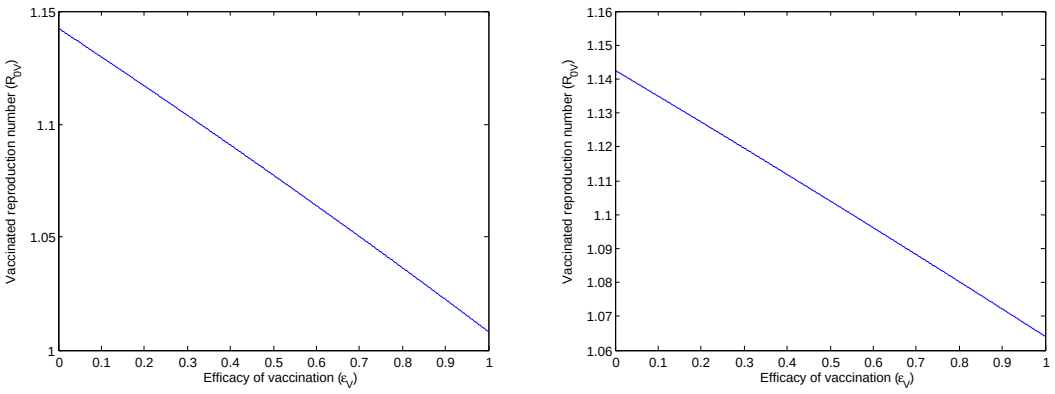

Figure 4.3: Vaccinated reproduction number (R_{0V}) as a function of efficacy of vaccination with fractionated 3-fold and 5-fold vaccines.

4.2.4.6 Global stability of $\mathcal{E}_3$

Here, conditions for global asymptotic stability of the DFE ($\mathcal{E}_3$) are explored using the method described by [77]. The same approach was employed by [45, 46, 78]. Using the property of the DFE, the system given by (4.2.5) can be rewritten in a pseudo-triangular form as follows,

$$\begin{aligned}\frac{dS_H}{dt} &= b_H - c_V S_H - \beta_{HV}(1-c_B)\frac{I_V}{N_H}S_H - \mu_H S_H,\\ &= b_H - c_V S_H - \beta_{HV}(1-c_B)\frac{I_V}{N_H}S_H - \mu_H S_H - b_H + c_V S_H^* + \mu_H S_H^*,\\ &= -K_1(S_H - S_H^*) - \beta_{HV}(1-c_B)\frac{I_V}{N_H}S_H.\end{aligned} \tag{4.2.24}$$

Similarly the equation of vaccinated humans is rewritten as

$$\begin{aligned}\frac{dV_H}{dt} &= c_V S_H - \beta_{HV}(1-c_B)(1-\epsilon)\frac{I_V}{N_H}V_H - \mu_H V_H,\\ &= c_V S_H - \beta_{HV}(1-c_B)(1-\epsilon)\frac{I_V}{N_H}V_H - \mu_H V_H - c_V S_H^* + \mu_H V_H^*,\\ &= -\mu_H(V_H - V_H^*) + c_V(S_H - S_H^*) - \beta_{HV}(1-c_B)(1-\epsilon)\frac{I_V}{N_H}V_H.\end{aligned} \tag{4.2.25}$$

Likewise the equation of non-infectious aquatic mosquitoes can be rewritten as

$$\begin{aligned}\frac{dA_N}{dt} =&\phi_V\Big(1-\frac{A}{\mathcal{K}}\Big)S_V+\phi_V\Big(1-\frac{A}{\mathcal{K}}\Big)(1-\eta_V)I_V-b_VA_N-\mu_AA_N-c_LA_N,\\ =&-(A_N-A_N^*)\Big(K_4+\phi_V\frac{S_V}{\mathcal{K}}\Big)+\frac{\phi_V}{N_0}(S_V-S_V^*)+\phi_V(1-\eta_V)\Big(1-\frac{A}{\mathcal{K}}\Big)I_V\\ &-\phi_V\frac{S_V}{\mathcal{K}}A_I,\end{aligned} \tag{4.2.26}$$

while

$$\begin{aligned}\frac{dS_V}{dt} &= b_VA_N-\beta_{HV}(1-c_B)\frac{I_H}{N_H}S_V-\mu_VS_V-c_AS_V,\\ &=-K_5(S_V-S_V^*)+b_V(A_N-A_N^*)-\beta_{HV}(1-c_B)\frac{I_H}{N_H}S_V.\end{aligned} \tag{4.2.27}$$

Following the above simplification, the system given by (4.2.5) can therefore be re-written in a pseudo-triangular form as

$$\begin{cases}\dot{\mathbf{x}_1} &= A_{11}(\mathbf{x})\big(\mathbf{x}_1-\mathbf{x}_1^*\big)+A_{12}(\mathbf{x})\mathbf{x}_2\\ \\ \dot{\mathbf{x}_2} &= A_{22}(\mathbf{x})\mathbf{x}_2\end{cases} \tag{4.2.28}$$

Where $\mathbf{x}_1=(S_H,V_H,R_H,A_N,S_V)^T$ represents the naive (uninfected) component of the model (4.2.5), $\mathbf{x}_2=(E_H,I_H,A_I,I_V)^T$ represents the infectious part of (4.2.5),

$\mathbf{x}_1^* = (S_H^*, V_H^*, R_H^*, A_N^*, S_V^*)^T$ is the DFE and

$$A_{11}(\mathbf{x}) = \begin{pmatrix} -K_1 & \omega_H & 0 & 0 & 0 \\ c_V & -\mu_H & 0 & 0 & 0 \\ 0 & 0 & -\mu_H & 0 & 0 \\ 0 & 0 & 0 & -(K_4 + \frac{\phi_V S_V}{\mathcal{K}}) & \frac{\phi_V}{N_0} \\ 0 & 0 & 0 & b_V & -K_5 \end{pmatrix},$$

$$A_{12}(\mathbf{x}) = \begin{pmatrix} 0 & 0 & 0 & -\beta_{HV}(1-c_B)\frac{S_H}{N_H} \\ 0 & 0 & 0 & -\beta_{HV}(1-c_B)(1-\epsilon)\frac{S_H}{N_H} \\ 0 & \tau_H & 0 & 0 \\ 0 & 0 & -\frac{\phi_V S_V}{\mathcal{K}} & \phi_V(1-\eta_V)\left(1-\frac{A}{\mathcal{K}}\right) \\ 0 & -\beta_{HV}(1-c_B)\frac{S_V}{N_H} & 0 & 0 \end{pmatrix}, \quad (4.2.29)$$

$$A_{22}(\mathbf{x}) = \begin{pmatrix} -K_2 & 0 & 0 & \frac{\beta_{HV}(1-c_B)\left[S_H+(1-\epsilon)V_H\right]}{N_H} \\ \gamma_H & -K_3 & 0 & 0 \\ 0 & 0 & -K_4 & \phi_V\eta_V\left(1-\frac{A}{\mathcal{K}}\right) \\ 0 & \beta_{HV}(1-c_B)\frac{S_V}{N_H} & b_V & -K_5 \end{pmatrix}.$$

Theorem 4.2.6. Consider (4.2.5). Let $\Omega \subset \mathbb{R}_+^{n_1+n_2}$ be a positively-invariant set. If

1. The system (4.2.5) is defined on the positively invariant set $\Omega \subset \mathbb{R}_+^{n_1+n_2}$.
2. The sub-system $\dot{\mathbf{x}} = A_{11}(\mathbf{x})(\mathbf{x}_1 - \mathbf{x}_1^*)$ is globally asymptotically stable at the equilibrium $\mathbf{x}_1^*$.
3. For any $\mathbf{x} \in \Omega$, the matrix $A_{22}(\mathbf{x})$ is Metzler and irreducible.
4. There exists an upper bound matrix $\bar{A_{22}}$ for the set $\mathcal{M} = \{A_{22}(\mathbf{x})/\mathbf{x} \in \Omega\}$, with the property that either $\bar{A_{22}} \notin \mathcal{M}$ or if $\bar{A_{22}} \in \mathcal{M}$(i.e., $\bar{A_{22}} = \max_\Omega \mathcal{M}$), then for $\mathbf{x}^* \in \Omega$ such that $\bar{A_{22}} = A_{22}(\mathbf{x}^*)$, then $\mathbf{x}^* \in \mathbb{R}^7 \times \{0\}$ (the DFE sub-manifold contains the points where the maximum is attained).
5. The stability modulus of $\bar{A_{22}}$ satisfies $\alpha(\bar{A_{22}}) \leq 0$.

Then, the associated DFE is GAS in Ω [45, 77].

Recall that the model given by (4.2.5) is defined on a positively invariant domain given by Ω in (4.2.7). Also straightforward computation shows that the eigenvalues of $A_{11}(x)$ are real and negative. Therefore conditions 1 and 2 of (4.2.6) are satisfied, for condition 3 of (4.2.6), the following definition is used.

Definition 4.2.1. A square matrix $\mathbf{A}$ is said to be reducible if it has the form

$$\mathbf{A} = \begin{pmatrix} \mathbf{A}_1 & \mathbf{A}_2 \\ 0 & \mathbf{A}_3 \end{pmatrix} \quad (4.2.30)$$

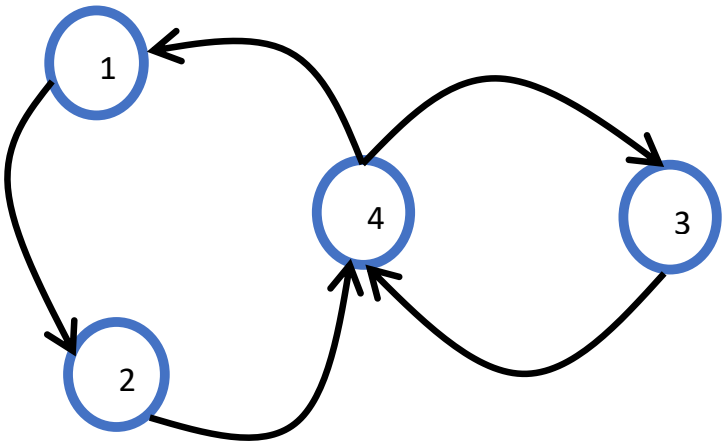

Figure 4.4: Strongly connected directed graph (di-graph) associated with the matrix $A_{22}(\mathbf{x})$. The square matrix $A_{22}(\mathbf{x})$ is irreducible (as the figure is strongly connected).

where $\mathbf{A}_1$ and $\mathbf{A}_3$ are square matrices of order at least 1 or if $\mathbf{A}$ can be transformed into the form (4.2.30) by simultaneous permutations of rows and columns [55]. It is irreducible otherwise. Alternatively, A square matrix is irreducible if and only if its associated digraph is strongly connected.

Figure 4.4 is the associated digraph of the matrix $A_{22}(x)$, and it is clear that it is strongly connected. Thus condition 3 is satisfied. Likewise since $S_V \leq \frac{\mathcal{K}b_V}{\mu_V+c_A} = S_V^* \frac{N_0}{N_0-1}$ in Ω, $A \leq \mathcal{K}$, $S_H + (1-\epsilon)V_H \leq N_H$, and $L_H^* = \frac{b_H}{\delta_H+\mu_H} \leq N_H \leq \frac{b_H}{\mu_H} = N_H^*$ then the matrix

$$\bar{A}_{22}(\mathbf{x}) = \begin{pmatrix} -K_2 & 0 & 0 & \beta_{HV}(1-c_B) \\ \gamma_H & -K_3 & 0 & 0 \\ 0 & 0 & -K_4 & \phi_V \eta_V \\ 0 & \frac{\beta_{HV}(1-c_B)S_V^* N_0}{L_H^*(N_0-1)} & b_V & -K_5 \end{pmatrix}, \tag{4.2.31}$$

is an upper bound of $A_{22}(x)$. For condition 5 of Theorem (4.2.6), the following result of [77] is applied.

Lemma 4.2.7. Let $\mathcal{M}$ be a Metzler matrix which is block decomposed

$$\mathcal{M} = \begin{pmatrix} \mathbb{A} & \mathbb{B} \\ \mathbb{C} & \mathbb{D} \end{pmatrix} \tag{4.2.32}$$

where $\mathbb{A}$ and $\mathbb{D}$ are square matrices. Then $\mathcal{M}$ is Metzler stable if and only if $\mathbb{A}$ and $\mathbb{D} - \mathbb{C}\mathbb{A}^{-1}\mathbb{B}$ are Metzler stable.

In the case of $\bar{A}_{22}(x)$ defined above, we have

$$\mathbb{A} = \begin{pmatrix} -K_2 & 0 \\ \gamma_H & -K_3 \end{pmatrix}, \quad \mathbb{B} = \begin{pmatrix} 0 & \beta_{HV}(1-c_B) \\ 0 & 0 \end{pmatrix}, \quad \mathbb{C} = \begin{pmatrix} 0 & 0 \\ 0 & \frac{\beta_{HV}(1-c_B)S_V^* N_0}{L_H^*(N_0-1)} \end{pmatrix},$$

$$\mathbb{D} = \begin{pmatrix} -K_4 & \phi_V \eta_V \\ b_V & -K_5 \end{pmatrix}, \quad \mathbb{D} - \mathbb{C}\mathbb{A}^{-1}\mathbb{B} = \begin{pmatrix} -K_4 & \phi_V \eta_V \\ b_V & -K_5\big[1 - \frac{\beta_{HV}^2(1-c_B)^2 S_V^* N_0 \gamma_H}{L_H^* K_2 K_3 K_5 (N_0-1)}\big] \end{pmatrix}. \tag{4.2.33}$$

Therefore, $\mathbb{D} - \mathbb{C}\mathbb{A}^{-1}\mathbb{B}$ is Metzler matrix if

$$\frac{\beta_{HV}^2(1-c_B)^2 S_V^* N_0 N_H^* \gamma_H}{L_H^* K_2 K_3 K_5 (N_0-1) N_H^*} = R_{HV} R_{VH} \frac{N_0 N_H^*}{L_H^*(N_0-1)} < 1 \tag{4.2.34}$$

and it is stable if

$$\begin{gathered} K_4 K_5 \Big(1 - R_{HV} R_{VH} \frac{N_0 N_H^*}{L_H^*(N_0-1)} - R_{VV} N_0\Big) > 0 \\ \text{which implies } R_{HV} R_{VH} \frac{N_0 N_H^*}{L_H^*(N_0-1)} + R_{VV} N_0 \leq 1. \end{gathered} \tag{4.2.35}$$

It should be noted that, condition (4.2.35) is a generalization of condition (4.2.34). Thus, satisfying condition (4.2.35) is sufficient for the GAS of the DFE, which is also equivalent to

$$R_{HV} R_{VH} + R_{VV}(N_0 - 1) \leq \Big(1 - \frac{1}{N_0}\Big) \frac{L_H^*}{N_H^*}. \tag{4.2.36}$$

Theorem 4.2.8. The disease free equilibrium $(\mathcal{E}_3)$ of the model (4.2.5) is globally asymptotically stable if $R_{HV} R_{VH} \frac{N_0 N_H^*}{L_H^*(N_0-1)} + R_{VV} N_0 \leq 1$.

Corollary 3. Consider the subset Ω^* of Ω defined in (4.2.7) given by

$$\begin{aligned} \Omega^* = \Bigg\{ & S_H, V_H, E_H, I_H, R_H, A_N, A_I, S_V, I_V \in \mathbb{R}_+^9 : S_H + V_H + E_H + I_H + R_H \leq \\ & \frac{b_H}{\mu_H}, \quad A_N \leq \mathcal{K}, \quad A_I \leq \mathcal{K}, \quad S_V + I_V \leq \frac{\mathcal{K} b_V}{\mu_V + c_A}, \quad S_V \leq S_V^* = \\ & \frac{\mathcal{K} b_V}{(\mu_V + c_A)}[1 - \frac{1}{N_0}], \quad (1 - \frac{1}{N_0}) \leq \frac{A}{\mathcal{K}} \Bigg\}, \end{aligned} \tag{4.2.37}$$

then the equilibrium $(\mathcal{E}_3)$ is globally asymptotically stable in the positively invariant set Ω^* if $\delta_H = 0$ and $\mathbb{R}_0 \leq 1$.

4.2.5 Type reproduction numbers

If K is the next generation matrix with large domain and hosts 1, 2 and 3 represent the populations of E_H, A_I and I_V. The type i reproduction number is given by

$$T_i = e^T K(I-(I-P)K)^{-1}e, \tag{4.2.38}$$

where I is an identity matrix, P is a projection matrix and e is a unit vector with all elements equal to zero except the ith. Let

$$K = \begin{pmatrix} 0 & 0 & k_{13} & k_{14} \\ 0 & 0 & 0 & 0 \\ 0 & 0 & k_{33} & k_{34} \\ k_{41} & k_{42} & 0 & 0 \end{pmatrix},$$

where,

$$k_{13} = \frac{\beta_{HV} b_V (1-c_B)\left[S_H^* + (1-\epsilon)V_H^*\right]}{N_H^* K_4 K_5}, \quad k_{14} = \frac{\beta_{HV}(1-c_B)\left[S_H^* + (1-\epsilon)V_H^*\right]}{N_H^* K_5},$$

$$K_{33} = \eta_V, \quad k_{34} = \frac{\phi_V \eta_V}{N_0 K_5}, \quad k_{41} = \frac{\beta_{HV} S_V^* (1-c_B)\gamma_H}{N_H^* K_2 K_3}, \quad k_{42} = \frac{\beta_{HV} S_V^* (1-c_B)}{N_H^* K_3}.$$

Notice that k_{ij} is expected number of cases of type i produced by one infected individual of type j, so that from (4.2.38) the type-reproduction number for infected humans is

$$\begin{aligned} T_1 &= k_{14}k_{41} + \frac{k_{13}k_{34}k_{41}}{1-k_{33}} \\ &= \frac{\beta_{HV}^2 (S_V^*)^2 (1-c_B)^2}{(N_H^*)^2 K_2^2} + \frac{\beta_{HV}^2 S_V^* (1-c_B)^2 b_V \gamma_V \phi_V \eta_V \left[S_H^* + (1-\epsilon)V_H^*\right]}{(N_H^*)^2 N_0 K_2 K_3 K_4 K_5^2 (1-\eta_V)}, \end{aligned}$$

Observe that $R_{0v} < 1$ implies

$$\frac{\beta_{HV}^2 S_V^* (1-c_B)^2 \left[S_H^* + (1-\epsilon)V_H^*\right]}{(N_H^*)^2 K_2 K_5} + \eta_V < 1 \tag{4.2.39}$$

Thus $T_1 < 1$ implies $R_{0v} < 1$. Similarly it can be shown that $T_3 < 1$ and $T_4 < 1$ implies $R_{0v} < 1$.

4.2.6 Existence of endemic equilibrium

Let $\lambda_V^{**} = \frac{\beta_{HV}(1-c_B)I_H^{**}}{N_H^{**}}$, $\lambda_H^{**} = \frac{\beta_{HV}(1-c_B)I_V^{**}}{N_H^{**}}$ and also recall that

$$\frac{dA}{dt} = \phi_V\left(1-\frac{A}{\mathcal{K}}\right)(S_V + I_V) - b_V A - \mu_A A - c_L A. \tag{4.2.40}$$

So that by solving for the fixed point of S_V and I_V in terms of A when $\lambda_V^{**} \neq 0$ we have

$$S_V^{**} = \frac{b_V A_N^{**}}{\lambda_V + K_5}, \quad I_V^{**} = \frac{b_V(\lambda_V^{**} + K_5)A_I^{**} + \lambda_V^{**} b_V A_N^{**}}{K_5(\lambda_V^{**} + K_5)}, \quad S_V^{**} + I_V^{**} = \frac{b_V A^{**}}{K_5}. \tag{4.2.41}$$

Thus, from (4.2.5) and (4.2.41), a unique non-zero endemic equilibrium is obtained when $N_0 > 1$ and it is given by

$$\begin{aligned}
S_H^{**} &= \frac{b_H + \omega_H V_H^*}{\lambda_H^{**} + \mu_H}, \quad V_H^{**} = \frac{b_H c_V}{\Big(\lambda_H^{**}(1-\epsilon) + \omega_H + \mu_H\Big)\big[\lambda_H^{**} + \mu_H\big]}, \\
E_H^{**} &= \frac{\lambda_H^{**}\Big(S_H^{**} + V_H^{**}(1-\epsilon)\Big)}{K_2}, \quad I_H^{**} = \frac{\lambda_H^{**}\gamma_H\Big(S_H^{**} + V_H^{**}(1-\epsilon)\Big)}{K_2 K_3}, \\
R_H^{**} &= \frac{\lambda_H^{**}\gamma_H\tau_H\Big(S_H^{**} + V_H^{**}(1-\epsilon)\Big)}{K_2 K_3 \mu_H}, \quad A^{**} = \frac{\mathcal{K}\Big(N_0 - 1\Big)}{N_0}, \\
A_N^{**} &= \frac{\phi_V\Big(S_V^{**} + \epsilon I_V^{**}\Big)}{N_0 K_4}, \quad A_I^{**} = \frac{\phi_V \eta_V I_V^{**}}{N_0 K_4}, \quad S_V^{**} = \frac{b_V\phi_V\Big(S_V^{**} + \epsilon I_V^{**}\Big)}{\Big(\lambda_V^{**} + K_5\Big)N_0 K_4}, \\
I_V^{**} &= \frac{\lambda_V^{**} K_2 b_V A^{**} + b_V\mu_V\phi_V\Big(1 - \frac{A^{**}}{\mathcal{K}}\Big)[1-\epsilon]I_V^{**}}{\Big(\lambda_V^{**} + \mu_V\Big)K_2\mu_V},
\end{aligned} \tag{4.2.42}$$

4.3 YF model for optimal control

Usually, incidences of YF and other vector borne diseases are seasonality dependent with their peaks during warm and rainy seasons, therefore it is reasonable to integrate time dependent controls in the model, the goal of which is to show the possibility of implementing time dependent controls while minimizing implementation cost.

Let the time dependent effort in preventing human-mosquito contacts through the use of treated bed nets be $u_1(t)$, so that the contact rate between mosquitoes and humans reduces by a factor $(1-u_1(t))$ where $0 \leq u_1(t) \leq 1$. The effort in vaccinating humans is $u_2(t) : 0 \leq u_2(t) \leq 1$. Similarly, the effort in the application of larvicides is $u_3(t) : 0 \leq u_3(t) \leq 1$, while that of spraying adulticides is $u_4(t) : 0 \leq u_4(t) \leq 1$. For instance, there is no any effort in controlling mosquitoes when $u_3(t) = u_4(t) = 0$, while aquatic and mature mosquitoes die at maximum possible rates c_L and c_A respectively, when $u_3(t) = u_4(t) = 1$. Maximum control is attained by the use of bed nets and vaccination when $u_1(t) = 1$ and $u_2(t) = 1$, respectively and no effort invested when $u_1(t) = u_2(t) = 0$. The autonomous system given by (4.2.5) is extended to include the aforementioned time dependent controls. Let $\Phi(t) = \omega_H(1 - u_2(t))$, then the

non-autonomous version of the model (4.2.5) is given by

$$\text{Humans}\begin{cases}\dfrac{dS_H}{dt} = b_H + \Phi(t)V_H - \beta_{HV}u_1(t)(1-c_B)\dfrac{I_V S_H}{N_H} - \mu_H S_H - c_V u_2(t)S_H,\\ \dfrac{dV_H}{dt} = c_V u_2(t)S_H - \beta_{HV}u_1(t)(1-c_B)(1-\epsilon)\dfrac{I_V V_H}{N_H} - \Phi(t)V_H - \mu_H V_H,\\ \dfrac{dE_H}{dt} = \beta_{HV}u_1(t)(1-c_B)\dfrac{I_V}{N_H}\Big[S_H + (1-\epsilon)V_H\Big] - \gamma_H E_H - \mu_H E_H,\\ \dfrac{dI_H}{dt} = \gamma_H E_H - \delta_H I_H - \tau_H I_H - \mu_H I_H,\\ \dfrac{dR_H}{dt} = \tau_H I_H - \mu_H R_H,\end{cases} \tag{4.3.43}$$

$$\text{Mosquitoes}\begin{cases}\dfrac{dA_N}{dt} = \phi_V\Big(1-\dfrac{A}{\mathcal{K}}\Big)\Big[S_V + (1-\eta_V)I_V\Big] - b_V A_N - \mu_A A_N - u_3(t)c_L A_N,\\ \dfrac{dA_I}{dt} = \phi_V\eta_V\Big(1-\dfrac{A}{\mathcal{K}}\Big)I_V - b_V A_I - \mu_A A_I - u_3(t)c_L A_I,\\ \dfrac{dS_V}{dt} = b_V A_N - \beta_{HV}u_1(t)(1-c_B)\dfrac{I_H}{N_H}S_V - \mu_V S_V - u_4(t)c_A S_V,\\ \dfrac{dI_V}{dt} = \beta_{HV}u_1(t)(1-c_B)\dfrac{I_H}{N_H}S_V + b_V A_I - \mu_V I_V - u_4(t)c_A I_V.\end{cases}$$

Following the non-autonomous system given by (4.3.43), an optimal control problem is formulated with the following objective (cost) functional

$$J\big(u_1(t),u_2(t),u_3(t),u_4(t)\big) = \int_0^T \Big(B_1E_H + B_2I_H + B_3A + B_4N_V + B_5c_V S_H + D_1u_1^2 + D_2u_2^2 + D_3u_3^2 + D_4u_4^2\Big)dt. \tag{4.3.44}$$

The interval $[0,T]$ represents the time through which various control measures are implemented. The cost incurred due to human infection of YF (which is proportional to the number of infected individuals) over the period of intervention is given by

$$\int_0^T \Big(B_1E_H + B_2I_H\Big)dt,$$

where B_1 and B_2 are positive weight constants associated with exposed and infected humans respectively. Similarly, the cost due to the presence of mosquitoes in the community, which is proportional to the number of aquatic and adult mosquitoes is given by

$$\int_0^T \Big(B_3A + B_4N_V\Big)dt,$$

where B_3 and B_4 are positive weight constants. Because of the short supply of YF vaccine, in order to optimize the available vaccines, there is need to minimize the total number of vaccines used over the period of intervention, thus the integral

$$\int_0^T B_5 c_V(t) S_H dt,$$

which measures the total number of vaccinated individuals during the period of intervention is included in the objective functional, with B_5 being a positive weight constant. The positive terms D_1, D_2, D_3 and D_4 are weight constants for efforts in the use of bed nets, vaccination, larvicides and adulticides respectively, and regularize the optimal control. $D_1 u_1^2$, $D_2 u_2^2$, $D_3 u_3^2$, and $D_4 u_4^2$ describe the cost associated with the aforementioned prevention and control measures. The degree of the cost functions follow from the non-linearity of controls and the convexity of quadratic functions [128]. Similar assumption has been used in optimal control problems in epidemiology, see for instance [18, 85, 107, 82, 119, 128] and some of the references therein.

The aim is to minimize infected humans and total mosquito population while optimizing limited vaccines and keeping the cost of vaccination, use of treated nets and application of pesticides low. Therefore we seek to optimize u_1^*, u_2^*, u_3^* and u_4^* such that

$$J(u_1^*, u_2^*, u_3^*, u_4^*) = \min_{u_1,u_2,u_3,u_4} \Big\{ J(u_1, u_2, u_3, u_4) | u_1, u_2, u_3, u_4 \in \mathcal{G} \Big\} \tag{4.3.45}$$

where

$$\mathcal{G} = \Big\{ (u_1, u_2, u_3, u_4) | u_i : [0, T] \longrightarrow [0, 1] \text{ is Lebesgue measurable, } i = 1, 2, 3, 4 \Big\}$$

is the control set. The impact of each control does depends on adherence and effort, if for example $u_1 = 1$, production and distribution of bed nets is at maximum, but its impact also depends on c_B, likewise the remaining control functions.

4.3.0.1 Existence of optimal control

The existence of optimal control solution can be established using Theorem 4.1 and Corollary 4.1 of [56].

Theorem 4.3.1. There exist an optimal control u_1^*, u_2^*, u_3^*, u_4^* and corresponding solution S_H^*, V_H^*, E_H^*, I_H^*, R_H^*, A_N^*, A_I^*, S_V^* and I_V^* that minimizes $J(u_1, u_2, u_3, u_4)$ over $\mathcal{G}$.

Proof. Clearly the set of controls and state variables are non-empty and the control set $\mathcal{G}$ is closed and convex. The integrand of the objective functional is convex on $\mathcal{G}$. Furthermore, the model is linear in the control variables and bounded by a linear system in the state variables, thus, the existence of an optimal control is guaranteed [18, 56].

4.3.1 Optimality system

The necessarily conditions that optimal controls and their corresponding states must satisfy are derived using Pontryagin's Maximum Principle [107, 118], where the problem of finding time-dependent control variables $u_1^*(t)$, $u_2^*(t)$, $u_3^*(t)$ and $u_4^*(t)$ that minimize J is equivalent to the problem of minimizing the Hamiltonian function defined as

$$H(t, \mathbf{x}, \mathbf{u}, \lambda) = g(t, \mathbf{x}, \mathbf{u}) + \lambda(t) f(t, \mathbf{x}, \mathbf{u})$$

where $g(t, \mathbf{x}, \mathbf{u})$ is the integrand of the objective functional (4.3.44) and $\lambda(t)$ is the adjoint vector such that $\lambda(t) = \Big(\lambda_{S_H}(t), \lambda_{V_H}(t), \lambda_{E_H}(t), \lambda_{I_H}(t), \lambda_{R_H}(t), \lambda_{A_N}(t), \lambda_{A_I}(t), \lambda_{S_V}(t), \lambda_{I_V}(t)\Big)$ satisfies

$$\frac{d\lambda_{S_H}}{dt} = -\frac{\partial H}{\partial S_H}, \quad \frac{d\lambda_{V_H}}{dt} = -\frac{\partial H}{\partial V_H}, \quad ..., \quad \frac{d\lambda_{I_V}}{dt} = -\frac{\partial H}{\partial I_V}.$$

The optimality equation is given by

$$\frac{\partial H}{\partial u_1} = \frac{\partial H}{\partial u_2} = \frac{\partial H}{\partial u_3} = \frac{\partial H}{\partial u_4} = 0,$$

and transversality conditions as $\lambda_{S_H}(T) = \lambda_{V_H}(T) = ... = \lambda_{I_V}(T) = 0$. Therefore,

$$\begin{aligned}
H =& B_1 E_H + B_2 I_H + B_3 A + B_4 N_V + B_5 c_V S_H + D_1 u_1^2 + D_2 u_2^2 + D_3 u_3^2 + D_4 u_4^2 \\
&+ \lambda_{S_H}\Big[b_H + \Phi(t) V_H - c_V u_2(t) S_H - \beta_{HV} u_1(t)(1 - c_B)\frac{I_V}{N_H} S_H - \mu_H S_H\Big] \\
&+ \lambda_{V_H}\Big[c_V u_2(t) S_H - \beta_{HV} u_1(t)(1 - c_B)(1 - \epsilon)\frac{I_V}{N_H} V_H - \Phi(t) V_H - \mu_H V_H\Big] \\
&+ \lambda_{E_H}\Big[\beta_{HV} u_1(t)(1 - c_B)\frac{I_V}{N_H}\Big\{S_H + (1 - \epsilon) V_H\Big\} - \gamma_H E_H - \mu_H E_H\Big] \\
&+ \lambda_{I_H}\Big[\gamma_H E_H - \delta_H I_H - \tau_H I_H - \mu_H I_H\Big] + \lambda_{R_H}\Big[\tau_H I_H - \mu_H R_H\Big] \\
&+ \lambda_{A_N}\Big[\phi_V\Big(1 - \frac{A}{\mathcal{K}}\Big)\Big[S_V + (1 - \eta_V) I_V\Big] - b_V A_N - \mu_A A_N - u_3(t) c_L A_N\Big] \\
&+ \lambda_{A_I}\Big[\phi_V \eta_V\Big(1 - \frac{A}{\mathcal{K}}\Big) I_V - b_V A_I - \mu_A A_I - u_3(t) c_L A_I\Big] \\
&+ \lambda_{S_V}\Big[b_V A_N - \beta_{HV} u_1(t)(1 - c_B)\frac{I_H}{N_H} S_V - \mu_V S_V - u_4(t) c_A S_V\Big] \\
&+ \lambda_{I_V}\Big[\beta_{HV} u_1(t)(1 - c_B)\frac{I_H}{N_H} S_V + b_V A_I - \mu_V I_V - u_4(t) c_A I_V\Big],
\end{aligned} \tag{4.3.46}$$

where $\lambda_{S_H}, ...\lambda_{I_V}$ are adjoint functions.

Theorem 4.3.2. Given an optimal control $(u_1^*, u_2^*, u_3^*, u_4^*)$ and the corresponding state solutions of the non-autonomous system given by (4.3.43), there exist adjoint functions

satisfying

$$\frac{d\lambda_{S_H}}{dt} =\mu_H\lambda_{S_H} + u_2(t)c_V\big[\lambda_{S_H} - \lambda_{V_H}\big] + \beta_{HV}u_1(t)(1-c_B)\big[\lambda_{S_H} - \lambda_{E_H}\big]\frac{I_V}{N_H} + \beta_{HV}$$
$$u_1(t)(1-c_B)\big[\lambda_{I_V} - \lambda_{S_V}\big]\frac{I_H S_V}{(N_H)^2} + \beta_{HV}u_1(t)(1-c_B)\big[\lambda_{E_H} - \lambda_{S_H}\big]\frac{I_V S_H}{(N_H)^2} +$$
$$\beta_{HV}u_1(t)(1-c_B)(1-\epsilon)\big[\lambda_{E_H} - \lambda_{V_H}\big]\frac{I_V V_H}{(N_H)^2} - B_5 c_V,$$

$$\frac{d\lambda_{V_H}}{dt} =\mu_H\lambda_{V_H} + \beta_{HV}u_1(t)(1-c_B)\big[\lambda_{E_H} - \lambda_{S_H}\big]\frac{I_V S_H}{N_H^2} + \beta_{HV}u_1(t)(1-c_B)\big[\lambda_{I_V} -$$
$$\lambda_{S_V}\big]\frac{I_H S_V}{N_H^2} + \beta_{HV}u_1(t)(1-c_B)(1-\epsilon)\frac{I_V}{N_H}\big[\lambda_{V_H} - \lambda_{E_H}\big] + \beta_{HV}u_1(t)(1-$$
$$c_B)(1-\epsilon)\big[\lambda_{E_H} - \lambda_{V_H}\big]\frac{I_V V_H}{N_H^2} - \omega_H(1-u_2(t))\big[\lambda_{V_H} - \lambda_{S_H}\big],$$

$$\frac{d\lambda_{E_H}}{dt} =\mu_H\lambda_{E_H} + \gamma_H\big[\lambda_{E_H} - \lambda_{I_H}\big] + \beta_{HV}u_1(t)(1-c_B)\big[\lambda_{E_H} - \lambda_{S_H}\big]\frac{I_V S_H}{N_H^2} + \beta_{HV}$$
$$u_1(t)(1-c_B)\big[\lambda_{I_V} - \lambda_{S_V}\big]\frac{I_H S_V}{N_H^2} + \beta_{HV}u_1(t)(1-c_B)(1-\epsilon)\big[\lambda_{E_H} - \lambda_{V_H}\big]$$
$$\frac{I_V V_H}{N_H^2} - B_1,$$

$$\frac{d\lambda_{I_H}}{dt} =(\delta_H + \mu_H)\lambda_{I_H} + \tau_H\big[\lambda_{I_H} - \lambda_{R_H}\big] + \beta_{HV}u_1(t)(1-c_B)\big[\lambda_{E_H} - \lambda_{S_H}\big]\frac{I_V S_H}{N_H^2} +$$
$$\beta_{HV}u_1(t)(1-c_B)\big[\lambda_{S_V} - \lambda_{I_V}\big]\frac{S_V}{N_H} + \beta_{HV}u_1(t)(1-c_B)(1-\epsilon)\big[\lambda_{E_H} - \lambda_{V_H}\big]$$
$$\frac{I_V V_H}{N_H^2} + \beta_{HV}u_1(t)(1-c_B)\big[\lambda_{I_V} - \lambda_{S_V}\big]\frac{I_H S_V}{N_H^2} - B_2,$$

$$\frac{d\lambda_{R_H}}{dt} =\mu_H\lambda_{R_H} + \beta_{HV}u_1(t)(1-c_B)\big[\lambda_{E_H} - \lambda_{S_H}\big]\frac{I_V S_H}{N_H^2} + \beta_{HV}u_1(t)(1-c_B)\big[\lambda_{I_V} -$$
$$\lambda_{S_V}\big]\frac{I_H S_V}{N_H^2} + \beta_{HV}u_1(t)(1-c_B)(1-\epsilon)\big[\lambda_{E_H} - \lambda_{V_H}\big]\frac{I_V V_H}{N_H^2},$$

$$\frac{d\lambda_{A_N}}{dt} =(\mu_A + u_3 c_L)\lambda_{A_N} + b_V\big[\lambda_{A_N} - \lambda_{S_V}\big] + \frac{\lambda_{A_N}\phi_V(S_V+I_V)}{\mathcal{K}} + \frac{I_V\phi_V\eta_V}{\mathcal{K}}\big[\lambda_{A_I} -$$
$$\lambda_{A_N}\big] - B_3,$$

$$\frac{d\lambda_{A_I}}{dt} =(\mu_A + u_3 c_L)\lambda_{A_I} + b_V\big[\lambda_{A_I} - \lambda_{I_V}\big] + \frac{\lambda_{A_N}\phi_V(S_V+I_V)}{\mathcal{K}} + \frac{I_V\phi_V\eta_V}{\mathcal{K}}\big[\lambda_{A_I} -$$
$$\lambda_{A_N}\big] - B_3,$$

$$\frac{d\lambda_{S_V}}{dt} =(\mu_V + u_4c_A)\lambda_{S_V} + \beta_{HV}u_1(t)(1-c_B)\big[\lambda_{S_V} - \lambda_{I_V}\big]\frac{I_H}{N_H} - \phi_V\Big(1-\frac{A}{\mathcal{K}}\Big)\lambda_{A_N}$$
$$- B_4,$$
$$\frac{d\lambda_{I_V}}{dt} =(\mu_V + u_4c_A)\lambda_{I_V} + \beta_{HV}u_1(t)(1-c_B)(1-\epsilon)\big[\lambda_{V_H} - \lambda_{E_H}\big]\frac{V_H}{N_H} + \beta_{HV}u_1(t)$$
$$(1-c_B)\big[\lambda_{S_H} - \lambda_{E_H}\big]\frac{S_H}{N_H} + \Big(1-\frac{A}{\mathcal{K}}\Big)\phi_V\eta_V\big[\lambda_{A_N} - \lambda_{A_I}\big] - \phi_V\Big(1-\frac{A}{\mathcal{K}}\Big)\lambda_{A_N}$$
$$- B_4,$$

with final time condition as $\lambda_i(T) = 0, i = 1, ..., 9$. In addition, the optimal control $u_j^*, j = 1, 2, 3, 4$ are given by

$$u_1^* = \begin{cases} 0, & \text{if} \quad \Big(\frac{\beta_{HV}(1-c_B)}{2N_HD_1}\Big)Q_0 < 0 \\ \Big(\frac{\beta_{HV}(1-c_B)}{2N_HD_1}\Big)Q_0, & \text{if} \quad 0 < \frac{\beta_{HV}(1-c_B)}{2N_HD_1}Q_0 < 1 \\ 1, & \text{if} \quad \Big(\frac{\beta_{HV}(1-c_B)}{2N_HD_1}\Big)Q_0 > 1 \end{cases} \tag{4.3.47}$$

where $Q_0 = \Big(I_VS_H\big[\lambda_{S_H} - \lambda_{E_H}\big] + I_VV_H(1-\epsilon)\big[\lambda_{V_H} - \lambda_{E_H}\big] + I_HS_V\big[\lambda_{S_V} - \lambda_{I_V}\big]\Big)$, while u_2^* is given by

$$u_2^* = \begin{cases} 0, & \text{if} \quad \frac{(c_VS_H+\omega_HV_H)}{2D_2}\big[\lambda_{S_H} - \lambda_{V_H}\big] < 0 \\ \frac{(c_VS_H+\omega_HV_H)}{2D_2}\big[\lambda_{S_H} - \lambda_{V_H}\big], & \text{if} \quad 0 < \frac{(c_VS_H+\omega_HV_H)}{2D_2}\big[\lambda_{S_H} - \lambda_{V_H}\big] < 1 \\ 1, & \text{if} \quad \frac{(c_VS_H+\omega_HV_H)}{2D_2}\big[\lambda_{S_H} - \lambda_{V_H}\big] > 1, \end{cases} \tag{4.3.48}$$

also u_3^* is given by

$$u_3^* = \begin{cases} 0, & \text{if} \quad \frac{c_V}{2D_3}\Big(\lambda_{A_N}A_N + \lambda_{A_I}A_I\Big) < 0 \\ \frac{c_V}{2D_3}\Big(\lambda_{A_N}A_N + \lambda_{A_I}A_I\Big), & \text{if} \quad 0 < \frac{c_V}{2D_3}\Big(\lambda_{A_N}A_N + \lambda_{A_I}A_I\Big) < 1 \\ 1, & \text{if} \quad \frac{c_V}{2D_3}\Big(\lambda_{A_N}A_N + \lambda_{A_I}A_I\Big) > 1 \end{cases} \tag{4.3.49}$$

and u_4^* is given by

$$u_4^* = \begin{cases} 0, & \text{if} \quad \frac{c_L}{2D_4}\left[\lambda_{S_V} S_V + \lambda_{I_V} I_V\right] < 0 \\ \frac{c_L}{2D_4}\left[\lambda_{S_V} S_V + \lambda_{I_V} I_V\right], & \text{if} \quad 0 < \frac{c_L}{2D_4}\left[\lambda_{S_V} S_V + \lambda_{I_V} I_V\right] < 1 \\ 1, & \text{if} \quad \frac{c_L}{2D_4}\left[\lambda_{S_V} S_V + \lambda_{I_V} I_V\right] > 1 \end{cases} \tag{4.3.50}$$

Proof. The non-autonomous system given by (4.3.43) together with the objective functional given by (4.3.44) and (4.3.45) are converted into a problem of minimizing the Hamiltonian, H, defined by (4.3.46). Therefore applying Pontryagin's Maximum Principle [107, 118], the proof follows.

4.4 Sensitivity analysis and numerical simulation

In this section, global sensitivity analysis using partial rank correlation coefficient (PRCC) for the basic offspring number and vaccinated reproduction number are conducted. Numerical simulations of the optimal control model given by (4.3.43) is also presented.

4.4.1 Sensitivity analysis

Local sensitivity analysis is used to provide direct information on the effect of small parameter perturbation, it evaluates the relative change in a function due to change in a single parameter, where other parameters are kept at constant values. It does not indicate the effect of simultaneous large perturbations in all model parameters. Thus, the need for a more robust form of sensitivity analysis for a multidimensional parameter space. The PRCC is a robust sensitivity measure for a non-linear but monotonic relationships between inputs and output, with little correlation between the inputs [91].

The PRCC of the basic offspring number (N_0) and that of the vaccinated reproduction number (R_{0v}) are computed with parameter ranges as presented in Table 4.1. The PRCC for N_0 shows that the threshold is more sensitive to c_A and c_L which are negatively correlated to the threshold, while ϕ_V is the most positively correlated as presented by Figure 4.5. On the other hand, R_{0V} is most positively correlated to η_V, which is followed by β_{HV} then $\mathcal{K}$, while it is most negatively correlated to c_A, c_B and then b_H as presented by Figure 4.6.

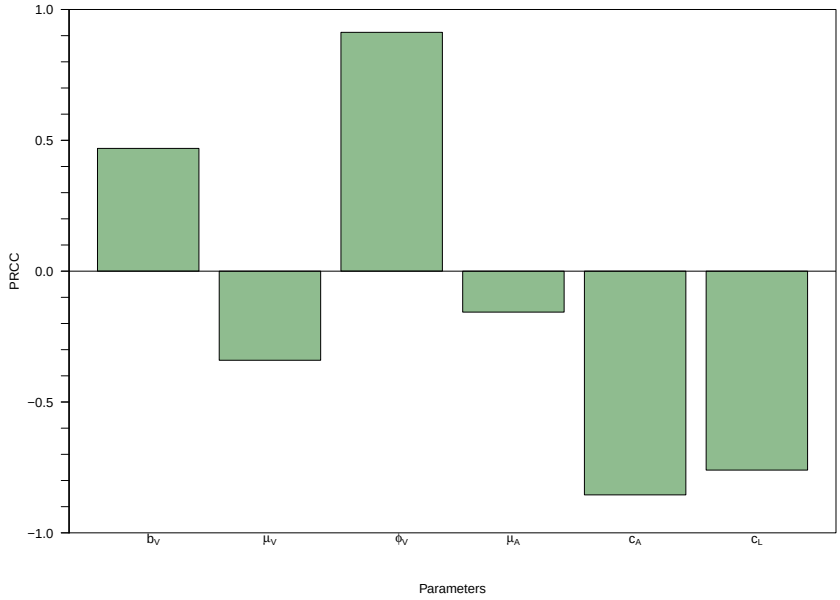

Figure 4.5: Partial rank correlation coefficient plots of the various parameters of the model (4.2.5) using N_0 as the output function.

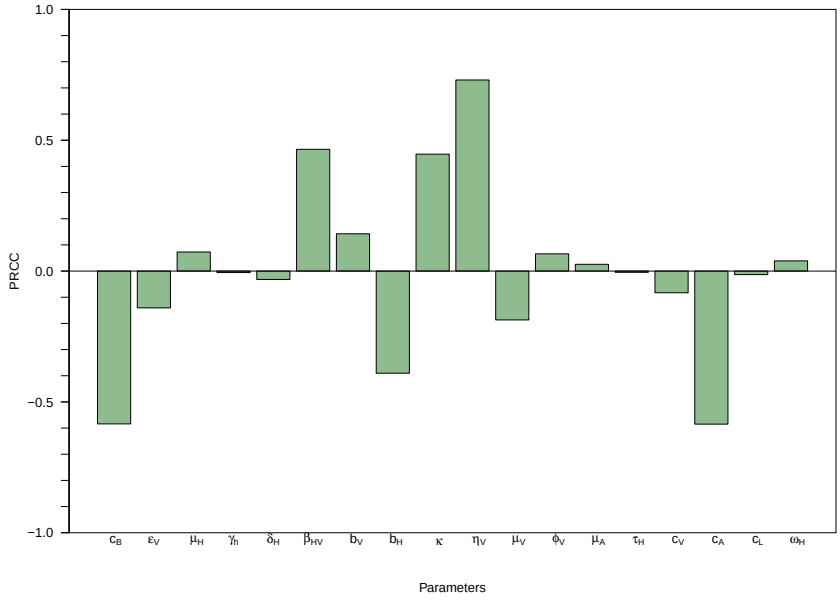

Figure 4.6: Partial rank correlation coefficient plots of the various parameters of the model (4.2.5) using R_{0V} as the output function.

4.4.2 Numerical simulations

In this section, we use numerical simulations to investigate impacts of the optimal control strategies employed in the model for the transmission dynamics of yellow fever. We can numerically calculate the optimal control using a forward-backward sweep method described by [86].

Basically, all the methods applied in solving optimal control problems can be classified in two different types; direct and indirect approaches [143]. Optimal control problem in direct methods is transformed into a nonlinear programing problem. The method directly optimize the cost functional using the parametrization of control by approximating control and state vector with a sum of function expansion [113, 143]. Although it has the advantage of robust numerics with respect to initial guess, low accuracy of results is noticed [113]. The indirect method (used in this thesis) is based on Pontryaguines minimum principle, in this case, numerical simulations converge quickly and the solutions are accurate if one starts with a good initial guess [113].

Using an iterative method with the fourth order Runge-Kutta procedure, solutions for the state equations and their corresponding adjoint equations can be obtained. We start with an initial guess for the adjoint variables, which is then used to solve the state system by a forward Runge-Kutta fourth order procedure in time. The guessed optimal control and the obtained solution to the state system are used as input to the adjoint system, which is solved numerically in backward scheme using the transversality condition. The controls are then updated using convex combination of the previous controls and the value from the characterizations [86]. This updated control replaces the initial control and the iterative process is repeated until the successive iterates of control values are sufficiently close to the ones at the present iterations.

The following numerical values for the model parameters are used as in Table 4.1:

$$b_H = 50; \beta_{HV} = 0.375; c_B = 0.5; \omega_H = 0.01; \mu_H = 0.0000421; c_V = 0.3; \epsilon = 0.95;$$

$$\gamma_H = 0.3; \delta_H = 0.0001; \tau_H = 0.143; b_V = 0.1; \phi_V = 50; \kappa = 800000; \eta_V = 0.01;$$

$$\mu_A = 0.22; \mu_V = 0.29; c_A = 0.2; c_L = 0.2.$$

For the numerical values of the weight constants in the objective functional J, it is important to note that the choices are made only for simulation purposes. Two different set of values for the weight constants are considered in our simulations, in both instances, minimizing the number of infected humans is given more priority over minimizing adult mosquitoes, then aquatic mosquitoes i.e $B_2 \geq B_1 > B_4 > B_3$ but with the same cost ($D_1 = D_2 = D_3 = D_4$). However, in both the two cases, because E_H, I_H and S_H are at the same scale and smaller than mosquito populations, values of their weight constants are chosen to be the same (i.e $B_1 = B_2 = B_5$) and smaller than those of mosquitoes, while $B_3 < B_4$ because aquatic mosquitoes are more than adult mosquitoes. The weight constants for the controls (D_1, D_2, D_3, D_4) balance cost associated with them, therefore two different choices were made for smaller and higher costs, simulations were carried out for the two different choices.

Because controls for mosquito borne disease are not done throughout the year (seasonal diseases), simulations are carried out for 200 days only.

Using initial human populations of

$$S_H(0) = 2000; V_H(0) = 500; E_H(0) = 500; I_H(0) = 200; R_H(0) = 50,$$

while those of mosquitoes as

$$A_N(0) = 25000; A_I(0) = 200; S_V(0) = 1000; I_V(0) = 500,$$

the impact of control and that of using different weight constants for the objective functional is assessed. In order to regularize the objective functional, smaller constants were chosen for the coefficients of the populations while larger constants for the control functions. Populations of infected mosquitoes, exposed, infected and recovered humans are depicted.

1. Case 1: Simulations of the optimal control problem is carried out for the case when

   $$B_1 = 0.1; B_2 = 0.1; B_3 = 0.001; B_4 = 0.005; B_5 = 0.1; D_1 = 500; D_2 = 500;$$

   $$D_3 = 500; D_4 = 500.$$

   Control profiles are given by Figure 4.7 and Figure 4.8, while populations of exposed and infected humans with and without control are given by Figure 4.9A and Figure 4.9B respectively. Exposed and infected humans reach the DFE faster with control, initially, infected humans with control sparked up (which is due to the imperfection of vaccination) before quickly reaching the DFE. Figure 4.10A shows the population of recovered humans where the population with control is bigger than those without control, this may be attributed to the fact that recovery confers permanent immunity. Infectious mosquitoes (both aquatic and adult) is presented by Figure 4.10B.

2. Case 2: In this case, simulations are carried out for the case when the weight constants are taken as

   $$B_1 = 0.01; B_2 = 0.01; B_3 = 0.0001; B_4 = 0.0005; B_5 = 0.1; D_1 = 50; D_2 = 50;$$

   $$D_3 = 50; D_4 = 50.$$

   Similarly, control profiles are given by Figure 4.11 and Figure 4.12. Population of exposed humans shows similar dynamics as that of Case 1 and it is presented by Figure 4.13A, while simulation of infected humans, where population with control shoot up before falling to the DFE is presented by Figure 4.13B. The population of recovered humans shows wider margin between cases with and without control in this instance compared to Case 1 as depicted by Figure 4.14A, also, population of infected mosquitoes sporadically bumps up before reaching DFE as shown in Figure 4.14B. Notice that, less effort and less costs are expended in this case in comparison to Case 1.

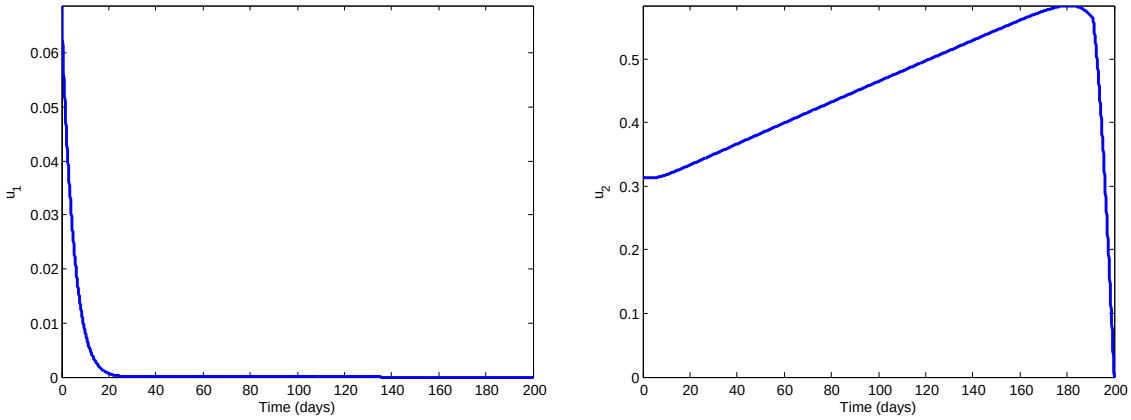

Figure 4.7: Simulations of the model (4.3.43) showing control profiles U_1 and U_2 for the case when $B_1 = 0.1$; $B_2 = 0.1$; $B_3 = 0.0001$; $B_4 = 0.00001$; $B_5 = 0.1$; $D_1 = 100$; $D_2 = 100$; $D_3 = 100$; $D_4 = 100$.

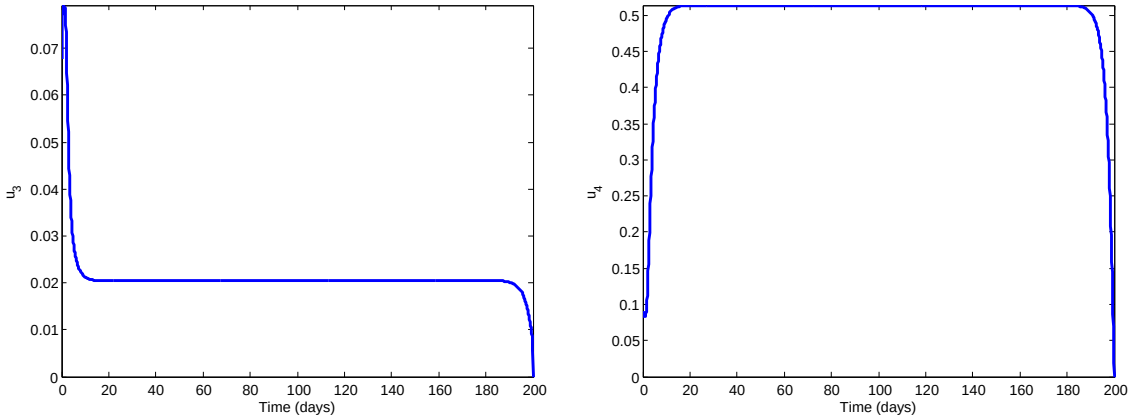

Figure 4.8: Simulations of the model (4.3.43) showing control profiles U_3 and U_4 for the case when $B_1 = 0.1$; $B_2 = 0.1$; $B_3 = 0.0001$; $B_4 = 0.00001$; $B_5 = 0.1$; $D_1 = 100$; $D_2 = 100$; $D_3 = 100$; $D_4 = 100$.

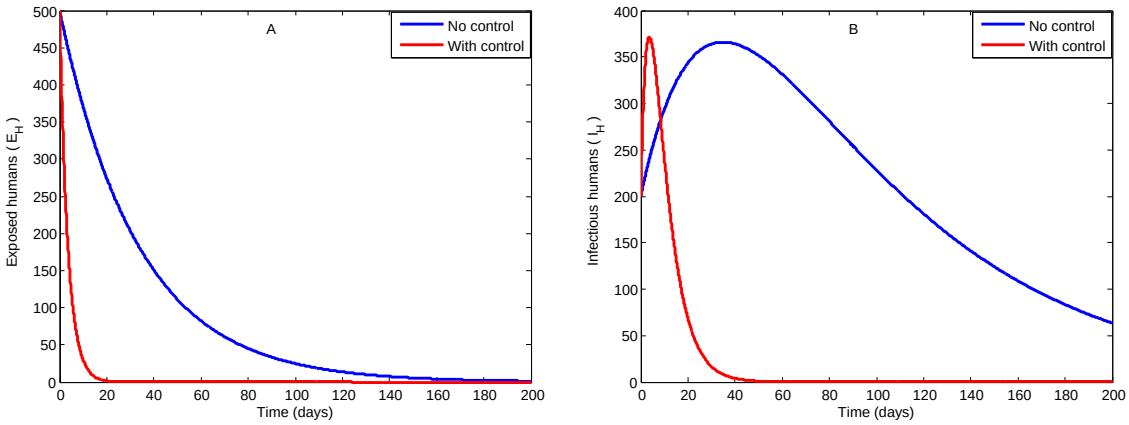

Figure 4.9: Simulations of the model (4.3.43) showing exposed humans and infected humans for the case when $B_1 = 0.1$; $B_2 = 0.1$; $B_3 = 0.0001$; $B_4 = 0.00001$; $B_5 = 0.1$; $D_1 = 100$; $D_2 = 100$; $D_3 = 100$; $D_4 = 100$.

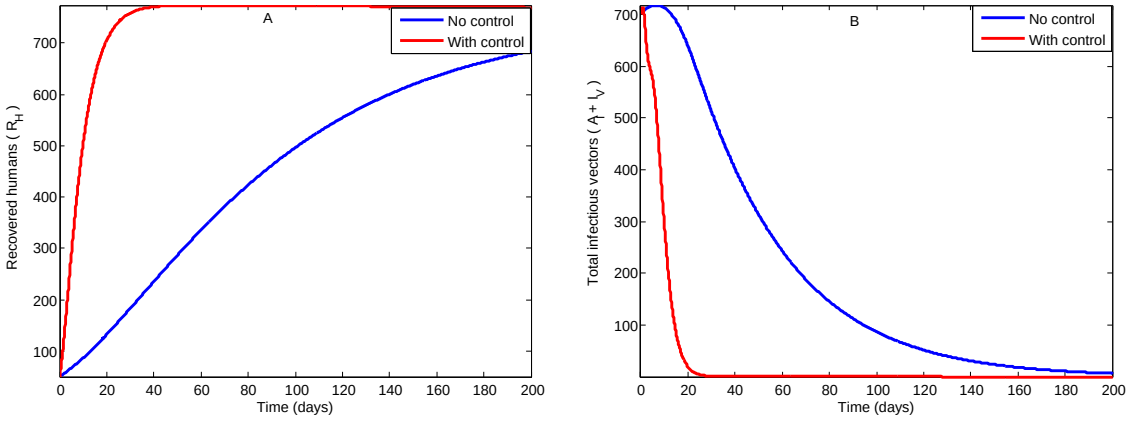

Figure 4.10: Simulations of the model (4.3.43) showing recovered humans and populations of infected mosquitoes for the case when $B_1 = 0.1$; $B_2 = 0.1$; $B_3 = 0.0001$; $B_4 = 0.00001$; $B_5 = 0.1$; $D_1 = 100$; $D_2 = 100$; $D_3 = 100$; $D_4 = 100$.

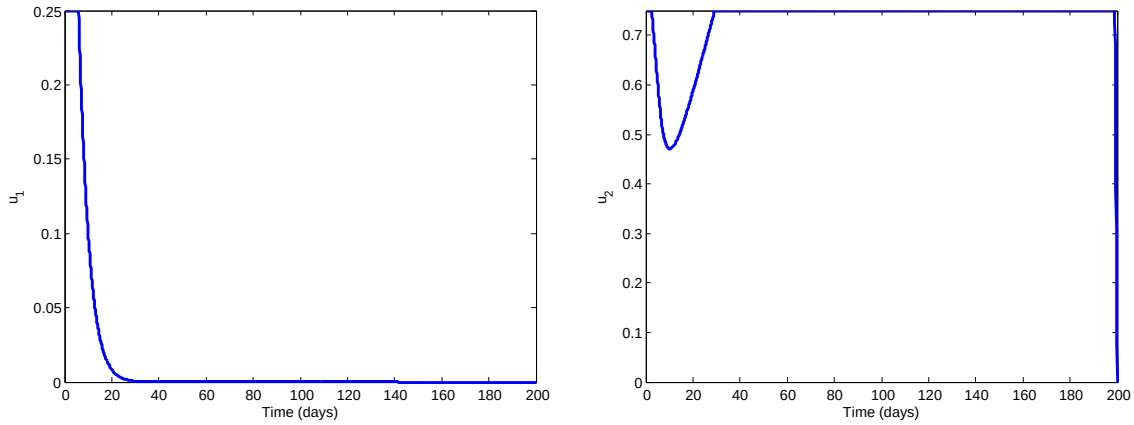

Figure 4.11: Simulations of the model (4.3.43) showing control profiles U_1 and U_2 for the case when $B_1 = 0.1$; $B_2 = 0.1$; $B_3 = 0.0001$; $B_4 = 0.00001$; $B_5 = 0.1$; $D_1 = 100$; $D_2 = 100$; $D_3 = 100$; $D_4 = 100$.

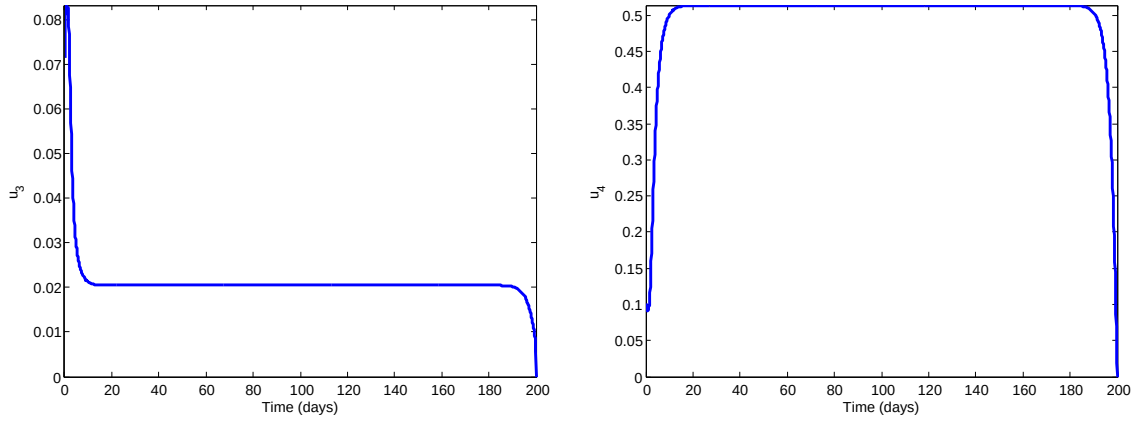

Figure 4.12: Simulations of the model (4.3.43) showing control profiles U_3 and U_4 for the case when $B_1 = 0.07$; $B_2 = 0.09$; $B_3 = 0.000001$; $B_4 = 0.00000001$; $B_5 = 0.05$; $D_1 = 1000$; $D_2 = 4000$; $D_3 = 1000$; $D_4 = 4000$.

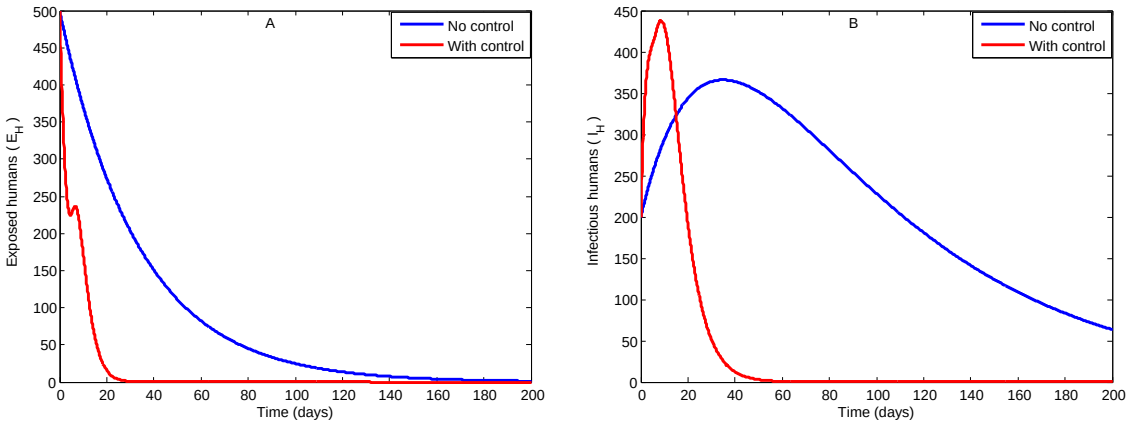

Figure 4.13: Simulations of the model (4.3.43) showing exposed humans and infected humans for the case when $B_1 = 0.07$; $B_2 = 0.09$; $B_3 = 0.000001$; $B_4 = 0.00000001$; $B_5 = 0.05$; $D_1 = 1000$; $D_2 = 4000$; $D_3 = 1000$; $D_4 = 4000$.

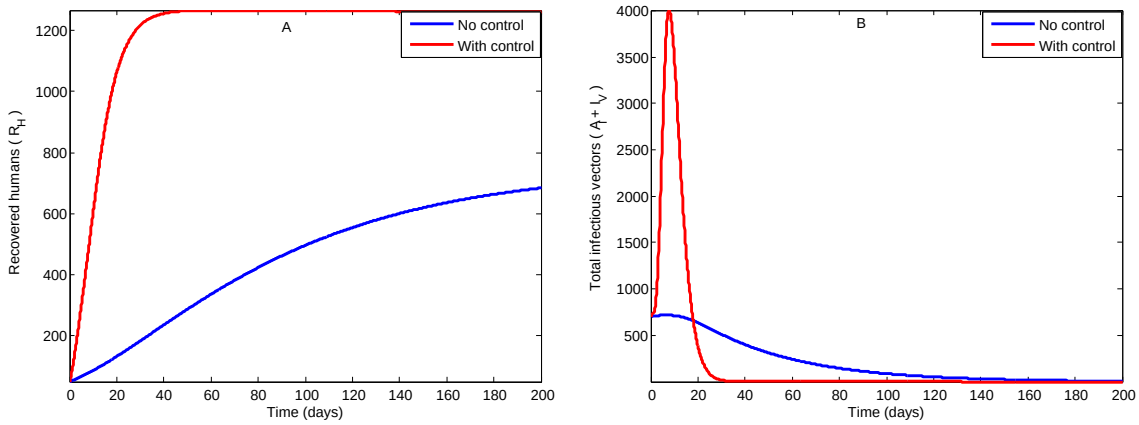

Figure 4.14: Simulations of the model (4.3.43) showing recovered humans and populations of infected mosquitoes for the case when $B_1 = 0.07$; $B_2 = 0.09$; $B_3 = 0.000001$; $B_4 = 0.00000001$; $B_5 = 0.05$; $D_1 = 1000$; $D_2 = 4000$; $D_3 = 1000$; $D_4 = 4000$.

Conclusion

A yellow fever model with standard incidence force of infection is constructed and analysed in this study. The model incorporated the use of treated bed nets and vaccination as forms of prevention in humans, while the use of larvicides and adulticides is used in controlling mosquito population. Some of the key results obtained include:

- There is a threshold that controls the persistent of mosquito population or otherwise, the threshold is a reducing function of the rate of death of mosquitoes due to use of larvicides and adulticides.
- The autonomous model has a locally-asymptotically stable disease-free equilibrium when the vaccinated reproduction number (R_{0V}) is less than unity. Although there is the threshold vaccination required to bring the vaccinated reproduction number to below unity, the threshold (R_{0V}) is a reducing function of the fraction of vaccinated reproduction number.
- The effect of dose fraction of vaccination is simulated by plotting the vaccinated reproduction number as a function of single, 2, 3 and 5 fold vaccines. For the parameter values used, for a single dose, 0.4 and above vaccine efficacy can reduce R_{0V} to below 1, while over 0.8 efficacy is needed for 2-fold. Even a 100% effective vaccine can not bring R_{0V} to below unity for 3 and 5-fold vaccine.
- The DFE of the autonomous model is GAS in the positively invariant region Ω provided $R_{HV}R_{VH}\frac{N_0N_H^*}{L_H^*(N_0-1)} + R_{VV}N_0 < 1$, while the DFE in the positively invariant subset Ω^* of Ω if $R_{0V} \leq 1$.
- Using Pontryagins maximum principle, the non-autonomous system is analysed and the necessary conditions for existence of an optimal control were determined.
- Numerical simulations of the non-autonomous model (with optimal control) using different weight constants show that slight increase in control effort show wide difference in the impact of control.
- Using sensitivity analysis, the vaccinated reproduction is most sensitive and positively correlated to the rate of vertical transmission, thus making it the most important parameter to target in controlling R_{0V}.

Chapter 5

Modeling the effect of temperature variability on Malaria control strategies

General introduction

In this chapter, a malaria model that takes into account temperature changes is constructed and rigorously analysed in the presence of control. The model has a notable feature of wholly susceptible class separated from other susceptible, as well as having compartments with and without history of vaccination. The work is under review [38].

Abstract

In this study, a non-autonomous (temperature dependent) and autonomous (temperature independent) models for the transmission dynamics of malaria in a population are designed and rigorously analysed. The models are used to assess the impact of temperature changes (which causes seasonality) on various control strategies. The autonomous model is shown to exhibit the phenomenon of backward bifurcation, where an asymptotically-stable disease-free equilibrium (DFE) co-exists with an asymptotically-stable endemic equilibrium when the associated reproduction number is less than unity. This phenomenon is shown to arise due to the presence of imperfect vaccines and disease-induced mortality rate. Threshold quantities (such as the basic offspring number, vaccination and host type reproduction numbers) and their interpretations for the models are presented. Conditions for local asymptotic stability of the disease -free solutions are computed. Sensitivity analysis using temperature data obtained from Kwazulu Natal Province of South Africa [111] is used to assess the parameters that have the most influence on malaria transmission. The effect of various control strategies (bed nets, adulticides and vaccination) were assessed *via* numerical simulations.

5.1 Introduction

Malaria is an important mosquito borne disease with a global distribution and significant public health burden. It is a life-threatening infection that is caused by Plas-

modium parasite, spread and sustained through bites by female Anopheles mosquitoes on susceptible and infected humans [150]. There are more than hundred species of Plasmodium that can infect different animal species such as reptiles, birds and various mammals [138], among which five species (P. falciparum, P. vivax, P. ovale, P. malariae, and, P. knowlesi) specifically cause human infections [50, 150]. Out of the aforementioned species, P. vivax (which is the dominant malaria parasite outside of sub-Saharan Africa) and P. falciparum (the most prevalent malaria parasite on the African continent and responsible for most malaria-related deaths globally) were responsible for 891,000 deaths in the period 2015-2016 [150].

The most important environmental variables that affect mosquito population are suitable temperature and appropriate aquatic breeding sites. Temperature affects both survival and development rate of mosquitoes while surface wetness limits the population size of aquatic mosquitoes [127]. In addition, temperature is a key determinant of environmental suitability for transmission of human malaria, modulating endemicity in some regions and preventing transmission in others. The spatial limits of the distribution and seasonal activities of malaria are sensitive to climate factors, as well as the local capacity to control the disease [25]. The dynamics and distribution of malaria strongly depend on the interplay between the parasite, the mosquitoes and the environment [106, 116], it has recently been shown that mosquito and parasite biology are influenced not only by average temperature, but also by the extent of the daily temperature variation [17]. At the extremes, temperature regimes constrain the geographical extent of the disease and, within this envelope, contribute to determining its intensity [65]. These constraints are temporally dynamic, with fluctuations in transmission suitability and intensity driven by seasonal and inter-annual temperature cycles. The importance of temperature as an environmental determinant of malaria endemicity arises from a series of effects on the life cycles of the plasmodium parasite and anopheles mosquitoes [65].

A number of mathematical models have been developed in the literature to gain insights into the effects of temperature change in the transmission dynamics of mosquito borne diseases in a community, see for instance [1, 3, 6, 50, 65, 89, 102, 106, 111, 116, 124, 153]. In particular, malaria has received lots of attention. Mordecai et al [102] considered a non-linear response of mosquito and malaria parasite to temperature which are closely consistent with field data, the work which changed predictions on how temperature change affects malaria predicts optimal malaria transmission at 25^0C. A malaria transmission model with periodic birth rate and age structure for the vector population was rigorously analysed by Loy and Zhao [89]. The examination of the process via which parasite development within the mosquito (extrinsic incubation period) is expected to vary over time and space, as depending on the diurnal temperature range and baseline mean temperature in Kenya and across Africa was presented by Blanford et al. [17]. Agusto et al. [3] considered a temperature-dependent deterministic model that gave some qualitative insights into the effects of temperature variability on malaria transmission dynamics, the model incorporated gradual increase in infection-acquired immunity via repeated exposure to malaria infection. The impact of variability in temperature and rainfall on the transmission dynamics of malaria in age-structured population, with the dynamics of immature and mature mosquitoes was also considered by Okuneye and Gumel [111]. A malaria model that qualitatively

studied the effect of seasonal variations (wet and dry seasons) on the spread of malaria was introduced and analysed by Dembele et al. [40], an explicit formulation for the basic reproduction ratio and stability analysis of the disease free equilibrium was presented. Eikenberry and Gumel extensively review the idea of mathematical modeling of climate change in the transmission dynamics of malaria [50].

Although, there have been tremendous success in the reduction of malaria cases especially in Africa, nevertheless, mortality due to the disease incidences still remains high in comparison to other infections. Over the years, there have been several initiatives aimed at ending malaria cases, some of which include WHOs Roll Back Malaria program, the Multilateral Initiative in Malaria, the Medicines for Malaria Venture, the Malaria Vaccine Initiative, and the Global Fund to Fight AIDS, TB and Malaria, which supports the implementation of prevention and treatment programs [138]. In fact, there is no single way of preventing malaria, however, there are a number of ways to decrease the transmission of the disease which include the use of treated nets, as well as the use of larvicides and adulticides to clear mosquito breeding sites and kill adult mosquitoes, respectively. Although there is no specific effective vaccine for malaria at the moment, a number of candidate vaccines targeting different stages of the malaria parasite life-cycle have been developed or are currently under development, in particular, RTS,S/AS01 is a strong candidate for the prevention of Plasmodium falciparum infection (the deadliest), in fact phase 3 trials of the vaccine has been completed [142].

Predicting the public health impact of a candidate malaria vaccine requires using clinical trial data to estimate the vaccines efficacy profile, initial efficacy after vaccination and the pattern through which the vaccine efficacy wanes over time. With an estimated vaccine efficacy profile, the effects of vaccination on malaria transmission can be simulated with the aid of mathematical models [142].

In this study, we consider both autonomous and non-autonomous deterministic model for the transmission dynamics of malaria with control in the presence of temperature variability. Notable feature of the model is that the host population is basically divided according to their vaccination status and the use of multiple control and prevention strategies. The model further assumed that recovered individuals do not become wholly susceptible. The work is organized as follows: A deterministic non-autonomous malaria model is developed in Section 5.1. Basic dynamical properties of the model are discussed in Section 5.2. In Section 5.3, analysis of the autonomous model is performed, while backward bifurcation analysis is discussed in Section 5.4. Analysis of the non-autonomous model is performed in Section 5.5, effect of control strategies are discussed in Section 5.6. Sensitivity analysis and numerical simulations are presented in Section 5.7.

5.2 Model formulation

The total human population at time t, denoted by $N_H(t)$ is divided into populations of vaccinated and non-vaccinated individuals. The sub-population of non-vaccinated individuals are further sub-divided into 5 mutually exclusive sub-population of wholly susceptible (without ever been infected) $(S_U(t))$, susceptible after recovery $(W_U(t))$, exposed $(E_U(t))$, infected $(I_U(t))$ and recovered $(R_U(t))$ humans. Similarly, the sub-

population of vaccinated individuals are sub-divided into wholly susceptible $(S_V(t))$, susceptible after recovery $(W_V(t))$, exposed $(E_V(t))$, infected $(I_V(t))$ and recovered $(R_V(t))$ humans, so that the total human population at time t is given by

$$N_H(t) = S_U(t)+S_V(t)+W_U(t)+W_V(t)+E_U(t)+E_V(t)+I_U(t)+I_V(t)+R_U(t)+R_V(t).$$

In order to assess the potential effect of temperature (seasonal) dependent oviposition of mosquitoes, the population of mosquitoes are divided into aquatic and non-aquatic stages. The aquatic stage (which involves egg, larva and pupa) is represented by a single equation $(A_M(t))$. The non-aquatic (matured) stage is further divided into susceptible $(M_U(t))$, exposed $(M_E(t))$ and infected $(M_I(t))$ mosquitoes. Thus, the total adult mosquito population (in the non-aquatic stage) is given by

$$N_V(t) = M_U(t) + M_E(t) + M_I(t).$$

Note that, in this study only female mosquitoes are considered as male mosquitoes are non-infectious. The model incorporates the use of larvicides (to clear aquatic mosquitoes) and adulticides (to kill matured mosquitoes). In either case, the death rates due to the use of larvicides and adulticides are proportional to successful rates of applications of larvicides and adulticides.

5.2.1 Dynamics of humans

It is assumed that the population of wholly susceptible humans is generated by birth (or immigration) at a constant rate Π_H. This population increases through the loss of vaccination-acquired immunity by wholly vaccinated individuals (at a waning rate ω_V). It is decreased by vaccination (at a rate ξ_V which move to the class of wholly vaccinated humans). Proportion of this individuals (in S_U class) acquire malaria infection following effective contact with infectious mosquitoes in M_I class at a temperature (seasonal) dependent rate $\lambda_H(T)$, given by

$$\lambda_H(T) = \frac{\beta_{VH} M_I(t)}{N_V(t)}(1 - \epsilon_B\alpha_B)a_M(T),$$

where, the parameter β_{VH} is a transmission probability from infectious mosquitoes to susceptible humans. The parameter $a_M(T)$ is a temperature dependent biting rate of mosquitoes, $0 < \epsilon_B < 1$ represents efficacy rate of bed nets and α_B measure compliance rate in the use of bed nets. Therefore $\epsilon_B\alpha_B$ represents the use of insect repellents to minimize contacts with mosquitoes. Natural mortality occurs in all human classes at a rate μ_H so that

$$\frac{dS_U(t)}{dt} = \Pi_H + \omega_V S_V(t) - \xi_V S_U(t) - \lambda_H(T)S_U(t) - \mu_H S_U(t).$$

The population of a wholly vaccinated individuals S_V is generated by vaccination of susceptible individuals at the rate ξ_V. This population decreases due to waning of vaccine (at the rate ω_V), infection at the rate $\lambda_H(T)(1-\epsilon_V)$ (where $0 < \epsilon_V < 1$ is a vaccine efficacy) and by natural death (at the rate μ_H) so that

$$\frac{dS_V(t)}{dt} = \xi_V S_U(t) - \lambda_H(T)(1-\epsilon_V)S_V(t) - \omega_V S_V(t) - \mu_H S_V(t).$$

The populations of non-vaccinated (W_U) and vaccinated (W_V) susceptible individuals (who are partially immune due to prior infection) is generated following loss of partial immunity by recovered individuals that are non-vaccinated and vaccinated at the rates τ_U and τ_V, respectively. These populations decrease by secondary infection at a reduced rate $\lambda_H(T)(1-\epsilon_W)$ (where ϵ_W is a protection rate due to prior malaria infection) and by natural death, so that

$$\frac{dW_U(t)}{dt} = \tau_U R_U(t) - \lambda_H(T)(1-\epsilon_W)W_U(t) - \mu_H W_U(t),$$
$$\frac{dW_V(t)}{dt} = \tau_V R_V(t) - \lambda_H(T)(1-\epsilon_W)W_V(t) - \mu_H W_V(t).$$

The populations of non-vaccinated exposed (E_U) and vaccinated exposed (E_V) individuals are generated by the infection of non-vaccinated (S_U, W_U) and vaccinated (S_V, W_V) individuals at the rates λ_H, $\lambda_H(T)(1-\epsilon_W)$ and $\lambda_H(1-\epsilon_V)$, $\lambda_H(T)(1-\epsilon_W)$, respectively. These populations reduces by progressing to non-vaccinated and vaccinated infectious classes at the rates σ_U and σ_V, respectively, and by natural death, this gives

$$\frac{dE_U(t)}{dt} = \lambda_H(T)S_U(t) + \lambda_H(T)(1-\epsilon_W)W_U(t) - \sigma_U E_U(t) - \mu_H E_U(t),$$
$$\frac{dE_V(t)}{dt} = \lambda_H(T)(1-\epsilon_V)S_V(t) + \lambda_H(T)(1-\epsilon_W)W_V(t) - \sigma_V E_V(t) - \mu_H E_V(t).$$

The populations of non-vaccinated infectious (I_U) and vaccinated infectious (I_V) individuals are generated by progression of non-vaccinated and vaccinated exposed individuals to the infectious classes at the rates σ_U and σ_V, respectively. These populations decreases by recovery at the rates γ_U and γ_V, respectively, natural death and disease-induced death at the rates δ_U and δ_V, respectively. This gives

$$\frac{dI_U(t)}{dt} = \sigma_U E_U(t) - \gamma_U I_U(t) - \delta_U I_U(t) - \mu_H I_U(t),$$
$$\frac{dI_V(t)}{dt} = \sigma_V E_V(t) - \gamma_V I_V(t) - \delta_V I_V(t) - \mu_H I_V(t).$$

The populations of non-vaccinated recovered (R_U) and vaccinated recovered (R_V) individuals are generated by recovery of non-vaccinated and vaccinated infectious individuals at the rates γ_U and γ_V, respectively. The populations are reduces by loss of partial immunity at the rates τ_U and τ_V, respectively, and natural death. So that

$$\frac{dR_U(t)}{dt} = \gamma_U I_U(t) - \tau_U R_U(t) - \mu_H R_U(t),$$
$$\frac{dR_V(t)}{dt} = \gamma_V I_V(t) - \tau_V R_V(t) - \mu_H R_V(t).$$

5.2.2 Dynamics of mosquitoes

In the presence of intervention (using larvicides), the population of aquatic mosquitoes (eggs, larvae and pupae) increases through oviposition by reproductive mosquitoes at a temperature dependent rate $\phi_A(T)\Big(1-\alpha_L\epsilon_L\Big)$, where α_L is a rate of applying larvicides and ϵ_L is an efficacy of larvicides (so that $\alpha_L\epsilon_L = c_L$ accounts for effectiveness of larvicides). The growth of aquatic mosquitoes is moderated by a constant environmental carrying capacity $\mathcal{K}$. This population decreases by maturation at a temperature dependent rate $\sigma_A(T)$, die naturally and due to the use of larvicides at a rate $\mu_A(T)\Big(1+\alpha_L\epsilon_L\Big)$, where $\mu_A(T)$ is a temperature dependent death rate. Thus

$$\frac{dA_M(t)}{dt} = \phi_A(T)\Big(1-\alpha_L\epsilon_L\Big)\Big(1-\frac{A_M(t)}{\mathcal{K}}\Big)N_V(t)-\Big[\sigma_A(T)-\mu_A(T)\big(1+\alpha_L\epsilon_L\big)\Big]A_M(t).$$

The population of susceptible adult female mosquitoes ($M_U(t)$) is generated by maturation of aquatic mosquitoes at the temperature dependent rate $\sigma_A(T)$. It decreases by acquiring infection following a substantial contact with an infectious human at a temperature dependent infection rate $\lambda_V(T)$, given by

$$\lambda_V(T) = \frac{\beta_{HV}}{N_H(t)}(1-\epsilon_B\alpha_B)a_M(T)\Big[I_U(t)+\eta_I I_V(t)+\eta_U R_U+\eta_V R_V\Big],$$

where, β_{HV} is the probability of infection from infectious humans to susceptible mosquitoes. The parameters η_I, η_U and η_V are modification parameters which account for the reduction in the infectivity of individuals in I_V, R_U and R_V classes in comparison to those in I_U class, respectively. Similarly, the population is further decreases at a rate $\mu_V(T)\Big(1+\alpha_A\epsilon_A\Big)$, where $\mu_V(T)$ is a temperature dependent death in the absence of intervention, α_A is a rate of applying adulticides and ϵ_A is an efficacy of adulticides (so that $\alpha_A\epsilon_A = c_A$ accounts for effectiveness of indoor residual spraying). Thus

$$\frac{dM_U(t)}{dt} = \sigma_A(T)A_M(t)-\lambda_V(T)M_U(t)-\mu_V(T)\Big(1+\alpha_A\epsilon_A\Big)M_U(t).$$

The population of exposed mosquitoes in the $M_E(t)$ class is generated by the infection of adult mosquitoes in the $M_U(t)$ class at the rate $\lambda_V(T)$. This population decreases by progression to infectious class at a temperature dependent rate $\sigma_M(T)$ and die naturally and due to the use of adulticides at the rate $\mu_V(T)\Big(1+\alpha_A\epsilon_A\Big)$. Hence

$$\frac{dM_E(t)}{dt} = \lambda_V(T)M_U(t)-\sigma_M(T)M_E(t)-\mu_V(T)\Big(1+\alpha_A\epsilon_A\Big)M_E(t).$$

Finally, the population of infectious mosquitoes in the $M_I(t)$ class is generated by progression of mosquitoes in the $M_E(t)$ class to $M_I(t)$ class at the temperature dependent rate $\sigma_M(T)$. It decreases due to natural death and the use of adulticides at

the rate $\mu_V(T)\Big(1+\alpha_A\epsilon_A\Big)$. This gives

$$\frac{dM_I(t)}{dt} = \sigma_M(T)M_E(t) - \mu_V(T)\Big(1+\alpha_A\epsilon_A\Big)M_I(t).$$

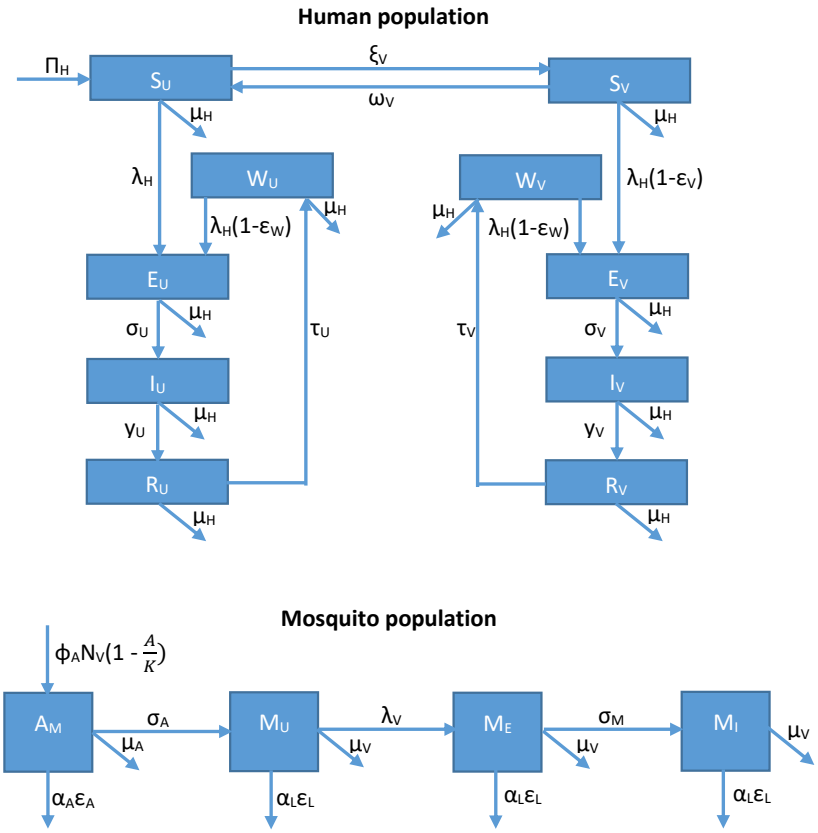

Figure 5.1: *Schematic diagram of the model* (5.2.1).

5.2.3 Model equations

The above formulation is represented by the following non-autonomous deterministic system of non-linear ordinary differential equations (a flow diagram of the model is depicted by Figure 5.1 and the state variables and parameters of the model are described

in Table 5.1 and Table 5.8 respectively):

$$
\begin{aligned}
\frac{dS_U(t)}{dt} &= \Pi_H + \omega_V S_V(t) - \xi_V S_U(t) - \lambda_H(T) S_U(t) - \mu_H S_U(t),\\
\frac{dS_V(t)}{dt} &= \xi_V S_U(t) - \lambda_H(T)(1-\epsilon_V) S_V(t) - \omega_V S_V(t) - \mu_H S_V(t),\\
\frac{dW_U(t)}{dt} &= \tau_U R_U(t) - \lambda_H(T)(1-\epsilon_W) W_U(t) - \mu_H W_U(t),\\
\frac{dW_V(t)}{dt} &= \tau_V R_V(t) - \lambda_H(T)(1-\epsilon_W) W_V(t) - \mu_H W_V(t),\\
\frac{dE_U(t)}{dt} &= \lambda_H(T) S_U(t) + \lambda_H(T)(1-\epsilon_W) W_U(t) - \sigma_U E_U(t) - \mu_H E_U(t),\\
\frac{dE_V(t)}{dt} &= \lambda_H(T)(1-\epsilon_V) S_V(t) + \lambda_H(T)(1-\epsilon_W) W_V(t) - \sigma_V E_V(t) - \mu_H E_V(t),\\
\frac{dI_U(t)}{dt} &= \sigma_U E_U(t) - \gamma_U I_U(t) - \delta_U I_U(t) - \mu_H I_U(t),\\
\frac{dI_V(t)}{dt} &= \sigma_V E_V(t) - \gamma_V I_V(t) - \delta_V I_V(t) - \mu_H I_V(t),\\
\frac{dR_U(t)}{dt} &= \gamma_U I_U(t) - \tau_U R_U(t) - \mu_H R_U(t),\\
\frac{dR_V(t)}{dt} &= \gamma_V I_V(t) - \tau_V R_V(t) - \mu_H R_V(t),\\
\frac{dA_M(t)}{dt} &= \phi_A(T)\Big(1-\alpha_L\epsilon_L\Big)\Big(1-\frac{A_M(t)}{\mathcal{K}}\Big)N_V(t) - \Big[\sigma_A(T) + \mu_A(T)\big(1+\alpha_L\epsilon_L\big)\Big]A_M(t),\\
\frac{dM_U(t)}{dt} &= \sigma_A(T) A_M(t) - \lambda_V(T) M_U(t) - \mu_V(T)\Big(1+\alpha_A\epsilon_A\Big)M_U(t),\\
\frac{dM_E(t)}{dt} &= \lambda_V(T) M_U(t) - \sigma_M(T) M_E(t) - \mu_V(T)\Big(1+\alpha_A\epsilon_A\Big)M_E(t),\\
\frac{dM_I(t)}{dt} &= \sigma_M(T) M_E(t) - \mu_V(T)\Big(1+\alpha_A\epsilon_A\Big)M_I(t).
\end{aligned}
\tag{5.2.1}
$$

For simulation purpose, a generalized temperature function given by,

$$
T(t) = T_0\left[1 + T_1\cos\left(\frac{2\pi}{365}(\omega t + \phi)\right)\right], \tag{5.2.2}
$$

will be used, where T_0 is the mean annual temperature, T_1 represents the variation about the mean, ω measures the periodicity of the function and ϕ is the phase shift of the function. Therefore the time dependent temperature $T = T(t)$, the temperature dependent parameters $\phi_A(T)$, $\sigma_A(T)$, $\mu_A(T)$, $\mu_V(T)$, $a_M(T)$ and $\sigma_M(T)$ are continuous, bounded, positive and $\omega-$periodic functions. That is they belong to $L^\infty_+(0,\omega,\mathbb{R}_+)$.

Using similar argument to those in [27, 34, 35, 62, 89, 108] (and some of the references therein) and the basic fact that for mosquito-borne diseases (such as malaria), the total number of bites made by mosquitoes must equal the total number of bites received by humans. Thus, for the number of bites to be conserved, the following equation must hold

$$\beta_{HV} N_V = \beta_{VH}(N_H, N_V) N_H,$$

so that

$$N_V = \frac{\beta_{VH}(N_H, N_V)}{\beta_{HV}} N_H.$$

Thus, the force of infection in human populations is now given by

$$\lambda_H(T) = \frac{\beta_{HV} M_I(t)}{N_H(t)} (1 - \epsilon_B \alpha_B) a_M(T). \tag{5.2.3}$$

The non-autonomous malaria model (5.2.1), to the author's knowledge is the first to incorporate various control measures. The model extends some malaria transmissions models in the literature, such as those in [1, 3, 6, 50, 65, 89, 106, 111, 116, 153], by *inter alia*:

(I) Assuming that recovered individuals do not revert to wholly-susceptible class because they enjoy reduced susceptibility to new malaria infection [3, 6];

(II) Incorporating vaccination and the use of treated bed nets in humans (this was not considered in [3, 6, 111]);

(III) Including both the use of larvicides and adulticides in mosquito populations (this was not considered in [1, 3, 6, 50, 65, 89, 106]);

(IV) Dividing human population into compartments based on malaria infection in line with their vaccination status (this was not considered in [3, 6, 111]);

(V) Considering a reduced disease induced death rate, faster recovery rate and slower winning of immunity for vaccinated humans, i.e $\delta_V \leq \delta_U$, $\gamma_V \geq \gamma_U$ and $\tau_V \leq \tau_U$, this was also not considered in [1, 3, 6, 50, 65, 89, 106, 116];

(VI) Incorporating the effect of endemicity of malaria by differentiating wholly susceptible from susceptible with prior infection, this was not considered in [3, 6, 65, 89, 106, 116, 153].

5.2.4 Temperature dependent parameters

Temperature is known to directly affects vector borne diseases in host vectors; insects are poikilothermic and hence their internal temperature is greatly influenced by environmental temperature, which affect their physiology, as well as exposing the pathogen they carry to environmental temperature [116]. Using the formulations in [23, 102, 124], the temperature dependent parameters of malaria model (5.2.1) are defined either as Briere or Quadratic functions as follows. The temperature dependent:

1. Oviposition rate ($\phi_A(T)$) of mosquitoes is given by

$$\phi_A(T) = -0.153T^2 + 8.61T - 0.487.$$

2. Maturation rate ($\sigma_A(T)$) of aquatic mosquitoes is given by

$$\sigma_A(T) = 0.000111(T - 14.7)\sqrt{34 - T}, \quad (0 \leq T \leq 34).$$

3. Death rate of aquatic mosquitoes is obtained from the formulation in [124] as

$$\mu_A = 0.0025T^2 - 0.094T + 0.9.$$

4. Daily survival probability of adult mosquitoes (a function of the adult mosquito mortality rate) also follows from [102] as

$$\rho_M(T) = e^{-\mu_V(T)} = -0.000828T^2 + 0.0367T + 0.522,$$

so that the temperature dependent mortality rate of adult mosquitoes ($\mu_V(T)$) is given by

$$\mu_V(T) = -\ln(\rho_M(T)) = -\ln(-0.000828T^2 + 0.0367T + 0.522).$$

5. Biting rate (a_M) and parasite development rate ($\sigma_M(T)$) of adult mosquitoes are respectively given by

$$a_M(T) = -0.000203T(T - 11.7)\sqrt{42.3 - T}, \quad (0 \leq T \leq 42.3)$$

and

$$\sigma_M(T) = 0.000111(T - 14.7)\sqrt{34.4 - T}, \quad (0 \leq T \leq 34.4).$$

6. Finally the temperature dependent vector competence defined as the product of the proportion of the bites by infective mosquitoes that infect susceptible humans and the bites by susceptible mosquitoes on infectious humans that infect susceptible mosquitoes [102] is given by

$$V(T) = -0.54T^2 + 25.2T - 206.$$

The graphical representations of the temperature dependent parameters are presented by Figure 5.2, Figure 5.3, Figure 5.4 and Figure 5.5.

Table 5.1: Description of variables and parameters used for the model given by (5.2.1).

Variable	**Interpretation**
$S_U(t)$	Population of non-vaccinated wholly susceptible humans
$S_V(t)$	Population of vaccinated wholly susceptible humans
$W_U(t)$	Population of non-vaccinated partially immune susceptible humans
$W_V(t)$	Population of vaccinated partially immune susceptible humans
$E_U(t)$	Population of non-vaccinated exposed humans
$E_V(t)$	Population of vaccinated exposed humans
$I_U(t)$	Population of non-vaccinated infected humans
$I_V(t)$	Population of vaccinated infected humans
$R_U(t)$	Population of non-vaccinated recovered humans
$R_V(t)$	Population of vaccinated recovered humans
$N_H(t)$	Total human population
$A_M(t)$	Population of aquatic mosquitoes
$M_U(t)$	Population of susceptible adult female mosquitoes
$M_E(t)$	Population of exposed adult female mosquitoes
$M_I(t)$	Population of infected adult female mosquitoes
$N_V(t)$	Total population of adult mosquitoes
Parameter	**Interpretation**
Π_H	Recruitment rate of humans
ξ_V, ϵ_V	Rate, efficacy of vaccine
ω_V	Waning rate of vaccine
μ_H	Natural death rate of humans
α_B, ϵ_B	Rate of using and efficacy of bed nets
ϵ_W	Rate of protection due to prior infection
σ_U	Progression rate of non-vaccinated exposed humans to infected class
σ_V	Progression rate of vaccinated exposed humans to infected class
γ_V, γ_U	Recovery rate of vaccinated, non-vaccinated infected humans
δ_V, δ_U	Disease induced death rate of vaccinated, non-vaccinated infected humans
τ_V	Rate of loosing partial immunity by recovered vaccinated humans
τ_U	Rate of loosing partial immunity by recovered non-vaccinated humans
η_I	Reduction parameter for transmission by vaccinated infected humans
η_V	Reduction parameter for transmission by vaccinated recovered humans
η_U	Reduction parameter for transmission by non-vaccinated recovered humans
$\mathcal{K}$	Carrying capacity of aquatic mosquitoes
α_L, α_A	Rate of applying larvicides and adulticides
ϵ_L, ϵ_A	Efficacy of larvicides and adulticides
β_{VH}	Probability of transmission from infected mosquito to humans
β_{HV}	Probability of transmission from infected humans to mosquito
$a_M(T)$	Temperature dependent biting rate of mosquitoes
$\phi_A(T)$	Temperature dependent oviposition rate of mosquitoes
$\sigma_A(T)$	Temperature dependent maturation rate of aquatic mosquitoes
$\sigma_M(T)$	Temperature dependent progression rate of mosquitoes from M_E to M_I
$\mu_A(T)$	Temperature dependent natural death rate of aquatic mosquitoes
$\mu_V(T)$	Temperature dependent natural death rate of non-aquatic mosquitoes

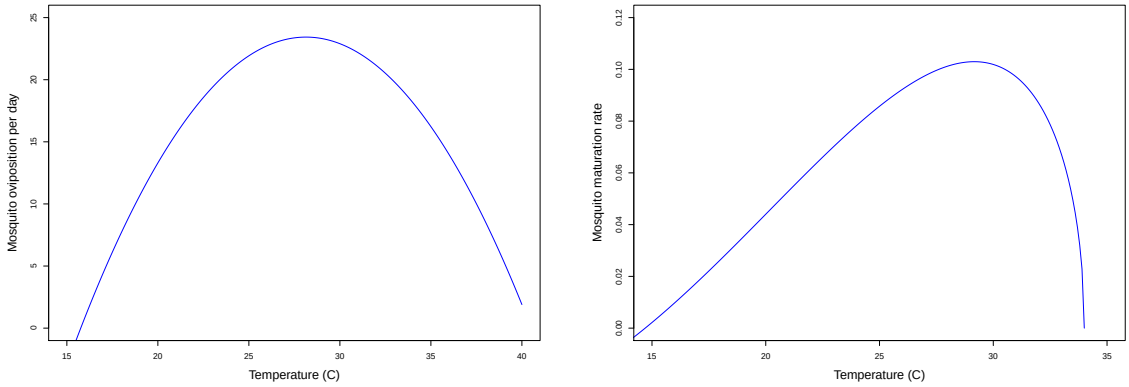

Figure 5.2: Simulation of temperature (T) dependent oviposition rate of adult mosquitoes given by $\phi_A(T) = -0.153T^2 + 8.61T - 97.7$ and maturation rate of aquatic mosquitoes given by $\sigma_A(T) = 0.000111T(T - 14.7)\sqrt{34 - T}$.

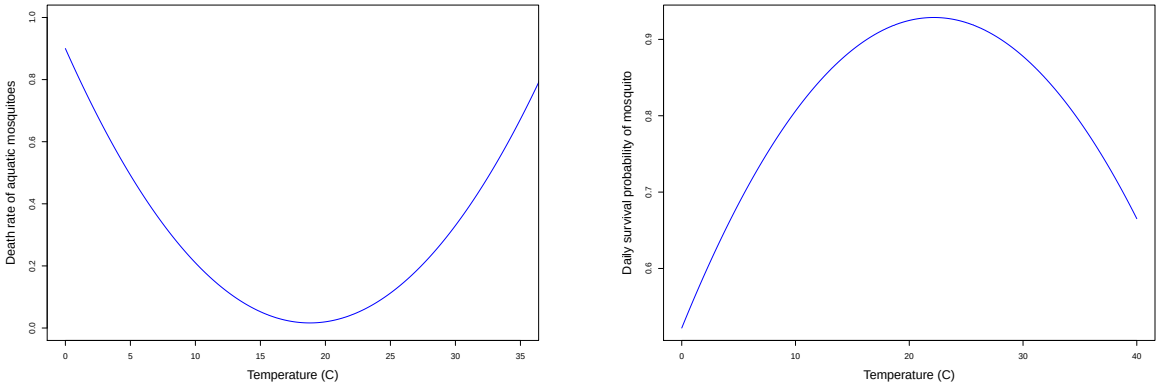

Figure 5.3: Simulation of temperature (T) dependent death rate of aquatic mosquitoes given by $\mu_A(T) = 0.0025T^2 - 0.09T + 0.9$ and daily survival probability of adult mosquitoes given by $\sigma_M(T) = -0.000828T^2 + 0.0367T + 0.522$.

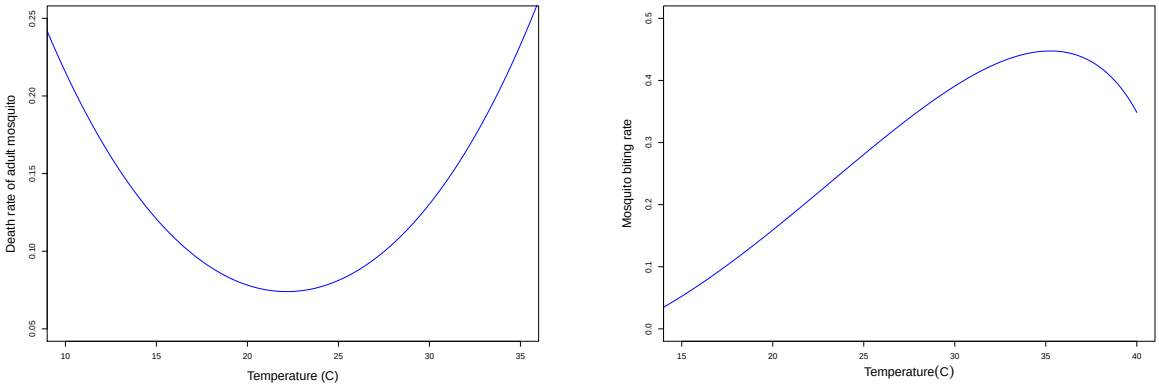

Figure 5.4: Simulation of temperature (T) dependent death rate of adult mosquitoes given by $\mu_V(T) = -\ln(-0.000828T^2 + 0.0367T + 0.522)$ and biting rate of adult mosquitoes given by $a_M(T) = 0.000203T(T - 11.7)\sqrt{42.3 - T}$.

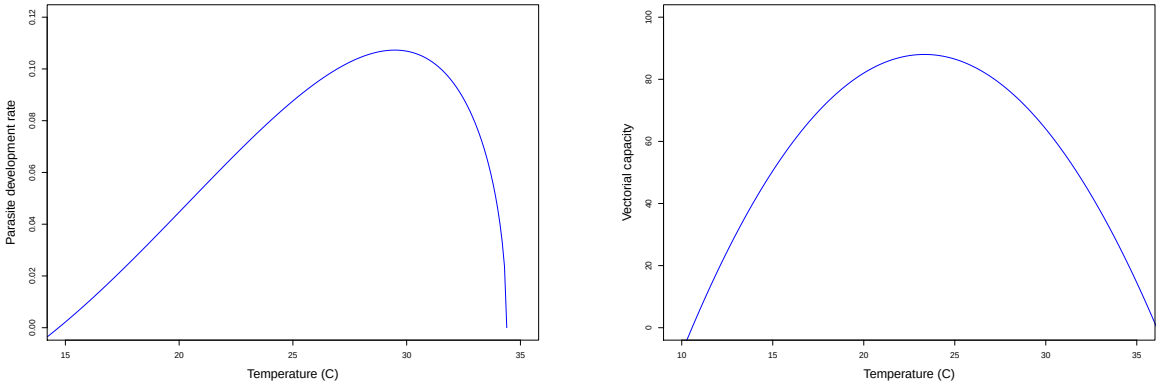

Figure 5.5: Simulation of temperature (T) dependent parasite development rate in mosquitoes given by $\sigma_M(T) = 0.000111T(T-14.7)\sqrt{34.4-T}$ and vectorial capacity of mosquitoes given by $V(T) = -0.54T^2 + 25.2T - 206$.

5.2.5 Basic properties of the model (5.2.1)

The basic dynamical properties of the non-autonomous system given by (5.2.1) is explored. Adding the first ten equations of the model (5.2.1) gives

$$\frac{dN_H}{dt} = \Pi_H - \mu_H N_H - \delta_U I_U - \delta_V I_V. \tag{5.2.4}$$

Since

$$\frac{dN_H}{dt} \leq \Pi_H - \mu_H N_H. \tag{5.2.5}$$

It follows that $dN_H/dt < 0$ if $N_H(t) > \Pi_H/\mu_H$. Thus, a standard comparison theorem can be used to show that $N_H(t) \leq N_H(0)e^{-\mu_H t} + \frac{\Pi_H}{\mu_H}\Big(1 - e^{-\mu_H t}\Big)$, which is bounded. Furthermore, letting $\mu_M(T) = \min\{\mu_A(T), \mu_V(T)\}$, and $c_M = \min\{\alpha_L\epsilon_L, \alpha_A\epsilon_A\}$, the total mosquito population (in both aquatic and non-aquatic stages) satisfies

$$\frac{dN_V}{dt} \leq \phi_A(T)\Big(1 - c_M\Big)\Big(1 - \frac{A_M(t)}{\mathcal{K}}\Big)N_V(t) - \mu_M(T)(1 + c_M)N_V.$$

Using similar approach to that of [89] and Gronwall's lemma, the mosquito population has a globally asymptotically periodic solution satisfying

$$N_V^*(t) = e^{-\int_0^t \mu_M(s)(1+c_M)ds}\Bigg[\int_0^t \Big\{\phi_A(s)(1-c_M)(1-\frac{A_M(s)}{\mathcal{K}})N_V(s)e^{\int_0^s \mu_M(k)(1+c_M)dk}$$

$$\Big\}d(s) + \frac{\int_0^\omega \Big\{\phi_A(s)(1-c_M)(1-\frac{A_M(s)}{\mathcal{K}})N_V(s)e^{\int_0^u \mu_M(n)(1+c_M)dn}\Big\}d(s)}{e^{\int_0^\omega \mu_M(n)(1+c_M)dn} - 1}\Bigg]. \tag{5.2.6}$$

Also from [89], it is assumed that the mosquito population stabilizes at a periodic state, thus for the continuous, bounded, positive and $\omega-$periodic functions $\phi_A(T)$, $\sigma_A(T)$, $\mu_A(T)$, $\mu_V(T)$, $a_M(T)$ and $\sigma_M(T)$, there exist a positive number h_0, such

that

$$\phi_A(T)(1-c_M)\Big(1-\frac{A_M(t)}{\mathcal{K}}\Big)L(t)-\mu_M(T)(1+c_M)L<0, \quad \text{for all } L\geq h_0. \quad (5.2.7)$$

Lemma 5.2.1. Consider the non-autonomous model (5.2.1) with non-negative initial condition for all $t \geq 0$. Then for any $x \in C([0],\mathbb{R}^{14}_+)$, the model has a unique non-negative solution through x that is ultimately bounded and uniformly bounded.

Let $X \in C([0],\mathbb{R}^{14}_+)$ and $G(t,x) := B(X)X + Z$ be the right hand side of (5.2.1), where $X = (S_U, S_V, W_U, W_V, E_U, E_V, I_U, I_V, R_U, R_V, A_M, M_U, M_E, M_I)^T$, $B(X)$ is the 14×14 matrix of coefficients of the non-constant part of (5.2.1), while $Z = (\Pi_H, 0, 0, 0, 0, 0, 0, 0, 0, 0, 0, 0, 0, 0)^T$.
It is clear that for all $x \in C([0],\mathbb{R}^{14}_+)$, $G(t,x)$ is continuous, and Lipschitzian in x, in addition, $\frac{\partial G_j(t,x)}{\partial x_i} > 0$ for all $i = 1, 2, ...14$ whenever $x_i \geq 0$ and $x_j = 0$, thus existence and uniqueness of solution through $(0, X)$ is guaranteed [89]. Following the approach of [45, 46, 111] and the fact that $B(X)$ is Metzler and $Z > 0$, the system is positively invariant in $C([0],\mathbb{R}^{14}_+)$.

Moreover it follows from (5.2.5) and (5.2.7), that $\limsup_{t\longrightarrow\infty} N_H(t) \leq \frac{\Pi_H}{\mu_H}$ and $\limsup_{t\longrightarrow\infty}(A_M + M_U + M_E + M_I - N^*_V(t)) \leq 0$, where $N^*_V(t)$ is the unique $\omega-$periodic solution defined by (5.2.6). Furthermore, $\frac{dN_H(t)}{dt} < 0$ whenever $N_H(t) > \frac{\Pi_H}{\mu_H}$ and $\frac{dN_V(t)}{dt} < 0$ if $N_V(t) > h_0$. Hence all solutions for the system given by (5.2.1) are positive, ultimately and uniformly bounded [89].

5.3 Analysis of the Autonomous Model

In this section, we analyse the dynamics of the autonomous form of the model (5.2.1). That is the case when the model parameters are temperature independent. Thus

$$a_M(T) = a_M, \quad \phi_A(T) = \phi_A, \quad \sigma_A(T) = \sigma_A, \quad \mu_A(T) = \mu_A, \quad \sigma_M(T) = \sigma_M,$$
$$\mu_V(T) = \mu_V.$$

We first of all analyse mosquito-only model in the absence of interaction with humans for its basic dynamical features.

5.3.1 Mosquito-only population model

In this section, we carry out analysis of mosquito-only population model in the absence of interaction with humans. In the absence of humans, the model (5.2.1), reduces to the following mosquito-only system:

$$\begin{aligned}\frac{dA_M(t)}{dt} &= \phi_A(1-\epsilon_L\alpha_L)\Big(1-\frac{A_M(t)}{\mathcal{K}}\Big)N_V(t) - (\sigma_A+\mu_A\epsilon_L\alpha_L+\mu_A)A_M(t),\\ \frac{dM_U(t)}{dt} &= \sigma_A A_M(t) - (1+\epsilon_A\alpha_A)\mu_V M_U(t).\end{aligned} \tag{5.3.8}$$

The system (5.3.8) has a threshold quantity called the basic offspring number denoted by N_0, given by

$$N_0 = \frac{\phi_A(1-\epsilon_L\alpha_L)\sigma_A}{(\sigma_A+\mu_A\epsilon_L\alpha_L+\mu_A)(1+\epsilon_A\alpha_A)\mu_V}. \tag{5.3.9}$$

The threshold quantity N_0 can be interpreted as follows: The average time spent by mosquito in the aquatic stage is given by $1/(\sigma_A+\mu_A\epsilon_L\alpha_L+\mu_A)$, where σ_A is the rate at which aquatic mosquitoes develop into an adult mosquito, so that the probability that an aquatic mosquito develop into an adult female mosquito is given by

$$\frac{\sigma_A}{\sigma_A+\mu_A\epsilon_L\alpha_L+\mu_A}. \tag{5.3.10}$$

In the absence of disease, the average life expectancy of an adult female mosquito is given by $\frac{1}{(1+\epsilon_A\alpha_A)\mu_V}$, so that the average eggs laid by an adult female mosquito throughout her life span is given by

$$\frac{\phi_A(1-\epsilon_L\alpha_L)}{(1+\epsilon_A\alpha_A)\mu_V}. \tag{5.3.11}$$

Thus, the product of (5.3.10) and (5.3.11) gives the basic offspring number of the mosquito-only population model.

The mosquito-only model (5.3.8) has two equilibria depending on N_0. If $N_0 \leq 1$, then, the system (5.3.8) has only the trivial equilibrium called an extinction equilibrium (E_0) given by

$$E_0 = (0,0).$$

If $N_0 > 1$. Then, the system (5.3.8) has a non-trivial equilibrium given by

$$E_1 = \Big[\mathcal{K}\Big(1-\frac{1}{N_0}\Big), \frac{\mathcal{K}\sigma_A}{(1+\epsilon_A\alpha_A)\mu_V}\Big(1-\frac{1}{N_0}\Big)\Big].$$

It is worth mentioning that the trivial equilibrium (E_0) is biologically less attractive since mosquitoes go extinct in the population. Rewriting the mosquito-only model (5.3.8) in the form $\dot{x} = f(x)$, where $\Omega^* \subseteq \mathbb{R}^2_+$ and $f : \Omega^* \to \mathbb{R}^2_+$ is continuous. Then we have the following results.

Theorem 5.3.1. The extinction equilibrium (E_0) is globally asymptotically stable (GAS) when $N_0 \leq 1$ and unstable otherwise. The non-trivial equilibrium (E_1) exists and is locally asymptotically stable (LAS) when $N_0 > 1$.

We shall give the proof of the first part of Theorem 5.3.1 using similar approach to

that in [8]. In particular, Theorem 6 of [8] reproduced below for convenience, will be used.

Theorem 5.3.2. [8] Let $a, b \in \Omega^*$ be such that $a < b$, $[a, b] \subseteq \Omega^*$ and $f(b) \leq 0 \leq f(a)$. Then the system defines a (positive) dynamical system on $[a, b]$. Moreover, if $[a, b]$ contains a unique equilibrium q then q is globally asymptotically stable on $[a, b]$.

Proof. To apply Theorem 5.3.2 to system (5.3.8), let $q > 0$ and let A_{Mq} be so large that the following inequalities hold:

$$\begin{aligned} A_{Mq} &\geq q, \\ M_{Uq} &= \frac{(\sigma_A + \mu_A \epsilon_L \alpha_L + \mu_A) A_{Mq}}{\phi_A (1 - c_M)} \geq q. \end{aligned} \tag{5.3.12}$$

Let $[a, b] = [0, b] \subseteq \mathbb{R}^2_+$, where $b = (A_{Mq},\ M_{Uq})'$. It is easy to see that $f(0) = 0$ and

$$f(b) = \begin{pmatrix} -\left[\sigma_A + \epsilon_L \alpha_L + \mu_A\right] \frac{A^2_{Mq}}{\mathcal{K}} \\ \sigma_A A_{Mq} [1 - \frac{1}{N_0}] \end{pmatrix} \tag{5.3.13}$$

so that $f(b) < 0$, provided $N_0 \leq 1$.

Therefore $f(b) \leq 0 \leq f(0)$, whenever $N_0 < 1$. Thus the mosquito component of model (5.2.1) defines a positive dynamical system on $[0, b]$ and E_0 is GAS on $[0, b]$. But since q is arbitrary, b can be extended and the result holds on $\mathbb{R}^2_+$. The second part of the proof follows straightforward by linearization. □

The epidemiological implication of Theorem (5.3.1) is that if the basic offspring number can be brought to a value less than unity, then mosquito population will goes to extinction and the diseases dies out in time (since no horizontal transmission).

5.3.2 Disease free equilibrium

The disease-free equilibrium (DFE) is the steady-state solution of the autonomous system (form of model (5.2.1)) obtained in the absence of disease. The autonomous form of (5.2.1) has two disease free equilibria depending on the magnitude of N_0. Suppose $N_0 \leq 1$ and the diseased compartments are zero, then the model has a mosquito extinction DFE, E_2, given by

$$\begin{aligned} E_2 &= \left(S^*_U, S^*_V, W^*_U, W^*_V, E^*_U, E^*_V, I^*_U, I^*_V, R^*_U, R^*_V, A^*_M, M^*_U, M^*_E, M^*_I \right) \\ &= \left(\frac{\Pi_H (\omega_V + \mu_H)}{\mu_H (\omega_V + \mu_H + \xi_V)}, \frac{\Pi_H \xi_V}{\mu_H (\omega_V + \mu_H + \xi_V)}, 0, 0, 0, 0, 0, 0, 0, 0, 0, 0, 0, 0 \right). \end{aligned} \tag{5.3.14}$$

If $N_0 > 1$, then the model has a non-mosquito extinction DFE, E_3 given by

$$E_3 = \left(\frac{\Pi_H(\omega_V + \mu_H)}{\mu_H(\omega_V + \mu_H + \xi_V)}, \frac{\Pi_H \xi_V}{\mu_H(\omega_V + \mu_H + \xi_V)}, 0, 0, 0, 0, 0, 0, 0, 0, \mathcal{K}\left(1 - \frac{1}{N_0}\right), \right.$$
$$\left. \frac{\mathcal{K}\sigma_A}{(1 + \alpha_A \epsilon_A)\mu_V}\left(1 - \frac{1}{N_0}\right), 0, 0 \right). \tag{5.3.15}$$

Notice that E_2 is biologically less attractive (due to absence of mosquitoes), thus we concentrate on E_3. The local stability of E_3 can be established using the next generation method [139]. Let

$$K_1 = \xi_V + \mu_H, \quad K_2 = \omega_V + \mu_H, \quad K_3 = \sigma_U + \mu_H, \quad K_4 = \sigma_V + \mu_H,$$
$$K_5 = \gamma_U + \delta_U + \mu_H, \quad K_6 = \gamma_V + \delta_V + \mu_H, \quad K_7 = \tau_U + \mu_H, \quad K_8 = \tau_V + \mu_H,$$
$$K_9 = \sigma_A + \mu_A + \mu_A \alpha_L \epsilon_L, \quad K_{10} = \mu_V + \mu_V \alpha_A \epsilon_A, \quad K_{11} = \sigma_M + \mu_V + \mu_V \alpha_A \epsilon_A. \tag{5.3.16}$$

The matrices for new infection terms (F) and of the transition terms (V) are respectively given by

$$F = \begin{pmatrix} 0 & 0 & 0 & 0 & 0 & 0 & 0 & \frac{C_1 S_U^*}{N_H^*} \\ 0 & 0 & 0 & 0 & 0 & 0 & 0 & \frac{C_2 S_V^*}{N_H^*} \\ 0 & 0 & 0 & 0 & 0 & 0 & 0 & 0 \\ 0 & 0 & 0 & 0 & 0 & 0 & 0 & 0 \\ 0 & 0 & 0 & 0 & 0 & 0 & 0 & 0 \\ 0 & 0 & 0 & 0 & 0 & 0 & 0 & 0 \\ 0 & 0 & \frac{C_1 M_U^*}{N_H^*} & \frac{C_1 \eta_I M_U^*}{N_H^*} & \frac{C_1 \eta_U M_U^*}{N_H^*} & \frac{C_1 \eta_V M_U^*}{N_H^*} & 0 & 0 \\ 0 & 0 & 0 & 0 & 0 & 0 & 0 & 0 \end{pmatrix},$$

and

$$V = \begin{pmatrix} K_3 & 0 & 0 & 0 & 0 & 0 & 0 & 0 \\ 0 & K_4 & 0 & 0 & 0 & 0 & 0 & 0 \\ -\sigma_U & 0 & K_5 & 0 & 0 & 0 & 0 & 0 \\ 0 & -\sigma_V & 0 & K_6 & 0 & 0 & 0 & 0 \\ 0 & 0 & -\gamma_U & 0 & K_7 & 0 & 0 & 0 \\ 0 & 0 & 0 & -\gamma_V & 0 & K_8 & 0 & 0 \\ 0 & 0 & 0 & 0 & 0 & 0 & K_{11} & 0 \\ 0 & 0 & 0 & 0 & 0 & 0 & -\sigma_M & K_{10} \end{pmatrix}.$$

and FV^{-1} is given by,

$$\begin{pmatrix} 0 & 0 & 0 & 0 & 0 & 0 & \frac{C_1\sigma_M S_U^*}{K_{11}K_{10}N_H^*} & \frac{C_1 S_U^*}{K_{10}N_H^*} \\ 0 & 0 & 0 & 0 & 0 & 0 & \frac{C_2\sigma_M S_V^*}{K_{11}K_{10}N_H^*} & \frac{C_2 S_V^*}{K_{10}N_H^*} \\ 0 & 0 & 0 & 0 & 0 & 0 & 0 & 0 \\ 0 & 0 & 0 & 0 & 0 & 0 & 0 & 0 \\ 0 & 0 & 0 & 0 & 0 & 0 & 0 & 0 \\ 0 & 0 & 0 & 0 & 0 & 0 & 0 & 0 \\ \frac{C_1\sigma_U M_U^*}{K_3K_5N_H^*}C_3 & \frac{C_1\sigma_V M_U^*}{K_4K_6N_H^*}C_4 & \frac{C_1 M_U^*}{K_5N_H^*}C_5 & \frac{C_1 M_U^*}{K_6N_H^*}C_6 & \frac{C_1 M_U^*\eta_U}{K_7N_H^*} & \frac{C_1\eta_V M_U^*}{K_8N_H^*} & 0 & 0 \\ 0 & 0 & 0 & 0 & 0 & 0 & 0 & 0 \end{pmatrix}$$

where

$$C_1 = \beta_{HV}a_M(1-\epsilon_B\alpha_B), \quad C_2 = C1(1-\epsilon_V), \quad C_3 = \Big(1+\frac{\eta_U\gamma_U}{K_7}\Big),$$
$$C_4 = \Big(\eta_I + \frac{\eta_V\gamma_V}{K_8}\Big). \tag{5.3.17}$$

Using the approach of [44], the next generation matrix with small domain $K = E^T(FV^{-1})E$ is given by

$$K_S = \begin{pmatrix} 0 & 0 & \frac{C_1\sigma_M S_U^*}{K_{11}K_{10}N_H^*} \\ 0 & 0 & \frac{C_2\sigma_M S_V^*}{K_{11}K_{10}N_H^*} \\ \frac{C_1\sigma_U M_U^*}{K_3K_5N_H^*}C_3 & \frac{C_1\sigma_V M_U^*}{K_4K_6N_H^*}C_4 & 0 \end{pmatrix}$$

where,

$$E = \begin{pmatrix} 1 & 0 & 0 \\ 0 & 1 & 0 \\ 0 & 0 & 0 \\ 0 & 0 & 0 \\ 0 & 0 & 0 \\ 0 & 0 & 0 \\ 0 & 0 & 1 \\ 0 & 0 & 0 \end{pmatrix}.$$

The dominant eigenvalue of K_S is the vaccinated reproduction number (R_{0V}) given by It follows then that the vaccinated reproduction number, denoted by, R_{0V}, is given by

$$\sqrt{\frac{\beta_{HV}^2 M_U^*\sigma_M a_M^2(1-\epsilon_B\alpha_B)^2}{(N_H^*)^2K_{11}K_{10}}\Big[\frac{S_U^*\sigma_U}{K_3K_5}\Big(1+\frac{\gamma_U\eta_U}{K_7}\Big)+\frac{S_V^*\sigma_V(1-\epsilon_V)}{K_4K_6}\Big(\eta_I+\frac{\gamma_V\eta_V}{K_8}\Big)\Big]}$$

$$= \sqrt{Q_1+Q_2}. \tag{5.3.18}$$

where

$$Q_1 = \frac{\beta_{HV}^2 a_M^2 (1-\epsilon_B\alpha_B)^2 \sigma_M \sigma_U M_U^* S_U^*}{(N_H^*)^2 K_3 K_5 K_{10} K_{11}} \left(1 + \frac{\gamma_U \eta_U}{K_7}\right)$$

and

$$Q_2 = \frac{\beta_{HV}^2 a_M^2 (1-\epsilon_B\alpha_B)^2 (1-\epsilon_V) \sigma_M \sigma_V S_V^* M_U^*}{(N_H^*)^2 K_4 K_6 K_{10} K_{11}} \left(\eta_I + \frac{\gamma_V \eta_V}{K_8}\right). \tag{5.3.19}$$

Following Theorem 2 of [139], the following result is established.

Lemma 5.3.3. The DFE of the model (5.2.1) is locally asymptotically stable if $R_{0V} < 1$, and unstable if $R_{0V} > 1$.

The threshold quantity R_{0V}, is the vaccinated reproduction number of the disease. It represents the average number of secondary malaria cases that one infected case can generate if introduced into a population where fraction are vaccinated and the aforementioned control strategies (bed nets, adulticides and larvicides) are used. It can be interpreted as follows.

Infection in humans occurs either in the class of non-vaccinated susceptible or vaccinated susceptible (due to vaccine failure and imperfection) classes. The number of new human cases in S_U class by an infected mosquito is the product of the infection rate of infected mosquito $(\frac{\beta_{HV} a_M (1-\epsilon_B\alpha_B)}{N_H^*})$, probability that a mosquito survives the exposed class and move to infected class $(\frac{\sigma_M}{K_{11}})$, the average life span of an infected mosquito $(\frac{1}{K_{10}})$ and the total number of non-vaccinated susceptible humans at the DFE. Thus we have

$$\frac{\beta_{HV} a_M (1-\epsilon_B\alpha_B) \sigma_M S_U^*}{N_H^* K_{10} K_{11}} = \frac{\beta_{HV} a_M (1-\epsilon_B\alpha_B) \sigma_M \Pi_H (\omega_V + \mu_H)}{N_H^* K_{10} K_{11} \mu_H (\omega_V + \mu_H + \xi_V)}. \tag{5.3.20}$$

Similarly, the number of infections generated by an infected mosquito in the S_V class is the product of the infection rate of infected mosquito $(\frac{\beta_{HV} a_M (1-\epsilon_B\alpha_B)}{N_H^*})$, the probability that a mosquito survives the exposed class and move to infected class $(\frac{\sigma_M}{K_{11}})$, the average life span of an infected mosquito $(\frac{1}{K_{10}})$, the reduced infection due to vaccination $(1-\epsilon_V)$, and the total number of non-vaccinated susceptible humans at the DFE. So that we have

$$\frac{\beta_{HV} a_M (1-\epsilon_B\alpha_B) \sigma_M (1-\epsilon_V) S_V^*}{N_H^* K_{10} K_{11}} = \frac{\beta_{HV} a_M (1-\epsilon_B\alpha_B) \sigma_M (1-\epsilon_V) \Pi_H \xi_V}{N_H^* K_{10} K_{11} \mu_H (\omega_V + \mu_H + \xi_V)}. \tag{5.3.21}$$

Mosquitoes get infection after sufficient contact with humans in either of I_U, I_V, R_U or R_V classes. The number of infections caused by an individual in class I_U is the product of the infection rate of infectious humans $(\frac{\beta_{HV} a_M (1-\epsilon_B\alpha_B)}{N_H^*})$, the probability that an individual survives E_U and move to I_U class $(\frac{\sigma_U}{K_3})$, the average time spent in I_U class $(\frac{1}{K_5})$ and the total number of susceptible mosquitoes at the DFE. Therefore

we have

$$\frac{\beta_{HV}a_M(1-\epsilon_B\alpha_B)\sigma_U M_U^*}{N_H^* K_3 K_5} = \frac{\beta_{HV}a_M(1-\epsilon_B\alpha_B)\sigma_U K\sigma_A r}{N_H^* K_3 K_5(\alpha_A\epsilon_A+\mu_V)}\left(1-\frac{1}{N_0}\right). \quad (5.3.22)$$

Using similar argument as above, with η_I accounting for reduced infectivity of vaccinated infectious humans, the number of infections caused by humans in compartment I_V is given as

$$\frac{\beta_{HV}a_M(1-\epsilon_B\alpha_B)\sigma_V\eta_I M_U^*}{N_H^* K_4 K_6} = \frac{\beta_{HV}a_M(1-\epsilon_B\alpha_B)\sigma_V\eta_I\mathcal{K}\sigma_A r}{N_H^* K_4 K_6(\alpha_A\epsilon_A+\mu_V)}\left(1-\frac{1}{N_0}\right). \quad (5.3.23)$$

The number of mosquito cases generated by humans in class R_U is the product of the infection rate of humans ($\frac{\beta_{HV}a_M(1-\epsilon_B\alpha_B)}{N_H^*}$), the probability that an individual survives E_U and move to I_U class ($\frac{\sigma_U}{K_3}$), the probability that an individual survives I_U and move to R_U ($\frac{\gamma_U}{K_5}$), the average time spent in R_U compartment $\frac{1}{K_7}$, and the total number of susceptible mosquitoes at DFE. With η_U accounting for the reduced infectivity of recovered humans of class R_U we have

$$\frac{\beta_{HV}a_M(1-\epsilon_B\alpha_B)\sigma_U\gamma_U\eta_U M_U^*}{N_H^* K_3 K_5 K_7} = \frac{\beta_{HV}a_M(1-\epsilon_B\alpha_B)\sigma_U\gamma_U\eta_U\mathcal{K}\sigma_A r}{N_H^* K_3 K_5 K_7(\alpha_A\epsilon_A+\mu_V)}\left(1-\frac{1}{N_0}\right). \quad (5.3.24)$$

Using similar approach as above, with $\eta_V \leq \eta_U$ accounting for the reduced infectivity of humans in compartments R_V we have

$$\frac{\beta_{HV}a_M(1-\epsilon_B\alpha_B)\sigma_V\gamma_V\eta_V M_U^*}{N_H^* K_4 K_6 K_8} = \frac{\beta_{HV}a_M(1-\epsilon_B\alpha_B)\sigma_V\gamma_V\eta_V\mathcal{K}\sigma_A r}{N_H^* K_4 K_6 K_8(\alpha_A\epsilon_A+\mu_V)}\left(1-\frac{1}{N_0}\right). \quad (5.3.25)$$

The total mosquito infection by non-vaccinated humans is the sum of (5.3.22) and (5.3.24), while mosquito infection by vaccinated humans is the sum of (5.3.23) and (5.3.25). Therefore the total mosquito to non-vaccinated humans and non-vaccinated humans to mosquito infections is given by the product of (5.3.20) and ((5.3.22) + (5.3.24)) given by

$$Q_1 = \frac{\beta_{HV}^2 a_M^2(1-\epsilon_B\alpha_B)^2\sigma_M\sigma_U M_U^* S_U^*}{(N_H^*)^2 K_3 K_5 K_{10} K_{11}}\left(1+\frac{\gamma_U\eta_U}{K_7}\right) \quad (5.3.26)$$

while those between vaccinated humans and mosquitoes is given by product of (5.3.21) and ((5.3.23) + (5.3.25)) as

$$Q_2 = \frac{\beta_{HV}^2 a_M^2(1-\epsilon_B\alpha_B)^2(1-\epsilon_V)\sigma_M\sigma_V S_V^* M_U^*}{(N_H^*)^2 K_4 K_6 K_{10} K_{11}}\left(\eta_I+\frac{\gamma_V\eta_V}{K_8}\right) \quad (5.3.27)$$

Thus, the square root of the sum of (5.3.26) and (5.3.27) given by (5.3.18) gives the vaccinated reproduction number.

5.3.3 Analysis of vaccine impact

The vaccinated reproduction number is such an important threshold that is used to determine whether a disease invade a community or dies out, such that reduction in the vaccinated reproduction number reduces disease burden. On the other hand, it was observed in the trial for RTS,S/AS01 vaccine that, the potential malaria vaccine is expected to be imperfect, thus it is important to investigate whether or not any widespread use of the malaria vaccine in a community will be beneficial (or not). This can simply be assessed by differentiating the vaccinated reproduction number R_{0V} with respect to the fraction of vaccinated individuals at steady state $V_H^* = \frac{S_V^*}{N_H^*}$. Let the basic reproduction number (in the absence of vaccine when $\xi_V = 0$) be given by

$$R_0 = \sqrt{\frac{\beta_{HV}^2 M_U^* \sigma_M \sigma_U a_M^2 (1-\epsilon_B\alpha_B)^2}{N_H^* K_3 K_5 K_{11} K_{10}}\left(1+\frac{\gamma_U \eta_U}{K_7}\right)}, \tag{5.3.28}$$

furthermore, let $F_1 = \min\{K_7, K_8\}$, $F_2 = \max\{C_3, C_4\}$, $F_3 = \min\{K_3, K_4\}$, $F_4 = \min\{K_5, K_6\}$, and $\sigma = \max\{\sigma_U, \sigma_V\}$, then it is easy to see that

$$R_{0V} \leq R_{0M} = \sqrt{\frac{\beta_{HV}^2 M_U^* F_2 \sigma_M a_M^2 (1-\epsilon_B\alpha_B)^2 \sigma}{N_H^* K_{11} K_{10} N_H^* F_3 F_4}\left[\frac{S_U^*}{N_H^*} + \frac{S_V^*(1-\epsilon_V)}{N_H^*}\right]},$$

since $R_{0V} \leq R_{0M}$ then

$$\frac{\partial R_{0V}}{\partial V_H^*} \leq \frac{\partial R_{0M}}{\partial V_H^*} = -\frac{\epsilon_V R_0}{2(1-\epsilon_V V_H^*)} < 0, \text{ since } (1-\epsilon_V V_H^*) > 0.$$

Thus, the vaccinated reproduction number is a decreasing function of V_H^*. Therefore an imperfect malaria vaccine would have a positive impact in the community (that is an increase in the fraction of vaccinated individuals leads to a corresponding decrease in malaria burden). Threshold quantities for vaccination (V_C^*) and efficacy of vaccination (ϵ_C^*) can be obtained by letting $R_{0V}(V_H^*) = 1$, so that

$$V_C^* = \frac{S_U^* K_4 K_6 \sigma_U (1+\frac{\gamma_U\eta_U}{K_7})}{N_H^* K_3 K_5 \sigma_V (1-\epsilon_V)(\eta_I + \frac{\gamma_V \eta_V}{K_8})}\left(\frac{N_H^*}{R_0^2 S_H^*} - 1\right)$$

and

$$\epsilon_C^* = 1 - \frac{S_U^* K_4 K_6 \sigma_U (1+\frac{\gamma_U\eta_U}{K_7})}{N_H^* K_3 K_5 V_H^* \sigma_V (\eta_I + \frac{\gamma_V \eta_V}{K_8})}\left(\frac{N_H^*}{R_0^2 S_H^*} - 1\right).$$

Lemma 5.3.4. The DFE (E_3) of the model (5.2.1) is locally asymptotically stable if $V_H^* > V_C^*$ and unstable otherwise.

The proof is consequence of Lemma 5.5.3 and the fact that $R_{0V} < 1$ provided $V_H^* > V_C^*$.

5.3.4 Type reproduction number

For a homogeneous system, the vaccinated reproduction number can be seen as the control threshold required to eliminate the disease from a community. The case is different in the case of multiple host types. The type-reproduction number ($\mathbf{T}$) is defined as

$$\mathbf{T}_i = e^{\mathbf{T}} K(I-(I-P)K)^{-1}e, \tag{5.3.29}$$

where I is an identity matrix, P is a projection matrix, e is a unit vector with all elements equal to zero except the ith term and $K = FV^{-1}$ is the next generation matrix with large domain. The type reproduction number correctly determines the critical control effort for heterogeneous populations [72].
We should note from the next generation matrix ($K = FV^{-1}$) that new infections occur only in compartments E_U, E_V and M_E, and therefore it can not be used to compute the type reproduction number for other infected/infectious compartments without new infection. Let the type reproduction numbers of compartments E_U, E_V and M_E be respectively denoted by $\mathbf{T}_1$, $\mathbf{T}_2$ and $\mathbf{T}_3$. From (5.3.29), it can be shown that

$$\mathbf{T}_1 = \frac{\frac{C_1^2\sigma_M\sigma_U S_U^* M_U^* C_3}{K_3K_5K_{11}K_{10}(N_H^*)^2}}{1-\frac{C_2C_1\sigma_V\sigma_M S_V^* M_U^* C_4}{K_4K_6K_{11}K_{10}(N_H^*)^2}} = \frac{Q_1}{1-Q_2} > 0, \text{ so that } \mathbb{T}_1 < 1, \text{ implies } Q_1+Q_2 < 1. \tag{5.3.30}$$

Similarly,

$$\mathbf{T}_2 = \frac{\frac{C_2C_1\sigma_V\sigma_M S_V^* M_U^* C_4}{K_4K_6K_{11}K_{10}(N_H^*)^2}}{1-\frac{C_1^2\sigma_M\sigma_U S_U^* M_U^* C_3}{K_3K_5K_{11}K_{10}(N_H^*)^2}} = \frac{Q_2}{1-Q_1} > 0, \text{so that } \mathbf{T}_2 < 1, \text{ implies } Q_1+Q_2 < 1 \tag{5.3.31}$$

and,

$$\mathbf{T}_3 = \frac{C_1^2\sigma_M\sigma_U S_U^* M_U^* C_3}{K_3K_5K_{11}K_{10}(N_H^*)^2} + \frac{C_2C_1\sigma_V\sigma_M S_V^* M_U^* C_4}{K_4K_6K_{11}K_{10}(N_H^*)^2} = Q_1+Q_2 = R_{0V}^2. \tag{5.3.32}$$

But

$$R_{0V}^2 < 1 \Longleftrightarrow \frac{C_1^2\sigma_M\sigma_U S_U^* M_U^* C_3}{K_3K_5K_{11}K_{10}(N_H^*)^2} + \frac{C_2C_1\sigma_V\sigma_M S_V^* M_U^* C_4}{K_4K_6K_{11}K_{10}(N_H^*)^2} < 1. \tag{5.3.33}$$

Hence it follows from (5.3.30), (5.3.31) and (5.3.32) that $\mathbb{T}_i < 1$ (for $i = 1, 2, 3$) implies $R_{0V} < 1$ (and vice versa).

$\mathbb{T}_i$ is the expected number of cases in compartment i caused by one infected individual of type i in a population where fractions are vaccinated, the infection might be directly or through chains of infections passing through individuals of other types, it singles out the required control effort when targeting the population of type i [72].

5.4 Endemic equilibrium and backward bifurcation

In this section, a unique endemic equilibrium of the model is computed and the conditions for the existence of backward bifurcation are also computed. In addition, impact of backward bifurcation on disease control is also evaluated.

5.4.1 Endemic equilibrium

Let the endemic equilibrium (the case when $\lambda_H \neq 0$ and $\lambda_V \neq 0$) of the model (5.2.1) be denoted by $E^{**} = \Big(S_U^{**}, S_V^{**}, W_U^{**}, W_V^{**}, E_U^{**}, E_V^{**}, I_U^{**}, I_V^{**}, R_U^{**}, R_V^{**}\Big)$, where

$$
\begin{aligned}
S_U^{**} &= \frac{M_0\Pi_H}{M_0M_2 - \omega_V\xi_V}, \quad S_V^{**} = \frac{\Pi_H\xi_V}{M_0M_2 - \omega_V\xi_V},\\
W_U^{**} &= \frac{M_0\Pi_H\lambda_H^{**}\sigma_U\gamma_U\tau_U}{\Big(M_0M_2 - \omega_V\xi_V\Big)\Big(K_3K_5K_7M_1 - \lambda_H^{**}M_3\Big)},\\
W_V^{*} &= \frac{M_0\Pi_H\lambda_H^{**}\sigma_V\gamma_V\tau_V}{\Big(M_0M_2 - \omega_V\xi_V\Big)\Big(K_4K_6K_8M_1 - \lambda_H^{**}M_4\Big)},\\
E_U^{**} &= \frac{\lambda_H^{**}\Big[S_U^{**} + (1-\epsilon_W)W_U^{**}\Big]}{K_3},\\
E_V^{**} &= \frac{\lambda_H^{**}\Big[S_V^{**} + (1-\epsilon_W)W_V^{**}\Big]}{K_4}, \quad I_U^{**} = \frac{\lambda_H^{**}\sigma_U\Big[S_U^{**} + (1-\epsilon_W)W_U^{**}\Big]}{K_3K_5},\\
I_V^{**} &= \frac{\lambda_H^{**}\sigma_V\Big[S_V^{**} + (1-\epsilon_W)W_V^{**}\Big]}{K_4K_6}, \quad R_U^{**} = \frac{\lambda_H^{**}\sigma_U\gamma_U\Big[S_U^{**} + (1-\epsilon_W)W_U^{**}\Big]}{K_3K_5K_7},\\
R_V^{**} &= \frac{\lambda_H^{**}\sigma_V\gamma_V\Big[S_V^{**} + (1-\epsilon_W)W_V^{**}\Big]}{K_4K_6K_8},\\
A_M^{**} &= \mathcal{K}\left[1 - \frac{K_9K_{10}\big[\lambda_V^{**} + \mu_V + \alpha_A\epsilon_A\big]}{\phi_V\sigma_A\big[K_{10} + \lambda_V^{**}\big]}\right],\\
M_U^{**} &= \frac{A_M^{**}\sigma_A}{K_{10} + \lambda_V^{**}}, \quad M_E^{**} = \frac{A_M^{**}\lambda_V^{**}\sigma_A}{K_{11}\big(K_{10} + \lambda_V^{**}\big)}, \quad M_I^{**} = \frac{A_M^{**}\lambda_V^{**}\sigma_M\sigma_A}{K_{10}K_{11}\big(K_{10} + \lambda_V^{**}\big)}
\end{aligned}
\tag{5.4.34}
$$

so that

$$
\begin{aligned}
N_H^{**} &= S_U^{**} + S_V^{**} + W_U^{**} + W_V^{**} + E_U^{**} + E_V^{**} + I_U^{**} + I_V^{**} + R_U^{**} + R_V^{**},\\
M_0 &= \lambda_H^{**}(1-\epsilon_V) + \omega_V + \mu_H, \quad M_1 = \lambda_H^{**}(1-\epsilon_V) + \mu_H, \quad M_2 = \lambda_H^{**} + \xi_V + \mu_H,\\
M_3 &= \sigma_U\gamma_U\tau_U(1-\epsilon_W), \quad M_4 = \sigma_V\gamma_V\tau_V(1-\epsilon_W),
\end{aligned}
$$

with

$$\lambda_H^{**}(T) = \frac{\beta_{HV} M_I^{**}(t)}{N_H^{**}(t)}(1-\epsilon_B\alpha_B)a_M(T),$$

and

$$\lambda_V^{**}(T) = \frac{\beta_{HV}}{N_H^{**}(t)}(1-\epsilon_B\alpha_B)a_M(T)\left[I_U^{**}(t) + \eta_I I_V^{**}(t) + \eta_U R_U^{**} + \eta_V R_V^{**}\right]$$

5.4.2 Backward bifurcation

Here we apply the method described in [26, 139] which is based on the use of centre manifold theory to prove the existence of backward bifurcation for the model (5.2.1). To apply that method, we carry out the following changes of variables. Let

$$S_U = x_1, S_V = x_2, W_U = x_3, W_V = x_4, E_U = x_5, E_V = x_6, I_U = x_7, I_V = x_8,$$
$$R_U = x_9, R_V = x_{10}, A_M = x_{11}, M_U = x_{12}, M_E = x_{13}, M_I = x_{14},$$

so that

$$N_H = x_1 + x_2 + x_3 + x_4 + x_5 + x_6 + x_7 + x_8 + x_9 + x_{10}, \quad N_V = x_{12} + x_{13} + x_{14},$$
and $N_V = x_{12} + x_{13} + x_{14}$.

The transformed malaria model (5.2.1) is represented by,

$$\begin{aligned}
\frac{dx_1}{dt} &= \Pi_H + \omega_V x_2 - \xi_V x_1 - \lambda_H x_1 - \mu_H x_1,\\
\frac{dx_2}{dt} &= \xi_V x_1 - \lambda_H(1-\epsilon_V)x_2 - \omega_V x_2 - \mu_H x_2,\\
\frac{dx_3}{dt} &= \tau_U x_9 - \lambda_H(1-\epsilon_W)x_3 - \mu_H x_3,\\
\frac{dx_4}{dt} &= \tau_V x_{10} - \lambda_H(1-\epsilon_W)x_4 - \mu_H x_4,\\
\frac{dx_5}{dt} &= \lambda_H x_1 + \lambda_H(1-\epsilon_W)x_3 - \sigma_U x_5 - \mu_H x_5,\\
\frac{dx_6}{dt} &= \lambda_H(1-\epsilon_V)x_2 + \lambda_H(1-\epsilon_W)x_4 - \sigma_V x_6 - \mu_H x_6,\\
\frac{dx_7}{dt} &= \sigma_U x_5 - \gamma_U x_7 - \delta_U x_7 - \mu_H x_7\\
\frac{dx_8}{dt} &= \sigma_V x_6 - \gamma_V x_8 - \delta_V x_8 - \mu_H x_8
\end{aligned} \tag{5.4.35}$$

$$\frac{dx_9}{dt} = \gamma_U x_7 - \tau_U x_9 - \mu_H x_9$$
$$\frac{dx_{10}}{dt} = \gamma_V x_8 - \tau_V x_{10} - \mu_H x_{10}$$
$$\frac{dx_{11}}{dt} = \phi_A\Big(1 - \frac{x_{11}}{\mathcal{K}}\Big)N_V - \sigma_A x_{11} - \alpha_L \epsilon_L x_{11} - \mu_A x_{11}$$
$$\frac{dx_{12}}{dt} = \sigma_A x_{11} - \lambda_V x_{12} - \mu_V x_{12} - \alpha_A \epsilon_A x_{12}$$
$$\frac{dx_{13}}{dt} = \lambda_V x_{12} - \sigma_M x_{13} - \mu_V x_{13} - \alpha_A \epsilon_A x_{13}$$
$$\frac{dx_{14}}{dt} = \sigma_M x_{13} - \mu_V x_{14} - \alpha_A \epsilon_A x_{14},$$

with the associated forces of infection given by

$$\lambda_H = \frac{\beta_{HV} x_{14(t)}}{N_H}(1 - \epsilon_B \alpha_B)a_M,$$

and

$$\lambda_V = \frac{\beta_{HV}}{N_H(t)}(1 - \epsilon_B \alpha_B)a_M\Big[x_7 + \eta_I x_8 + \eta_U x_9 + \eta_V x_{10}\Big].$$

By letting $R_{0V} = 1$ we have,

$$\frac{\beta_{HV}^2 M_U^* \sigma_M a_M^2 (1 - \epsilon_B \alpha_B)^2}{(N_H^*)^2 K_{10} K_{11}}\Big(\frac{S_U^* \sigma_U}{K_3 K_5}[1 + \frac{\gamma_U \eta_U}{K_7}] + \frac{S_V^* \sigma_V (1 - \epsilon_V)}{K_4 K_6}[\eta_I + \frac{\gamma_V \eta_V}{K_8}]\Big) = 1, \tag{5.4.36}$$

suppose, further that $\beta_{HV} = \beta_{HV}^*$ is chosen to be the bifurcation parameter. The Jacobian matrix (J^*) at the DFE with $\beta_{HV} = \beta_{HV}^*$ is given by

$$J^* = \begin{bmatrix} P_1 & P_2 \\ P_3 & P_4 \end{bmatrix},$$

where

$$P_1 = \begin{bmatrix} -K_1 & \omega_V & 0 & 0 & 0 & 0 & 0 \\ \xi_V & -K_2 & 0 & 0 & 0 & 0 & 0 \\ 0 & 0 & -\mu_H & 0 & 0 & 0 & 0 \\ 0 & 0 & 0 & -\mu_H & 0 & 0 & 0 \\ 0 & 0 & 0 & 0 & -K_3 & 0 & 0 \\ 0 & 0 & 0 & 0 & 0 & -K_4 & 0 \\ 0 & 0 & 0 & 0 & \sigma_U & 0 & -K_5 \end{bmatrix},$$

while,

$$P_2 = \begin{bmatrix} 0 & 0 & 0 & 0 & 0 & 0 & -Q_0 \\ 0 & 0 & 0 & 0 & 0 & 0 & -Q_1 \\ 0 & \tau_U & 0 & 0 & 0 & 0 & 0 \\ 0 & 0 & \tau_V & 0 & 0 & 0 & 0 \\ 0 & 0 & 0 & 0 & 0 & 0 & Q_0 \\ 0 & 0 & 0 & 0 & 0 & 0 & Q_1 \\ 0 & 0 & 0 & 0 & 0 & 0 & 0 \end{bmatrix} \quad P_3 = \begin{bmatrix} 0 & 0 & 0 & 0 & 0 & \sigma_V & 0 \\ 0 & 0 & 0 & 0 & 0 & 0 & \gamma_U \\ 0 & 0 & 0 & 0 & 0 & 0 & 0 \\ 0 & 0 & 0 & 0 & 0 & 0 & 0 \\ 0 & 0 & 0 & 0 & 0 & 0 & -Q_2 \\ 0 & 0 & 0 & 0 & 0 & 0 & Q_2 \\ 0 & 0 & 0 & 0 & 0 & 0 & 0 \end{bmatrix},$$

and

$$P_4 = \begin{bmatrix} -K_6 & 0 & 0 & 0 & 0 & 0 & 0 \\ 0 & -K_7 & 0 & 0 & 0 & 0 & 0 \\ \gamma_V & 0 & -K_8 & 0 & 0 & 0 & 0 \\ 0 & 0 & 0 & -K_9 N_0 & \frac{\phi_V}{N_0} & \frac{\phi_V}{N_0} & \frac{\phi_V}{N_0} \\ -Q_2\eta_I & -Q_2\eta_U & -Q_2\eta_V & \sigma_A & -K_{10} & 0 & 0 \\ Q_2\eta_I & Q_2\eta_U & Q_2\eta_V & 0 & 0 & -K_{11} & 0 \\ 0 & 0 & 0 & 0 & 0 & \sigma_M & -K_{10} \end{bmatrix}.$$

where,

$$Q_0 = \frac{\beta^*_{HV} S^*_U (1-\epsilon_B\alpha_B)}{N^*_H}, \quad Q_1 = \frac{\beta^*_{HV} S^*_V (1-\epsilon_B\alpha_B)(1-\epsilon_V)}{N^*_H},$$
$$Q_2 = \frac{\beta^*_{HV} M^*_U (1-\epsilon_B\alpha_B)}{N^*_H}.$$

The Jacobian (J^*) of the linearized system has a simple zero eigenvalue (with all other eigenvalues having negative real parts). Hence the theory based on center manifold theory [26, 139] can be used to analysed the dynamics of the system (5.4.35). We obtained the left eigenvector (v) corresponding to the zero eigenvalue denoted by $v = \Big[v_1, v_2, v_3, v_4, v_5, v_6, v_7, v_8, v_9, v_{10}, v_{11}, v_{12}, v_{13}, v_{14}\Big]^T$, where

$$v_1 = 0, \quad v_2 = 0, \quad v_3 = 0, \quad v_4 = 0, \quad v_5 = \frac{Q_2\sigma_M\sigma_U}{K_3K_5K_{11}}\Big(1 + \frac{\gamma_U\eta_U}{K_7}\Big)v_{14},$$
$$v_6 = \frac{Q_2\sigma_M\sigma_V}{K_4K_6K_{11}}\Big(\eta_I + \frac{\gamma_V\eta_V}{K_8}\Big)v_{14}, \quad v_7 = \frac{Q_2\sigma_M}{K_5K_{11}}\Big(1 + \frac{\gamma_U\eta_U}{K_7}\Big)v_{14},$$
$$v_8 = \frac{Q_2\sigma_M}{K_6K_{11}}\Big(\eta_I + \frac{\gamma_V\eta_V}{K_8}\Big)v_{14}, \quad v_9 = \frac{Q_2\sigma_M\eta_U}{K_7K_{11}}v_{14}, \quad v_{10} = \frac{Q_2\sigma_M\eta_V}{K_8K_{11}}v_{14},$$
$$v_{11} = 0, \quad v_{12} = 0, \quad v_{13} = \frac{\sigma_M}{K_{11}}v_{14} \quad v_{14} = (\beta^*_{HV})^2(1-\alpha_B\epsilon_B)^2 M^*_U\sigma_M\big(S^*_U\sigma_U Q_{11}$$
$$+ S^*_V\sigma_V(1-\epsilon_V)Q_{12}\big) + (N^*_H)^2K_{11}\big[K_{10}+K_{11}\big]\big(K_3K_4K_5K_6K_7K_8\big)^2, \tag{5.4.37}$$

where

$$Q_{11} = \left[K_7(K_3+K_5)(K_7+\gamma_U\eta_U) + K_3K_5\gamma_U\eta_U\right]\left(K_4K_6K_8\right)^2, \quad Q_{12} = \left[K_8(K_4+K_6)\right. \quad \left.(K_8\eta_I+\gamma_V\eta_V) + K_4K_6\gamma_V\eta_V\right]\left(K_3K_5K_7\right)^2.$$

The right eigenvector (w) is denoted by $w = \left[w_1, w_2, w_3, w_4, w_5, w_6, w_7, w_8, w_9, w_{10}, w_{11}, w_{12}, w_{13}, w_{14}\right]^T$, with

$$w_1 = \frac{-\left(Q_1K_2+Q_2\omega_V\right)}{\left(K_1K_2-\omega_V\xi_V\right)}w_{14}, \quad w_2 = \frac{-\left(Q_1\xi_V+Q_2K_1\right)}{\left(K_1K_2-\omega_V\xi_V\right)}w_{14},$$

$$w_3 = \frac{Q_1\sigma_U\gamma_U\tau_U}{K_3K_5K_7\mu_H}w_{14}, \quad w_4 = \frac{Q_2\sigma_U\gamma_V\tau_V}{K_4K_6K_8\mu_H}w_{14},$$

$$w_5 = \frac{Q_1}{K_3}w_{14}, \quad w_6 = \frac{Q_2}{K_4}w_{14}, \quad w_7 = \frac{Q_1\sigma_U}{K_3K_5}w_{14}, \quad w_8 = \frac{Q_2\sigma_V}{K_4K_6}w_{14},$$

$$w_9 = \frac{Q_1\sigma_U\gamma_U}{K_3K_7K_5}w_{14}, \quad w_{10} = \frac{Q_2\sigma_V\gamma_Vw_{14}}{K_4K_6K_8}, \quad w_{11} = 0, \quad w_{12} = \frac{K_{11}}{\sigma_M}w_{14},$$

$$w_{13} = \frac{K_{10}}{\sigma_M}w_{14}, \quad w_{14} = (N_H^*)^2K_{11}\left(K_3K_4K_5K_6K_7K_8\right)^2,$$

The eigenvalues v_{14} and w_{14} are chosen so that the classical requirement that the dot product of v and w satisfies $v.w = 1$. Clearly $v_i \geq 0$ while w_1, w_2 are negative (for variables that are non-zero at DFE), such choice is justified by Remark 1 of [26] which states;

Remark. The requirement that w is non-negative in the theorem is not necessary. When some components in w are negative, we still can apply this theorem, but one has to compare w with the actual equilibrium because the general parametrization of the Centre Manifold before the coordinate change is,

$$W^c = \left\{x_0 + c(t)w + h(c,\phi_V) : v.h(c,\phi_V) = 0, |c| \leq c_0, c(0) = 0\right\},$$

provided that x_0 is a non-negative equilibrium of interest (usually x_0 is the disease-free equilibrium). Hence, $x_0 - \frac{2b\phi_V}{a} > 0$ requires that $w_j > 0$ whenever $x_0(j) = 0$. If $x_0(j) > 0$, then $w(j)$ need not be positive [26].

It can be verified that $v.w = 1$, thus all the necessarily conditions for the application of Lemma 3 and Theorem 4 of [139] as well as Theorem 4.1 of [26] are satisfied. After

series of computations and simplifications we obtained

$$\mathbf{a} = \sum_{k,i,j=1}^{n} v_k w_I w_j \frac{\partial^2 f_k}{\partial x_I \partial x_j}(0,0) = -\frac{2(\beta^*_{HV})^2(1-\epsilon_B\alpha_B)^2 w_{14}^2 v_{14}}{(N^*_H)^2}\Big\{\frac{M^*_U P_1(1-\epsilon_B\alpha_B)}{K_{11}}$$
$$\Big(P_3+P_5-P_6-P_7\Big)\sigma_M + N^*_H P_1 + P_9 S^*_V(1-\epsilon_B\alpha_B)(1-\epsilon_V)\Big(P_3+P_4-P_6\Big)$$
$$+ P_8 S^*_U(1-\epsilon_B\alpha_B)\Big(P_2+P_5-P_7\Big) + P_8 P_{10}(1-\epsilon_B\alpha_B)\Big(N^*_H\epsilon_W - S^*_V\Big) + P_9 P_{11}$$
$$(1-\epsilon_B\alpha_B)\Big(N^*_H\epsilon_W - S^*_U\Big) + P_9 P_{11} S^*_V(1-\epsilon_B\alpha_B)\epsilon_V + P_8 P_6 S^*_V(1-\epsilon_B\alpha_B) +$$
$$P_9 P_7 S^*_U(1-\epsilon_B\alpha_B)(1-\epsilon_V)\Big\}$$

where,

$$P_1 = \frac{S^*_U\beta^*_{HV}\sigma_U}{N^*_H K_3 K_5}\Big(1+\frac{\gamma_U\eta_U}{K_7}\Big) + \frac{S^*_V\beta^*_{HV}\sigma_V(1-\epsilon_V)}{N^*_H K_4 K_6}\Big(\eta_I + \frac{\gamma_V\eta_V}{K_8}\Big),$$
$$P_2 = \frac{S^*_U\beta^*_{HV}}{N^*_H K_3}\Big(1+\frac{\sigma_U}{K_5}+\frac{\sigma_U\gamma_U}{K_5K_7}\Big), \quad P_3 = \frac{S^*_U\beta^*_{HV}}{N^*_H K_3}\Big(1+\frac{\sigma_U}{K_5}+\frac{\sigma_U\gamma_U}{K_5K_7}+\frac{\tau_U\sigma_U\gamma_U}{K_5K_7\mu_H}\Big),$$
$$P_4 = \frac{S^*_V\beta^*_{HV}(1-\epsilon_V)}{N^*_H K_4}\Big(1+\frac{\sigma_V}{K_6}+\frac{\sigma_V\gamma_V}{K_6K_8}\Big),$$
$$P_5 = \frac{S^*_V\beta^*_{HV}(1-\epsilon_V)}{N^*_H K_4}\Big(1+\frac{\sigma_V}{K_6}+\frac{\sigma_V\gamma_V}{K_6K_8}+\frac{\tau_V\sigma_V\gamma_V}{K_6K_8\mu_H}\Big),$$
$$P_6 = \frac{\beta^*_{HV}\big(S^*_U K_2 + S^*_V\omega_V(1-\epsilon_V)\big)}{N^*_H\big(K_1K_2-\omega_V\xi_V\big)}, \quad P_7 = \frac{\beta^*_{HV}\big(S^*_U\xi_V + S^*_V K_1(1-\epsilon_V)\big)}{N^*_H\big(K_1K_2-\omega_V\xi_V\big)},$$
$$P_8 = \frac{\beta^*_{HV}M^*_U\sigma_M\sigma_U}{K_3K_5K_{11}N^*_H}\Big(1+\frac{\gamma_U\eta_U}{K_7}\Big), \quad P_9 = \frac{\beta^*_{HV}M^*_U\sigma_M\sigma_V}{K_4K_6K_{11}N^*_H}\Big(\eta_I+\frac{\gamma_V\eta_V}{K_8}\Big),$$
$$P_{10} = \frac{\beta^*_{HV}S^*_U\sigma_U\gamma_U\tau_U}{N^*_H K_3K_5K_7\mu_H}, \quad P_{11} = \frac{\beta^*_{HV}S^*_V\sigma_U\gamma_V\tau_V(1-\epsilon_V)}{N^*_H K_4K_6K_8\mu_H},$$

while,

$$\mathbf{b} = \sum_{k,i=1}^{n} v_k w_I \frac{\partial^2 f_k}{\partial x_I \partial \phi_V}(0,0) = \frac{\beta^*_{HV}M^*_U\sigma_M v_{14}w_{14}}{(N^*_H)^2}\Big[\frac{S^*_U\sigma_U}{K_3K_5K_{11}}\Big(1+\frac{\gamma_U\eta_U}{K_7}\Big)+$$
$$\frac{S^*_V\sigma_V}{K_4K_6K_{11}}\Big(\eta_I+\frac{\gamma_V\eta_V}{K_8}\Big)\Big] + \Big[\frac{\beta^*_{HV}S^*_U\sigma_M\gamma_U\sigma_U}{N^*_H K_3K_5K_7}\Big(1+\frac{\gamma_U\eta_U}{K_5}\Big) + \frac{\beta^*_{HV}S^*_V(1-\epsilon_V)}{N^*_H K_4K_6}$$
$$\sigma_M\sigma_V\Big(\eta_I+\frac{\gamma_V\eta_V}{K_8}\Big)\Big]\frac{M^*_U\sigma_M v_{14}w_{14}}{N^*_H K_{11}} > 0$$

Since $\mathbf{b} > 0$, the direction of bifurcation depends on the sign of $\mathbf{a}$, which can be positive or negative, and $\mathbf{a} > 0$ means the model (5.2.1) undergo backward bifurcation

at $R_{0V} = 1$ [26, 139]. Thus we claim the following result.

Theorem 5.4.1. The autonomous malaria model (5.2.1) undergo backward bifurcation at $R_{0V} = 1$ whenever the bifurcation coefficient **a** is positive.

5.4.3 Non-existence of backward bifurcation

It is well known that disease induced death rate and imperfect vaccination are some of the major causes of backward bifurcation in vector borne disease models. Let $\delta_U = \delta_V = \omega_V = 0$, then **a** reduces to

$$\mathbf{a} = \sum_{k,i,j=1}^{n} v_k w_I w_j \frac{\partial^2 f_k}{\partial x_I \partial x_j}(0,0) = -\frac{2(\beta^*_{HV})^2(1-\epsilon_B\alpha_B)^2 w_{14}^2 v_{14}}{(N^*_H)^2}\Bigg\{ N^*_H P_1 + P_4 P_9 S^*_V(1-\epsilon_V) + P_2 P_8 S^*_U + P_8 P_{10}\Big(N^*_H\epsilon_W - S^*_V\Big) + P_9 P_{11}\Big(N^*_H\epsilon_W - S^*_U\Big) + P_9 P_{11} S^*_V \epsilon_V + P_8 P_6 S^*_V + P_9 P_7 S^*_U(1-\epsilon_V)\Bigg\}$$

which is less than zero provided $\epsilon_W \geq \max\left\{\frac{S^*_V}{N^*_H}, \frac{S^*_U}{N^*_H}\right\}$

Lemma 5.4.2. The model (5.2.1) does not undergo backward bifurcation at $R_{0V} = 1$ provided $\delta_U = \delta_V = \omega_V = 0$ and $\epsilon_W \geq \max\left\{\frac{S^*_V}{N^*_H}, \frac{S^*_U}{N^*_H}\right\}$.

5.4.4 Impact of backward bifurcation on disease control

Since the direction of bifurcation at $R_{0V} = 1$ depends on the sign of **a**, it is important to investigate the effect of control measures on the direction of backward bifurcation. Let $\mathbf{a} = 0$, then we have

$$\epsilon^*_B = \frac{1}{\alpha_B}\left\{1 + \frac{N^*_H P_1 K_{11}}{Z_1}\right\} \tag{5.4.38}$$

where,

$$\begin{aligned} Z_1 =& M^*_U P_1(1-\epsilon_B\alpha_B)\sigma_M\Big(P_3 + P_5 - P_6 - P_7\Big) + P_9 S^*_V K_{11}(1-\epsilon_B\alpha_B)(1-\epsilon_V)\Big(P_3 \\ &+ P_4 - P_6\Big) + P_8 S^*_U K_{11}(1-\epsilon_B\alpha_B)\Big(P_2 + P_5 - P_7\Big) + P_8 P_{10} K_{11}(1-\epsilon_B\alpha_B) \\ &\Big(N^*_H\epsilon_W - S^*_V\Big) + P_9 P_{11} K_{11}(1-\epsilon_B\alpha_B)\Big(N^*_H\epsilon_W - S^*_U\Big) + P_9 P_{11} S^*_V K_{11}(1- \\ &\epsilon_B\alpha_B)\epsilon_V + P_8 P_6 S^*_V K_{11}(1-\epsilon_B\alpha_B) + P_9 P_7 S^*_U K_{11}(1-\epsilon_B\alpha_B)(1-\epsilon_V), \end{aligned}$$

therefore for the direction of bifurcation at R_{0V} to be forward, the vaccine efficacy ϵ_B should be greater than ϵ_B^*. Similarly,

$$\epsilon_V^* = \frac{Z_2}{Z_3}, \tag{5.4.39}$$

where,

$$\begin{aligned} Z_2 =& \frac{M_U^* P_1(1-\epsilon_B\alpha_B)\sigma_M}{K_{11}}\Big(P_3+P_5-P_6-P_7\Big)+N_H^*P_1+P_9S_V^*(1-\epsilon_B\alpha_B)\Big(P_3+\\ & P_4-P_6\Big)+P_8S_U^*(1-\epsilon_B\alpha_B)\Big(P_2+P_5-P_7\Big)+P_8P_{10}(1-\epsilon_B\alpha_B)\Big(N_H^*\epsilon_W-S_V^*\Big)\\ & +P_9P_{11}(1-\epsilon_B\alpha_B)\Big(N_H^*\epsilon_W-S_U^*\Big)+P_8P_6S_V^*(1-\epsilon_B\alpha_B)+P_9P_7S_U^*(1-\epsilon_B\alpha_B), \end{aligned}$$

and,

$$Z_3 = P_9S_V^*(1-\epsilon_B\alpha_B)\Big(P_3+P_4-P_6\Big)+P_9P_7S_U^*(1-\epsilon_B\alpha_B)-P_9P_{11}S_V^*(1-\epsilon_B\alpha_B),$$

and thus, for the direction of bifurcation at $R_{0V}=1$ to be forward, then $\epsilon_V > \epsilon_V^*$.

5.5 Analysis of non-autonomous model

Consider the non-autonomous model given by (5.2.1) where the time dependent basic offspring number given by

$$N_0(t) = \frac{\phi_A(T)\sigma_A(T)r}{(\sigma_A(T)+\epsilon_L\alpha_L+\mu_A(T))(\mu_V(T)+\epsilon_A\alpha_A)} \tag{5.5.40}$$

is strictly greater than 1. To find the disease-free state of the system given by (5.2.1), we let $E_U(t)=E_V(t)=I_U(t)=I_V(t)=R_U(t)=R_V(t)=M_E(t)=M_I(t)=0$ and obtained a non-trivial disease-free state given by

$$\begin{aligned} E_4 =& \left(S_U^{**},S_V^{**},W_U^{**},W_V^{**},E_U^{**},E_V^{**},I_U^{**},I_V^{**},R_U^{**},R_V^{**},A_M^{**},M_U^{**},M_E^{**},M_I^{**}\right)=\\ & \left(\frac{\Pi_H(\omega_V+\mu_H)}{\mu_H(\omega_V+\mu_H+\xi_V)},\frac{\Pi_H\xi_V}{\mu_H(\omega_V+\mu_H+\xi_V)},0,0,0,0,0,0,0,0,A_M^{**},M_U^{**},0,0\right) \end{aligned}$$

where the pair (A_M^{**},M_U^{**}) is the unique positive $\omega-$periodic solution of

$$\begin{aligned} \frac{dA_M^{**}(t)}{dt} &= \phi_A(T)\Big(1-\frac{A_M^{**}(t)}{\mathcal{K}}\Big)N_V^{**}(t)-\sigma_A(T)A_M^{**}(t)-\alpha_L\epsilon_LA_M^{**}(t)-\mu_A(T)A_M^{**}(t)\\ \frac{dM_U^{**}(t)}{dt} &= \sigma_A(T)A_M^{**}(t)-\mu_V(T)M_U^{**}(t)-\alpha_A\epsilon_AM_U^{**}(t), \end{aligned}$$

which is obtained when $N_0(t) > 1$. On the other hand, a unique positive trivial non-periodic solution is obtained when $N_0(t) \leq 1$.

5.5.1 Basic reproduction ratio

The local asymptotic stability of the positive periodic disease-free state (E_4) can be established using a threshold parameter called the basic reproduction ratio [141]. The basic reproduction ratio for the model (5.2.1) is computed using the theory developed by [141] and used for many periodic models such as [1, 3, 106, 89, 111, 153] and some of the references therein.

Consider the disease classes of the model (5.2.1) given by

$$\begin{aligned}
\frac{dE_U(t)}{dt} &= \lambda_H(T)S_U(t) + \lambda_H(T)(1-\epsilon_W)W_U(t) - \sigma_U E_U(t) - \mu_H E_U(t),\\
\frac{dE_V(t)}{dt} &= \lambda_H(T)(1-\epsilon_V)S_V(t) + \lambda_H(T)(1-\epsilon_W)W_V(t) - \sigma_V E_V(t) - \mu_H E_V(t),\\
\frac{dI_U(t)}{dt} &= \sigma_U E_U(t) - \gamma_U I_U(t) - \delta_U I_U(t) - \mu_H I_U(t)\\
\frac{dI_V(t)}{dt} &= \sigma_V E_V(t) - \gamma_V I_V(t) - \delta_V I_V(t) - \mu_H I_V(t)\\
\frac{dR_U(t)}{dt} &= \gamma_U I_U - \tau_U R_U - \mu_H R_U\\
\frac{dR_V(t)}{dt} &= \gamma_V I_V - \tau_V R_V - \mu_H R_V\\
\frac{dM_E(t)}{dt} &= \lambda_V(T)M_U(t) - \sigma_M(T)M_E(t) - \mu_V(T)M_E(t) - \alpha_A\epsilon_A M_E(t)\\
\frac{dM_I(t)}{dt} &= \sigma_M(T)M_E(t) - \mu_V(T)M_I(t) - \alpha_A\epsilon_A M_I(t),
\end{aligned} \tag{5.5.41}$$

where $\lambda_H(T)$ and $\lambda_V(T)$ are as defined in (5.2.3). The matrix of new infection terms $F(t)$ and matrix of transfer in and out of infectious compartments $V(t)$ are respectively given by

$$F(t) = \begin{pmatrix}
0 & 0 & 0 & 0 & 0 & 0 & 0 & \frac{S_H^* G_0}{N_H^*}\\
0 & 0 & 0 & 0 & 0 & 0 & 0 & \frac{S_V^* G_0(1-\epsilon_V)}{N_H^*}\\
0 & 0 & 0 & 0 & 0 & 0 & 0 & 0\\
0 & 0 & 0 & 0 & 0 & 0 & 0 & 0\\
0 & 0 & 0 & 0 & 0 & 0 & 0 & 0\\
0 & 0 & 0 & 0 & 0 & 0 & 0 & 0\\
0 & 0 & \frac{G_0 M_U^*}{N_H^*} & \frac{G_0\eta_I M_U^*}{N_H^*} & \frac{G_0\eta_U M_U^*}{N_H^*} & \frac{G_0\eta_V M_U^*}{N_H^*} & 0 & 0\\
0 & 0 & 0 & 0 & 0 & 0 & 0 & 0
\end{pmatrix},$$

while,

$$V(t) = \begin{pmatrix} G_1 & 0 & 0 & 0 & 0 & 0 & 0 & 0 \\ 0 & G_2 & 0 & 0 & 0 & 0 & 0 & 0 \\ -\sigma_U & 0 & G_3 & 0 & 0 & 0 & 0 & 0 \\ 0 & -\sigma_V & 0 & G_4 & 0 & 0 & 0 & 0 \\ 0 & 0 & -\gamma_U & 0 & G_5 & 0 & 0 & 0 \\ 0 & 0 & 0 & -\gamma_V & 0 & G_6 & 0 & 0 \\ 0 & 0 & 0 & 0 & 0 & 0 & G_7 & 0 \\ 0 & 0 & 0 & 0 & 0 & 0 & -\sigma_M & G_8 \end{pmatrix},$$

where,

$$G_0 = \beta_{HV}(1-\epsilon_B\alpha_B)a_M(T), \quad G_1 = \sigma_U + \mu_H, \quad G_2 = \sigma_V + \mu_H,$$
$$G_3 = \gamma_U + \delta_U + \mu_H, \quad G_4 = \gamma_V + \delta_V + \mu_H, \quad G_5 = \tau_U + \mu_H, \quad G_6 = \tau_V + \mu_V,$$
$$G_7 = \sigma_M(T) + \mu_V(T) + \alpha_A\epsilon_A, \quad G_8 = \mu_V(T) + \alpha_A\epsilon_A.$$

Notice that $F(t)$ is non-negative and $-V(t)$ is cooperative. Let $K(t) = \big(E_U(t), E_V(t), I_U(t), I_V(t), R_U(t), R_V(t), M_E(t), M_I(t)\big)^T$, then the linearization of (5.5.41) can be re-written in the form

$$\frac{dK}{dt} = \Big(F(t) - V(t)\Big)K(t).$$

Following the approach of [89, 141], let $Y(t,s)$ and $\Phi_T = Y(t,0)$ respectively be the evolution operator and monodromy matrix of the linear $\omega-$periodic system $\frac{dy}{dt} = -Vy(t)$, $t \geq s$, that is for each $s \in \mathbb{R}$, the 8×8 matrix $Y(t,s)$ satisfies

$$\frac{dY}{dt} = -VY(t,s), \quad Y(s,s) = I, \quad t \geq s,$$

where I is the identity matrix of order 8. Let Z_T be the Banach space of all ω-periodic functions equipped with the maximum norm and an ω-periodic function of s denoted by $\alpha(s)$ be the initial distribution of infectious individuals in the community, then the rate at which new infections are produced by an infected individual in the community who were introduced at time s is given by $F(s)\alpha(s)$ [3, 89, 141]. Likewise the distribution of new infected individuals from infections at time s and remain in the infected compartments at a later time t is $Y(t,s)F(s)\alpha(s)$. Therefore

$$\theta(t) = \int_{-\infty}^{t} Y(t,s)F(s)\alpha(s)ds = \int_{0}^{\infty} Y(t,t-a)F(t-a)\alpha(t-a)da \qquad (5.5.42)$$

gives the cumulative distribution of new infections at time t that are produced by all infected individuals $(\alpha(s))$ introduced at sometimes before t.
Define the linear operator $\mathcal{L} : Z_T \longrightarrow Z_T$ by

$$(\mathcal{L}\alpha)(s) = \int_{0}^{\infty} Y(t,t-a)F(t-a)\alpha(t-a)da \quad \forall t \in \mathbb{R}, \quad \alpha \in Z_T. \qquad (5.5.43)$$

If $\rho(\mathcal{L})$ is the spectral radius of $\mathcal{L}$, the basic reproduction ratio (R_{0T}) is given by $\rho(\mathcal{L})$

[141]. It is easy to show that, in addition to Assumptions A1 to A5 satisfied by the autonomous system, the non-autonomous model (5.2.1) can be shown to satisfy the additional Assumptions A6 and A7 of [141]. Thus the following result follows from Theorem

Theorem 5.5.1. The disease free state (E_4), of the non-autonomous model (5.2.1) is LAS if $R_{0T} < 1$ and unstable if $R_{0T} > 1$ provided $N_0(t) > 1$.

5.6 Effect of control strategies

In this section, numerical simulations to assess impact of different control measures (single or in combination) are carried out for both the autonomous and non-autonomous models.

Simulations to assess effects of control strategies for the non-autonomous model were carried out for the cities of Kigali, Niamey and Gulu, where values of the parameters for the generalized temperature function given by (5.2.2) were used (as given in Table 3 of [3]). In addition, more simulations for the autonomous model (where temperature values are fixed) based on control measures are also presented.

5.6.1 Effects of control on the non-autonomous model

Using the generalized temperature function given by (5.2.2), simulations were done to assess the impact of low (administered at 0.1), medium (at 0.3) and high (at 0.5) control measures. Three different control strategies are considered, namely;

(i) Bed nets and vaccination strategy;

(ii) Mosquito control (larvicides and adulticides) strategy;

(iii) Bed nets, vaccination and mosquito control strategy (Hybrid strategy).

Simulations are carried out for the functional form of a_M, ϕ_A, σ_A, μ_A, σ_M and μ_V (temperature dependent), while

$$\Pi_H = 70, \beta_{HV} = 0.64, \epsilon_W = 0.5, \omega_V = 0.1, \tau_U = 0.1, \tau_V = 0.02, \gamma_U = 0.015,$$

$$\delta_U = 0.004, \delta_V = 0.003, \sigma_U = 0.08, \sigma_V = 0.07, \eta_I = 0.7, \eta_U = 0.3, \eta_V = 0.1,$$

$$\mathcal{K} = 100000, \mu_H = 0.0000548, \gamma_V = 0.017.$$

The generalized temperature parameter values were fitted for some selected sub-Saharan African countries from 2011-2013 and presented in Table 3 of [3]. Three cities are selected for our simulations and parameters presented as follows:

City of Kigali with latitude -1.961 and longitude 30.078 has,

$$T_0 = 20.5, T_1 = 0.0455, \omega = 0.9503, \phi = -150.499.$$

The city of Gulu, Uganda with latitude 2.763 and longitude of 32.294 has,

$$T_0 = 23.5, T_1 = 0.131, \omega = 1.0349, \phi = -125.4224.$$

Similarly, Niamey of Niger republic with latitude 13.516 and longitude 2.140 has,

$$T_0 = 29.9, T_1 = -0.139, \omega = 0.9256, \phi = -282.5711.$$

It should be observed that, Kigali has the lowest mean annual temperature, followed by Gulu then Niamey, also Niamey has the smallest phase shift, then Kigali and Gulu.

As expected, the hybrid control is the most effective in reaching the DFE, reducing the number of infected humans and cycles of infections in the three cities as presented by Figure 5.12, Figure 5.13 and Figure 5.14. Similarly, the use of vaccination and bed nets (Figure 5.9, Figure 5.10 and Figure 5.11) is more effective in reaching the DFE, reducing the number of infected humans and cycles of infections in comparison with the use of larvicides and adulticides (Figure 5.6, Figure 5.7 and Figure 5.8). Observe that control is more effective in Kigali, the city with the smallest mean annual temperature and moderate phase shift, where for hybrid control, the DFE is reached after 1,600 days in comparison to Gulu (4,500 days) and Niamey (4,000 days). Although the mean annual temperature of Gulu is smaller than that of Niamey, control is more effective in Niamey, this is attributed to the phase shift, where that of Gulu is bigger, thus, in addition to mean annual temperature, phase shift also affects the impact of control.

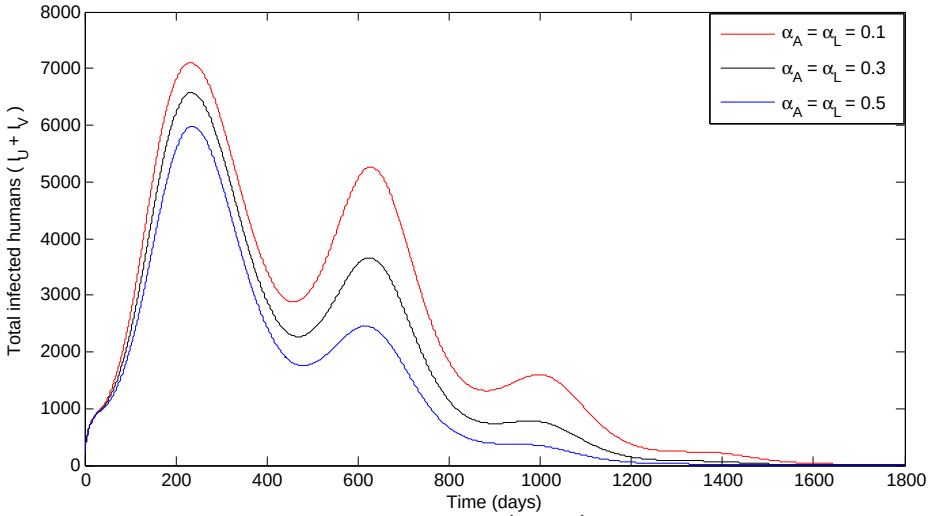

Figure 5.6: Simulations of the model (5.2.1) showing the total number of infected humans $(I_U + I_V)$ with varying temperature for the city Kigali in Rwanda and the use of larvicides and adulticides.

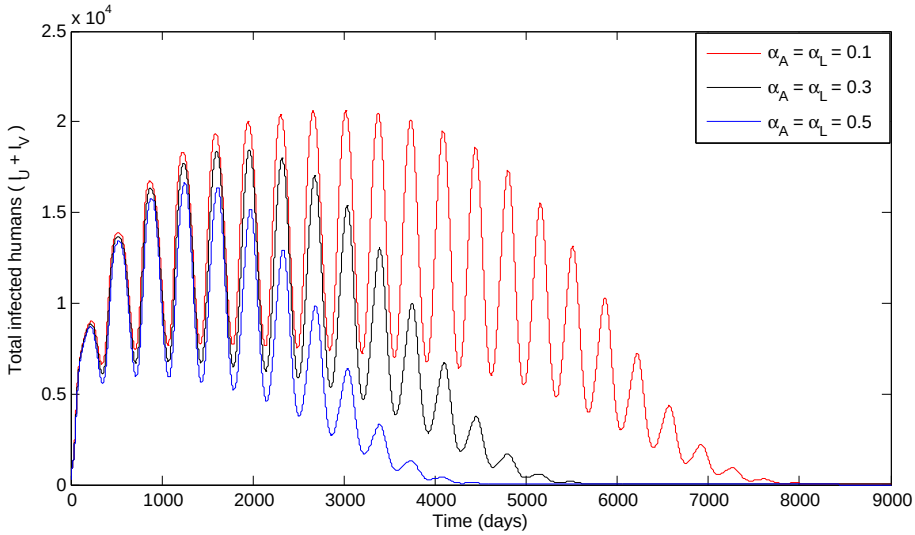

Figure 5.7: Simulations of the model (5.2.1) showing the total number of infected humans $(I_U + I_V)$ with varying temperature for the city Gulu in Uganda and the use of larvicides and adulticides.

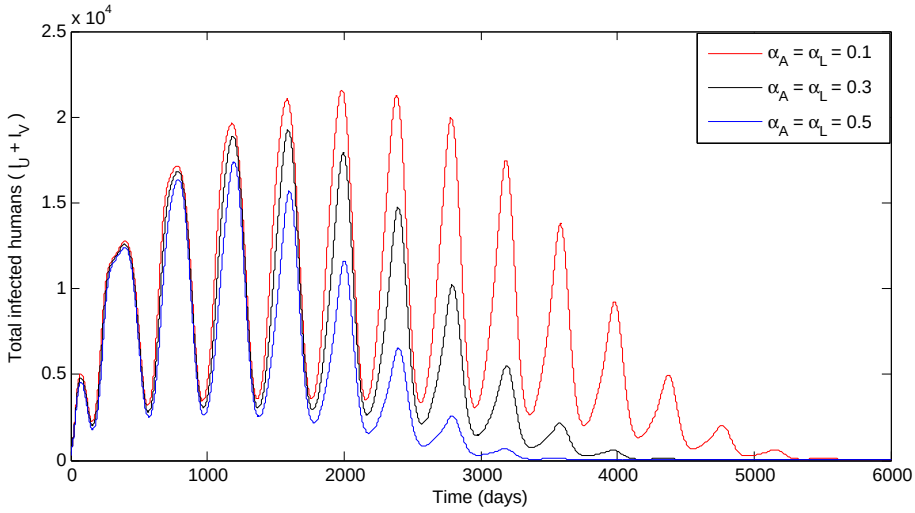

Figure 5.8: Simulations of the model (5.2.1) showing the total number of infected humans $(I_U + I_V)$ with varying temperature for the city Niamey in Niger republic and the use of larvicides and adulticides.

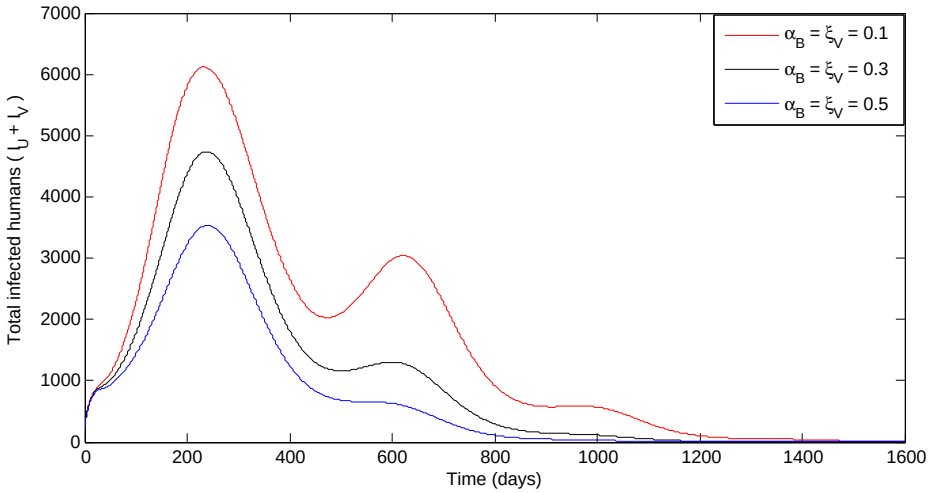

Figure 5.9: Simulations of the model (5.2.1) showing the total number of infected humans ($I_U + I_V$) with varying temperature for the city Kigali in Rwanda and the use of larvicides and adulticides.

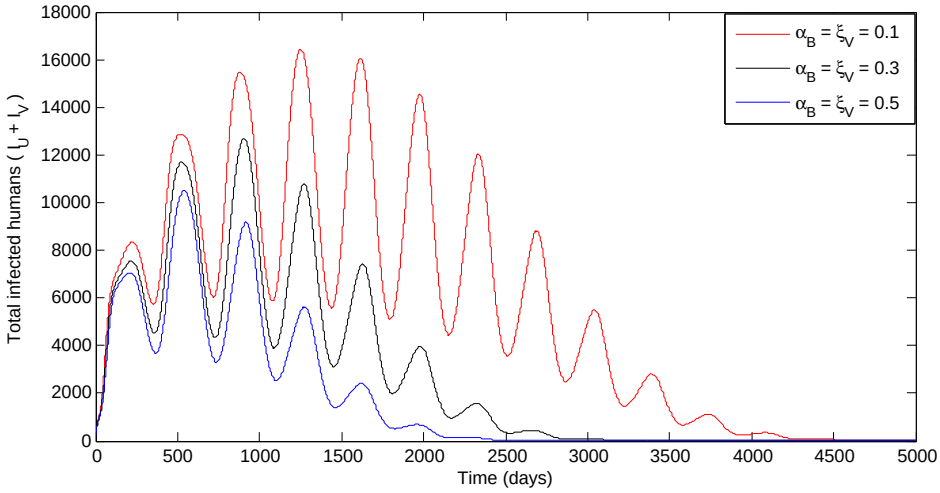

Figure 5.10: Simulations of the model (5.2.1) showing the total number of infected humans ($I_U + I_V$) with varying temperature for the city Gulu in Uganda and the use of larvicides and adulticides.

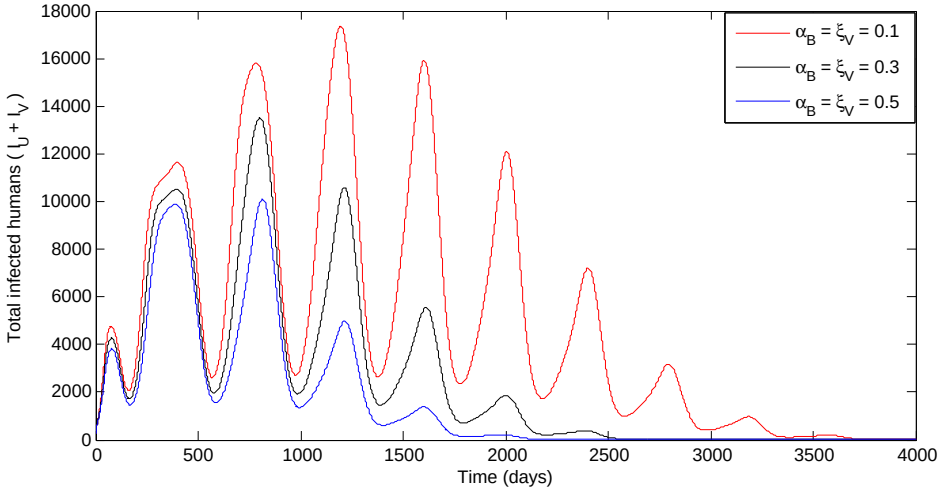

Figure 5.11: Simulations of the model (5.2.1) showing the total number of infected humans ($I_U + I_V$) with varying temperature for the city Niamey in Niger republic and the use of larvicides and adulticides.

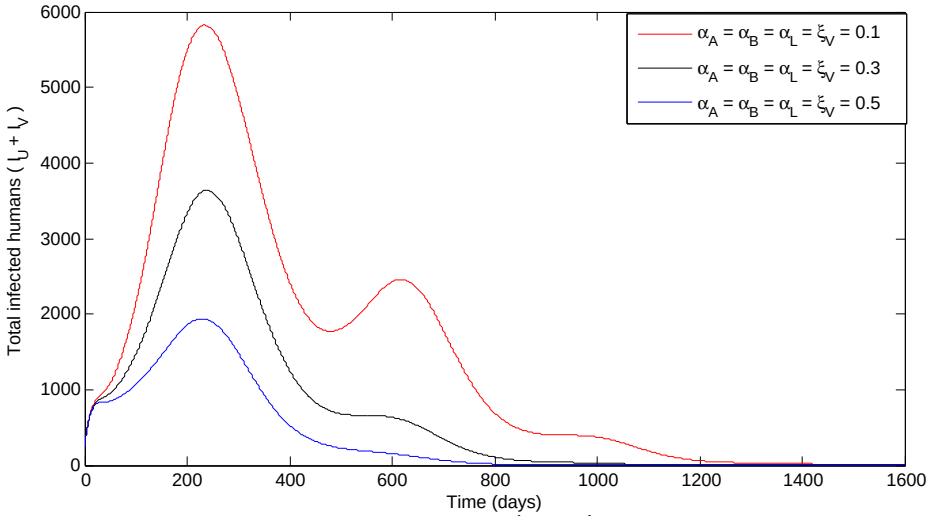

Figure 5.12: Simulations of the model (5.2.1) showing the total number of infected humans ($I_U + I_V$) with varying temperature for the city Kigali in Rwanda and the use of larvicides and adulticides.

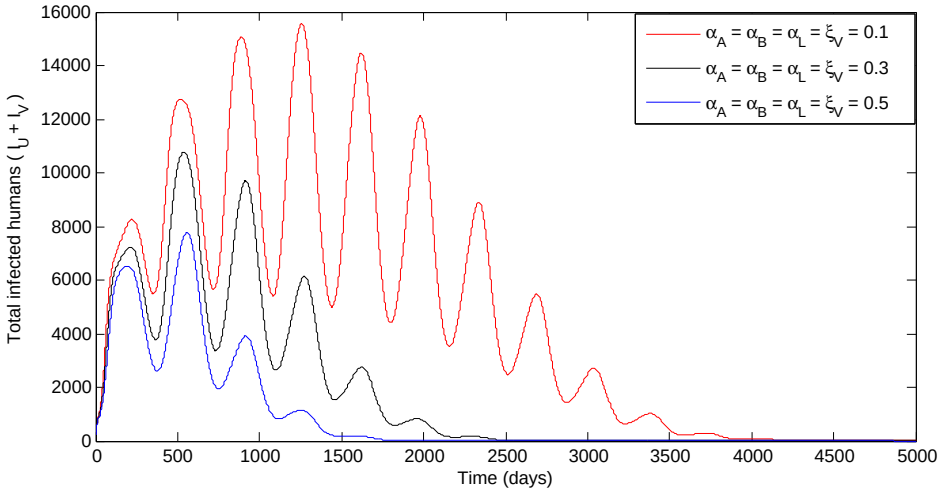

Figure 5.13: Simulations of the model (5.2.1) showing the total number of infected humans ($I_U + I_V$) with varying temperature for the city Gulu in Uganda and the use of larvicides and adulticides.

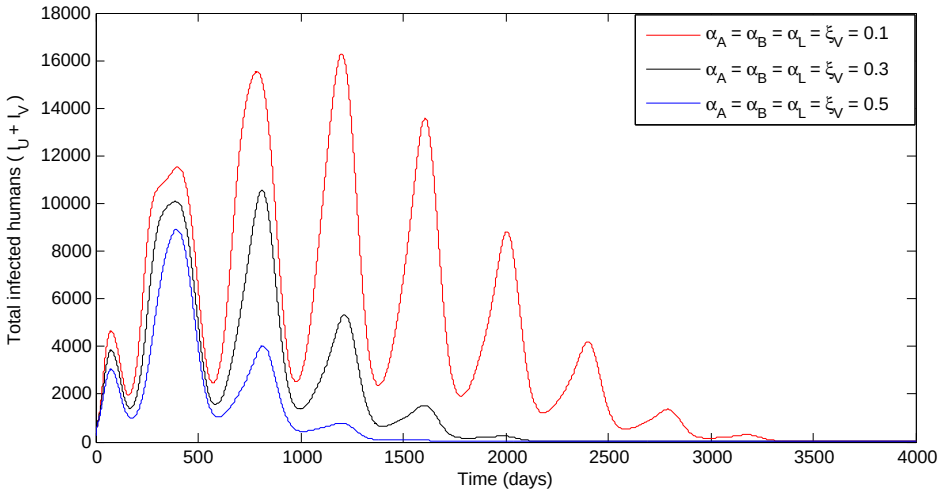

Figure 5.14: Simulations of the model (5.2.1) showing the total number of infected humans ($I_U + I_V$) with varying temperature for the city Niamey in Niger republic and the use of larvicides and adulticides.

5.6.2 Effects of control on the autonomous model

In this section, we consider five main control strategies for the autonomous form of the model, namely:

(i) Bed nets-only strategy;

(ii) Vaccination-only strategy;

(iii) Mosquito control-only (larvicides) strategy;

(iv) Bed nets and vaccination strategy;

(v) Bed nets, vaccination and mosquito control strategy (Hybrid strategy).

Using the functional definitions of a_M, ϕ_A, σ_A, μ_A, σ_M and μ_V with fixed temperature values at $T = 20, 25$ and 30 degrees (to obtain constant values), together with the following parameter values:

$$\Pi_H = 450, \beta_{HV} = 0.64, \epsilon_W = 0.5, \omega_V = 0.1, \eta_V = 0.1, \eta_U = 0.3, \tau_U = 0.1,$$

$$\tau_V = 0.02, \gamma_U = 0.015, \gamma_V = 0.017, \delta_U = 0.004, \delta_V = 0.003, \sigma_U = 0.08,$$

$$\sigma_V = 0.07, \eta_I = 0.7, \mathcal{K} = 150000, \mu_H = 0.0000342.$$

The model will be simulated to assess the effectiveness of these strategies (implemented singly or in combination).

Since we are interested in exploring the feasibility of disease elimination, these simulations are carried out for the special case of the model where backward bifurcation does not occur. In order to analyse the effect of the aforementioned control strategies in the presence of temperature changes, three different sets of numerical simulations are carried out, that is the cases where temperature (T) is 20^0C, 25^0C and 30^0C.

5.6.3 Bed nets-only strategy

Here, the effect of using bed nets-only is assessed, by setting all other parameters related to vaccination and mosquito control to zero, that is the case when $\xi_V = \epsilon_V = \alpha_A = \epsilon_A = \alpha_L = \epsilon_L = 0$. The model is simulated using the following levels of bed nets effectiveness (with bed nets efficacy of 0.5):

(i) Low bed nets effectiveness: $\alpha_B = 0.1$ (i.e., only 10% of individuals uses bed nets effectively);

(ii) Moderate bed nets effectiveness: $\alpha_B = 0.2$ (i.e., only 20% of individuals uses bed nets effectively);

(iii) High bed nets effectiveness: $\alpha_B = 0.5$ (i.e., only 50% of individuals uses bed nets effectively).

As expected, an increase in the rate of bed net use leads to a decrease in the number of infected individuals. For instance, the resulting number of individuals corresponding

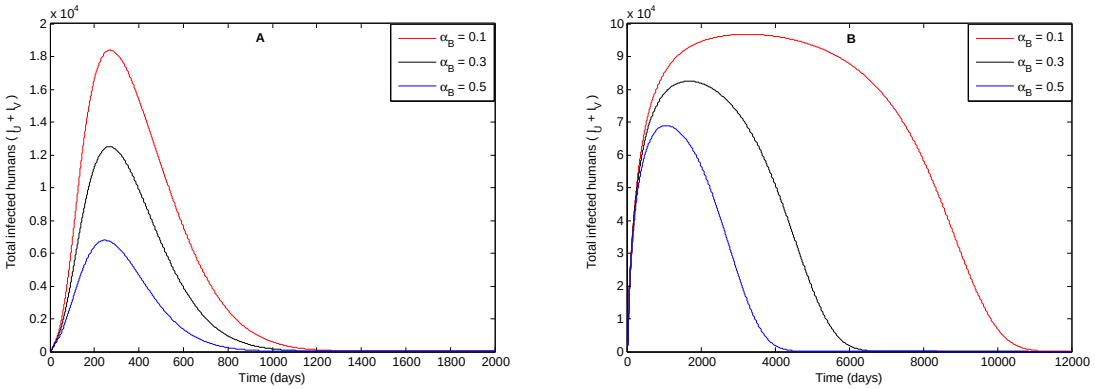

Figure 5.15: Simulations of the model (5.2.1) showing the total number of infected humans $(I_U + I_V)$ with: **(A)** When $T = 20$ having; $R_{0V} = 0.1233$ when $\alpha_B = 0.1$, $R_{0V} = 0.1103$ when $\alpha_B = 0.3$, and $R_{0V} = 0.0973$ when $\alpha_B = 0.5$ with $N_0 = 116.9812$. **(B)** When $T = 25$ having; $R_{0V} = 0.3492$ when $\alpha_B = 0.1$, $R_{0V} = 0.3125$ when $\alpha_B = 0.3$, and $R_{0V} = 0.2757$ when $\alpha_B = 0.5$ also with $N_0 = 116.7733$.

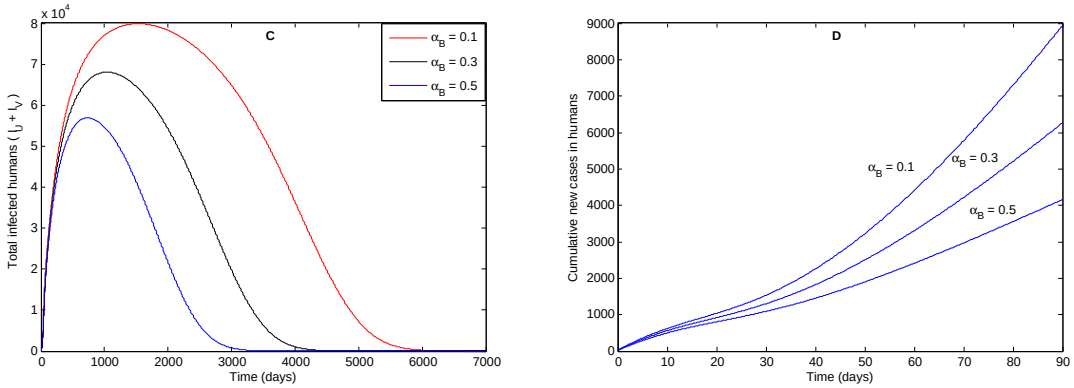

Figure 5.16: Simulations of the model (5.2.1) showing: **(C)** The total number of infected humans $(I_U + I_V)$ with $T = 30$, showing $R_{0V} = 0.3052, N_0 = 41.4528$ when $\alpha_B = 0.1$, $R_{0V} = 0.2731, N_0 = 41.4528$ when $\alpha_B = 0.3$, and $R_{0V} = 0.2410, N_0 = 41.4528$ when $\alpha_B = 0.5$. **(D)** Cumulative new cases in humans at $T = 20^0$C with different levels of applications.

to the low, moderate and high bed nets use (for the case when the temperature is taken to be 20^0C) is 18,000, 12,200 and 6,100, respectively (Table 5.2). Figure 5.15 shows the simulations of the model using different temperature levels and bed nets use, from which it is evident that the use of bed nets is more effective when temperature is 20^0C (as in Figure 5.15**A**), where the total number of infected humans is lower and approach the DFE faster. The DFE is reached by the total infected humans when $T = 30^0$C (as shown in Figure 5.16**C**) at almost half the time taken to reach the DFE when $T = 25^0$C (where the total infected humans are at their peak when $T = 25^0$C; Figure 5.15**B**). The cumulative number of new cases in humans with low, medium and high rates of applying bed nets at $T = 20^0$C is depicted in Figure 5.16**D**.

Table 5.2: Number of infected individuals using bed nets-only strategy.

Level of bed net use	**Temp at 20^0C**	**Temp at 25^0C**	**Temp at 30^0C**
Low ($\alpha_B = 0.1$)	18000	98000	80000
Moderate ($\alpha_B = 0.3$)	12200	82000	67000
High ($\alpha_B = 0.5$)	6100	68000	56000

5.6.4 Vaccination-only strategy

The effect of the use of vaccination only for temperatures of $T = 20^0$C, $T = 25^0$C and $T = 30^0$C with vaccine efficacy of 0.75 is investigated. For the vaccination-only strategy, we have $\alpha_A = \epsilon_A = \alpha_B = \epsilon_B = \alpha_L = \epsilon_L = 0$. Simulation of the model (5.2.1) are carried out to assess the impact of vaccination in reducing the malaria burden under the following levels of vaccination effectiveness.

(i) Low vaccination effectiveness: $\xi_V = 0.1$ (i.e., only 10% of individuals are vaccinated effectively);

(ii) Moderate vaccination effectiveness: $\xi_V = 0.3$ (i.e., only 30% of individuals are vaccinated effectively);

(iii) High vaccination effectiveness: $\xi_V = 0.5$ (i.e., only 50% of individuals are vaccinated effectively).

Similar to the use of bed nets, vaccination is more effective in reducing the total number of infected humans and time taken to reach the DFE when the temperature is 20^0C (Figure 5.17**A**), where as similar effect for both temperatures of 25^0C (Figure 5.17**B**) and 30^0C (Figure 5.18**C**) are obtained. A cumulative number of new cases in humans with low, medium and high rates of vaccine application at $T = 20^0$C is depicted in Figure 5.18**D**.

As expected the vaccination reproduction number decreases with increase in the rate of application of vaccines. At $T = 20^0$C, total infected humans reach the DFE in less than 1,200 days at most, while it reaches the DFE in about 8,000 days for the case when $T = 25^0$C and less than 5,000 days when $T = 30^0$C as in Figure 5.17**A**, Figure 5.17**B** and Figure 5.18**C**.

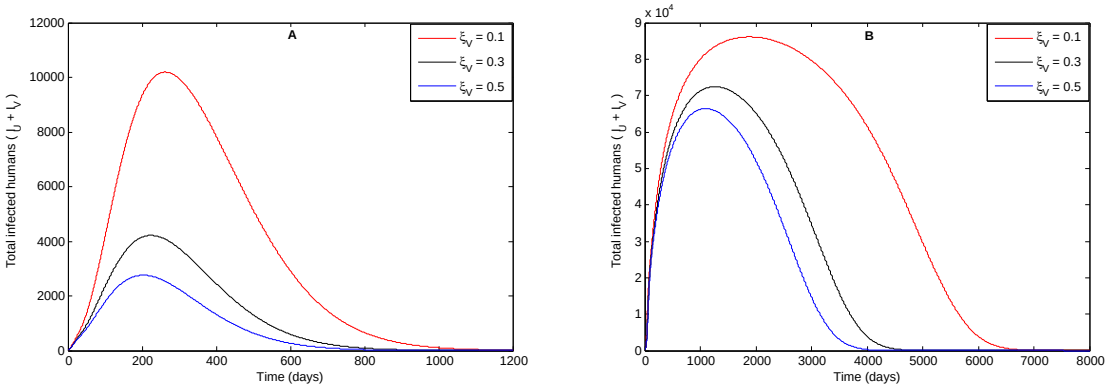

Figure 5.17: Simulations of the model (5.2.1) showing the total number of infected humans $(I_U + I_V)$ with: **(A)** $T = 20$ such that $R_{0V} = 0.2838$ for $\xi_V = 0.1$, $R_{0V} = 0.3353$ for $\xi_V = 0.3$, $R_0 = 0.3508$ for $\xi_V = 0.5$ and $N_0 = 116.9812$. **(B)** $T = 25$ such that $R_{0V} = 0.8036$ for $\xi_V = 0.1$, $R_{0V} = 0.9493$ for $\xi_V = 0.3$, $R_{0V} = 0.9931$ for $\xi_V = 0.5$ and $N_0 = 116.7733$.

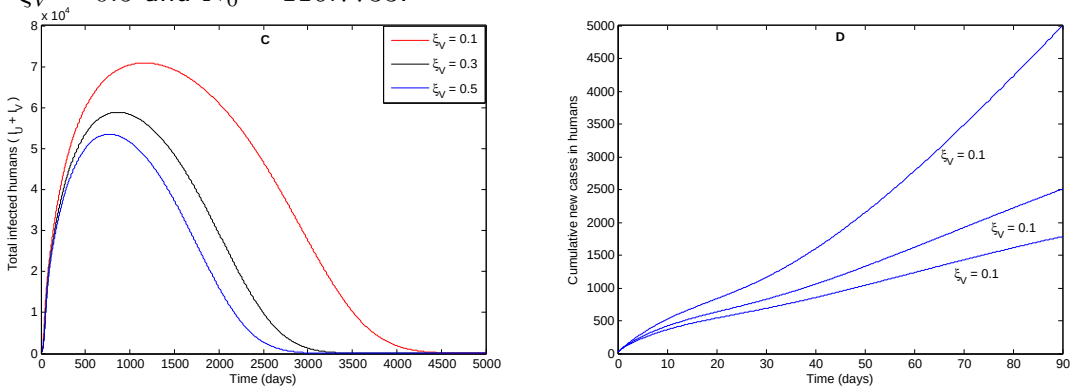

Figure 5.18: Simulations of the model (5.2.1) showing: **(C)** The total number of infected humans $(I_U + I_V)$ with $T = 30$ which implies $R_{0V} = 0.7000$ for $\xi_V = 0.1$, $R_{0V} = 0.8267$ for $\xi_V = 0.3$, $R_{0V} = 0.8648$ for $\xi_V = 0.5$ and $N_0 = 41.4528$. **(D)** Cumulative number of new human cases for $T = 20$ with different levels of applications.

5.6.5 Mosquito control-only strategy (adulticides strategy)

Here, the effect of the use of adulticides only with efficacy of 0.5 is simulated, that is when $\alpha_B = \epsilon_B = \alpha_L = \epsilon_L = \xi_V = \epsilon_V = 0$. Notice that the use of larvicides only show no effect in the dynamics of infected humans (it mainly affects the basic offspring number).
Further simulations were carried out to assess the impact of mosquito control-only strategy using adulticides. The following levels of adulticides effectiveness are considered:

(i) Low adulticides effectiveness: $\alpha_A = 0.1$ (i.e., only 10% applies adulticides effective);

(ii) Moderate adulticides effectiveness: $\alpha_A = 0.3$ (i.e., only 30% applies adulticides effective);

(iii) High adulticides effectiveness: $\alpha_A = 0.5$ (i.e., only 50% applies adulticides effective).

This control strategy shows the biggest positive effect in both reducing the total number of infected individuals and the effect of using different levels of controls for different temperatures compared to other forms of single controls. For $T = 20^0$C (as shown in Figure 5.19**A**), mosquito control measure at the rate $\alpha_A = 0.5$ pushes the total number of infected humans to reach the DFE at the shortest period in comparison to when $T = 25^0$C (as in Figure 5.19**B**), and when $T = 30^0$C (Figure 5.20**C**). The cumulative number of new cases in humans with low, medium and high rates of applying adulticides at $T = 20^0$C is depicted in Figure 5.20**D**.

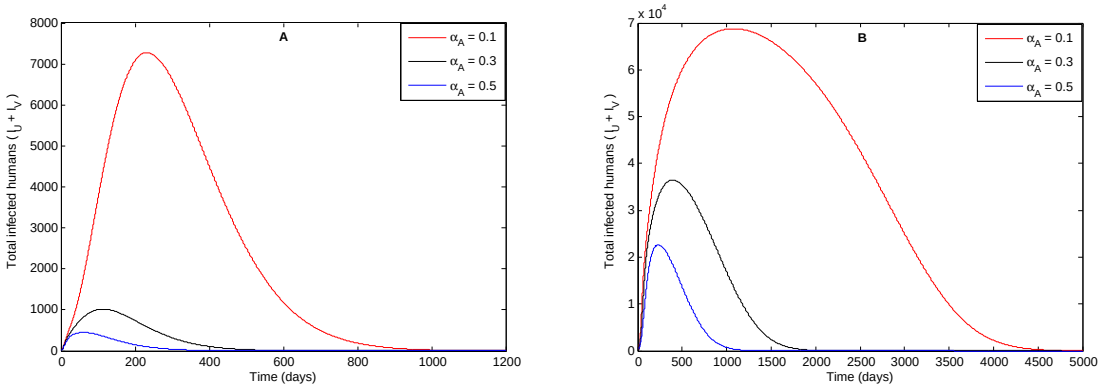

Figure 5.19: Simulations of the model (5.2.1) showing the total number of infected humans (I_U+I_V) with: **(A)** Obtained for $T = 20$, where $R_{0V} = 0.0957, N_0 = 93.1507$ for $\alpha_A = 0.1$, $R_{0V} = 0.0600, N_0 = 66.1852$ for $\alpha_A = 0.3$, and $R_{0V} = 0.0420, N_0 = 51.3270$ for $\alpha_A = 0.5$. **(B)** Obtained for $T = 25$, with $R_{0V} = 0.2786, N_0 = 93.6979$ for $\alpha_A = 0.1$, $R_{0V} = 0.1810, N_0 = 67.1564$ for $\alpha_A = 0.3$, and $R_{0V} = 0.1299, N_0 = 52.3324$ for $\alpha_A = 0.5$.

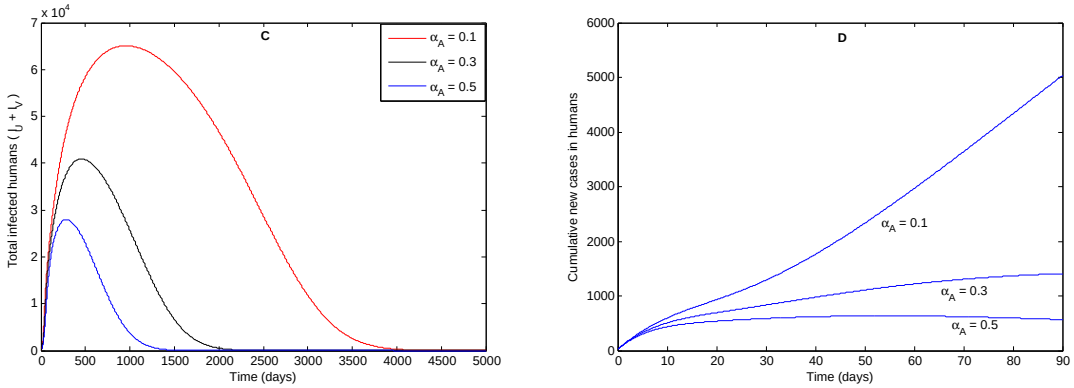

Figure 5.20: Simulations of the model (5.2.1) showing: **(C)** The total number of infected humans $(I_U + I_V)$ with $T = 30$, where $R_{0V} = 0.2670, N_0 = 35.9381$ for $\alpha_A = 0.1$, $R_{0V} = 0.1954, N_0 = 28.3856$ for $\alpha_A = 0.3$, and $R_{0V} = 0.1510, N_0 = 23.4562$ for $\alpha_A = 0.5$. **(D)** Cumulative number of new cases in humans with different level of interventions and $T = 20^0$C.

5.6.6 Bed nets and vaccination strategy

The combined effect of the use of bed nets and imperfect vaccination are explored here. Vaccine efficacy of 0.75 and bed net efficacy of 0.5 are used. For this simulation, parameters related to other control strategies are set to zero (i.e., $\epsilon_A = \alpha_A = \epsilon_B = \alpha_B = 0$).
The model is simulated using the following levels of bed nets and vaccination effectiveness at various temperature levels (20^0C, 25^0C and 30^0C):

(i) Low bed nets and vaccination effectiveness: $\alpha_B = \xi_V = 0.1$ (i.e., only 10% of individuals uses bed nets and vaccinated effectively);

(ii) Moderate bed nets and vaccination effectiveness: $\alpha_B = \xi_V = 0.3$ (i.e., only 30% of individuals uses bed nets and vaccinated effectively);

(iii) High bed nets and vaccination effectiveness: $\alpha_B = \xi_V = 0.5$ (i.e., only 50% of individuals uses bed nets and vaccinated effectively).

As expected, the combined use of bed nets and vaccination is more effective than the singular use of bed nets or vaccine. Figure 5.23 and Figure 5.24 depict the simulations of the model (5.2.1) with the use of bed nets and vaccination, from which it is evident that the total infected humans reach the DFE (for low, medium and high application of controls) faster than the separate use of the controls for both $T = 20^0$ (Figure 5.21**A**), $T = 25^0$C (Figure 5.21**B**), and $T = 30^0$C (Figure 5.22**C**). The cumulative number of new cases in humans with low, medium and high rates of applying bed nets and vaccines at $T = 20^0$C is depicted in Figure 5.22**D**.

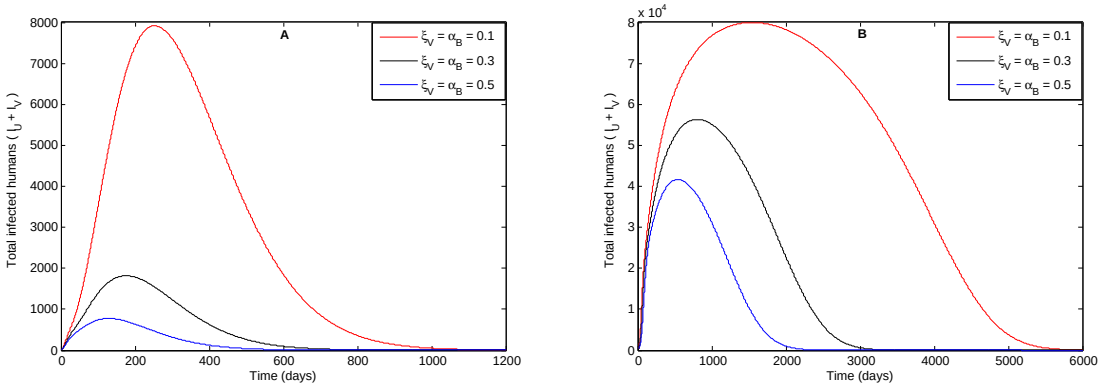

Figure 5.21: Simulations of the model (5.2.1) showing the total number of infected humans $(I_U + I_V)$ with: **(A)** Obtained for $T = 20$, so that $R_{0V} = 0.2696$ for $\alpha_V = \alpha_B = 0.1$, $R_{0V} = 0.2850$ for $\alpha_V = \alpha_B = 0.3$, and $R_{0V} = 0.2631$ for $\alpha_V = \alpha_B = 0.5$ with $N_0 = 116.9812$. **(B)** Obtained for $T = 25$, so that $R_{0V} = 0.7634$ for $\alpha_V = \alpha_B = 0.1$, $R_{0V} = 0.8069$ for $\alpha_V = \alpha_B = 0.3$, and $R_{0V} = 0.7448$ for $\alpha_V = \alpha_B = 0.5$ with $N_0 = 116.7733$.

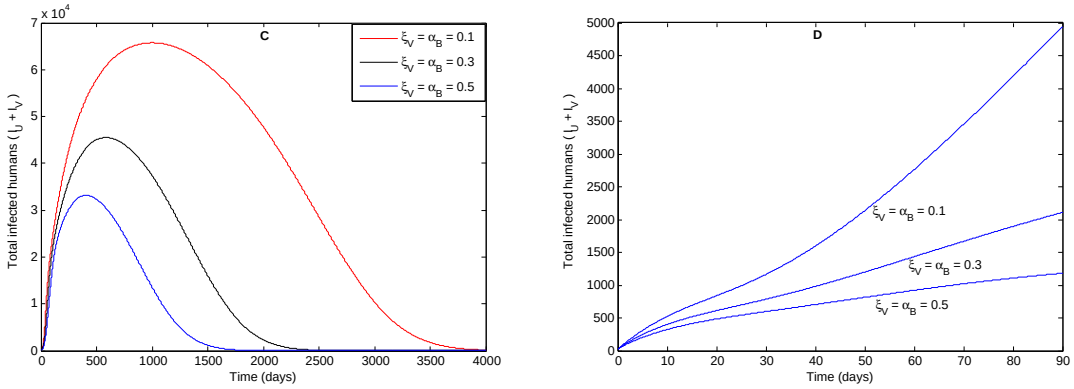

Figure 5.22: Simulations of the model (5.2.1) showing; **(C)** The total number of infected humans $(I_U + I_V)$ with $T = 30$, such that $R_{0V} = 0.6650$ for $\alpha_V = \alpha_B = 0.1$, $R_{0V} = 0.7027$ for $\alpha_V = \alpha_B = 0.3$, $R_{0V} = 0.6486$ for $\alpha_V = \alpha_B = 0.5$ and $N_0 = 41.4528$. **(D)** Cumulative number of cases in humans with different levels of applications and $T = 20^0$C.

5.6.7 Hybrid strategy

The potential impact of using all controls are examined, using the following effectiveness levels:

(i) Low effectiveness: $\epsilon_A = \epsilon_L = \alpha_B = \xi_V = 0.1$ (i.e., combined measures at only 10% effectiveness);

(ii) Moderate effectiveness: $\epsilon_A = \epsilon_L = \alpha_B = \xi_V = 0.3$ (i.e., combined measures at only 30% effectiveness);

(iii) High effectiveness: $\epsilon_A = \epsilon_L = \alpha_B = \xi_V = 0.5$ (i.e., combined measures at only 50% effectiveness).

For high levels of intervention, the total number of infected humans is lower and reach the DFE at a very short time for the different temperature levels used. For instance, the total infected humans reach the DFE in less than 1,000 days when $T = 20^0$C as depicted in (Figure 5.23**A**) and it reaches the DFE in about 3,000 days when $T = 25^0$C (Figure 5.23**B**) and $T = 30^0$C (Figure 5.24**C**). The cumulative number of new cases in humans with low, medium and high rates of applying bed nets, vaccines and adulticides at $T = 20^0$C is depicted in Figure 5.24**D**.

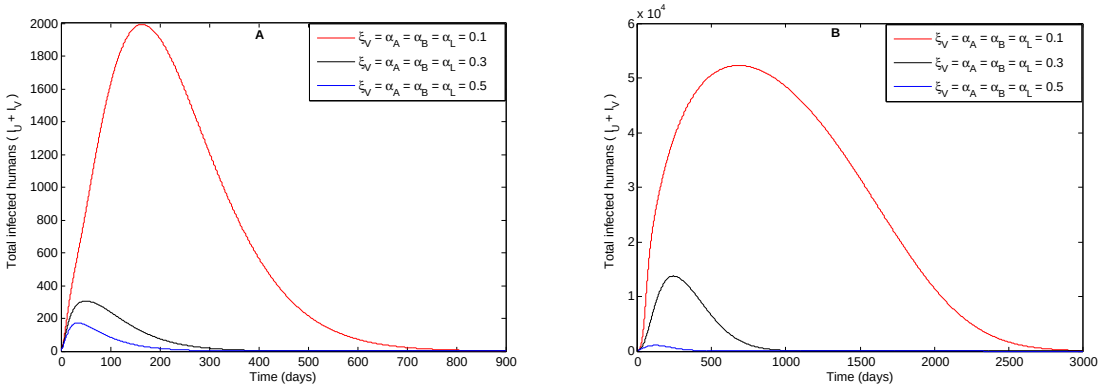

Figure 5.23: Simulations of the model (5.2.1) showing the total number of infected humans $(I_U + I_V)$ with: **(A)** Obtained when $T = 20$, such that $R_{0V} = 0.0692, N_0 = 70.9784$ for low, $R_{0V} = 0.0309, N_0 = 34.1664$ for medium, and $R_{0V} = 0.0171, N_0 = 20.0347$ for high controls. **(B)** Obtained when $T = 25$, such that $R_{0V} = 0.2017, N_0 = 85.1115$ for low, $R_{0V} = 0.0937, N_0 = 51.5536$ for medium, and $R_0 = 0.0533, N_0 = 34.7858$ for high controls.

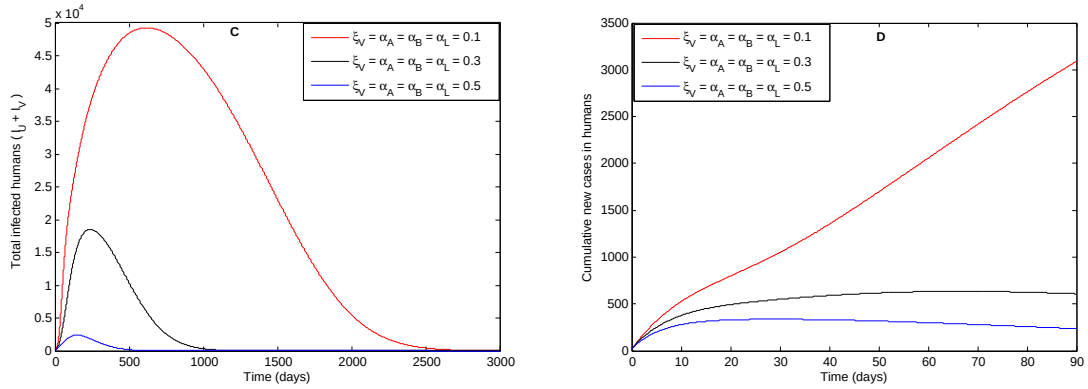

Figure 5.24: Simulations of the model (5.2.1) showing: **(C)** The total number of infected humans $(I_U + I_V)$ when $T = 30$, such that $R_0 = 0.1932, N_0 = 34.3476$ for low, $R_{0V} = 0.1010, N_0 = 24.9232$ for medium, and $R_{0V} = 0.0619, N_0 = 19.0463$ for high controls. **(D)** Cumulative new cases in humans when $T = 20$ with different levels of interventions.

5.7 Sensitivity analysis and Numerical simulation

In this section, the partial rank correlation coefficient (PRCC) of the parameters of the vaccinated reproduction number for different temperature ranges are given. In addition, numerical simulations of the model are also presented.

5.7.1 Sensitivity analysis

The partial rank correlation coefficient is a sampling based sensitivity index that measures the strength of the linear associations between a dependent variable (in this

case the vaccinated reproduction number), and independent variables (its parameters) after removing the linear effect of other parameter values. We consider the cases for constant and various temperatures. Using the vaccinated reproduction number as the output for temperature values for ranges 15^0C-20^0C, 20^0C-25^0C, 25^0C-30^0C, 30^0C-35^0C and that of constant parameter values with a confidence interval of 95% and 1000 number of boots, the PRCC are obtained.

Table 5.3, Table 5.4, Table 5.5, Table 5.6 and Table 5.7 show the PRCC values, bias, standard error, minimum and maximum confidence interval for each of the 27 parameters of the basic reproduction ratio with the aforementioned temperature intervals and constant temperature, respectively. Similarly, Figures 5.25, 5.26 and 5.27 show the bar plot of the PRCC of the parameters of the basic reproduction ratio as temperature varies and constant temperature. For the different temperature ranges, the rate of vaccination ξ_V, efficacy of vaccination ϵ_V and rate of successful use of bed nets C_B show little variation as temperature varies. The rate of vaccination is positively correlated to R_{0V} due to the imperfect vaccine (not 100% effective), thus vaccinated individuals can still be acquire infections.

The use of larvicides is positively correlated to R_{0V} for temperature ranging from 15^0C-20^0C with PRCC value of $+0.4099$, but when the temperature range is from 20^0C-25^0C, the PRCC becomes negatively correlated to R_{0V} with value of -0.0179, it remains negative with PRCC value of -0.1008 when the temperature is between 25^0C-30^0C and returns to positive for temperature of 30^0C-35^0C having PRCC of $+0.1099$, where as the PRCC is negative with value of -0.0381 in a constant temperature settings. For the use of adulticides, negative correlation with R_{0V} are obtained with PRCC values of -0.8184, -0.7572, -0.6391, -0.7671 and -0.6159 for temperature ranges of 15^0C-20^0C, 20^0C-25^0C, 25^0C-30^0C, 30^0C-35^0C and constant respectively.

Disease induced death rates, which have been shown to be main causes of backward bifurcations in mosquito borne diseases such as [27, 35, 62, 111] show wide variations as temperature changes for both non-vaccinated infected and vaccinated infected humans, PRCC values of $\delta_V = +0.0038$, $\delta_V = -0.0103$, $\delta_V = +0.0065$, $\delta_V = -0.0227$, and $\delta_V = +0.0318$ were obtained for temperature ranges of 15^0C-20^0C, 20^0C-25^0C, 25^0C-30^0C, 30^0C-35^0C and constant respectively. Similarly for the same temperature ranges and constant, the PRCC values of $\delta_U = +0.0532$, $\delta_U = -0.0379$, $\delta_U = +0.0326$, $\delta_U = +0.0422$, and $\delta_U = +0.0325$ were respectively obtained. Variations occur in other temperature dependent and temperature independent parameters as presented in the Tables and Figures for the global sensitivity analysis.

Table 5.3: PRCC for parameters of the basic reproduction ratio with temperature of 15^0C -20^0C

Para	PRCC	Bias	Std. error	Min. c.i.	Max. c.i.
σ_U	$+0.0116573$	-0.0007059	0.0327846	-0.0507698	$+0.0733284$
σ_V	-0.0232599	-0.0011866	0.0319199	-0.0859427	$+0.0387305$
σ_A	$+0.0176615$	$+0.0002679$	0.0319108	-0.0446594	$+0.0827357$
σ_M	$+0.1055920$	$+0.0002096$	0.0336147	$+0.0399197$	$+0.1682346$
μ_H	$+0.1216671$	-0.0004487	0.0335058	$+0.0583749$	$+0.1891785$
μ_V	-0.0390433	-0.0011569	0.0330434	-0.1020185	$+0.0305234$
μ_A	$+0.0176899$	$+0.0013925$	0.0323228	-0.0455994	$+0.0791484$
δ_V	$+0.0038029$	-0.0010111	0.0340335	-0.0611271	$+0.0690736$
δ_U	$+0.0532007$	-0.0004144	0.0324357	-0.0115217	$+0.1187615$
γ_U	-0.2641840	$+0.0003395$	0.0308615	-0.3282315	-0.2061550
γ_V	-0.2422403	-0.0005914	0.0328178	-0.3056412	-0.1780375
τ_U	-0.0734964	-0.0015532	0.0319108	-0.1341357	-0.0135771
τ_V	$+0.0115517$	-0.0025839	0.0312943	-0.0466292	$+0.0706519$
Π_H	-0.3772186	-0.0032223	0.0320140	-0.4432971	-0.3160064
ϕ_A	-0.4343937	-0.0007132	0.0294558	-0.4954435	-0.3774096
c_A	-0.8183722	-0.0026977	0.0121513	-0.8432971	-0.7961376
c_L	$+0.4098845$	$+0.0020502$	0.0294757	$+0.3485913$	$+0.4682076$
c_B	-0.6670218	$+0.0000797$	0.0181261	-0.7034560	-0.6336552
κ	$+0.4298697$	-0.0008229	0.0302802	$+0.3714995$	$+0.4885408$
β_{HV}	$+0.4945893$	$+0.0010630$	0.0263685	$+0.4471908$	$+0.5457829$
a_M	$+0.2805036$	$+0.0014569$	0.0311481	$+0.2195653$	$+0.3425459$
ϵ_V	-0.3686739	-0.0058365	0.0293159	-0.4263527	-0.3100787
ω_V	$+0.2823186$	-0.0010166	0.0321963	$+0.2227506$	$+0.3458825$
η_U	$+0.0454152$	$+0.0035739$	0.0338749	-0.0191098	$+0.1110642$
η_V	$+0.0339887$	$+0.0004213$	0.0347059	-0.0376288	$+0.0972901$
η_I	$+0.3039816$	-0.0003942	0.0318035	$+0.2397632$	$+0.3678769$
ξ_V	$+0.5238138$	$+0.0097502$	0.0259621	$+0.4761949$	$+0.5741889$

Table 5.4: PRCC for parameters of the basic reproduction ratio with temperature of 20^0C-25^0C.

Para	Original	Bias	Std. error	Min. c.i.	Max. c.i.
σ_U	$+0.0272416$	-0.0007902	0.0327054	-0.0360532	$+0.0937781$
σ_V	-0.0073296	-0.0006006	0.0328427	-0.0699371	$+0.0585221$
σ_A	$+0.0924912$	$+0.0014401$	0.0316656	$+0.0281105$	$+0.1533272$
σ_M	$+0.0944706$	-0.0000784	0.0325518	$+0.0332401$	$+0.1623727$
μ_H	$+0.1127021$	$+0.0000767$	0.0316062	$+0.0482402$	$+0.1711439$
μ_V	-0.0200803	-0.0008417	0.0328245	-0.0830335	$+0.0488403$
μ_A	-0.0566776	-0.0001684	0.0329911	-0.1215934	$+0.0070602$
δ_V	-0.0102746	-0.0017691	0.0340915	-0.0700897	$+0.0622394$
δ_U	-0.0379350	$+0.0007999$	0.0340594	-0.0300189	$+0.1049511$
γ_U	-0.2487736	$+0.0008432$	0.0326861	-0.3148316	-0.1842316
γ_V	-0.2480796	-0.0003195	0.0310429	-0.3157813	-0.1869417
τ_U	-0.0495361	-0.0009234	0.0334424	-0.1146326	$+0.0179481$
τ_V	$+0.0197085$	-0.0015089	0.0331141	-0.0439765	$+0.0853165$
Π_H	-0.3473466	$+0.0000988$	0.0300609	-0.4084650	-0.2871868
ϕ_A	-0.0364459	$+0.0007974$	0.0319624	-0.1012336	$+0.0273710$
c_A	-0.7571855	$+0.0003732$	0.0133595	-0.7854990	-0.7318509
c_L	-0.0179992	$+0.0005700$	0.0318969	-0.0796521	$+0.0423534$
c_B	-0.6201653	$+0.0006721$	0.0187960	-0.6598916	-0.5838745
κ	$+0.3893278$	-0.0013335	0.0307154	$+0.3278164$	$+0.4527466$
β_{HV}	$+0.4631499$	-0.0003937	0.0267489	$+0.4131450$	$+0.5186893$
a_M	$+0.1232240$	$+0.0008872$	0.0325427	$+0.0600620$	$+0.1882611$
ϵ_V	-0.3162192	$+0.0003416$	0.0295568	-0.3722439	-0.2576412
ω_V	$+0.2622113$	-0.0003436	0.0309711	$+0.2010132$	$+0.3242911$
η_U	$+0.0545866$	$+0.0010445$	0.0324711	-0.0074782	$+0.1179109$
η_V	$+0.0385358$	$+0.0002086$	0.0330906	-0.0253969	$+0.1084278$
η_I	$+0.2768270$	$+0.0003028$	0.0297059	$+0.2187766$	$+0.3324457$
ξ_V	$+0.4844347$	$+0.0001834$	0.0251479	$+0.4376538$	$+0.5357899$

Table 5.5: PRCC for parameters of the basic reproduction ratio with temperature of 25^0C-30^0C.

Para	Original	Bias	Std. error	Min. c.i.	Max. c.i.
σ_U	$+0.0483804$	-0.0004057	0.0333765	-0.0186168	$+0.1125817$
σ_V	$+0.0114802$	-0.0011647	0.0309363	-0.0532153	$+0.0730034$
σ_A	$+0.0597791$	$+0.0012013$	0.0332133	-0.0042205	$+0.1216877$
σ_M	$+0.0445856$	-0.0004296	0.0327879	-0.0216979	$+0.1082284$
μ_H	$+0.1068126$	-0.0004946	0.0321849	$+0.0445602$	$+0.1664874$
μ_V	-0.0645414	-0.0009126	0.0331577	-0.1262763	$+0.0088067$
μ_A	-0.0559747	$+0.0003682$	0.0329798	-0.1186303	$+0.0069229$
δ_V	$+0.0064994$	-0.0015801	0.0336362	-0.0546403	$+0.0768521$
δ_U	$+0.0326299$	$+0.0003169$	0.0335178	-0.0318403	$+0.1004987$
γ_U	-0.2750038	$+0.0006289$	0.0326875	-0.3405111	-0.2100418
γ_V	-0.2766534	-0.0002737	0.0313243	-0.3389869	-0.2153664
τ_U	-0.0510142	-0.0006659	0.0335426	-0.1156434	$+0.0156466$
τ_V	$+0.0060012$	-0.0001283	0.0326736	-0.0553695	$+0.0731931$
Π_H	-0.3874218	-0.0007302	0.0297809	-0.4455378	-0.3277662
ϕ_A	$+0.0033342$	$+0.0010076$	0.0331209	-0.0621007	$+0.0649226$
c_A	-0.6390782	$+0.0002818$	0.0202658	-0.6832559	-0.6026203
c_L	-0.1007759	$+0.0001927$	0.0337962	-0.1660626	-0.0351183
c_B	-0.6519635	$+0.0003658$	0.0185159	-0.6902679	-0.6162609
κ	$+0.4161619$	-0.0017819	0.0299235	$+0.3567321$	$+0.4768279$
β_{HV}	$+0.5029739$	$+0.0005889$	0.0264660	$+0.4526908$	$+0.5545998$
a_M	$+0.0784946$	-0.0001587	0.0333855	$+0.0185815$	$+0.1444017$
ϵ_V	-0.3477630	-0.0004523	0.0290541	-0.4048732	-0.2903114
ω_V	$+0.3007633$	-0.0007619	0.0301747	$+0.2451951$	$+0.3628431$
η_U	$+0.0854023$	$+0.0002371$	0.0335750	$+0.0193157$	$+0.1534979$
η_V	$+0.0207561$	$+0.0000308$	0.0335975	-0.0416263	$+0.0882889$
η_I	$+0.3051394$	-0.0001698	0.0303403	$+0.2476859$	$+0.3683635$
ξ_V	$+0.4968967$	$+0.0000247$	0.0254239	$+0.4482705$	$+0.5473321$

Table 5.6: PRCC for parameters of the basic reproduction ratio with temperature of 30^0C-35^0C.

Para	Original	Bias	Std. error	Min. c.i.	Max. c.i.
σ_U	$+0.0451980$	-0.0005944	0.03296141	-0.0155342	$+0.1097078$
σ_V	$+0.0080809$	-0.0014946	0.03216838	-0.0561889	$+0.0695945$
σ_A	-0.0232658	$+0.0007003$	0.03218964	-0.0884070	$+0.0367905$
σ_M	$+0.1068015$	-0.0000438	0.03214870	$+0.0438982$	$+0.1708055$
μ_H	$+0.1069910$	-0.0004608	0.03147377	$+0.0463622$	$+0.1691896$
μ_V	-0.1075564	-0.0004600	0.03417210	-0.1743457	-0.0394728
μ_A	$+0.0040081$	$+0.0001087$	0.03221020	-0.0606068	$+0.0692966$
δ_V	-0.0226984	-0.0014608	0.03351764	-0.0894162	$+0.0425969$
δ_U	$+0.0422372$	$+0.0004247$	0.03338551	-0.0233578	$+0.1107938$
γ_U	-0.2767289	$+0.0009461$	0.03165590	-0.3407932	-0.2150720
γ_V	-0.2379078	-0.0005803	0.03091655	-0.3003231	-0.1780435
τ_U	-0.0707100	-0.0003518	0.03182795	-0.1300137	-0.0067869
τ_V	$+0.0068589$	-0.0008134	0.03346120	-0.0575232	$+0.0741217$
Π_H	-0.4010288	-0.0003367	0.02914214	-0.4605973	-0.3408796
ϕ_A	-0.0889220	$+0.0013691$	0.03294498	-0.1566463	-0.0267232
c_A	-0.7671031	$+0.0004052$	0.01390989	-0.7967973	-0.7413719
c_L	$+0.1099999$	$+0.0016757$	0.03264374	$+0.0441499$	$+0.1753972$
c_B	-0.6612125	$+0.0007278$	0.01704738	-0.6980249	-0.6295967
κ	$+0.4223961$	-0.0016396	0.02881096	$+0.3652521$	$+0.4794296$
β_{HV}	$+0.5113951$	$+0.0002744$	0.02441461	$+0.4649900$	$+0.5586622$
a_M	$+0.0072425$	-0.0000582	0.03334982	-0.0593828	$+0.0734986$
ϵ_V	-0.3639675	$+0.0002173$	0.02810343	-0.4221400	-0.3112162
ω_V	$+0.2973694$	-0.0006766	0.03052003	$+0.2401928$	$+0.3577935$
η_U	$+0.0610768$	$+0.0009632$	0.03264673	-0.0017988	$+0.1241164$
η_V	$+0.0234672$	$+0.0000817$	0.03262804	-0.0404243	$+0.0881068$
η_I	$+0.3308712$	$+0.0002972$	0.02985926	$+0.2721758$	$+0.3928036$
ξ_V	$+0.5098077$	$+0.0006601$	0.02482458	$+0.4606819$	$+0.5583210$

Table 5.7: PRCC for parameters of the basic reproduction ratio with constant.

Para	Original	Bias	Std. error	Min. c.i.	Max. c.i.
σ_U	$+0.0537072$	-0.0000335	0.03142014	-0.0065539	$+0.1154683$
σ_V	-0.0270326	-0.0013361	0.03069721	-0.0909801	$+0.0308928$
σ_A	$+0.4461772$	$+0.0000156$	0.02649914	$+0.3933939$	$+0.4959988$
σ_M	$+0.3510576$	$+0.0009426$	0.03105527	$+0.2909725$	$+0.4157925$
μ_H	$+0.1090479$	-0.0010750	0.03327486	$+0.0467657$	$+0.1769173$
μ_V	-0.1843498	$+0.0007244$	0.03158123	-0.2477469	-0.1209180
μ_A	$+0.0215627$	-0.0000023	0.03148113	-0.0402444	$+0.0853352$
δ_V	$+0.0317568$	-0.0012651	0.03219245	-0.0305051	$+0.1000426$
δ_U	$+0.0324881$	-0.0003282	0.03379430	-0.0318886	$+0.0979736$
γ_U	-0.2687226	$+0.0001583$	0.03116736	-0.3283692	-0.2040955
γ_V	-0.2629236	-0.0001416	0.03073967	-0.3235758	-0.2050292
τ_U	-0.0525523	$+0.0005959$	0.03168751	-0.1132575	$+0.0147820$
τ_V	$+0.0380073$	$+0.0001263$	0.03334126	-0.0272727	$+0.1051935$
Π_H	-0.3428469	-0.0007563	0.03105764	-0.4012005	-0.2843012
ϕ_A	$+0.0174543$	-0.0002773	0.03422852	-0.0476062	$+0.0827469$
c_A	-0.6159261	$+0.0004929$	0.02160704	-0.6576728	-0.5746723
c_L	-0.0381227	$+0.0020628$	0.03327691	-0.1092252	$+0.0236732$
c_B	-0.6559501	$+0.0002602$	0.01775010	-0.6918969	-0.6237530
κ	$+0.4245334$	-0.0012985	0.02804146	$+0.3755547$	$+0.4856456$
β_{HV}	$+0.5049071$	$+0.0003461$	0.02369151	$+0.4600162$	$+0.5533423$
a_M	$+0.5617064$	$+0.0004058$	0.02354306	$+0.5165672$	$+0.6088471$
ϵ_V	-0.3690131	-0.0001147	0.02917487	-0.4256369	-0.3135196
ω_V	$+0.2531897$	-0.0001845	0.03223262	$+0.1924038$	$+0.3192285$
η_U	$+0.0561337$	$+0.0008215$	0.03287014	-0.0142383	$+0.1240309$
η_V	$+0.0144269$	-0.0013924	0.03449365	-0.0490704	$+0.0864574$
η_I	$+0.3183981$	$+0.0001165$	0.02926591	$+0.2595554$	$+0.3769897$
ξ_V	$+0.4727052$	$+0.0002722$	0.02628378	$+0.4225355$	$+0.5231252$

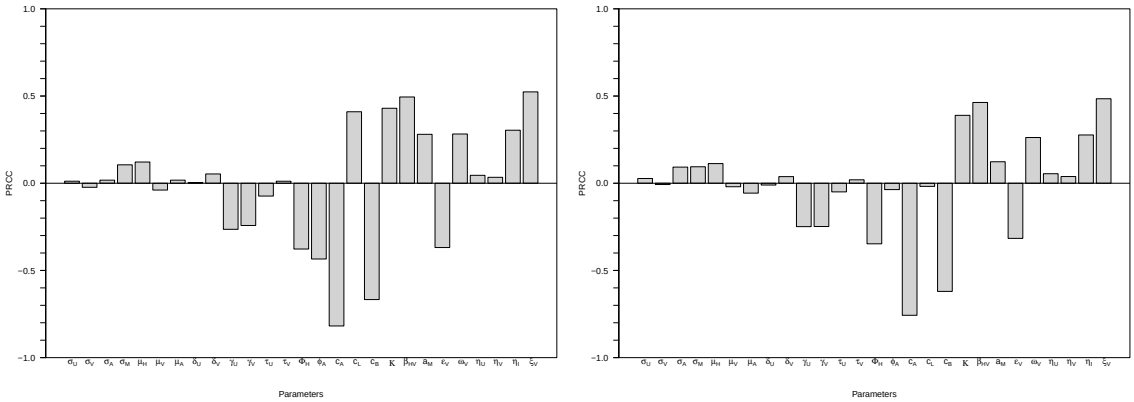

Figure 5.25: Partial rank correlation coefficient (PRCC) of the model parameters with R_{0V} as the output function for temperature between 15^0C - 20^0C and between 20^0C - 25^0C respectively.

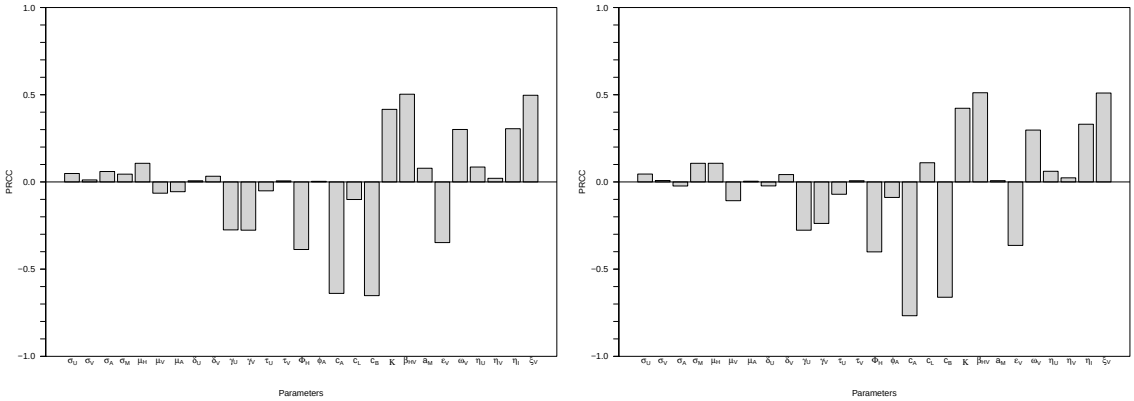

Figure 5.26: Partial rank correlation coefficient (PRCC) of the model parameters with R_{0V} as the output function for temperature between 25^0C - 30^0C and 30^0C - 35^0C respectively.

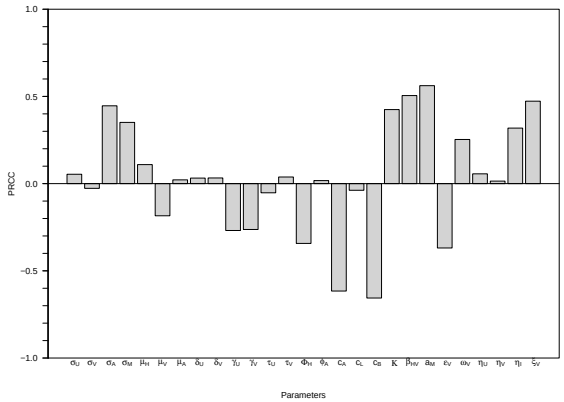

Figure 5.27: Partial rank correlation coefficient (PRCC) of the model parameters with R_{0V} as the output function and constant temperature.

5.7.2 Numerical simulations

We fix temperature values for the non-autonomous model (5.2.1), so that each of the temperature dependent parameter becomes constant. For simulation purposes, two different sets of parameter values that give $R_{0V} = 0.297 < 1$, $N_0 = 14.2$ and $R_{0V} = 6.457 > 1$, $N_0 = 104.4$ were chosen within the ranges given in Table 5.8. Initial populations are given by $S_U(0) = 2000$; $S_V(0) = 1000$; $W_U(0) = 1000$; $W_V(0) = 500$; $E_U(0) = 500$; $E_V(0) = 300$; $I_U(0) = 200$; $I_V(0) = 50$; $R_U(0) = 150$; $R_V(0) = 40$; $A_M(0) = 2500$; $M_U(0) = 1500$; $M_E(0) = 1000$; $M_I(0) = 800$. In order to simulate the effect seasonal variation, we use the generalized temperature function given by [3] as follows where T_0 is the mean annual temperature, T_1 represents the variation about the mean, ω measures the periodicity of the function and ϕ is the phase shift of the function.

The solution profile of the model (5.2.1) showing the total number of infected humans $(I_U + I_V)$ when $R_{0V} < 1$ and when $R_{0V} > 1$ are given in Figure 5.28 and Figure 5.29 respectively. The total infected humans approach the DFE when $R_{0V} < 1$ and approach an endemic equilibrium when $R_{0V} > 1$. Figure 5.30 and Figure 5.31 respectively show disease prevalence in humans as a function of rate of successful use of larvicides (c_A) and function of vaccine efficacy (ϵ_V) with other control variables been fixed. Figure 5.32 also show disease prevalence as a function of the successful rate of using bed nets (c_B) with other controls fixed. It should be noted that the rate of successful use adulticides have a small marginal effect in the disease prevalence. Figure 5.33 show the vaccinated reproduction number as a function of vaccine efficacy when $R_{0V} = 6.457 > 1$ with $R_{0V} < 1$ when the efficacy of the vaccination is above 90%.

For the simulation of the seasonal variations, the constants coefficients of (5.2.2) are chosen from the values in Table 3 of [3]. Simulation for the total infected humans $(I_U + I_V)$ of the autonomous and non-autonomous models are compared for the city of Ati in republic of Chad by Figure 5.34 (where $T_0 = 29.1$, $T_1 = 0.1137$, $\omega = 1.0159$ and $\phi = -155.5315$), while that of Tchibanga in Gabon with coefficients $T_0 = 24.8$, $T_1 = 0.0434$, $\omega = 1.0044$ and $\phi = -71.74437$ is given by Figure 5.35. Similarly, the comparison for Lodwar in Kenya (where $T_0 = 26.3$, $T_1 = 0.129$, $\omega = 1.0023$ and $\phi = -128.2092$) is given by Figure 5.36, and Figure 5.37 depict the comparison for the city of Bamako Mali where $T_0 = 27.2$, $T_1 = 0.120$, $\omega = 0.9734$ and $\phi = -109.7449$. In each of the cases there are fluctuations in the periodic case while the constant approach an endemic equilibrium point, although they have different frequencies and amplitude, they all fluctuate within the same region.

Simulation of the model (5.2.1) showing the total number of infected mosquitoes with periodic temperature function given by $T(t) = T_0\big[1 + T_1 \cos\big(\frac{2\pi}{365}(\omega t + \phi)\big)\big]$, where the population fluctuates without extincting over a long period of time for the city of Ati in republic of Chad and Lodwar in Kenya are respectively given by Figure 5.38 and Figure 5.39.

Table 5.8: Values and ranges for the temperature-independent parameters of the model given by (5.2.1). Two choices of parameter values for which $R_{0V} < 1$ and $R_{0V} > 1$ for the autonomous system are respectively given in column three and column four.

Para	Ranges	$R_{0V} < 1$	$R_{0V} < 1$	References
Π_H	10-800/day	100	30	[3, 62]
ω_V	0-1/day	0.1	0.1	Assumed
ξ_V	0-1/dose	0.3	0.6	[117]
ϵ_V	0-1/dose	0.3	0.3	[117, 142]
μ_H	0.00003-0.00006/day	0.0000342	0.0000548	[27, 62, 109]
α_B	0-1	0.2	0.8	[117]
ϵ_B	0-1	0.5	0.5	Assumed
ϵ_W	0-1	0.5	0.5	Assumed
τ_U	0.000055-0.011/day	0.1	0.1	[3, 27, 109]
τ_V	0.000055-0.011/day	0.02	0.02	[3, 27, 109]
η_I	0 - 1	0.6	0.7	[62, 111]
η_U	0 - 1	0.3	0.3	[62, 111]
η_V	0 - 1	0.1	0.1	[62, 111]
σ_U	0.067-0.2/day	0.08	0.08	[27, 109, 89]
σ_V	0.077-0.2/day	0.07	0.07	[27, 109, 89]
γ_U	0.0014-0.017/day	0.015	0.015	[3, 27, 109]
γ_V	0.0014-0.017/day	0.016	0.017	[3, 27, 109]
δ_U	0.0001-0.0004/day	0.0015	0.004	[3, 27, 109]
δ_V	0.0001-0.0003/day	0.001	0.003	[3, 27, 109]
$\mathcal{K}$	50-3300000	10000	50000	[3, 83, 124]
ϕ_A	1-500/day	20	40	[83, 89, 124]
σ_A	0.02-0.27/day	0.2	0.2	[109, 83, 124]
α_L	0-1	0.6	0.2	Assumed
α_A	0-1	0.625	0.375	Assumed
ϵ_L	0-1	0.5	0.5	Assumed
ϵ_A	0-1	0.8	0.8	Assumed
σ_M	0.029-0.33/day	0.5	0.7	[109, 27, 89]
μ_A	0.001-0.2/day	0.1	0.019	[3, 109, 89]
μ_V	0.04762-0.07143/day	0.0529	0.04762	[27, 62, 109]
a_M	0.1-1/day	0.4	0.6	[3, 27, 109]
β_{VH}	0.0027-0.64/day	0.44	0.64	[3, 27, 62]
β_{HV}	0.072-0.64/day	0.44	0.64	[3, 27, 109]

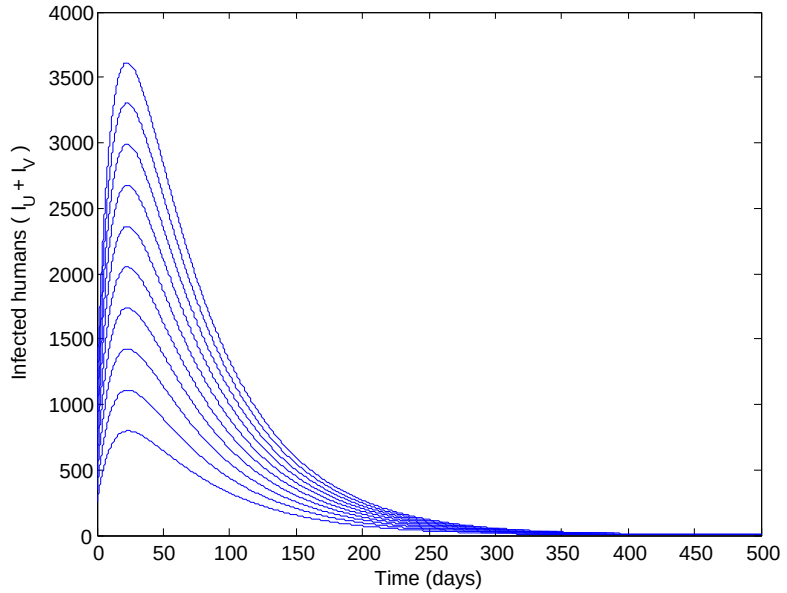

Figure 5.28: Simulation of the model (5.2.1) showing the total number of infected humans $(I_U + I_V)$ with different initial conditions approaching the disease free equilibrium when $R_{0V} < 1$.

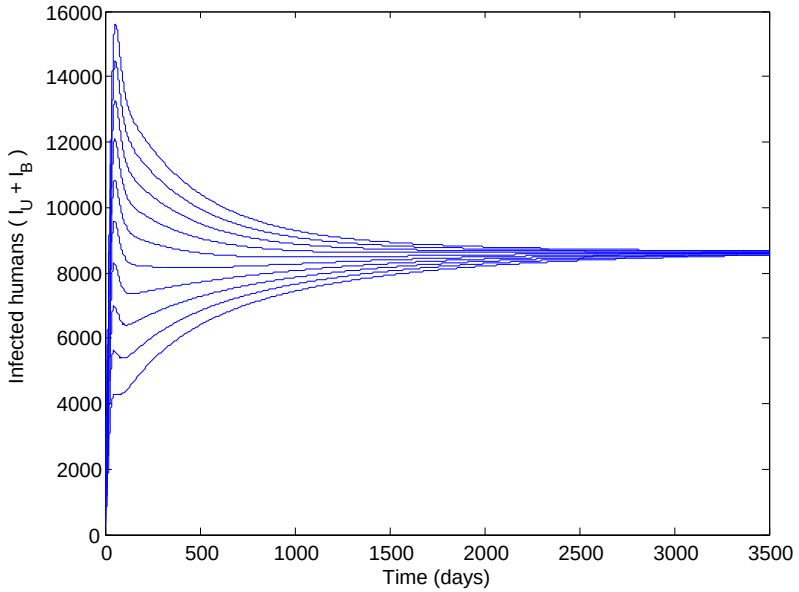

Figure 5.29: Simulation of the model (5.2.1) showing the total number of infected humans $(I_U + I_V)$ with different initial conditions approaching an endemic equilibrium when $R_{0V} > 1$.

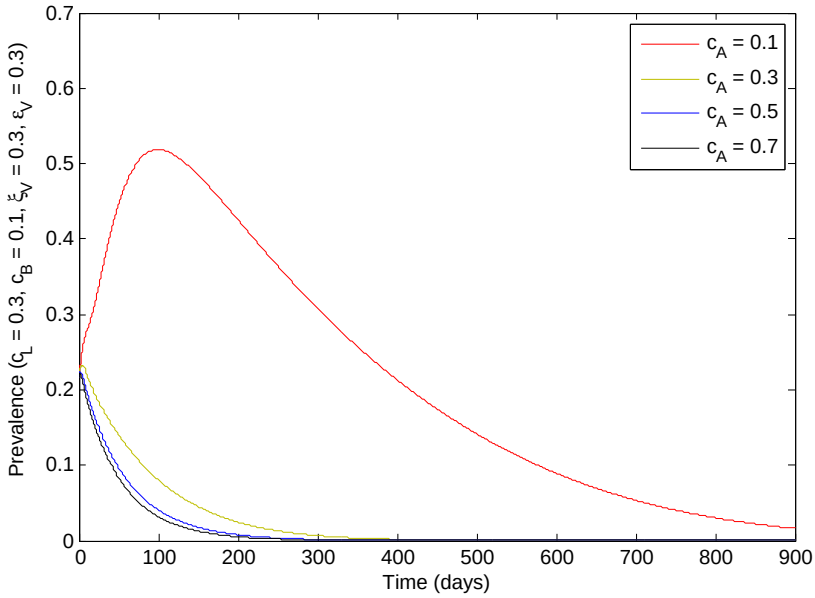

Figure 5.30: Simulation of the model (5.2.1) showing the disease prevalence with different rate of successful use of adulticides and $R_{0V} < 1$.

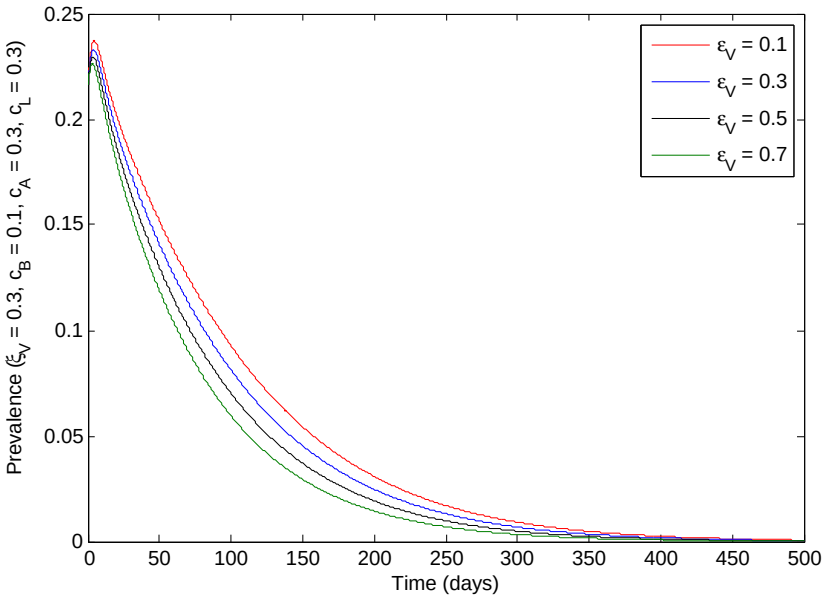

Figure 5.31: Simulation of the model (5.2.1) showing the disease prevalence when $R_{0V} < 1$ with different efficacy of vaccine.

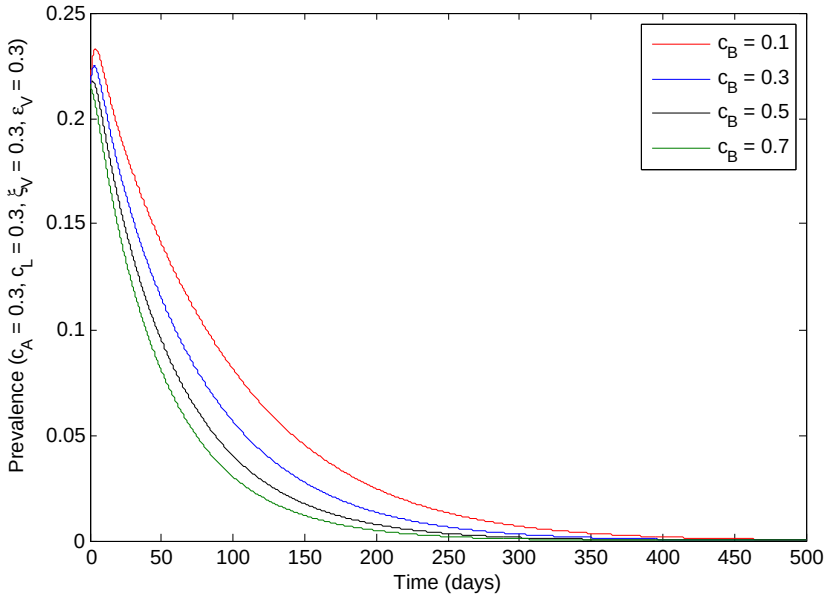

Figure 5.32: Simulation of the model (5.2.1) showing the disease prevalence with different rate of successful use of bed nets and $R_{0V} < 1$.

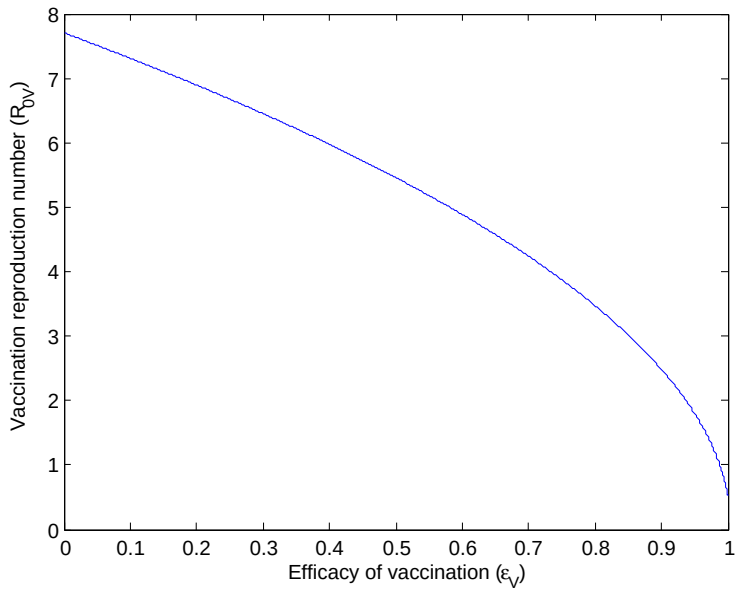

Figure 5.33: Simulation of the vaccinated reproduction number (R_{0V}) as a function of the efficacy of vaccination (ϵ_V).

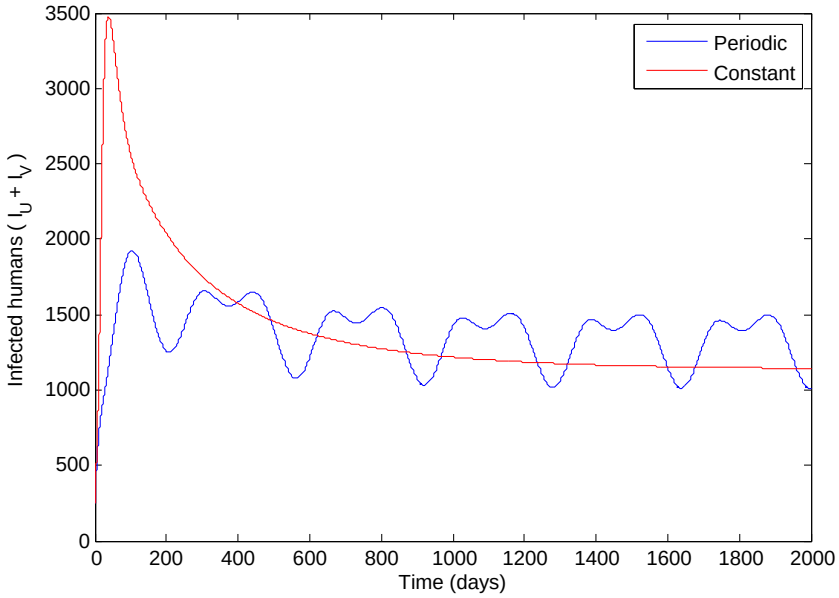

Figure 5.34: Simulation of the model (5.2.1) showing the total number of infected humans with constant and periodic temperature given by the generalized temperature function $T(t) = T_0\left[1+T_1\cos\left(\frac{2\pi}{365}(\omega t+\phi)\right)\right]$ for the city of Ati in Chad when $R_{0V} > 1$.

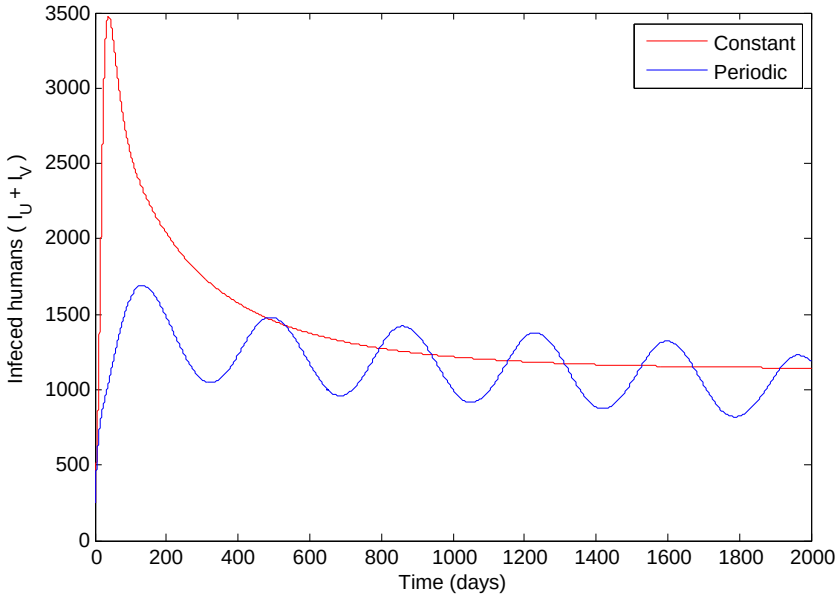

Figure 5.35: Simulation of the model (5.2.1) showing the total number of infected humans with constant and periodic temperature given by the generalized temperature function $T(t) = T_0\left[1+T_1\cos\left(\frac{2\pi}{365}(\omega t+\phi)\right)\right]$ for the city of Tchibanga in Gabon when $R_{0V} > 1$.

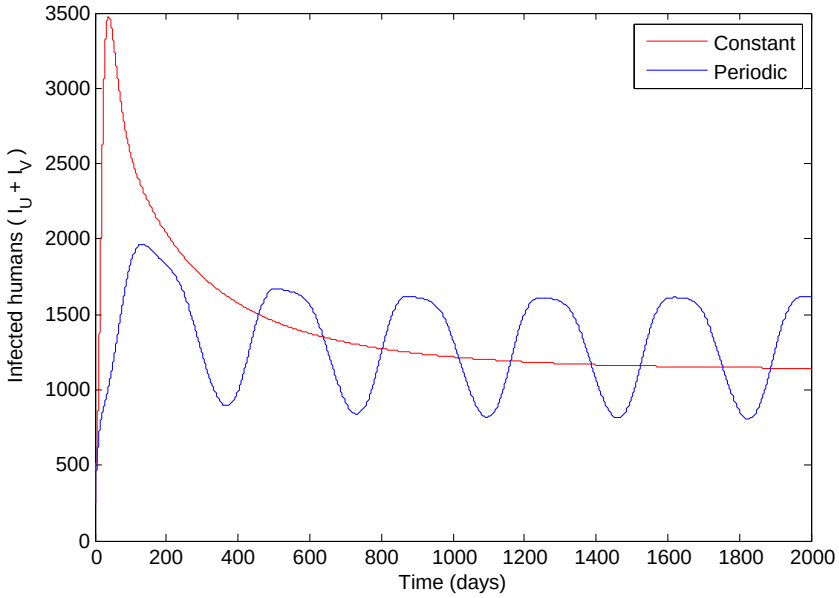

Figure 5.36: Simulation of the model (5.2.1) showing the total number of infected humans with constant and periodic temperature given by the generalized temperature function $T(t) = T_0\left[1 + T_1 \cos\left(\frac{2\pi}{365}(\omega t + \phi)\right)\right]$ for the city of Lodwar in Kenya when $R_{0V} > 1$.

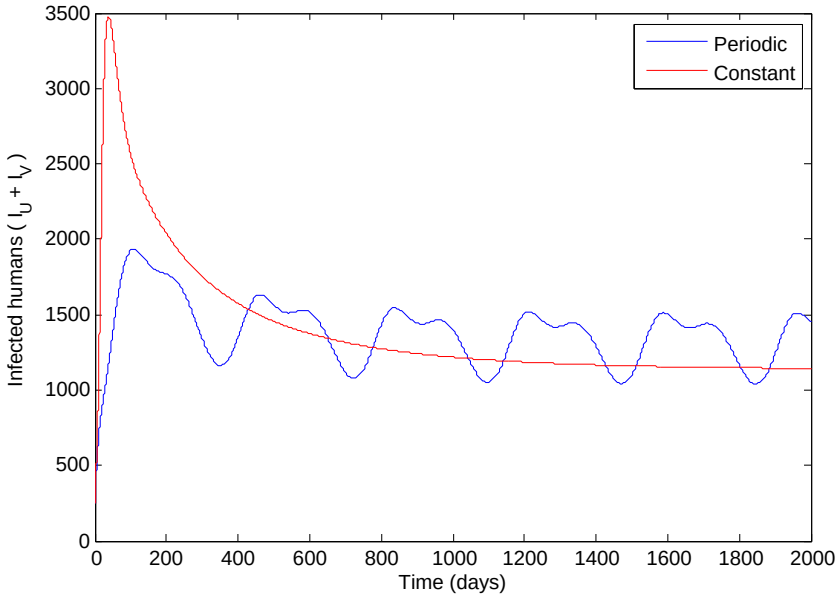

Figure 5.37: Simulation of the model (5.2.1) showing the total number of infected humans with constant and periodic temperature given by the generalized temperature function $T(t) = T_0\left[1 + T_1 \cos\left(\frac{2\pi}{365}(\omega t + \phi)\right)\right]$ for the city of Bamako in Mali when $R_{0V} > 1$.

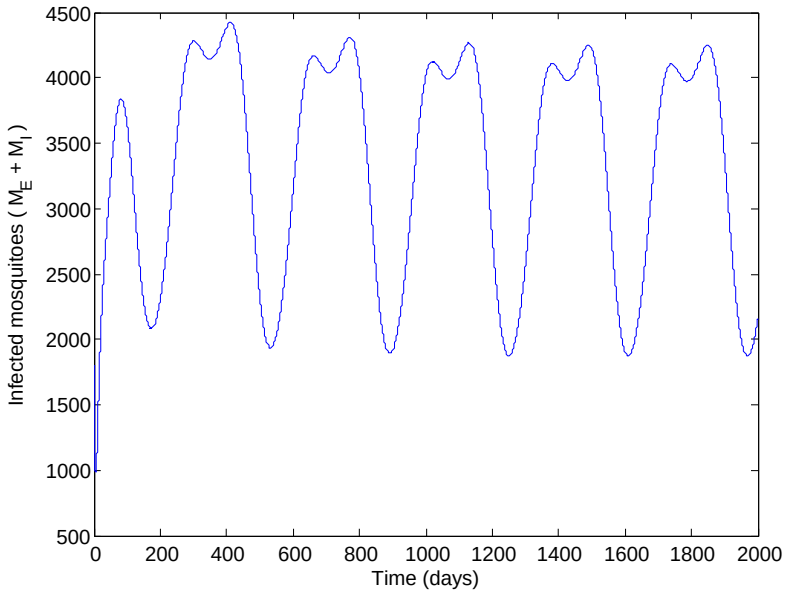

Figure 5.38: Simulation of the model (5.2.1) showing the total number of infected mosquitoes with periodic temperature given by the generalized temperature function $T(t) = T_0\left[1 + T_1 \cos\left(\frac{2\pi}{365}(\omega t + \phi)\right)\right]$ for the city of Ati in Chad when $R_{0V} > 1$.

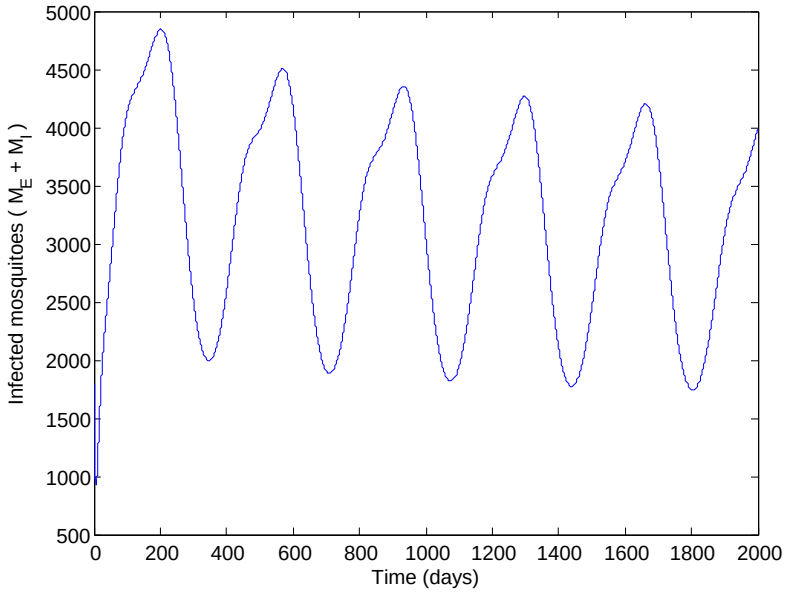

Figure 5.39: Simulation of the model (5.2.1) showing the total number of infected mosquitoes with periodic temperature given by the generalized temperature function $T(t) = T_0\left[1 + T_1 \cos\left(\frac{2\pi}{365}(\omega t + \phi)\right)\right]$ for the city of Lodwar in Kenya when $R_{0V} > 1$.

Conclusion

A new mathematical model to assess the effect of temperature on control strategies in the transmission dynamics of malaria, is constructed and analysed. Some of the main findings of this study are summarized below:

(I) The autonomous mosquito-only model has a threshold quantity called the basic offspring number with the property that, if the threshold quantity (N_0) is less than or equal to unity, the mosquito population goes to extinction, and it establishes if $(N_0) > 1$.

(II) The autonomous model version of system (5.2.1) has two disease-free equilibria, the mosquito-extinction equilibrium (E_2) which is globally-asymptotically stable (GAS) when the basic offspring number (N_0) is less than unity and the non-mosquito-extinction equilibrium (E_3) which is locally asymptotically stable when $R_{0V} \leq 1$.

(III) The autonomous model undergoes the phenomenon of backward bifurcation, which could be removed for a special case when malaria induced death rates ($\delta_U = 0$ and $\delta_V = 0$) and the vaccine waning rate are negligible ($\omega_V = 0$).

(IV) Relationship between the vaccinated reproduction number and the type reproduction numbers is established, where it is shown that $T_i < 1$ $(i = 1, 2, 3)$, provided $R_{0V} < 1$ (and $T_i \Leftrightarrow R_{0V}$). This result suggest that, malaria can be control by targeting certain groups in the population.

(V) The non-autonomous model (5.2.1) has a disease-free equilibrium (E_4), which is locally asymptotically stable whenever the associated reproduction ratio is less than one and unstable otherwise.

(VI) The partial rank correlation coefficient for the use of larvicides is positively correlated with the vaccinated reproduction number when the temperature ranges between 15^0C-20^0C and 30^0C-35^0C, thus within those temperature intervals, use of larvicides may impede effort aimed at reducing malaria infection.

(VII) The successful use of adulticides (c_A), bed nets (c_B) and vaccine efficacy (ϵ_V) are negatively correlated with the vaccinated reproduction number within all the temperature ranges.

(VIII) For non-control parameters, the most positively correlated parameters within all ranges are the mosquito carrying capacity $(\mathcal{K})$, probability of disease transmission (β_{HV}), reduction parameter in the transmission of infected vaccinated humans and rate of vaccination (ξ_V). On the other hand, recovery rates γ_U, γ_V and human recruitment rate (Π_H) are the most negatively correlated in all the temperature ranges.

(IX) Numerical simulation of the model, using appropriate demographic and epidemiological data for Kwazulu Natal province of South Africa, show that (for the case where backward bifurcation does not occur), the hybrid strategy which combines

all the strategies (that is combined use bed nets, vaccination and adulticides) is more effective than singular use of the aforementioned control strategies, that can lead to malaria elimination in the province.

(X) Simulations of the model show that high vaccine efficacy is required to reduce the vaccinated reproduction number to a value below unity. Further, a singular effective use of bed nets can result in effective control of malaria in a community provided the bed net coverage and the bed net efficacy are high enough (at least 60 % each).

Chapter 6

Conclusion and future work

This thesis considered three different mathematical models for the transmission dynamics of mosquito borne diseases. All the models studied were deterministic and standard incidence formulations were used in the construction of their forces of infections. In Chapter 2 and Chapter 3, models for the transmission of Zika virus were studied, while transmission dynamics of yellow fever was studied in Chapter 4, and in Chapter 5, autonomous and non-autonomous malaria models were studied.

6.0.3 Conclusion

Although conclusions at the end of Chapter 2, Chapter 3, Chapter 4 and Chapter 5 were given, general conclusions are given as follows;

1. In the case of mathematical models for the transmission dynamics of mosquito borne diseases, where aquatic stages of mosquito development are incorporated, population of mosquito has a threshold parameter called the basic offspring number (N_0), which controls the extinction or persistence of mosquito population, such that if the threshold is less than or equal to one, mosquito population dies out and persist otherwise. In the case of models with mosquito control, the threshold is a reducing function of the rate of death of mosquitoes due to use of control.

2. For models of mosquito borne diseases with human-human transmission, the requirement for the control of the disease in a population where $N_0 \leq 1$ is that, the associated human-human basic reproduction number to be less than or equal to unity.

3. The disease free equilibriums of the models when their respective basic offspring numbers are greater than one were shown to be locally-asymptotically stable when the associated basic reproduction numbers are less than unity.

4. In line with results from previously studied mosquito borne diseases with standard incidence force of infection. The model (with $N_0 > 1$) in the absence of direct transmission undergoes backward bifurcation, where the stable DFE co-exist with a stable endemic equilibrium when the associated reproduction number is

less than unity. It was shown that, disease induced death rate in humans is the major cause of the phenomenon for models without vaccination, where as imperfect vaccination is also another cause for models with vaccination.

5. Although the rate of direct human-human transmission is positively correlated to the basic reproduction number (increases disease burden), it was shown that it does not affect the existence or otherwise of backward bifurcation.

6. As the type reproduction number excludes total number of infections from one individual to individuals of its kind in a heterogeneous populations. There exist relationships between the type reproduction numbers and the basic reproduction number, with infected human type reproduction number (T_1) most closely related to the basic reproduction number.

7. Conditions for the global asymptotic stability of disease free equilibria were also established for the autonomous models.

8. For the models with vaccination, the threshold vaccination and vaccine efficacy required to bring the vaccinated reproduction number (R_{0V}) to below unity were computed, in addition, it was shown that the threshold (R_{0V}) is a reducing function of the fraction of vaccinated individuals.

9. In the models with vertical transmission, it was shown using sensitivity analysis that the vaccinated/basic reproduction numbers are most sensitive and positively correlated to the rate of vertical transmission, thus making it the most important parameter to target in controlling the threshold.

6.0.4 Future work

In the future, the model presented in Chapter 2 can be extended to incorporate vertical transmission within human population (as it was attributed to been the cause of congenital neurological disorder and auto-immune complications), to do this, the human population need to be extended to a sex structured form with a non-constant (varying) recruitment rate of humans, thereby substantially increasing the number of equations. In addition, density dependence mortality rate in humans, as well as temperature variations to capture seasonal variation can also be incorporated into the model.

For the model in Chapter 3, aside from extensions similar to those of Chapter 2, the model can be extended to incorporate time dependent release of sterilized mosquitoes (different release functions to capture different circumstances can be tested), thus a non-constant mating probability will be considered and optimal control analysis be done. The model in Chapter 4 can similarly incorporate temperature changes, as well as time dependent controls. The model in Chapter 5 can also incorporate a non-constant recruitment rate in humans and time dependent control, so as to consider an optimal control problem.

Bibliography

[1] Abdelrazec A, Gumel AB. Mathematical assessment of the role of temperature and rainfall on mosquito population dynamics. *Journal of mathematical biology*. 2017;74(6):1351-1395.

[2] Adams B, Boots M. How important is vertical transmission in mosquitoes for the persistence of dengue? Insights from a mathematical model. *Epidemics*. 2010;2(1):1-0.

[3] Agusto FB, Gumel AB, Parham PE. Qualitative assessment of the role of temperature variations on malaria transmission dynamics. *Journal of Biological Systems*. 2015;23(04):1550030.

[4] Agusto FB, Bewick S, Fagan WF. Mathematical model for Zika virus dynamics with sexual transmission route. *Ecological Complexity*. 2017;29:61-81.

[5] Agusto FB, Bewick S, Fagan WF. Mathematical model of Zika virus with vertical transmission. *Infectious Disease Modelling*. 2017.

[6] Alonso D, Bouma MJ, Pascual M. Epidemic malaria and warmer temperatures in recent decades in an East African highland. *Proceedings of the Royal Society of London B: Biological Sciences*. 2011;278(1712):1661-1669.

[7] Andraud M, Hens N, Marais C, Beutels P. Dynamic Epidemiological Models for Dengue Transmission: A Systematic Review of Structural Approaches. *PLoS one*. 2012;7(11):e49085.

[8] Anguelov R, Dumont Y, Lubuma J. Mathematical Modeling of Sterile Insect Technology for Control of Anopheles Mosquito. *Computers & Mathematics with Applications*. 2012;64(3):374-389.

[9] Bacar N, Guernaoui S. The epidemic threshold of vector-borne diseases with seasonality. *Journal of mathematical biology*. 2006;53(3):421-436.

[10] Bacar N. Approximation of the basic reproduction number R 0 for vector-borne diseases with a periodic vector population. *Bulletin of mathematical biology*. 2007;69(3):1067-1091.

[11] Bacaer N. *A short History of Mathematical Population Dynamics*. Springer London Dordrecht Heildelberg, New York, 2011.

[12] Barclay HJ, Van Den Driessche P. A sterile release model for control of a pest with two life stages under predation. *Rocky Mountain Journal of Mathematics*. 1990;20:847-855.

[13] Barnett ED. Yellow fever: epidemiology and prevention. *Clinical Infectious Diseases*. 2007;44(6):850-856.

[14] Barrett AD. Yellow fever in Angola and beyond-the problem of vaccine supply and demand. *New England Journal of Medicine*. 2016;375(4):301-303.

[15] Barrett AD, Monath TP. Epidemiology and ecology of yellow fever virus. *Advances in virus research*. 2003;61:291-317.

[16] Belmusto-Worn V.E., Sanchez J.L., McCARTHY K.A.R.E.N., Nichols R., Bautista C.T., Magill A.J., Pastor-Cauna G., Echevarria C., Laguna-Torres V.A., Samame B.K. and Baldeon M.E.. Randomized, double-blind, phase III, pivotal field trial of the comparative immunogenicity, safety, and tolerability of two yellow fever 17D vaccines (Arilvax and YF-VAX) in healthy infants and children in Peru. *The American journal of tropical medicine and hygiene*. 2005;72(2),:189-197.

[17] Blanford JI, Blanford S, Crane RG, Mann ME, Paaijmans KP, Schreiber KV, Thomas MB. Implications of temperature variation for malaria parasite development across Africa. *Scientific reports*. 2013;1300.

[18] Blayneh KW, Gumel AB, Lenhart S, Clayton T. Backward bifurcation and optimal control in transmission dynamics of West Nile virus. *Bulletin of mathematical biology*. 2010;72(4):1006-1028.

[19] Bowman C, Gumel AB, Van den Driessche P, Wu J, Zhu H. A mathematical model for assessing control strategies against West Nile virus. *Bulletin of mathematical biology*. 2005;67(5):1107-1133.

[20] Buonomo B, Della Marca R. Optimal bed net use for a dengue disease model with mosquito seasonal pattern. *Mathematical Methods in the Applied Sciences*. 2018;41(2):573-592.

[21] Brauer F, Castillo-Chavez C, Castillo-Chavez C. Mathematical models in population biology and epidemiology. *New York: Springer*; 2012.

[22] Brauer F, Castillo-Chavez C, Mubayi A, Towers S. Some models for epidemics of vector-transmitted diseases. *Infectious Disease Modelling*. 2016;1(1):79-87.

[23] Briere JF, Pracros P, Le Roux AY, Pierre JS. A novel rate model of temperature-dependent development for arthropods. *Environmental Entomology*. 1999;28(1):22-29.

[24] Buonomo B, Lacitignola D. On the backward bifurcation of a vaccination model with nonlinear incidence. *Nonlinear Analysis: Modelling and Control*. 2011;16(1):30-46.

[25] Caminade C, Kovats S, Rocklov J, Tompkins AM, Morse AP, Coln-Gonzlez FJ, Stenlund H, Martens P, Lloyd SJ. Impact of climate change on global malaria distribution. *Proceedings of the National Academy of Sciences*. 2014;111(9):3286-3291.

[26] Castillo-Chavez C, Song B. Dynamical model of tuberculosis and their applications. *Mathematical Bioscience and Engineering*. 2004;1(2):361-404.

[27] Chitnis N, Cushing JM, Hyman JM. Bifurcation analysis of a Mathematical model for malaria transmission. *Society for Industrial and Applied Mathematics*. 2006;67(1):24-45.

[28] Chitnis N, Cushing JM, Hyman JM. Determining important parameters in the spread of malaria through sensitivity analysis of a Mathematical model. *Bulletin of Mathematical Biology*. 2008;70(5):1272-1296.

[29] Chitnis N, Hyman JM, Manore CA. Modelling vertical transmission in vector-borne diseases with application to Rift Valley fever. *Journal of Biological Dynamics*. 2013;7(1):11-40.

[30] Chowell G, Hayman JM, Bettencourt LM, Castillo-Chavez C. *Mathematical and Statistical Estimation Approaches in Epidemiology*. Springer Dirdrecht Heidelberg, New York, 2009.

[31] Ciota AT, Bialosuknia SM, Ehrbar DJ, Kramer LD. Vertical transmission of Zika virus by Aedes aegypti and Ae. albopictus Mosquitoes. *Emerging Infectious Diseases*. 2017;23(5):880.

[32] Clemons A, Mori A, Haugen M, Severson D, Duman-Scheel M. *Aedes aegypti* Culturing and Egg Collection. *Cold Spring Harbor protocols*. 2010;pdb-prot5507.

[33] Coutinho FAB, Burattini MN, Lopez LF, Massad E. Threshold conditions for a non-autonomous epidemic system describing the population dynamics of dengue. *Bulletin of Mathematical Biology*. 2006;68(8):2263-2282.

[34] Danbaba UA, Garba SM, Analysis of model for the transmission dynamics of Zika with sterile insect technique, in R. Anguelov, M. Lachowicz (Editors), Mathematical Methods and Models in Biosciences. *Biomath Forum*, Sofia, 2018;81-99. $http://dx.doi.org/10.11145/texts.2018.01.083$

[35] Danbaba UA, Garba SM. Modeling the transmission dynamics of Zika with sterile insect technique. *Math Meth Appl Sci*. 2018;1-26. https://doi.org/10.1002/mma.5336.

[36] Danbaba A. Mathematical models and analysis for the transmission dynamics of malaria. Dissertation, University of Pretoria. 2016.

[37] Danbaba UA, Garba SM, Stability Analysis and Optimal Control for Yellow Fever Model with Vertical Transmission. International Journal of Applied and Computational Mathematics.

[38] Danbaba UA, Garba SM, Modeling the effect of temperature variability on malaria control strategies. Mathematical Modelling of Natural Phenomena.

[39] Deckard DT, Chung WM, Brooks JT, Smith JC, Woldai MS, Hennessey M, Kwit N. Male-to-Male Sexual Transmission of Zika Virus-Texas, January 2016. *Morbidity and Mortality Weekly Report (MMWR)*, 65(14): 372-374. DOI: 10.15585/mmwr.mm6514a3 PMID: 27078057, 2016.

[40] Dembele B, Friedman A, Yakubu AA. Malaria model with periodic mosquito birth and death rates. *Journal of biological dynamics*. 2009;3(4):430-445.

[41] Diallo M, Thonnon J, Fontenille D. Vertical transmission of the yellow fever virus by Aedes aegypti (Diptera, Culicidae): dynamics of infection in F1 adult progeny of orally infected females. *The American journal of tropical medicine and hygiene*. 2000;62(1):151-156.

[42] Musso D, Roche C, Robin E, Nhan T, Teissier A, Cao-Lormeau VM. Potential Sexual Transmission of Zika Virus. *Emerging Infectious Diseases*. 2015;21(2);359.

[43] Diekmann O, Heesterbeek JA, Metz JA. On the definition and computation of the basic reproduction ratio R_0 in models for the infectious diseases in heterogeneous populations. *Journal of Mathematical Biology*, **28**: 1990;365-382.

[44] Diekmann O, Heesterbeek JA, Roberts MG. The construction of next-generation matrices for compartmental epidemic models. *Journal of the Royal Society Interface*. 2010;7:873-885.

[45] Dumont Y, Choiroleu F, Domerg C. On a temporal model for the Chikungunya disease: Modeling, theory and numerics. *Mathematical Biosciences*. 2008;213(1):80-91.

[46] Dumont Y, Choiroleu F. Vector control for the Chikungunya disease. *Mathematical Bioscience and Engineering*. 2010;7(2):313-345.

[47] Dumont Y, Tchuenche JM. Mathematical studies on the sterile insect technique for the Chikungunya disease and Aedes albopictus. *Journal of Mathematical Biology*. 2012;65(25):809-854.

[48] DOrtenzio E, Matheron S, de Lamballerie X, Hubert B, Piorkowski G, Maquart M, Descamps D, Damond F, Yazdanpanah Y, Leparc-Goffart I. Evidence of Sexual Transmission of Zika Virus. *New England Journal of Medicine*. 2016;374(22):2195-2198.

[49] Dye C. Models for the population dynamics of the yellow fever mosquito, Aedes aegypti. *The Journal of Animal Ecology*. 1984:247-268.

[50] Eikenberry SE, Gumel AB. Mathematical modeling of climate change and malaria transmission dynamics: a historical review. *Journal of mathematical biology*. 2018:1-77.

[51] Esteva L, Yang HM. Mathematical model to assess the control of *Aedes aegypti* mosquitoes by sterile insect technique. *Mathematical Biosciences*. 2005;198(2):132-147.

[52] Esteva L, Yang HM. Control of Dengue Vector by the Sterile Insect Technique Considering Logistic Recruitment. *TEMA. Tendncias em Matemtica Aplicada e Computacional*. 2006;7(2):259-268.

[53] Fang J. Ecology: a world without mosquitoes. *Nature News*. 2010;466(7305):432-434.

[54] Ferreira-de-Brito A, Ribeiro IP, Miranda RM, Fernandes RS, Campos SS, Silva KA, Castro MG, Bonaldo MC, Brasil P, Loureno-de-Oliveira R. First detection of natural infection of Aedes aegypti with Zika virus in Brazil and throughout South America. *Memrias do Instituto Oswaldo Cruz*. 2016;111(10):655-658.

[55] Fiedler M. *Special matrices and their applications in numerical mathematics*. Courier Corporation; 2008.

[56] Fleming WH, Rishel RW. *Deterministic and stochastic optimal control*. Springer Science & Business Media; 2012.

[57] Fontenille D, Diallo M, Mondo M, Ndiaye M, Thonnon J. First evidence of natural vertical transmission of yellow fever virus in Aedes aegypti, its epidemic vector. *Transactions of the Royal Society of Tropical Medicine and Hygiene*. 1997;91(5):533-535.

[58] Foy BD, Kobylinski KC, Foy JLC, Blitvich BJ, da Rosa AT, Haddow AD, Lanciotti RS, Tesh RB. Probable NonVector-borne Transmission of Zika Virus, Colorado, USA. *Emerging Infectious Diseases*. 2011;17(5):880-882.

[59] Fred B, and Castillo-Chavez C. *Mathematical models in population Biology and Epidemiology*, Second edition. Springer New york Dordrecht Heidelberg London, 2012.

[60] Frour T, Miralli S, Hubert B, Splingart C, Barriere P, Maquart M, Leparc-Goffart I. Sexual transmission of Zika virus in an entirely asymptomatic couple returning from a Zika epidemic area, France, April 2016. *Eurosurveillance*. 2016;21(23):1-3.

[61] Gao D, Lou Y, He D, Porco DC, Kuang Y, Chowell G, Ruan S. Prevention and Control of Zika as a Mosquito-Borne and Sexually Transmitted Disease: A Mathematical Modeling Analysis. *Scientific Reports*. 2016;6(28070).

[62] Garba SM, Gumel AB, Abu Bakar MR. Backward bifurcation in dengue transmission dynamics. *Mathematical Bioscience*. 2008;215(1):11-25.

[63] Garba SM, Gumel AB. Effect of cross-immunity on the transmission dynamics of two strains of dengue. *International Journal of Computer Mathematics*. 2010;87(10): 2361-2384.

[64] Garba SM, Safi MA. Mathematical Analysis of West Nile Virus Model with Discrete Delays. *Acta Mathematica Scientia*. 2013;33(5):1439-1462.

[65] Gething PW, Van Boeckel TP, Smith DL, Guerra CA, Patil AP, Snow RW, Hay SI. Modelling the global constraints of temperature on transmission of Plasmodium falciparum and P. vivax. *Parasites & vectors*. 2011;4(1):92.

[66] Gumel AB. Causes of backward bifurcations in some epidemiological models. *Journal of Mathematical Analysis and Applications*. 2012;395(1):355-365.

[67] Gotuzzo E, Yactayo S, Crdova E. Efficacy and duration of immunity after yellow fever vaccination: systematic review on the need for a booster every 10 years. *The American journal of tropical medicine and hygiene*. 2013;89(3):434-444.

[68] Gutirrez-Bugallo G, Rodriguez-Roche R, Daz G, Vzquez AA, Alvarez M, Rodrguez M, Bisset JA, Guzman MG. First record of natural vertical transmission of dengue virus in Aedes aegypti from Cuba. *Acta Tropica*. 2017.

[69] Hanley KA, Monath TP, Weaver SC, Rossi SL, Richman RL, Vasilakis N. Fever versus fever: the role of host and vector susceptibility and interspecific competition in shaping the current and future distributions of the sylvatic cycles of dengue virus and yellow fever virus. *Infection, Genetics and Evolution*. 2013;19:292-311.

[70] Harbach RE, Besansky NJ. Mosquitoes. *Current Biology*. 2014;24(1):R14-15.

[71] Hayes EB. Zika Virus Outside Africa. *Emerging Infectious Diseases*. 2009;15(9):1347-1350.

[72] Heesterbeek JA, Roberts MG. The type-reproduction number T in models for infectious disease control. *Mathematical biosciences*. 2007;206(1):3-10.

[73] Hole PI, Knols BGJ, Malaria J.8 (Suppl. 2) (2009) S8. http://dx.doi.org/10.1186/1475-2875-8-s2-s8. [Accessed February, 2018].

[74] Imran M, Usman M, Dur-e-Ahmad M, Khan A. Transmission Dynamics of Zika Fever: A SEIR Based Model. *Differential Equations and Dynamical Systems*. 2017:1-24.

[75] Jain J, Kushwah RB, Singh SS, Sharma A, Adak T, Singh OP, Bhatnagar RK, Subbarao SK, Sunil S. Evidence for natural vertical transmission of chikungunya viruses in field populations of Aedes aegypti in Delhi and Haryana states in Indiaa preliminary report. *Acta tropica*. 2016;162:46-55.

[76] Johansson MA, Arana-Vizcarrondo N, Biggerstaff BJ, Staples JE. Incubation periods of yellow fever virus. The American journal of tropical medicine and hygiene. 2010;83(1):183188

[77] Kamgang JC, Sallet G. Global asymptotic stability for the disease free equilibrium for epidemiological models. *Comptes Rendus Mathematique*. 2005;341(7):433-438.

[78] Kamgang JC, Tchoumi SY. A model of the dynamic of transmission of Malaria, integrating SEIRS, SEIS, SIRS and SIS organization in the host-population. *Journal of Applied Analysis and Computation*. 2015;5(4):688-703.

[79] Kang Y, Castillo-Chavez C. Dynamics of SI models with both horizontal and vertical transmissions as well as Allee effects. *Mathematical biosciences*. 2014;248:97-116.

[80] Knipling EF. Possibilities of insect control or eradication through the use of sexually sterile males. *Journal of Economic Entomology*. 1955;48(4):459-462.

[81] Korn GA, Korn TM. *Mathematical Handbook for Scientists and Engineers: Definitions, Theorems, and Formulas for Reference and Review*. Courier Corporation. 2000.

[82] Kumar A, Srivastava PK. Vaccination and treatment as control interventions in an infectious disease model with their cost optimization. *Communications in Nonlinear Science and Numerical Simulation*. 2017;44:334-343.

[83] Laperriere V, Brugger K, Rubel F. Simulation of the seasonal cycles of bird, equine and human West Nile virus cases. *Preventive veterinary medicine*. 2011;98(2-3):99-110.

[84] LaSalle JP. *The Stability of Dynamical Systems*. Society for Industrial and Applied Mathematics. 1976.

[85] Lee J, Kim J, Kwon HD. Optimal control of an influenza model with seasonal forcing and age-dependent transmission rates. *Journal of theoretical biology*. 2013;317:310-320.

[86] Lenhart S, Workman JT. Optimal Control Applied to Biological Models. Boca Raton, FL: Chapman & Hall/CRC; 2007.

[87] Lequime S, Lambrechts L. Vertical transmission of arboviruses in mosquitoes: a historical perspective. *Infection, Genetics and Evolution*. 2014;28:681-690.

[88] Li CX, Guo XX, Deng YQ, Xing D, Sun AJ, Liu QM, Wu Q, Zhang YM, Zhang HD, Cao WC, Qin CF. Vector competence and transovarial transmission of two Aedes aegypti strains to Zika virus. *Emerging microbes & infections*. 2017;6(4):e23.

[89] Lou Y, Zhao XQ. A climate-based malaria transmission model with structured vector population. *SIAM Journal on Applied Mathematics*. 2010;70(6):2023-2044.

[90] Magalhaes T, Foy BD, Marques ET, Ebel GD, Weger-Lucarelli J. Mosquito-borne and sexual transmission of Zika virus: Recent developments and future directions. *Virus Research*. 2017.

[91] Marino S, Hogue IB, Ray CJ, Kirschner DE. A methodology for performing global uncertainty and sensitivity analysis in systems biology. *Journal of theoretical biology*. 2008;254(1):178-197.

[92] Marquardt WH, editor. *Biology of disease vectors*. Elsevier; 2004.

[93] Andraud M, Hens N, Marais C, Beutels P. Dynamic Epidemiological Models for Dengue Transmission: A Systematic Review of Structural Approaches. *PLoS one*. 2012;7(11):e49085.

[94] Martorano Raimundo S, Amaku M, Massad E. Equilibrium analysis of a yellow fever dynamical model with vaccination. *Computational and mathematical methods in medicine*. 2015.

[95] Matthews G. Integrated vector management: controlling vectors of malaria and other insect vector borne diseases. *John Wiley & Sons*. 2011.

[96] Maxian O, Neufeld A, Talis EJ, Childs LM, Blackwood JC. Zika virus dynamics: When does sexual transmission matter?. *Epidemics*. 2017.

[97] Meiss JD. *Differential dynamical systems*. SIAM; 2007.

[98] Oliveira Melo AS, Malinger G, Ximenes R, Szejnfeld PO, Alves Sampaio S, Bispo de Filippis AM. Zika virus intrauterine infection causes fetal brain abnormality and microcephaly: tip of the iceberg. *Ultrasound in Obstetrics and Gynecology*. 2016;47(1):6-7.

[99] Monath TP, Nichols R, Archambault WT, Moore L, Marchesani R, Tian J, Shope RE, Thomas N, Schrader R, Furby D, Bedford P. Comparative safety and immunogenicity of two yellow fever 17D vaccines (ARILVAX and YF-VAX) in a phase III multicenter, double-blind clinical trial. *The American journal of tropical medicine and hygiene*. 2002;66(5):533-541.

[100] Monath TP, Woodall JP, Gubler DJ, Yuill TM, Mackenzie JS, Martins RM, Reiter P, Heymann DL. Yellow fever vaccine supply: a possible solution. *The Lancet*. 2016;387(10028):1599-1600.

[101] Monica K, Livingstone SL, Francis S. Modelling and stability analysis of SVEIRS yellow fever two host model. *Gulf Journal of Mathematics*. 2015 3;3:106-129.

[102] Mordecai EA, Paaijmans KP, Johnson LR, Balzer C, BenHorin T, de Moor E, McNally A, Pawar S, Ryan SJ, Smith TC, Lafferty KD. Optimal temperature for malaria transmission is dramatically lower than previously predicted. *Ecology letters*. 2013;16(1):22-30.

[103] Musso D, Gubler DJ. Zika virus: following the path of dengue and chikungunya?. *The Lancet*. 2015;386(9990):243-244.

[104] Musso D, Roche C, Robin E, Nhan T, Teissier A, Cao-Lormeau VM. Potential Sexual Transmission of Zika Virus. *Emerging Infectious Diseases*. 2015;21(2);359.

[105] Musso D, Gubler DJ. Zika virus. *Clinical microbiology reviews*. 2016;29(3):487-524.

[106] Murdock CC, Sternberg ED, Thomas MB. Malaria transmission potential could be reduced with current and future climate change. *Scientific reports*. 2016;6:27771.

[107] Neilan RM, Lenhart S. An Introduction to Optimal Control with an Application in Disease Modeling. *DIMACS Series in Discrete Mathematics and Theoretical Computer Science*. 2010: 67-82.

[108] Ngwa GA, Shu WS. A mathematical model for endemic malaria with variable human and mosquito populations. *Mathematical and Computer Modelling*. 2000;32(7-8):747-763.

[109] Niger AM, Gumel AB. Mathematical analysis of the role of repeated exposure on malaria transmission dynamics. *Differential Equations and Dynamical Systems*. 2008;16(3):251-287.

[110] Nishiura H, Kinoshita R, Mizumoto K, Yasuda Y, Nah K. Transmission potential of Zika virus infection in the South Pacific. *International Journal of Infectious Diseases*. 2016;45:95-97.

[111] Okuneye K, Gumel AB. Analysis of a temperature- and rainfall-dependent model for malaria transmission dynamics. *Mathematical biosciences*. 2017;287:72-92.

[112] Oliva CF, Jacquet M, Gilles J, Lemperiere G, Maquart PO, Quilici S, Schooneman F, Vreysen MJ, Boyer S. The Sterile Insect Technique for Controlling Populations of Aedes albopictus (Diptera: Culicidae) on Reunion Island: Mating Vigour of Sterilized Males. *PLoS one*. 2012;7(11):e49414.

[113] Orellana JM. Optimal control for HIV therapy strategies enhancement. International Journal of Pure and Applied Mathematics.2010;59(1):39-57.

[114] Pan American Health Organization/World Health Organization. Epidemiological Update: Yellow Fever. 9 January, Washington, D.C.: PAHO/WHO; 2017.

[115] Parham PE, Michael E. Modeling the effects of weather and climate change on malaria transmission. *Environmental health perspectives*. 2009;118(5):620-626. doi:10.1289/ehp.0901256.

[116] Parham PE, Waldock J, Christophides GK, Hemming D, Agusto F, Evans KJ, Fefferman N, Gaff H, Gumel A, LaDeau S, Lenhart S. Climate, environmental and socio-economic change: weighing up the balance in vector-borne disease transmission. *Phil. Trans. R. Soc. B*. 2015;370(1665):20130551.

[117] Penny MA, Verity R, Bever CA, Sauboin C, Galactionova K, Flasche S, White MT, Wenger EA, Van de Velde N, Pemberton-Ross P, Griffin JT. Public health impact and cost-effectiveness of the RTS,S/AS01 malaria vaccine: a systematic comparison of predictions from four mathematical models. *The Lancet*. 2016;387(10016):367-375.

[118] Pontryagin LS, Mishchenko EF, Boltyanskii VG, Gamkrelidze RV. *The mathematical theory of optimal processes*. New York, Wiley. 1962.

[119] Prosper O, Ruktanonchai N, Martcheva M. Optimal vaccination and bednet maintenance for the control of malaria in a region with naturally acquired immunity. *Journal of theoretical biology*. 2014;353:142-156.

[120] Quereshi A. *Zika virus disease: From origin to outbreak*. Academic Press; 2017.

[121] Rahman MM. Insecticide substitutes for DDT to control mosquitoes may be causes of several diseases. *Environmental Science and Pollution Research*. 2013;20(4):2064-2069.

[122] Roberts L. *Mosquitoes and disease*. Science (New York, NY). 2002;298(5591):82-83.

[123] Roberts MG, Heesterbeek JA. A new method for estimating the effort required to control an infectious disease. *Proceedings of the Royal Society of London B: Biological Sciences*. 2003;270(1522):1359-1364.

[124] Rubel F, Brugger K, Hantel M, Chvala-Mannsberger S, Bakonyi T, Weissenbck H, Nowotny N. Explaining Usutu virus dynamics in Austria: model development and calibration. *Preventive veterinary medicine*. 2008;85(3-4):166-186.

[125] Sikka V, Chattu VK, Popli RK, Galwankar SC, Kelkar D, Sawicki SG, Stawicki SP, Papadimos TJ. The emergence of Zika virus as a global health security threat: a review and a consensus statement of the INDUSEM Joint Working Group (JWG). *Journal of global infectious diseases*. 2016;8(1):3.

[126] Shapiro H, Micucci S. Pesticide use for West Nile virus. *Canadian Medical Association Journal*. 2003;168(11):1427-1430.

[127] Shaman J, Spiegelman M, Cane M, Stieglitz M. A hydrologically driven model of swamp water mosquito population dynamics. *Ecological modelling*. 2006;194(4):395-404.

[128] Sharomi O, Malik T. Optimal control in epidemiology. *Annals of Operations Research*. 2017;251(1-2):55-71.

[129] Shearer FM, Moyes CL, Pigott DM, Brady OJ, Marinho F, Deshpande A, Longbottom J, Browne AJ, Kraemer MU, O'Reilly KM, Hombach J. Global yellow fever vaccination coverage from 1970 to 2016: an adjusted retrospective analysis. The Lancet infectious diseases. 2017;17(11):1209-1217.

[130] Sontag ED. Mathematical control theory: deterministic finite dimensional systems. Springer Science & Business Media; 2013.

[131] Strogatz SH, Fox RF. Nonlinear Dynamics and Chaos: With Applications to Physics, Biology, Chemistry and Engineering. *Physics Today*. 1995;48:93.

[132] Stock NK, Laraway H, Faye O, Diallo M, Niedrig M, Sall AA. Biological and phylogenetic characteristics of yellow fever virus lineages from West Africa. *Journal of virology*. 2013;87(5):2895-2907.

[133] Stuart A, Humphries AR. *Dynamical systems and numerical analysis*. Cambridge University Press; 1998.

[134] Takeuchi Y, Iwasa Y, Sato K, editors. *Mathematics for life science and medicine*. Springer Science & Business Media; 2007.

[135] Tangena JA, Thammavong P, Wilson AL, Brey PT, Lindsay SW. Risk and control of mosquito-borne diseases in Southeast Asian rubber plantations. *Trends in parasitology*. 2016;32(5):402-415.

[136] Tchoumi SY, Kamgang JC, Tieudjo D, Sallet G. A basic general model of vector-borne diseases. *Communications in Mathematical Biology and Neuroscience*. 2018:Article-ID.

[137] Thangamani S, Huang J, Hart CE, Guzman H, Tesh RB. Vertical transmission of Zika virus in Aedes aegypti mosquitoes. *The American journal of tropical medicine and hygiene*. 2016;95(5):1169-1173.

[138] Tuteja R. Malaria-an overview. *The FEBS journal*. 2007;274(18):4670-4679.

[139] Van den Driessche P, Watmough J. Reproduction numbers and sub-threshold endemic equilibria for compartmental models of the disease transmission. *Mathematical Bioscience*. 2012;180(1):29-48.

[140] Wang L, Zhao H, Oliva SM, Zhu H. Modeling the transmission and control of Zika in Brazil. *Scientific reports*. 2017;7(1):7721.

[141] Wang W, Zhao XQ. Threshold Dynamics for Compartmental Epidemic Models in Periodic Environments. *Journal of Dynamics and Differential Equations*. 2008;20(3):699-717.

[142] White MT, Verity R, Churcher TS, Ghani AC. Vaccine approaches to malaria control and elimination: Insights from mathematical models. *Vaccine*. 2015;33(52):7544-7550.

[143] Von Stryk O, Bulirsch R. Direct and indirect methods for trajectory optimization. Annals of Operations Research. 1992; 1;37(1):357-373

[144] World Health Organization. A global strategy to eliminate yellow fever epidemics (EYE) 2017-2026. *World Health Organization*; 2018.

[145] World Health Organization. *Handbook for integrated vector management*. 2012.

[146] World Health Organization. *Global strategic framework for integrated vector management*. Geneva: World Health Organization; 2004.

[147] Yellow fever. World Health Organization. Available at http://www.who.int/en/news-room/fact-sheets/detail/yellow-fever. Accessed on 1st May 2018.

[148] Yellow fever. Brazil. World Health Organization. Available at http://www.who.int/csr/don/09-march-2018-yellow-fever-brazil/en/. Accessed on 1st May 2018.

[149] Zika virus fact sheet. World Health Organization. Available: : //http://www.who.int/mediacentre/factsheets/Zika/en/. Accessed 02 March, 2017.

[150] Malaria: World Health Organization fact-sheets. Available at http://www.who.int/news-room/fact-sheets/detail/malaria. Accessed on 1st August 2018.

[151] Wiggins S. *Introduction to applied nonlinear dynamical systems and chaos*. Springer Science & Business Media; 2003.

[152] Wu JT, Peak CM, Leung GM, Lipsitch M. Fractional Dosing of Yellow Fever Vaccine to Extend Supply: A Modeling Study. The Lancet. 2016;388(10062):2904-2011.

[153] Yang HM. A mathematical model for malaria transmission relating global warming and local socioeconomic conditions. *Revista de saude publica*. 2001;35:224-231.

[154] Zhang H, Georgescu P, Hassan AS. Mathematical insights and integrated strategies for the control of Aedes aegypti mosquito. *Applied Mathematics and Computation*. 2016;273:1059-1089.

[155] Zhou J, Hethcote HW. Population size dependent incidence in models for diseases without immunity. *Journal of Mathematical Biology*. 1994;32(8):809-834.

[156] Zika Virus Vaccine. National Institute of Allergy and Infectious Diseases. //http://www.niaid.nih.gov/diseases-conditions/Zika-vaccines. Accessed 23 August, 2018.

[157] Zhao S, Stone L, Gao D, He D. Modelling the large-scale yellow fever outbreak in Luanda, Angola, and the impact of vaccination. PLoS neglected tropical diseases. 2018;12(1):e0006158.